CHEMOTAXIS SIGNAL TRANSDUCTION IN *CAMPYLOBACTER JEJUNI*

Thesis submitted for the degree of

Doctor of Philosophy

At the University of Leicester

By

Paul Ainsworth BSc

Department of Genetics

University of Leicester

2013

Supervised by Professor Julian Ketley

Abstract

The bacterium *Campylobacter jejuni* is the most common cause of food borne disease in the UK, causing a 5-7 day *enteritis* including profuse watery diarrhoea, abdominal pain, fever, headache and occasionally vomiting. In rare cases leading to the paralysing autoimmune disease, Guillain-Barré syndrome. *C. jejuni* are highly motile cells, propelled through the environment by flagella, their motility is directed through a behaviour called chemotaxis. Cells are able to detect attractants or repellents and reposition the cell accordingly. Chemotaxis is central to *C. jejuni* colonisation as non-motile and non-chemotactic mutant strains poorly colonise their usual hosts. In *Escherichia coli* chemotaxis is regulated by the Che proteins which form a two component phospho relay system. In previous studies *In silico* comparison of *E. coli* Che proteins identified homologues in *C. jejuni*, which display altered chemotactic phenotypes in Δ*che* mutant strains. Studies of interactions between the Che proteins using bacterial and yeast two hybrid systems, suggested ways in which the homologues may interact, but to further discern these mechanisms required *in vitro* study. For the purpose of this study the *C. jejuni* Che homologues were cloned, expressed and purified, for use in *in vitro* experiments. Radiolabelled Phosphotransfer assays confirmed CheA as a histidine kinase, and demonstrated Pi transfer to the response regulators of CheY, CheV and CheA, in that order of preference. Affinity tag pull-down assays found the predicted decrease in affinity between phosphorylated CheY and CheA, but also an increase in the affinity of phosphorylated CheV for the receptor, TLP_1. The results of this study confirm the two component backbone of the *C. jejuni* Che model, and suggest how CheV may regulate methylation adaption in a system devoid of a CheB response regulator.

Table of contents

Table of Figures and Tables

Page No.

Glossary of terms

Ac-P	Acetyl phosphate
ATP	Adenosine triphosphate
BSA	Bovine Serum Albumin
CetA/B	Candidate redox sensing TLP receptors
CheA	Histidine kinase
CheA RR	Native response regulator domain of the whole length CheA protein.
$CheA^{HK}$	Separately expressed histidine kinase domain of CheA
$CheA^{RR}$	Separately expressed response regulator domain of CheA
CheB	Methylesterase to TLP cytoplasmic domains
Chemotaxis	Directed cell motility toward attractant or away from repellent ligands
ChePep	A newly identified chemotaxis protein of unknown function
CheR	Methyltransferase to TLP cytoplasmic domains
CheV	Response regulator paired to CheA, with a CheW-like domain
CheW	Scaffolding protein found in complex with CheA and TLP receptors
CheY	Response regulator paired to CheA
CheZ	Phosphatase to CheY and CheB in *E. coli*
Cj0700	Candidate phosphatase, structurally homologous to HP0170 of *H. pylori*
Dhp domain	Dimerization and Histidine Phosphotransfer domain
DNA	Deoxyribonucleic Acid
DTT	Dithiothreitol
EDTA	Ethylenediaminetetraacetic acid
Energytaxis	Cell taxis directed by internal metabolic signals rather than external ligands
FliM	Flagella switch motor protein
GST	Glutathione S-transferase tag
HAMP	Domain of TLP/MCP receptors which communicates

	environmental signals to CheA
HAP	Hard Agar Plug assay
HIS	Polyhistidine tag
HP0170	*H. pylori* phosphatase, functionally homologous to CheZ
HQNO	2-n-Heptyl-4-hydroxyquinoline N-oxide
Hpt	Histidine phospho-transfer domain
IMAC	Immobilised Metal Ion Affinity Chromatography
IPTG	Isopropyl β-D-1-thiogalactopyranoside
MALDI-TOF	Matrix Assisted Laser Desorption/Ionisation-Time Of Flight
MCP	Methyl Accepting Proteins, transmembrane receptors sensing periplasmic ligands in *E. coli* and *B. Subtilis*
PAGE	Polyacrylamide gel electrophoresis
PAS	Sensing domain of TLP/MCP receptors
SDS	Sodium Dodecyl Sulfate
SPR	Surface Plasmon Resonance
TEMED	N,N,N',N'-Tetramethylethylenediamine
TLP	Transducer Like Proteins, *C. jejuni* transmembrane receptors sensing periplasmic ligands
Tris	Tris(hydroxymethyl)aminomethane
Tsr	Serine detecting MCP receptor of *E. coli*
Two component system	A paired histidine kinase and response regulator
Y2H/B2H	Yeast/Bacterial Two Hybrid system

Chapter 1: Introduction

1.1. Overview

C. jejuni is a Gram negative, helical, microaerophilic bacterium which is a common cause of gastroenteritis (Poly & Guerry 2008). Cells are between 0.2-0.8 µm wide and 0.5-5 µm long, they usually have single or bi-polar flagella and are highly motile. There are 16 subspecies within the *Campylobacter* genus of which *C. jejuni* is the most common cause of human enterocolitis. *C. jejuni* is part of the *Campylobacterales* order, which includes the closely related *Helicobacter pylori* noted for causing stomach ulcers. *C. jejuni* grow optimally at 42 °C but also well at 37 °C, their healthy growth at 42 °C may reflect an adaption toward the colonisation of birds in which they are commonly found. The *C. jejuni* NCTC11168 genome was first published in 2000 (Parkhill et al. 2000), many more have since been sequenced (Hofreuter et al. 2006; Pearson et al. 2007; Fouts et al. 2005). With the advent of next generation sequencing methods many hundreds more genomes are being sequenced (Sheppard et al. 2013). *C. jejuni* NCTC11168 has 1,641,481 bases and a GC content of 30.6%, low in comparison to that of *E. coli* which is approximately 50%.

Chemotactic motility is an essential virulence factor for *C. jejuni* and is heavily implicated in the colonisation of poultry, which are often presumed to be the reservoir of *C. jejuni* in human disease (Shreeve et al. 2013; Hood et al. 1988).

As the system for chemotactic control of motility is not well understood in *C. jejuni*, this study aims to investigate that mechanism.

1.1.1. Prevalence

The bacterium *Campylobacter* is the most common cause of food borne disease. In 2012 the Department for Food and Rural Affairs recorded 72,592 cases of Human *Campylobacter* infections in the UK (DEFRA 2013). Human sources of infection include sewage, contaminated water, poultry, pork, and unpasteurised milk. Undercooked contaminated poultry is a particularly common source of human disease as C*. jejuni* is common within chicken flocks (Shreeve et al. 2013; Hood et al. 1988),causing a largely asymptomatic colonisation although some pro-inflammatory response is observed (Smith et al. 2005). Flocks are found colonised after 3 weeks, typically 100% of the birds will be carriers (Corry & Atabay 2001). Surveys by the Food Standards Agency found *Campylobacter* present in 65.2% of chickens purchased from supermarkets (FSA 2009).

1.1.2. Disease

Symptoms of *Campylobacter* enteritis include profuse watery diarrhoea, abdominal pain, fever, headache and sometimes vomiting; symptoms typically last for 5-7 days. In rare cases infection may lead to Guillain-Barré syndrome, an autoimmune disease causing progressive ascending paralysis, recoverable with extensive treatment but fatal if untreated, or acute reactive arthritis, an autoimmune disease characterised by, but not limited to, painful inflammation of lower limb joints (Pope et al. 2010).

It is difficult to assess the impact of *C. jejuni* gastroenteritis as it is not a notifiable disease in the UK. In Sweden where infections are notifiable, the estimated economic cost of campylobacteriosis ranges from between £14,000,000 and £114,000,000 (Toljander et al. 2012), 82% of the estimated cost being due to reduced economic production. These costs remain approximations as *C. jejuni* infections are often not presented to health professionals in order to become notifiable.

For a human pathogen *C. jejuni* has a lack of identifiable toxins, only the cytolethal distending toxin (CDT) identified so far, and recent studies have found campylobacteriosis caused by Δ*cdt* strains to be indistinguishable from those caused by cells positive for a *cdt* gene (Mortensen et al. 2011). Colonisation and survival in the host appear more central to *C. jejuni* virulence (Szymanski & Gaynor 2012).

C. jejuni invasion of epithelial cells is the primary cause of the cell damage which leads to diarrhoea (Everest et al. 1992). *C. jejuni* traverse the surface mucosa of the intestine and are found deep in intestinal crypts during infection (Hugdahl et al. 1988). Directed cell motility is essential for this colonisation as non-motile *C. jejuni* do not colonise their usual hosts (Golden & Acheson 2002; Balaban & Hendrixson 2011; Hendrixson & DiRita 2004; Kanungpean et al. 2011b; Yao et al. 1997) and have attenuated cell invasion phenotypes (Golden & Acheson 2002). Interestingly, *C. jejuni* motility has been found to increase in viscous media, such as the intestinal mucus, and *in vitro* invasion of cell layers has been shown to increase when cells are bathed in more viscous medias (Szymanski et al. 1995). It is important to note that not all the affects noted may be directly due to motility,

as the flagellum also acts as a type III secretion system for a number of invasion associated factors (Guerry 2007), however motility and chemotaxis are important contributory factors in colonisation and invasion, during *C. jejuni* infection.

1.2. Motility and Chemotaxis

Several different bacteria have been utilised as models of bacterial chemotaxis, in many ways that of *E. coli* is the best studied and simplest with which to draw comparison, for this reason discussion begins in terms of a general overview of the *E. coli* model (Krell et al. 2011).

E. coli are peritrichous flagellate bacteria, their flagellae rotate together, forming a bundle of fibres that propel the cell forward. When a flagellum rotates counter clockwise, forces acting against the flagellum in this plane push it into an ordered, rigid structure which acts as a propeller pushing the cell forward, resulting in a straight swim (run). When the flagellum rotates clockwise, it is disordered and without structure so it flails randomly causing the cell to tumble, so randomly re-orientating the cell before it resumes straight swimming.

Chemotaxis is the result of directed motility, through manipulation of the bias between cell runs and tumbles (Fig.1.0*A*). When the cell senses an increasing attractant concentration the flagella will bias towards counter-clockwise rotation, resulting in straight swimming. When a decreasing attractant concentration or an increasing repellent concentration is detected, the cell will bias towards clockwise rotation, resulting in cell tumbling.

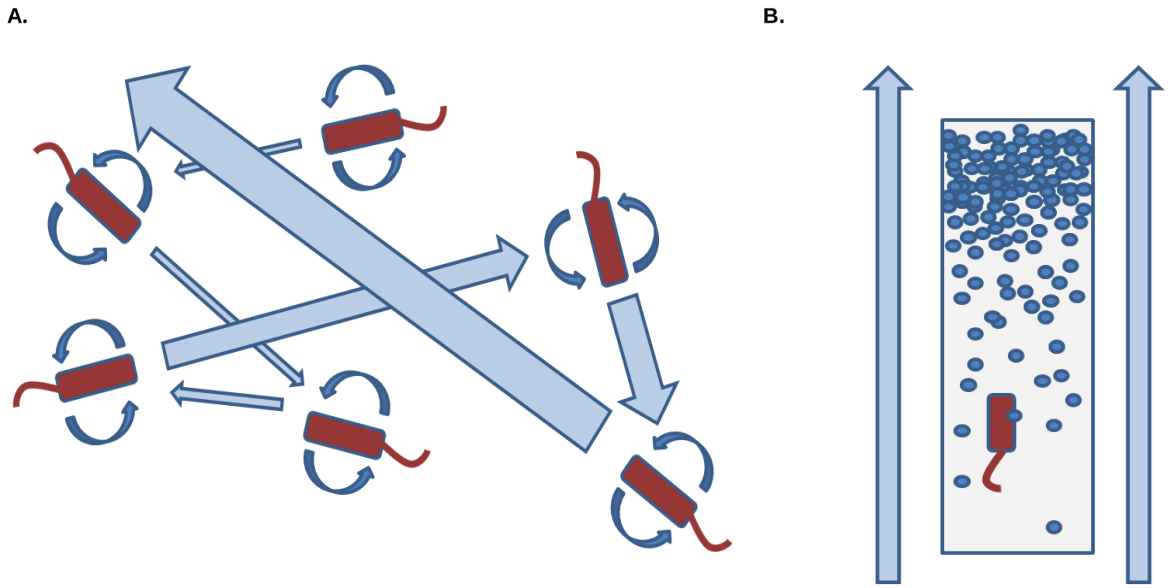

Figure 1.0. Motility and chemotaxis in *E. coli*. (A) *E.coli* negotiates its environment by switching between two types of motion, runs and tumbles. When the cell detects an increasing attractant concentration the cell will bias toward runs that propel the cell forward so that it will continue its movement toward the attractant. When the cell detects a decrease in attractant concentration it switches it's bias toward tumbling motions, that randomly reorientate the cell before resuming running. If the change in cell direction results in movement toward an attractant it's bias will switch toward runs, a continued decrease will cause further tumbling. (B) Modulation of the run/tumble bias results in the chemotactic movement of cells along concentration gradients, either toward attractants or away from repellents.

Re-orientation of a cell during tumbling is a random process and may result in the cell temporarily moving against an attractant gradient, however the cell will tumble again and then resume straight swimming. The process is repeated until an increase in attractant concentration is detected, when the bias will lean towards straight swimming and decrease tumbling events (Eisenbach 1996) (Fig.1.0*B*). To control this rotational bias *E. coli* use a simple two component phosphor relay system, this system, known as the Che system, integrates multiple inputs from surface receptors into a single output, that being the direction of flagellar rotation.

The *E. coli* modes of straight swimming interspersed with tumbling motions are not observed for *C. jejuni*. It appears *C. jejuni* may have a run/stop/reverse swim type which partly relies upon Brownian motion for reorientation (Shigematsu et al. 1998; Ferrero & Lee 1988). Some observations of *C. jejuni* motility have suggested the *C. jejuni* swimming mode may vary with viscosity and that in low viscosity media the cells run and tumble as *E. coli* would, but that in high viscosity media the cells seem to switch between run and pause (Szymanski et al. 1995). However, in high viscosity media cell reversals are apparent in other studies (Shigematsu et al. 1998; Ferrero & Lee 1988).

C. jejuni appears adapted to survival in viscous environments. The spiral morphology of *C. jejuni* may aid its movement through a viscous matrix as its motile velocity increases with the viscosity of the medium it traverses (Shigematsu et al. 1998). Other motile species, for example *E. coli, Vibrio cholerae*, *Pseudomonas aeruginosa* and *Salmonella enterica* show decreases in velocity with increase in matrix viscosity (Ferrero & Lee 1988; Shigematsu et al. 1998).

Motility and chemotaxis are understood to be essential to *C. jejuni* colonisation and pathogenicity (Ketley & Korolik 2008). Multiple studies of *C. jejuni* strains with parts of the flagella or signal transduction systems missing, show failure to colonise their usual hosts. These studies are covered in detail later in the chapter.

Central to the Che signal transduction system is a two component system, what follows is a discussion of these systems and their diverse functions.

1.3. Two Component Systems

1.3.1. A General Overview

A two component system forms the backbone of the chemotaxis signal transduction system. Two component regulators are sensory systems which are used by bacteria to interpret their environment and from that form an appropriate response. Two-component systems are an integral part of cellular survival and adaption to the environment and so are ubiquitous within the bacterial kingdom, with over 50,000 identified so far. Each system shares a common architecture, using modular domains adapted to detect a particular stimulus and perform a certain response (Gao & Stock 2009). *E. coli* possess 30 histidine kinases and [32] response regulators (Stock et al. 2000). With so many similar transduction systems within the cell, the components of each two component system are partnered to each other to prevent unwanted cross talk between unrelated systems (Szurmant & Hoch 2010).

Although there are variations in the arrangement and the number of proteins within a given two component regulator system, they are defined by the presence of two proteins, a histidine kinase and a response regulator. The histidine kinase responds to stimuli by autophosphorylating, this phosphate is then transferred to a response regulator protein (Foussard et al. 2001).

Binding of phosphate to a response regulator activates the protein allowing it to interact with its target within the cell. The majority of response regulators within *E. coli* are transcriptional regulators that bind DNA and promote or repress transcription, but response regulators are a diverse group that regulate the activity of a variety of proteins (Gao & Stock 2009).

Some histidine kinases contain stimuli sensing domains, which modulate activity of the kinase domains, whereas others outsource this sensing activity to an accessory protein with which they interact. EnvZ is an integral transmembrane protein of *E. coli* that senses changes in osmolarity in the periplasm and transduces this signal across the membrane to its own cytoplasmic histidine kinase domains (Cai & Inouye 2002). The NarX histidine kinase uses its integrated sensor to detect nitrate and nitrite (Noriega et al. 2008). The CheA histidine kinase of the chemotaxis system uses separate transmembrane sensors called methyl accepting chemotaxis proteins (MCP) to sense chemoattractants and modulate the activity of the separate cytoplasmic CheA histidine kinase (Falke et al. 1997). Two component systems may respond to external stimuli, or to internal stimuli such as metabolic signals. Systems detecting internal stimuli may have soluble histidine kinases free within the cell or anchored to the membrane.

There is a large variation in reaction rates of two component systems, they can effect rapid changes within the cell which may be short in duration, for example the chemotaxis system, which requires rapid switching of the flagella motor for fluent chemotaxis, while others may be active over a period of hours, for example those involved in the regulation of gene expression, which require chronic activation. OmpR is an example of a chronically activated response regulator, it is an *E. coli* transcriptional regulator controlled by a response regulator domain, paired to the histidine kinase EnvZ (Ames et al. 1999). Modulation of the phosphorylation state of OmpR differentially regulates transcription of porin genes *ompF* and *ompC,* which allow the cell to adapt to changes in osmolarity. PhoB is another transcriptional regulator whose activity is under control of a response regulator domain. PhoB becomes phosphorylated in response to low environmental concentrations of Pi , and regulates transcription of more than 47 identified genes, including the *pst* family of phosphate uptake genes (Lamarche et al. 2008).

Two component systems may also form phosphorelay systems. These systems use the same histidine kinase and response regulator domains but in addition use multiple accessory proteins form a cascade of phosphorylatable proteins that lead to an ultimate response regulator, or response regulators, that will affect the cell response (Medicine & Jolla 2002). The sporulation system of *B. subtilis* is a good example of a phosphorelay system, a histidine kinase transfers phosphate to an Asp residue of the response regulator Spo0F, which can transfer Pi to Spo0B, which in turn may transfer its phosphate to the terminal response regulator Spo0A, a phosphate controlled transcriptional regulator (Zapf et al. 1998;

Medicine & Jolla 2002). This kind of phosphorelay cascade increases the number of proteins required for a system but increases the opportunity for regulation and integration of signals, Spo0F can be phosphorylated by 5 different histidine kinases, multiple phosphatases target Spo0F to remove the Pi group and Spo0A itself is subject to transcriptional regulation by other systems and a phosphatase Spo0E but can be directly phosphorylated by the kinase KinC (Higgins & Dworkin 2012).

1.3.2. Histidine Kinases

Histidine kinases are multi-domain proteins which fall into two broad classes. The CheA protein involved in chemotaxis signal transduction is a Class II histidine kinase, and so for this reason discussion will focus on Class II.

Dimerisation of histidine kinases, via their dimerisation domain, is essential to their function, as they trans-phosphorylate their opposite number in the histidine kinase dimer using phosphate groups liberated from ATP (Baker et al. 2006).

The S domain of Class II kinases binds to response regulators, in the case of the CheA-CheY system, binding of CheY to the S domain causes conformational changes within CheY which increases its susceptibility to phosphorylation and also make it readily accessible to the histidine phospho-transfer (Hpt) domain, easing phosphotransfer (Gao & Stock 2009).

The catalytic domain contains the N, G1, F, G2 homology boxes which identify histidine kinases and define the nucleotide binding cleft (Stock et al. 2000). Between the F and G2 boxes a flexible region called the ATP lid stabilises ATP

binding by becoming more rigid and covering the ATP once it is bound (Gao & Stock 2009). Binding of ATP causes a conformational change that brings the Hpt domain into contact with the catalytic domain of its partner protein in the homodimer, allowing transfer of the gamma phosphate to a histidine residue in the Hpt domain (Baker et al. 2006). Phospho-transfer allows for the dissociation of Hpt and the release of ADP from the catalytic domain (Baker et al. 2006).

The CheW domain of CheA is responsible for interactions with the MCP sensor proteins, these interactions allow for regulation of the rate of autophosphorylation activity based on signals from the MCP.

Class I histidine kinases have phosphatase activity and remove the phosphate group from their respective response regulators, CheA is atypical in this respect as its phosphatase activity is “outsourced” to an accessory protein CheZ (Gao & Stock 2009). The functions of many of the separate domains of Class II histidine kinases are associated with a single Dhp domain in Class I histidine kinases, Class II kinases represent only around 5% of the histidine kinases identified so far (Gao & Stock 2009).

1.3.3. Response Regulators

The response regulator family of proteins share a conserved response regulator domain (RR) by which they interact with their paired histidine kinases, the RR domain has a simple structure of a 5 stranded β-sheet surrounded by 5 α-helices (Stock et al. 2000). Small variations in this RR domain confer specificity to the response regulator/histidine kinase interaction and prevent unwanted cross talk between two-component systems.

Response regulators usually consist of an N-terminal RR domain and a C-terminal output domain, whose activity is regulated by the phosphorylation state of its RR domain. The output domains have different functions although the majority form DNA binding sites. Many response regulators consist of a single RR domain and lack a specific output domain (Jenal & Galperin 2009). For these single domain response regulators, conformational changes within the RR domain allow them to interact directly with a cell target, which is activated or inactivated by RR binding (Jenal & Galperin 2009).

Magnesium is an essential factor for the function of response regulators, it causes conformational changes within RR domains which allow them to bind phosphate at an aspartate residue (Asp57). Mg^{2+} is only required for binding of the phosphate not to maintain phosphorylation once the Pi group is bound.

Response regulators have an inherent autodephosphorylation activity, the rate of which varies widely across two component systems, depending upon the role of the system within the cell. The cause of such variation in hydrolysis is of interest as the structure of response regulators is highly conserved. The efficiency of this action appears to be tuned by individual amino acids at key locations, for example the rate of Pi hydrolysis for *E. coli* CheY can be manipulated by single amino acid substitutions at Asn59 and Glu89 (Thomas et al. 2008). It appears the residues at these positions are selected for by their suitability in enhancing or retarding the rate of signal adaption of the two component system.

1.4. The *E. coli* Chemotaxis Model

The majority of chemotaxis proteins identified thus far in *C. jejuni* have been identified by their homology to those of *E. coli* and *H. pylori*. The two-component chemotaxis signal transduction of *E. coli* is the best characterised and simplest with which to make cross species comparisons. For this reason it will initially be the model with which I explain what we understand of the *C. jejuni* system so far.

1.4.1. System Overview

In the *E. coli* system methyl-accepting chemotaxis proteins (MCPs) sense changes in local concentrations of chemoattractants or repellents. MCPs are integral inner membrane proteins with periplasmic domains that bind environmental ligands. In the *E. coli* model, the MCP reacts to an absence of chemoattractant, and transduces this signal to its cytoplasmic domain, which is held in a complex with the histidine kinase CheA and a scaffold protein CheW.

The signal from the MCP increases the rate of CheA autophosphorylation, once CheA is phosphorylated it passes its Pi group to its cognate response regulator protein CheY (Falke et al. 1997) (Fig. 1.1). Phosphorylation of CheY causes a large conformational change in the protein which decreases its affinity for CheA and increases its affinity for the flagella motor switch protein FliM (Lee et al. 2001).

When greater than 70% of the population of CheY proteins is phosphorylated, the binding of activated CheY to FliM changes the bias of flagellar rotation towards

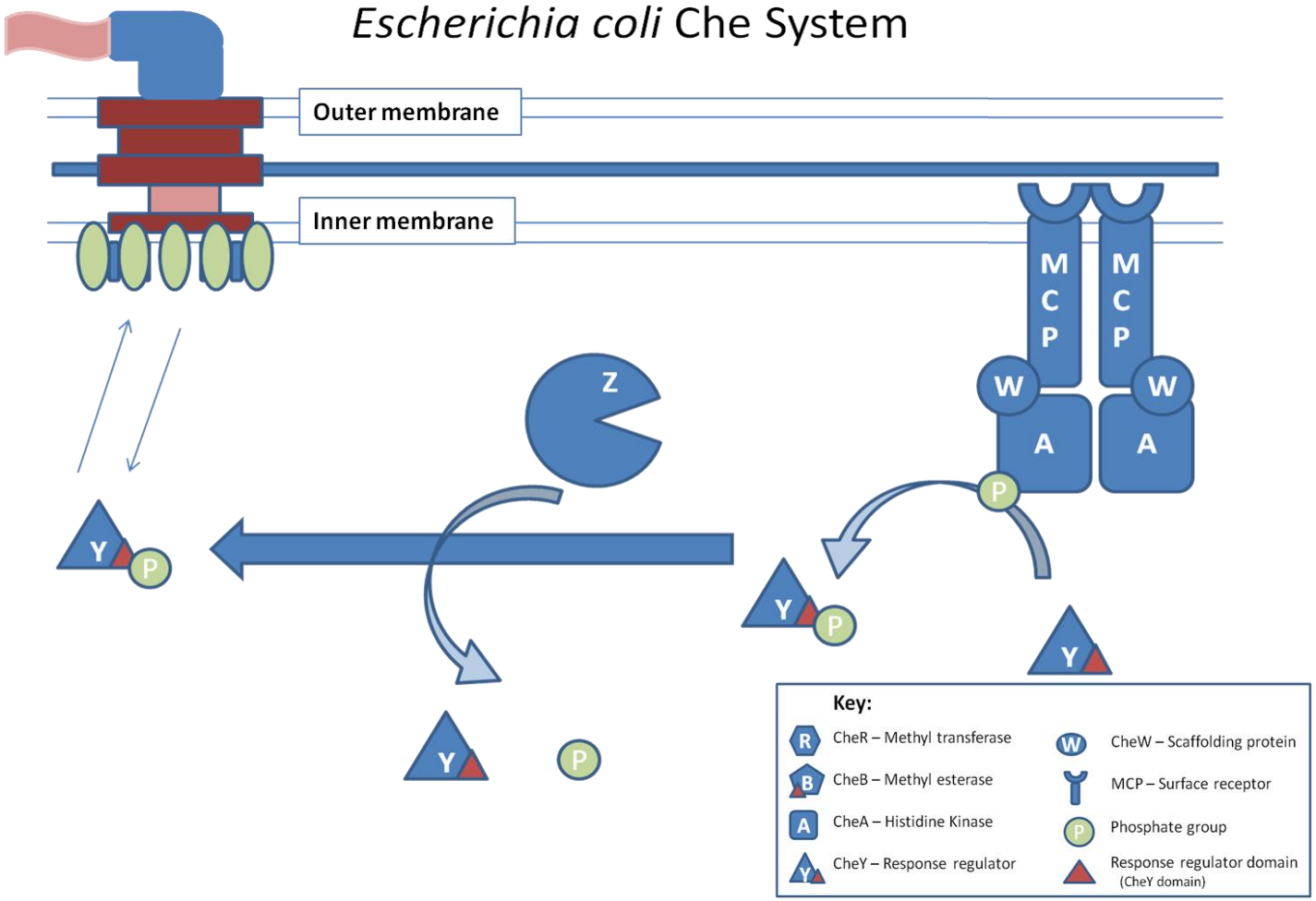

Figure 1.1. The model chemotaxis signal transduction system of *E. coli*. The periplasmic sensing domain of the methyl-accepting chemotaxis protein (MCP) detects environmental ligands such as attractants or repellents, and transduces this signal across the membrane to its cytoplasmic domain. The MCP cytoplasmic domain is held in a signalling complex with CheA and CheW. In response to a fall in attractant concentration or the presence of a repellent, the MCP increases CheA's rate of autophosphorylation. Phosphorylated CheA transfers its phosphate to CheY, which then dissociates from CheA to interact with the flagella motor switch. Once greater than 70% of the CheY population has phosphorylated and bound to the motor switch, the flagella changes its rotation bias towards clockwise rotation, so increasing cell tumbling motions. The phosphatase CheZ helps to reset the system by removing phosphate from CheY, so that it may dissociate from the flagella and re-associate with CheA. When an increasing attractant concentration is sensed the MCP suppresses CheA phosphorylation, reducing the population of phosphorylated CheY and biasing the flagella towards counter clockwise rotation, which propels the cell forward.

clockwise rotation (Bren & Eisenbach 2001), causing the cell to tumble and randomly re-orientate itself in space before the system resets and the cell resumes straight swimming. The system 'resets' by hydrolysing Pi from CheY, the phosphatase CheZ increases the rate of Pi hydrolysis, which decreases the population of phosphorylated CheY molecules. Reduction in the population of phospho CheY will decrease the probability of cell tumbling events, however CheA may still be active and continuing to transduce signal by phosphorylating CheY molecules (Porter et al. 2011).

The efficiency of signal transduction by the MCP to CheA is modulated by methylation of MCP receptors. CheR is a methyl-transferase which constitutively adds methyl groups to the cytoplasmic domain of MCPs, CheB is a methylesterase, regulated by a response regulator domain, which removes methyl groups from MCPs when it becomes phosphorylated by CheA (Porter et al. 2011) (Fig.1.2). Increased MCP methylation desensitises the receptor to its ligand, increasing the probability of it triggering autophosphorylation of CheA. Methylation and de-methylation adjust the sensitivity of the receptor and enable the cell to detect and move up or down a concentration gradient, by constantly altering the threshold concentration at which the system will become active (Kirby et al. 1997).

1.5. Previous Studies in *Campylobacter jejuni*

The *E. coli* model exemplifies the components of the chemotaxis system however there is variation in chemotaxis signal transduction systems across species, for example the *Rhodobacter sphaeroides* system (Fig.1.3) has 4 CheA and 6 CheY

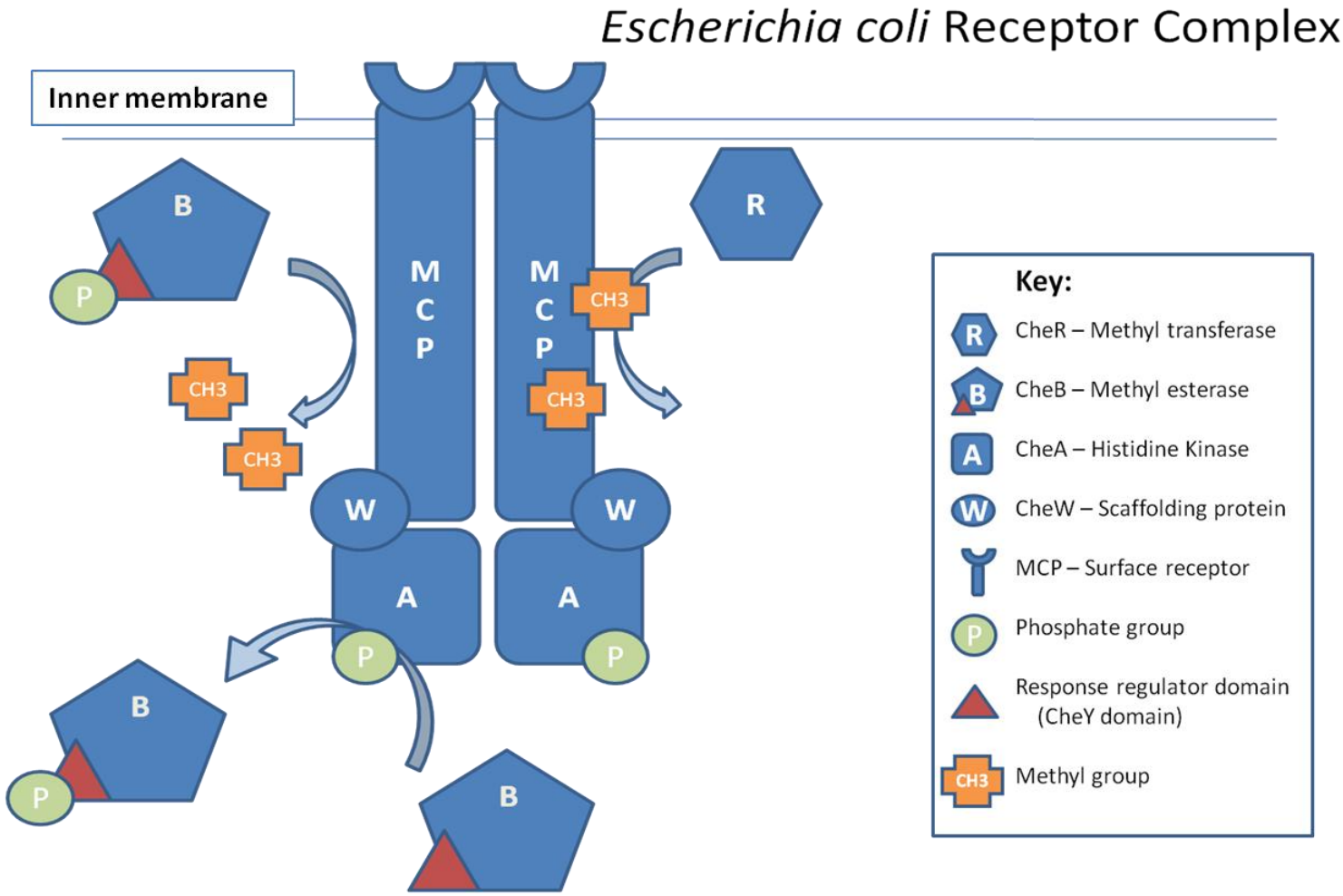

Figure 1.2. The signalling complex in the model chemotaxis signal transduction system of *E. coli*. The chemotaxis signalling complex consists of the cytoplasmic domain of MCP, CheA and CheW. CheB and CheR associate with the complex to adapt the sensitivity of the MCP receptors to their ligand, and so affect the probability of CheA autophosphorylation being triggered by MCP. CheB and CheR regulate MCP ligand sensitivity by modulating the methylation state of itscytoplasmic domain, CheR is a methyl-transferase which constitutively adds methyl groups to MCPs, whereas CheB is a methylesterase controlled by a response regulator domain. CheB removes methyl groups from MCPs when it becomes phosphorylated by CheA.

homologues that have diverse functions (Ferré et al. 2004) and *B. subtilis* (Fig.1.3) and *H. pylori* contain additional proteins not found within the *E. coli* model. While there are great similarities between the apparent *C. jejuni* system and that of *E. coli*, further study will be necessary to understand its transduction mechanism.

C. jejuni homologues of the *E. coli* chemotaxis Che proteins and MCP surface receptors were identified shortly after the first sequencing of the genome. Homologues to *E. coli cheA*, *cheW*, *cheY*, *cheB* and *cheR*, were located but no homologue to the phosphatase *cheZ* (Parkhill et al. 2000; Marchant et al. 2002). A homologue to the *B. subtilis* and *H. pylori* scaffold protein *cheV* was identified and the *C. jejuni* methylesterase CheB was found not to have an RR domain. In common with *H. pylori*, the *C. jejuni* CheA was found to have its own response regulator domain (Parkhill et al. 2000; Marchant et al. 2002). *C. jejuni* possesses a unique complement of Che proteins so a directly analogous model is not available for comparison.

CheV proteins seem common in other, non-*E.coli* chemotaxis systems. An analysis in 2009 of the 523 bacterial genomes sequenced at the time, found that 22% of them had a *cheV* homologue, some had more than one homologue. It is notable that only 20% of the genomes had an identifiable homologue to *E. coli cheZ* (Hamer et al. 2010)

The MCP chemoreceptors of *E. coli* also have homologues in *C. jejuni*, these are referred to as Transducer like proteins (TLP). There are ten putative TLP

A.

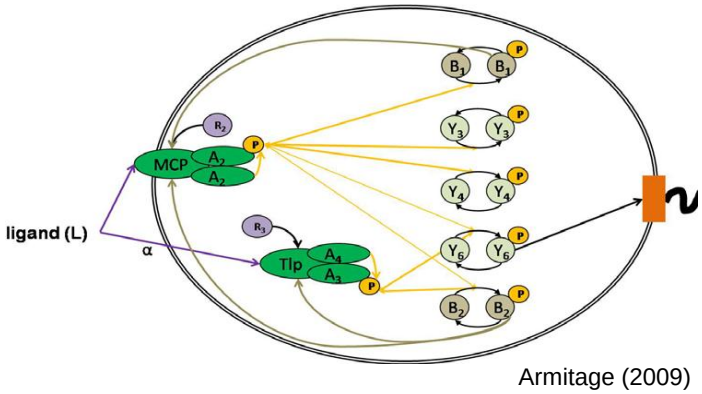

Armitage (2009)

B.

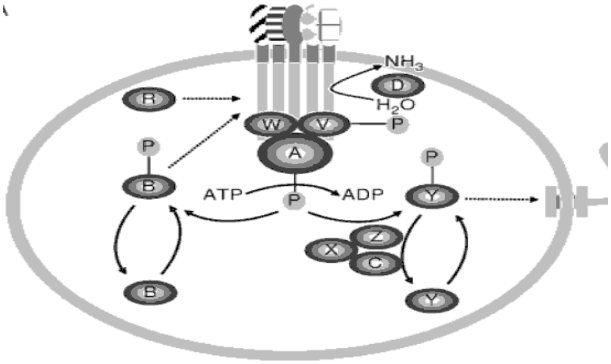

Miller (2009)

Figure 1.3. Chemotaxis signal transduction systems in *Rhodobacter sphaeroides* and *Bacillus subtilis*. (A) The chemotaxis signal transduction system of *Rhodobacter sphaeroides* uses four CheA, four CheW, six CheY, two CheB and two CheR homologues. Differential interactions between these kinases and response regulators, combine complex internal and external stimuli into a single rational chemotactic response (Hamer et al. 2010). (B) The chemotaxis signal transduction system of *Bacillus subtilis* possesses additional Che proteins not present within the *E.coli* model. CheC and CheD appear to be additional regulators of receptor methylation, activated by phosphorylated CheY, although the system has CheB and CheR homologues. The CheV protein, essentially a CheW with a response regulator, regulates receptor sensitivity and adaption (Rao *et al* 2009).

proteins in *C. jejuni* (TLP_{1-10}) and two potential *aer* homologues (Parkhill et al. 2000; Marchant et al. 2002).

The *cheV*, *cheA* and *cheW* genes appear to be present in an operon and are probably co-transcribed, as are *cheB* and *cheR* which appear together in the genome. *CheY* appears to be in an operon with four apparently unrelated genes, (Marchant et al. 2002).

Phenotypes of *C. jejuni* Δ*che* Mutant Strains

One of the most common methods to assess the chemotactic ability of motile cells is to measure their displacement in a swarm assay. Strains are inoculated onto the centre of a semisolid agar plate that allows for passage of the cells through the medium, the medium is incubated for a period of time appropriate to the species being tested, then the diameter of the zone of swarming is measured. The use of nutrients by the cells creates an expanding area of low concentration in the centre of the plate, which drives chemotaxis of the cells toward the periphery of the agar plate. Comparison of test strains with motile wild type and non-motile strains, which are used as positive and negative controls, demonstrates the zone diameter which should be achieved by chemotactic cells and that which would result from normal cell growth without the influence of chemotaxis. Cells could be non-motile rather than non-chemotactic, that is to say that they lack motile flagella rather than just the ability to move toward an attractant. To ensure a chemotactic phenotype was being observed, and not a non-motile phenotype, cells were observed by light microscopy to ensure they have flagella, and that the cells are in motion (Bridle 2007).

C. jejuni cheV, *cheA*, *cheW*, *cheR*, *cheB* and *cheY* homologues were implicated in chemotaxis by comparison of the chemotactic phenotype of *Δche* strains to that of wild type cells in swarm assays. All were observed to have an attenuated chemotaxis phenotype in swarming assays, indicating that the mutated genes were genuine Che homologues and that they are involved in *C. jejuni* chemotaxis (Bridle 2007; Reuter & van Vliet 2013; Yao et al. 1997).

Complementation of the Δ*che* strains was necessary to exclude the possibility that polar effects on downstream genes were responsible for observed changes in chemotactic phenotypes. Only *cheY*, *cheB* and *cheR* could be complemented at an alternate locus (Bridle 2007). The *cheV*, *cheA* and *cheW* genes were successfully reverted by natural transformation with a genome preparation from *C. jejuni* NCTC 11168. However, this method could not exclude that recombination had also occurred at loci other than those intended for reversion, and that changes at these loci may have been responsible for the observed phenotype (Bridle 2007).

In *in vivo* tests *C. jejuni* Δ*cheB* and Δ*cheR* strains were found to be attenuated in their ability to colonise chickens. A *cheB*/*cheR* double mutant colonised to 100 fold less than wild type cells at seven days post infection (Kanungpean et al. 2011b) and Δ*cheY* strains were completely unable to colonise their usual hosts (Yao et al. 1997)

The *C. jejuni* homologues of the MCP periplasmic receptor proteins of *B. subtilis* and *E. coli*, also appear to play an important role in *C. jejuni* chemotaxis. *C. jejuni* Δ*tlp* strains have a reduced ability to colonise mice (Hartley-Tassell et al. 2010;

Sandhu 2011) and Δ*tlp*$_4$ and Δ*tlp*$_{10}$ mutants have been found to be attenuated for colonisation in chickens (Hendrixson & DiRita 2004). A Δ*tlp*$_{10}$ mutant strain was found to be severly attenuated for chickens colonisation, reaching 10^{x6} less cells than the wild type *C. jejuni* strains (Hendrixson & DiRita 2004; Balaban & Hendrixson 2011). Strains with the putative cytoplasmic sensors c*etA* and *cetB* removed, have been shown to have attenuated invasion phenotypes, showing only 20% of wild type invasion in tissue culture, although a Δ*cetA*/*cetB* mutant was found to colonise chickens to near normal levels (Hendrixson & DiRita 2004; Golden & Acheson 2002; Hendrixson et al. 2001)

Che Protein Interaction Assays

Possible paths of interaction between *C. jejuni* chemotaxis homologues have been investigated previously using a small scale bacterial two-hybrid system (B2H) (Bridle 2007) to test for suspected interactions, and by a yeast two-hybrid system (Y2H) (Parrish et al. 2007) in a genome wide protein interaction assay. As the interactions detected in B2H and Y2H assays are numerous and their implication for the *C. jejuni* model requires greater attention, these previous results will be covered in depth in later chapters.

B2H and Y2H assays give indications of the interactions occurring in cells however it is important to keep in mind that these assays were not carried out in a *C. jejuni* background, and that the proteins were fused to portions of an adenylate cyclise. This may promote spurious interactions or prevent native interactions that should occur, so generating false positive or negative results. Auxiliary proteins may also be required for interaction between bait and prey proteins and as both assays excluded auxiliary proteins these interactions would not have

been detected. However, observation of an interaction in a B2H or Y2H assay is a good basis for further investigation.

That the Che proteins had been observed to interact in affinity assays, showed that the collection of Che homologues were acting as part of a single system and discounted the possibility that the chemotactic phenotype, observed in the Δ*che* swarming assays (Bridle 2007), may have been due to effects other than a direct impact of Δ*che* deletions upon the chemotaxis signal transduction system.

1.6. *C. jejuni* Chemotaxis Proteins

The previous section gave an overview of the evidence so far for a Che transduction system in *C. jejuni*. This section discusses the *C. jejuni* Che proteins in greater depth and uses cross species comparisons of the homologous proteins. For reference a representation of a proposed *C. jejuni* chemotaxis system is included (Fig. 1.4.)

1.6.1. CheA

Strong interactions have been observed between *C. jejuni* CheA and CheY in B2H and Y2H assays, supporting the hypothesis of a signal transduction system working in a manner similar to that of *E. coli* (Bridle 2007; Parrish et al. 2007). Δ*cheA* mutant strains have been found to be non-chemotactic and also have heavily attenuated invasive phenotypes (Golden & Acheson 2002; Bridle 2007), although the method used may have resulted in polar effects upon downstream genes. The *cheA* gene was mutated by the insertion of a large antibiotic resistance cassette. Because *cheA* is positioned between *cheV* and *cheW* in an

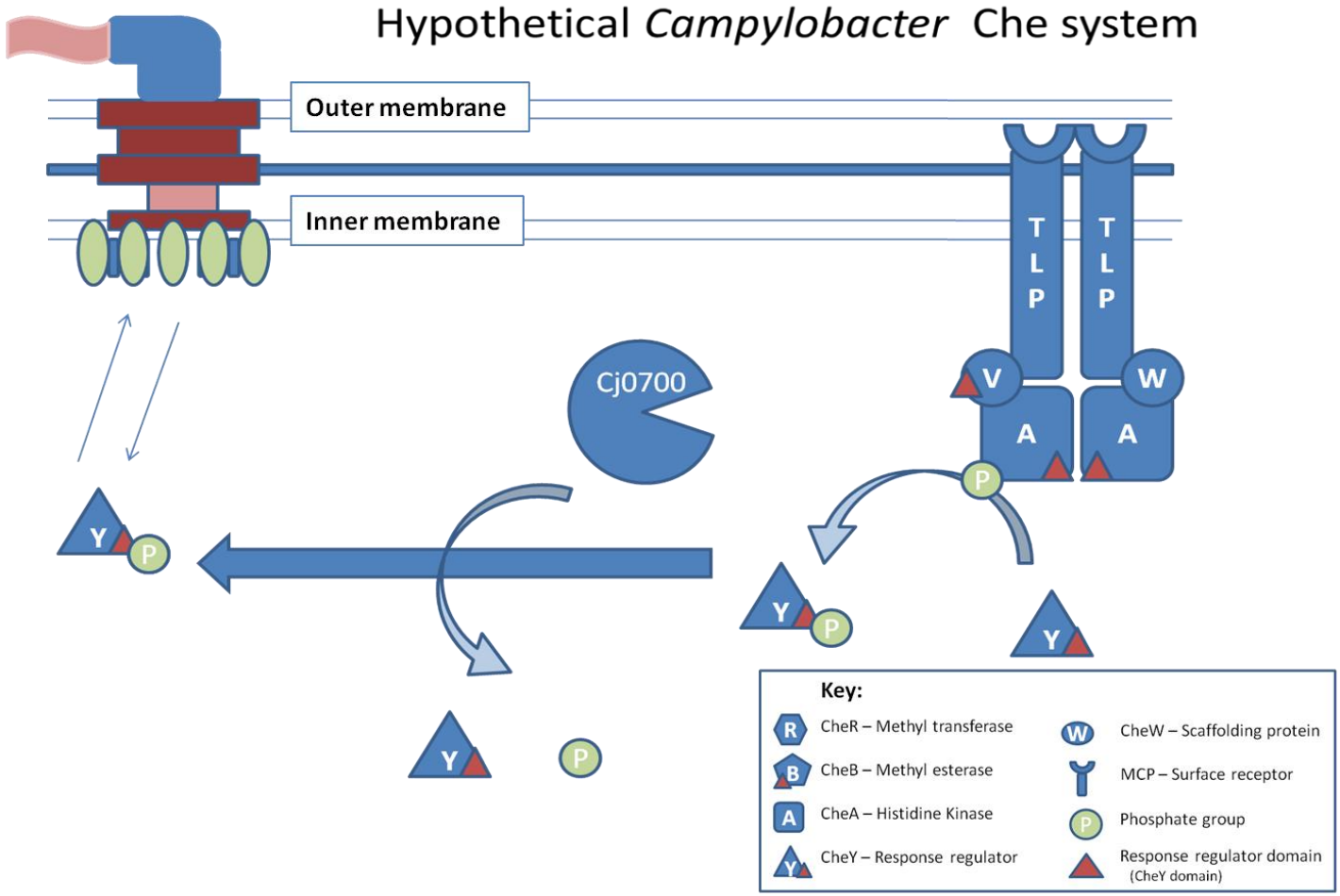

Figure 1.4. A putative model of the core *C. jejuni* chemotaxis transduction system. The periplasmic sensing domain of the transducer-like protein (TLP) detects environmental ligands such as attractants or repellents, and transduces this signal across the membrane to itscytoplasmic domain. The TLP cytoplasmic domain is held in a signalling complex with CheA and CheW/CheV. In response to changes in attractant or repellent concentration the MCP alters CheA's autophosphorylation rate. Phosphorylated CheA transfers itsphosphate to CheY, CheY dissociates from CheA to interact with the flagella motor switch and modulate the flagella rotation bias. A phosphatase Cj0700 resets the system by removing phosphate from CheY, so that it may dissociate from the flagella and re-associate with CheA. CheA is predicted to phosphorylate the putative response regulators of CheV and the CheA RR domain, but the function of these proteins is as yet unconfirmed.

operon, it is uncertain if the effects upon chemotaxis were due to interruption of the *cheA* gene, or a disruption of *cheW* transcription or translation.

The rate of CheA autophosphorylation is dependent upon stimulus by an MCP receptor. In *E. coli*, in the presence of CheW and an MCP receptor, CheY phosphorylation can increase 10-100 fold (Ninfa et al. 1991; Li et al. 2011), the level of activation of CheA by MCPs is relative to the concentration of MCP ligand present.

Unlike the CheA of the *E. coli* model, *C. jejuni* CheA has a response regulator domain at its C-terminus (CheA RR) the function of which is not known, however C*. jejuni* is not unique in having a CheA containing a response regulator domain. FrzE, the CheA homologue of *Myxococcus xanthus*, contains a response regulator domain which prevents any detectable autophosphorylation of the HK domain *in vitro*. Truncated forms of FrzE which exclude the CheA RR domain are able to autophosphorylate the HK domain, and separately expressed phosphorylated FrzE HK domains are able to trans-phosphorylate the FrzE respsonse regulator. This evidence suggests FrzE may be activated by phosphorylation of its CheA RR domain by another histidine kinase or perhaps interaction with part of the receptor complex may relax regulation of the HK domain, and so allow for positive feedback, this mechanism would add an additional layer of regulation of this two component system (Inclán et al. 2008). Perhaps the *C. jejuni* CheA RR may regulate the activity of the CheA histidine kinase domain in a similar manner.

H. pylori CheA also contains a CheA RR domain, deletion of which results in a severely attenuated chemotactic phenotype and a failure to colonise mice (Foynes et al. 2000). Observation of *H. pylori* Δ*cheY* and Δ*cheA-RR* mutant strains found them both to be strongly biased towards counter clockwise rotation resulting in straight swimming, the default rotation for *H. pylori* flagella. This evidence suggests the deletion of *cheA RR* had paralysed the transduction system, indicating a significant role for CheA RR domain in chemotaxis.

A number of roles have been suggested for the CheA RR domain. It has been speculated that CheA RR may associate with internal MCPs to form soluble signalling complexes to detect internal stimuli (Foynes et al. 2000). Radiolabelled phosphate studies have observed possible retro-phosphorylation from CheY to CheA RR domain (Foynes et al. 2000), and suggested phosphate may be recycled back into the system via this route. A phosphate sink theory suggests that systems lacking a phosphatase for CheY may use multiple response regulator domains, such as CheA RR domain, to reduce the availability of the phosphorylated HK domain of CheA to CheY (Marchant et al. 2002) .

The CheA RR domain could form an alternative input to the signal transduction system, integrating a signal from another two component system, or perhaps function as an output to a phosphorelay system. However, notwithstanding the previous hypotheses, the histidine kinase domain of *H. pylori* CheA has been found to phosphorylate both CheY and CheA RR, with a strong preference towards CheY (Jiménez-Pearson et al. 2005).

1.6.2. CheY

The role of CheY in *C. jejuni* chemotaxis is most likely conserved as the *C. jejuni cheY* homologue has been used to successfully complement a *H. pylori* Δ*cheY* mutant in swarming assays (Jiménez-Pearson et al. 2005). This complementation shows *C. jejuni* CheY is a functional orthologue to that of *H. pylori*, which has been shown to be the primary response regulator which interacts with the flagellum. The CheY of *H. pylori* has an 82% amino acid identity to that of *C. jejuni* and 4 of the 5 conserved amino acids of the active site are identical (Foynes et al. 2000).

CheY is a typical single domain response regulator, transfer of phosphate from CheA to CheY causes large conformational changes within the response regulator which allow the protein to dissociate from CheA, and interact with the flagellar motor protein, FliM (Lee et al. 2001). The response regulator domain of CheY is likely to have a different role to that of CheA or CheV as it shares greater homology with CheY proteins across multiple species than it does with the response regulator domains of CheA and CheV (Marchant et al. 2002).

Response regulator domains have their own autodephosphorylatory activity, which helps hydrolyse the Pi group from the RR domain and so 'reset' the transduction system (Terasawa et al. 2011). The autodephosphorylatory rate of CheY is the most rapid of all identified response regulators. The rate of hydrolysis of Pi on *E. coli* CheY is defined by residues at Asn59 and Glu89. Substitution mutations at Asn59 and Glu89 can increase the rate of hydrolysis of Pi by as much as 130 fold, or decrease it by as much as 40 fold from its native

rate (Thomas et al. 2008). For each response regulator the residues at Asn59 and Glu89 appear to be selected for by the required signal adaption rate of the two component system. Systems which require long term activation of a response regulator, such as those with DNA binding domains, generally have much slower Pi hydrolysis rates than those which require rapid adaption (Thomas et al. 2008). *C. jejuni* NCTC11168 CheY has Asn59 and Glu89 residues, suggesting a very rapid autodephosphorylatory rate, but one slower than that of *E. coli* CheB or *R. sphaeroides* $CheY_6$ (Thomas et al. 2008).

CheA is not the only route to CheY activation, as acetyl phosphate, a product of pyruvate and acetate metabolism, has been found to directly phosphorylate a number of response regulators including CheY. An *E. coli* Δ*cheA* deletion mutant strain which is normally unable to tumble, was found to be able to tumble when placed in conditions promoting acetyl phosphate production (McCleary & Stock 1994; McCleary et al. 1993). The metabolic path way and the enzymes responsible for acetyl phosphate production have homologues in *C. jejuni*. If the CheY of *C. jejuni* can use acetyl phosphate as a phosphate donor at physiologically relevant concentrations this may represent a mechanism for metabolism to influence cell taxis (McCleary et al. 1993; McCleary & Stock 1994).

Adaption of CheY may occur in *C. jejuni* via acetylation. *E. coli* CheY has 10 acetylation sites which have been identified *in vitro*, with the most common sites at Lys-92 and Lys-122. *In vivo* CheY acetylation has been confirmed using anti-acetyl-lysine antibodies against western blots of wild type cells. The majority of CheY molecules isolated from cells have between 0 and 3 acetyl groups (Yan et al. 2008). In *E. coli* high levels of CheY acetylation prevent its interaction with

CheA and dramatically reduce its binding to the phosphatase CheZ. Acetylated CheY also has a much lower affinity for the motor switch FliM (Liarzi et al. 2010). In *E. coli* the overall result of acetylation is to inhibit chemotaxis signal transduction and so promote straight swimming, the effect of this method of modulation, if at work in *C. jejuni,* is unknown but would perhaps generate a phenotype similar to that of a Δ*cheY* or Δ*cheA* strain.

1.6.3. CheV and CheW

CheW and Signal Amplification

This section will discuss CheV and CheW together as they appear to have overlapping functions and CheV is in essence a CheW protein with a response regulator domain.

The close homology of *C. jejuni* CheW to *E. coli* CheW suggests that it fulfils the same function and so will form a receptor complex with TLPs (the MCPs of *C. jejuni*) and CheA as found in the *E. coli* model. This is supported by the *C. jejuni* Y2H assay which found interactions between CheA and CheW, and between CheW and the TLPs 2, 3 and 4 (Parrish et al. 2007; Hartley-Tassell et al. 2010).

In *E. coli* CheW performs an essential function in amplifying the signal between MCP receptors and CheA, although CheA can associate with MCPs without CheW present. When CheW is present, MCPs can increase CheA activity 10 fold (Ninfa et al. 1991). The site at which CheA interacts with MCPs overlaps with that of CheW, and binds with a higher affinity than that of CheW. Assays using the *E. coli* MCP Tsr receptor against a variety of concentrations of purified CheA

and CheW found competition between the proteins for Tsr, with the addition of 10μM CheA caused a 30% reduction in the level of MCP associated CheW (Levit et al. 2002). When present at lower concentrations, the presence of CheW increases the amount of CheA found in Tsr receptor complexes (Francis et al. 2002; Levit et al. 2002). The CheW-like domain of CheA which binds to MCPs is very similar to that of CheW, CheW and CheA may therefore act as bridges between MCP receptors to form complexes of receptor clusters, which in turn may have implications for the role of CheV.

Deciphering a Role For CheV

The role of the response regulator domain of CheV is not known at present. CheV does not exist in the model *E. coli* system but has orthologues in *B. subtilis, S. enterica,* and three homologues in *H. pylori* (Foynes et al. 2000).

CheV is part of the chemotaxis signal transduction system, phosphorylation of CheV homologues by CheA has been confirmed in *B. subtilis* (Karatan et al. 2001) and *H. pylori* (Pittman et al. 2001). Interactions seen between *C. jejuni* CheA and CheV in B2H assays suggest the route of phosphorylation is the same for *C. jejuni* CheV. The non-chemotactic phenotype of a Δ*cheV* deletion mutant has confirmed CheV involvement in chemotactic movement, suggesting that the identified *C. jejuni* CheV is a real homologue to that of *B. subtilis* and *H. pylori* (Bridle 2007).

Although well studied, the role of CheV in *B. subtilis* and *H. pylori* is unclear, in the following sections the evidence for a putative function is discussed by study of CheV deletion mutants for each species.

Phenotypes of CheV mutants in *B. subtilis*

B. subtilis Δ*cheV* strains have attenuated chemotactic phenotypes in relation to that of wild type cells, with the mutants only displaying 45% of wild type chemotaxis in the presence of an attractant (Rosario el al. 1994). A *cheV* mutant expressing only the CheW-like portion of CheV retains 75% of it's chemotactic motility, suggesting that CheV might in part be functionally redundant to CheW, but the loss of chemotactic motility in the deletion mutant suggests the response regulator domain carries out a function essential to full wild type chemotaxis (Rosario et al. 1994).

A *B. subtilis cheV*/*cheW* double mutant, with a severe bias in its walk, can be partially complemented with a pointed mutated non-phosphorylatable *cheV*, and recovers its switching ability to near normal levels (Karatan et al. 2001). The cells show receptor adaptation when an asparagine attractant is added, but do not recover completely. A Δ*cheW* single mutant reacts to asparagine in the same manner as wild type cells. From these experiments the authors concluded that the phenotype of the *cheV*/*cheW* mutant must have been due to the inactivated non-phosphorylatable CheV response regulator domain (Karatan et al. 2001).

As a caveat to these studies it is important to note that only asparagine was used to assay the phenotype of *cheV* and *cheW* mutants. Previous experiments have shown a strong bias for some receptors to bind either CheV or CheW in *C. jejuni* (Hartley-Tassell et al. 2010), so although these results are compelling, the use of just asparagine as an attractant may not have allowed for the full phenotype of a *cheV,* or non-phosphorylatable *cheV* mutant to be observed. Interestingly all of the mutant strains show high pre-stimulus biases towards counter clockwise

rotation, suggesting that CheV and CheW are required to maintain wild type switching levels (Karatan et al. 2001).

Phenotypes of $CheV_{1-3}$ mutants in *H. pylori*

H. pylori has 3 different CheV homologues (Pittman et al. 2001). A study observing the migration of *cheV* deletion mutants on soft agar found Δ$cheV_1$ mutants to be non-chemotactic (Pittman et al. 2001), whereas Δ$cheV_2$ and Δ$cheV_3$ mutants showed no obvious change in phenotype. Soft agar migration assay observe the final result of chemotaxis, not the process or its efficiency. Motion tracking assays, which can observe movement of individual cells, found Δ$cheV_1$ and Δ$cheV_2$ mutants to carry a bias towards straight swimming and that Δ$cheV_3$ deletion mutant had displacement rates comparable to that expected of unaided diffusion (Lowenthal et al. 2009). A Δ$cheV_3$ mutant strain was found to be in an almost constant tumble (Pittman et al. 2001). The different swimming phenotypes observed suggests that the CheV homologues do not all have the same function, or at least not to the same extent, as if they were functionally redundant to each other, it could be expected that each deletion mutant would express roughly the same phenotype.

Differing results in colonisation assays using the Δ*cheV* strains support the notion that CheV homologues are not functionally redundant to each other. Colonisation assays in mice found Δ$cheV_2$ and Δ$cheV_3$ strains to colonise mice to comparable levels as wild type cells, whereas Δ$cheV_1$ mutant cells were 1000 fold less successful in comparison to wild type. Competition assays found all *cheV* mutants were able to colonise mice but that they could not compete with wild type cells when present together in a mouse model (Lowenthal et al. 2009).

CheV Localisation Within the Cell

The localisation of CheV *in situ* has been studied in order to understand its role in the chemotaxis system. Studies in *B. subtilis* found the location of CheV to be dynamic, unlike CheW which is predominantly found at cell poles (Wu et al. 2011). The addition of an attractant causes CheV to relocate. Before attractant is added CheV is found mostly laterally associated but on addition of attractant CheV was found to cluster at the poles. After one minute cells had adapted, presumably by methylation, and CheV had returned to its lateral positioning (Wu et al. 2011).

A strain created with a truncated CheV minus its RR domain ($CheV^{\Delta RR}$), and a strain with CheV with an introduced point mutation that rendered it non-phosphorylatable ($CheV^{57}$), were both found to locate permanently to the poles. The authors suggest this demonstrates that RR domain phosphorylation is required for CheV lateral localisation. However, the findings of this study seem to disagree its conclusion (Wu et al. 2011). *B. subtilis* increases autophosphorylation of CheA in environments of increased attractant concentration, the level of CheV phosphorylation presumably increases in proportion to the level of CheA phosphorylation as CheA is its partnered histidine kinase (Garrity & Ordal 1997). When attractant was added to wild type cells, so increasing CheA phosphorylation, wild type CheV was found to relocate to the poles not to lateral clusters, so the results of the attractant addition assays, using wild type cells, and the results of assays using $CheV^{\Delta RR}$ and $CheV^{57}$ seem to be in disagreement with the conclusions drawn (Wu et al. 2011).

The conflicting conclusions drawn from the assays described in the previous paragraph may be easier to understand if CheV^{57} showed a different phenotype to the CheV$^{\Delta RR}$ strain. If the RR domain of CheV was obscuring an active site of the CheW domain so that its removal led to a permanently 'active' state then perhaps it may share that phenotype with the wild type phosphorylated CheV, however the non-phosphorylatable CheV^{57} mutant also shows the same phenotype (Wu et al. 2011).

The inference commonly drawn is that CheV must in some way be controlling the receptor raft morphology. Localisation studies of *B. subtilis* MCPs in a Δ*cheV* background found that there was a reduction in the number of cells with polar clusters but that those polar clusters were more stable and less likely to diffuse or move laterally when attractant was added (Wu et al. 2011). CheV appears to be implicated in the localisation of receptor clusters but the mechanism of this action is not understood.

C. jejuni

There is very limited evidence available so far for the role of CheV in *C. jejuni*. One suggested role for CheV may be the regulation of TLP methylation, as *C. jejuni* CheB lacks the response regulator domain with which *E. coli* CheB is regulated (Parkhill et al. 2000). There is some evidence to support this hypothesis as individual Δ*cheW* and Δ*cheV* strains of *B. subtilis*, although having reduced levels of chemotaxis, had near normal levels of MCP methylation. A double *cheW*/*cheV* mutant had extremely low levels of methylation as well as being non-chemotactic (Rosario et al. 1994). However, if CheV was directly involved in regulating methylation of MCP receptors in *B. subtilis,* I could

reasonably expect to see a change in methylation level for the individual Δ*cheV* mutant, as even if its function was redundant to that of CheW, CheW lacks the regulatory domain possessed by CheV so there is no obvious method by which it could be activated and deactivated as CheV could. For reasons stated, the low levels of methylation observed for the double CheW/CheV mutant seem more likely due to a disruption of the chemoreceptor complex rather than a direct effect of the *cheW* and *cheV* deletions. Although *B. subtilis* contains a CheV protein similar to that of *C. jejuni*, it also contains a CheB with an intact response regulator domain, as the CheB of the *E. coli* model does, so it is difficult to draw obvious conclusions for the *C. jejuni* system from the previous evidence.

Although the theory of CheB regulation through CheV is compelling there is evidence in *C. jejuni* of a role for CheV more similar to that of CheW. Affinity tag pull down assays show interaction between *C. jejuni* CheV and TLP_1, and between TLP_1 and CheW, but show that TLP_1 and has greater affinity for CheV, although the interaction was found to be specific to the CheW domain of CheV (Hartley-Tassell et al. 2010). The B2H assays of *C. jejuni* suggest an interaction between full length CheA and CheV but not between the histidine kinase domain and CheV, although this may be due to the transient nature of a kinase interaction between these two domains or perhaps the interaction is dependent upon CheV phosphorylation (Bridle 2007). From these studies *C. jejuni* CheV seems to be in some way entwined with the function of TLP/CheA/CheW receptor clusters and that some part of this function is dependent upon its phosphorylation.

1.6.4. CheB and CheR

In the model *E. coli* system, the methylesterase CheB and the methyltransferase, CheR modulate the methylation level of the cytosolic domains of MCP receptors to alter their sensitivity to stimuli (Fig. 1.2). CheR is constitutively active in adding methyl groups to the cytosolic domains of MCPs, whereas CheB requires phosphorylation of its response regulator domain by CheA to become active and remove methyl groups from MCPs (Porter et al. 2011).

In this *E. coli* model system the cell senses the lack of environmental ligand rather than its presence. In increasing ligand concentration the chemotaxis signal transduction system is inactive and the MCPs do not activate CheA autophosphorylation (Fig.1.3), CheY does not become phosphorylated by CheA and so does not dissociate from CheA to interact with the flagellar motor switch. In the absence of a signal from the chemotaxis system the flagellum defaults to counter clockwise rotation and the cell continues straight swimming. As phospho CheA is not present to act as a kinase to CheB, CheB remains inactive, this allows for the accumulation of methyl groups on the MCP which are constitutively added by CheR (Porter et al. 2011) (Fig.1.5).

The sensitivity of MCP receptors for their ligand is decreased as their level of methylation increases, in effect this constantly increases the concentration of ligand required to keep the signal transduction system inactive and so maintain counter clockwise flagella rotation. Eventually the receptor becomes desensitised to a point where the MCP will activate the signal transduction system regardless of ligand concentration, triggering CheA autophosphorylation and so

phosphorylation and activation of CheY resulting in cell tumbling and phosphorylation and activation of CheB resulting in removal of methyl groups from MCPs (Fig.1.6) This moving threshold of activation created by the modulation of the MCP methylation state, works almost as a memory, allowing the cell to sense minute changes in ligand concentration rather than its absolute concentration (Stock & Levit 2000).

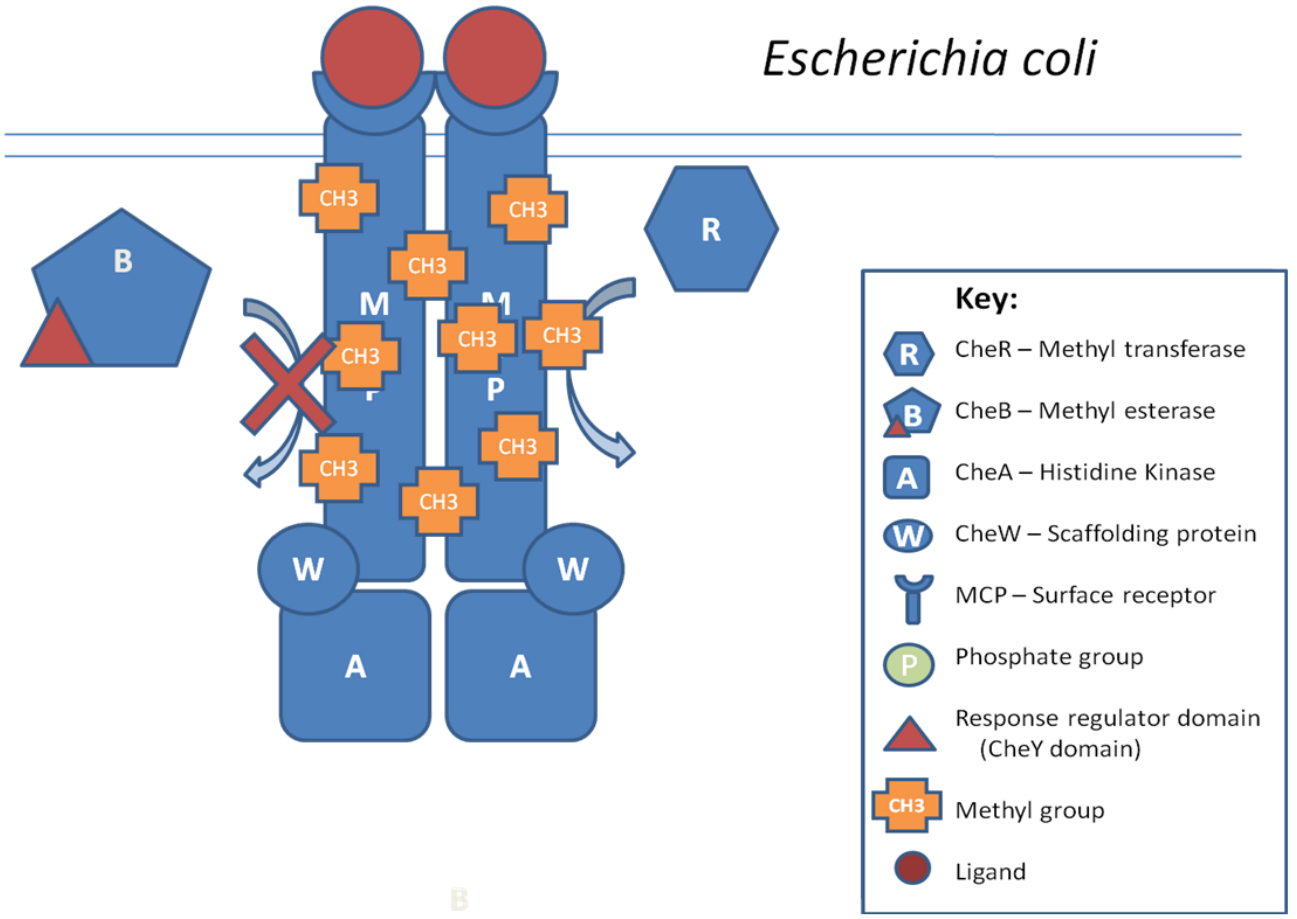

Figure 1.5. MCP desensitisation in the *E. coli* chemotaxis signal transduction model. In the *E. coli* system, when the MCP periplasmic sensing domain has attractant bound, it decreases the probability of CheA autophosphorylation and biases the cell toward runs rather than tumbles. CheA is unable to phosphorylate CheB and so CheB remains inactive, resulting in the accumulation of methyl groups upon MCP as the methyltransferase CheR is constitutively active. Increased methylation of MCP decreases the receptors sensitivity for its attractant ligands, continuously increasing the amount of ligand required to prevent its activation of CheA autophosphorylation.

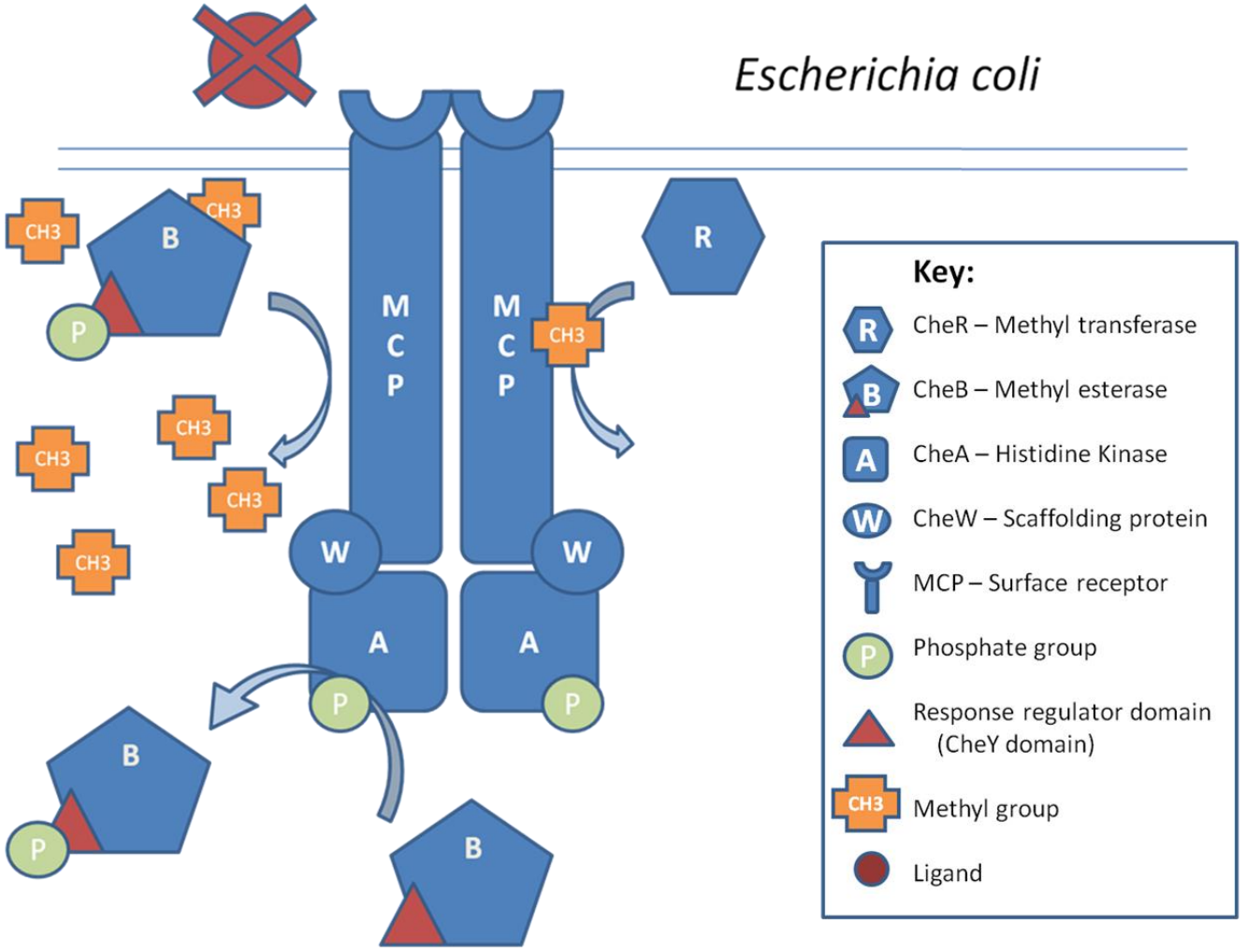

Figure 1.6. MCP sensitisation in the *E. coli* chemotaxis signal transduction model. Whether due to the lack of an attractant, the presence of a repellent, or the methylation dependent desensitisation of MCP to it's ligand, the MCP cytoplasmic domain signals CheA to autophosphorylate. CheY is phosphorylated by CheA and increases the probability of cell tumbling. CheB becomes phosphorylated by CheA, activating the methylesterase which rapidly removes methyl groups from MCP, increasing sensitivity of the MCP to it's attractant ligands and increasing the probability of CheA deactivation.

As *cheB* and *cheR* have homologues in *C. jejuni* it is likely that the same methylation adaptation system exists, currently the best models of this kind of adaptation exist in *B. subtilis* and *E. coli*. Methylation of *B. subtilis* MCP receptors is thought to stabilise the MCP/CheA complex by masking the negatively charged glutamate residues, increasing the efficiency of MCP interaction with CheA and increasing the probability of CheA autophosphorylation (Rao et al. 2008).

In the *E. coli* adaptation model, binding of phosphate to the RR domain of CheB changes the protein's conformation and exposes it's esterase domain, so that it can become active and interact with the methyl sites of MCP receptors. The homologues of CheB and CheR are present in *C. jejuni* but the CheB of *C. jejuni* does not possess a response regulator domain (Parkhill et al. 2000). If CheB and CheR proteins are constitutively active, and their action unaided or uninhibited by other factors, then there would be no net gain to the cell. This suggests that another method is being used to regulate the activity of either or both CheB and CheR.

Perhaps CheV may play a role in *C. jejuni* CheB regulation, where the RR domain of *C. jejuni* CheV may interact with CheB or CheR to form a feedback loop through which their action upon the methylation state of MCP could be modulated. This hypothesis is strengthened by B2H evidence of an interaction between CheV and CheB (Bridle 2007), however study of a *B. subtilis* strain with a truncated CheV found its MCPs to have comparable levels of methylation to that of wild type cells (Rosario et al. 1994). As the *B. subtilis* CheB protein also

possesses a response regulator domain, the relevance of direct comparison of methylation/demethylation processes, or the role of CheV within *C. jejuni* may be questionable.

Methanol concentrations are used as an indicator of CheB methylesterase activity *in situ*. In *E. coli* cells an increase in methanol concentration is found when ligand is removed, consistent with the model in which a decrease in ligand triggers CheA autophosphorylation, and so CheB activation and esterase activity against MCPs. In contrast studies in *B. subtilis* found methanol to be released both on addition and removal of attractant (Kirby et al. 1997).

Although the *B. subtilis* CheB possess an RR domain, unlike *C. jejuni*, and is activated by CheA, there is evidence of another type of regulation upon its activity. Rao *et al*. (2011) hypothesised that perhaps movement in the internal structure of MCP receptors, caused by ligand binding was exposing or guarding sites of methylation, and that the modulation of the kinase action of CheA in *B. subtilis* may be dictated not by overall methylation levels but rather by the methylation state of particular residues. This hypothesis was later supported by studies using amidation as a form of simulated methylation. Amidation at 1 site was found to increase receptor sensitivity, whereas amidation at two alternate sites reduced the receptor's sensitivity to its ligand (Glekas et al. 2011).

This selective methylation site model is complicated by observations that de-methylation of receptor clusters occurs within a minute whereas re-methylation of receptors may take up to 20 minutes (Kirby et al. 1999). It would be difficult to equate these rates with the rapid rates of adaption presumably required by a

chemotaxis system, although if viable this may explain the lack of a response regulator domain on *C. jejuni* CheB.

Comparison between the *H. pylori* and *C. jejuni* methylation models is problematic as *H. pylori* lacks identified CheB or CheR homologues (Jiménez-Pearson et al. 2005), however many of the glutamate residues targeted for the addition of methyl groups, are conserved in *H. pylori* MCP receptors, suggesting that perhaps a Che methylesterase and transferase are present but as yet unidentified (Pittman et al. 2001). Interestingly a Δ*cheV*$_3$ *H. pylori* mutant has a hyper switching phenotype, often changing direction, a similar phenotype to that of an *E. coli* Δ*cheB* mutant (Lowenthal et al. 2009), perhaps this could perhaps indicate a role for CheV in *C. jejuni* CheB regulation and/or modulation of an activation threshold.

1.6.5. Cj0700 (CheZ)

A direct homologue of *E. coli cheZ* has not been identified in C. *jejuni*, instead a candidate phosphatase was found by an indirect route (Terry et al. 2006). The *H. pylori* phosphatase HP0170 was identified by a chance observation in a Δ*cheW* mutant background, where a mutation of HP0170 returned chemotactic movement to the previously non-chemotactic Δ*cheW* mutant. A two dimensional SDS-PAGE gel resolved the protein HP0170, which showed decreased expression in Δ*cheW* mutants with the recovered chemotactic phenotype (Terry et al. 2006).

Once expressed and purified, a comparison of the resolved secondary structure of HP0170 found it to have structural homology to the phosphatase CheZ of *E.*

coli (Lowenthal et al. 2009). Radiolabelled phosphate assays confirmed HP0170 had phosphatase activity against *H. pylori* Che response regulators (Terry et al. 2006). Sequence comparison of HP0170 with the *C. jejuni* NCTC11168 genome identified *cj0700* as a putative orthologue to *hp0170*.

With a probable *C. jejuni* phosphatase identified, work began to confirm its position in the Che transduction system, however due to the limitations in techniques used at the time, a *C. jejuni* Δ*cj0700* mutant could not be successfully created, but a diploid *cj0700* strain did display attenuated chemotaxis. A B2H study by the same group found interactions between Cj0700 and CheY, CheV and CheA RR domain, suggesting an interaction with Che RR domains and implicating *cj0700* as a functioning *C. jejuni cheZ* orthologue (Bridle 2007). More recent studies have since successfully created a Δ*cj0700* deletion strain, which has been shown to be attenuated for chemotaxis, and recent radiolabelled phosphate assays observed phosphatase activity of Cj0700 against CheY and the CheA RR domain (Jama 2013).

The successful identification of a Che phosphatase in *C. jejuni* calls into question the phosphate sink hypotheses previously put forward to explain the additional response regulators present in the *C. jejuni* transduction system. However, the existence of an identified phosphatase and the possibility of phosphate sink are not mutually exclusive. In addition alternate unidentified phosphatases may act upon the Che response regulators as comparison of *hp0170* against sequenced bacterial genomes suggests CheZ homologues may be far more common than initially thought (Lertsethtakarn & Ottemann 2010).

E. coli CheZ localises to receptor complexes, this localisation is dependent upon a truncated CheA protein referred to as $CheA_{short}$. $CheA_{short}$ binding was also found to increase phosphatase activity of CheZ by 2.3 fold. The $CheA_{short}$ molecule is translated from a shortened transcript that uses an alternate start site at M98 (Cantwell et al. 2003). The alternative site is present in *C. jejuni*, however it is difficult to judge the relevance of $CheA_{short}$ to *C. jejuni* as the relationship between the Cj0700/CheZ proteins is based upon secondary structure rather than nucleotide or amino acid sequence (Terry et al. 2006).

1.6.6. Transducer Like proteins (TLPs)

Receptor Complexes and Their Function

Most of the recent work with chemotaxis receptors has focused upon the MCPs of *B. subtilis* and *E. coli*, therefore these systems will form the basis of the following discussion.

MCPs are periplasmic sensors that bind environmental ligands, causing a shift in their transmembrane helices. The conformational signal is communicated via a HAMP domain to a highly conserved domain (HCD) which interacts with CheA and CheW to transduce the environmental signal into the cell (Elliott & Dirita 2008). MCP receptors form into functional units in the periplasmic membrane, forming dimers which cluster into trimers of dimers. Trimers of MCP dimers are the optimum MCP cluster size for activation of CheA, resulting in up to 100 fold activation of CheA. Larger sizes of clusters have been tested but do not result in an increased level of activation (Li et al. 2011).

C. jejuni shares this trimer of dimers receptor arrangement, as under electron microscopy hexagonal TLP trimer formations were revealed (Briegel et al. 2009). The hexagonal formations consist of 6 trimers, which can be shared with neighbouring hexagons so that massive clusters or 'rafts' can form, consisting of thousands of receptor trimers (Briegel et al. 2009).

The signalling clusters responsible for transduction and amplification of signals from receptors, appear to be present in the *C. jejuni* system as well. Within the cytosol, CheA, CheW and CheV molecules associate with receptor cytosolic domains in order to receive the signal transduced from the receptors. Dimerised CheA molecules each associate with a CheW, so that three receptor dimers with two CheA and two CheW molecules will form an optimum signalling complex. The cytoplasmic domain of the receptors sits between CheW and its opposing CheA, with CheA running antiparallel to the receptor (Bhatnagar et al. 2010; Maddock & Shapiro 1993).

MCP/TLP Localisation

As CheV is implicated in receptor localisation, it is important to look at receptor raft localisation across species. The mechanisms driving MCP localisation are poorly understood.

Unlike *C. jejuni*, *E. coli* are peritrichous flagellated cells, however the MCP receptors of *E. coli* are not fixed around flagella but are situated at the poles of the cell. 80% of MCPs observed by electron microscopy are found associated with the poles (Maddock & Shapiro 1993). *E. coli* Δ*cheW* mutant strains show 25% of wild type MCP polar bias and a Δ*cheA* strain shows no reduction,

suggesting CheW, but not CheA, is involved in MCP localisation (Maddock & Shapiro 1993). The MCP receptor rafts of *B. subtilis* can be found in polar locations on the cell, but this localisation has been found to vary with attractant concentration. Upon addition of an attractant the receptor rafts became predominantly laterally located, once cells have adapted to the attractant concentration, after 1 minute, polar rafts reform (Wu et al. 2011). This dynamic MCP behaviour appears to be strongly linked to the phosphorylation state of CheV, as discussed previously, and as *C. jejuni* shares a CheV homologue it may be that this behaviour is shared by *C. jejuni* also; however these tests have not yet been carried out.

Polar rafts are observed in *C. jejuni* under electron microscopy (Briegel et al. 2009), however these assays were carried out under constant conditions and have not investigated the affect of varying attractant concentration, so it is unknown if the receptor rafts of *C. jejuni* are dynamic structures, as observed for *B. subtilis*. The movement of receptor rafts is an important phenomenon as it appears to be used as a form of adaptation, lateral clusters having a reduced rate of CheA kinase activity (Wu et al. 2011).

As well as relocation of receptor rafts there is evidence of direct modulation of their density by repellents and attractants. In *E. coli* repellents have been found to stabilise receptor clusters whereas attractants destabilise them (Borrok, Kolonko 2008), this provides an intuitive answer as to how CheA autophosphorylation rates could be manipulated in the presence/absence of a repellent or attractant. In the presence of an attractant *E. coli* cells default to straight swimming, when an attractant is not present or a repellent is, CheA

autophosphorylation is triggered and so CheY phosphorylation results in cell tumbling (Porter et al. 2011). Therefore a link between receptor stability and cell response appears intuitively correct. However, the same results are observed in the *B. subtilis* system in which attractant binding causes increased CheA autophosphorylatory activity, so the mechanism by which this system modulates CheA activity is not as intuitive as it at first appears (Borrok, Kolonko 2008).

C. jejuni TLP receptor specificity

Identification of chemoattractants and repellents for *C. jejuni* cells has been problematic so far. The ligand specificity of MCP or TLP receptors cannot be determined by *in silico* analysis as the predicted ligand binding domains lack conserved features, so experimental methods are required to pair attractants and repellents with individual TLP receptors.

Individual *C. jejuni* TLPs may react to multiple attractant and repellent ligands, the *E. coli* MCP Tar and Tsr receptors directly interact with some amino acids but can also interact with a range of periplasmic adaptor proteins which act as adaptors to broaden the range of ligands Tar can sense. These include carbohydrates, pH change (Manson 1992) and the autoinducing quorum sensing molecule AI-2 of *E. coli* (Hegde et al. 2011). The use of the Tar and Tsr receptors as transduction machines to these adaptor proteins, known as minor MCPs, offers an advantage to the cell as Tar and Tsr also form the vast majority of the receptors found in the membrane (Manson 1992). This economy saves the cell from having to produce additional receptors and signal transduction machinery for every ligand.

Typically chemo-attractants or repellents may be tested against cells using hard agar plug assays (HAP). In HAP assays agar plugs or filter paper in which a suspect attractant or repellent chemical has been dissolved, is placed on top of motility agar, onto which a bacterial lawn has been inoculated. Attractants should cause an increase in the density of cells around an attractant plug as they are drawn towards it, whereas repellents should cause a clearance zone of low cell density around the plug.

In HAP assays wild type *C. jejuni* have been found to be attracted to aspartate, serine, cysteine, fumarate, glutamate, pyruvate, fumarate, malate, succinate, serine and possibly towards α-ketoglutarate (Hartley-Tassell et al. 2010; Sandhu 2011; Vegge et al. 2009). Cholic acid, deoxycholic acid, taurocholic acid and glycocholic acid, constituents of bile, have been identified as repellents for *C. jejuni* strain NCTC 11168 (Vegge et al. 2009). Although bovine gall bladder bile, ox gall and chick gall bladder bile are attractants to *C. jejuni*, many of the individual bile components act as repellents (Hugdahl et al. 1988).

The results of HAP assays against *C. jejuni* have not been conclusive. There are outstanding issues with perceived accuracy of HAP assays as presumably non-chemotactic *C. jejuni* Δ*cheY* strains used in a HAP assays against α-ketoglutarate, glutatmate, fumarate, serine, and pyruvate, show apparently positive results (Kanungpean et al. 2011a), leading to some doubt over the validity of the attractants and repellents previously identified.

To pair TLP receptors with ligands *Δtlp* strains are created and the chemotactic phenotype of these strains assayed in relation to that of wild type cells, using

HAP assays or by observing the cells swarming phenotype on motility plates. However, Δ*tlp* mutant strains tested using these methods have shown unexpected results in chemotaxis assays. In one set of assays *C. jejuni* Δ*tlp*$_1$, Δ*tlp*$_2$ and Δ*tlp*$_4$ deletion mutant strains show altered chemotactic phenotypes that clearly implicated the receptors involvement in taxis on motility plates (Sandhu 2011). However, the phenotypes were not as expected, Δ*tlp1* strains showed greater swarming than wild type cells, Δ*tlp2* mutants showed reduced swarming diameter and formed irregular patterns at the leading edge of the swarm rather than a regular circumference (Sandhu 2011). Δ*tlp4* strains showed a reduced swarming zone with reduced density at the leading edge suggesting some reduction in the ability of cells to detect their optimum environment (Sandhu 2011).

Some studies observe no discernible difference in chemotactic responses in HAP assays of wild type and Δ*tlp* mutant strains (Vegge et al. 2009), however more recent investigations testing Δ*tlp*$_1$ mutant against aspartate found increased linear displacement and increases in swarming zones on Brucella agar and a loss of motility towards aspartate in HAP assays (Hartley-Tassell et al. 2010). The interaction of aspartic acid with TLP$_1$ has been verified using amino acid arrays to demonstrate binding of the predicted periplasmic region to aspartate, and is further supported by STD NMR spectra data (Hartley-Tassell et al. 2010). A Δ*tlp*$_7$ mutant has been shown to lose its attraction to formic acid (Tareen et al. 2010).

Sandhu (2011) suggests that a more complex interaction between the receptors and motility may be at play and that the method by which chemotaxis is assayed may be adversely affecting the results if the dominant form of taxis on motility

plates is in fact energytaxis (Sandhu 2011). As many of the identified *C. jejuni* attractants identified are electron donors or acceptors it has been speculated that external ligands sensed by chemotaxis receptors may not be the driver of directed motility.

Energytaxis in *C. jejuni*

There is speculation over the importance of the Che transduction system to *C. jejuni* taxis. The difficulties experienced in linking individual TLPs to attractants, particularly in motility assays, has led to speculation that the chemotaxis observed for *C. jejuni*, may in fact be due to internal metabolic signals rather than external stimuli sensed by the transmembrane receptors, this type of motility is referred to as energytaxis.

In one study of *C. jejuni* the authors attempted to separate possible energytaxis events from chemotaxis assays. Inhibitors of Cytochrome c oxidase were introduced to block oxygen linked respiration, and the affect of attractants and repellents in HAP assays observed. 2-n-Heptyl-4-hydroxyquinoline N-oxide (HQNO) was found to inhibit the action of recognised attractants with the exception of formate, although in the presence of HQNO wild type cells had attenuated motility. The authors were concerned the observed effects may be due to a reduction in motility caused by interference with normal cell metabolism, so ran control assays in the presence of known repellents, these assays showed no reduction in the repellent effect in the presence of HQNO (Vegge et al. 2009).

For wild type *C. jejuni* cells in the presence of HQNO and sodium azide, a 23% and ^{32}% reduction in motility on motility agar was observed, the authors

concluded from this that although there is an observable reduction in motility caused by the chemicals, this loss was not great enough to account for the observed loss in chemotactic movement (Vegge et al. 2009). The authors argued that their results indicate that previously observed motility towards attractants was in fact due to energytaxis, whilst repellent behaviour is due to chemotaxis since this was unaffected by HQNO or sodium azide (Vegge et al. 2009). However, the confirmed identification of a TLP_1 interaction with aspartate seems to refute this theory, at least in the case of this receptor (Hartley-Tassell et al. 2010; Sandhu 2011).

CetA/B (Aer Homologues)

CetA and CetB, the identified Aer homologue of *C. jejuni* may form one route by which this energytaxis informs the transduction system. CetA and CetB may co-operate to form an internal, membrane associated, cytosolic TLP which may inform the chemotaxis signal transduction system of the metabolic state of the cell.

C. jejuni cetA and *cetB* genes were identified in a random Tn mutagenesis screen, their connection to directed taxis was confirmed by an attenuated motility phenotype in Δ*cetA* and Δ*cetB* strains. Both deletion mutants displayed a reduced swarming phenotype on standard motility agar but also in supplemented media. The largest differences between swarming diameters of wild type and Δ*cet* strains were observed on plates supplemented with sodium pyruvate or fumarate, which increase cell metabolism rate, suggesting CetA and CetB are involved in a form of energytactic swarming (Hendrixson et al. 2001).

The Cet proteins are homologues of the *E. coli* Aer proteins. Aer proteins have 3 domains: PAS, HAMP and HCD, the CetA/B of *C. jejuni* posses these domains but split between the 2 co-transcribed proteins (Elliott & Dirita 2008; Marchant et al. 2002). CetB consists of a single PAS sensing domain, whereas CetA contains the HAMP and HCD domains predicted to interact with histidine kinases. CetA is a membrane protein consisting of 2 transmembrane helixes and a membrane anchor, and is found in the inner membrane as a homodimer similar to the *E. coli* receptors (Elliott & Dirita 2008).

Although translated separately there is compelling evidence that CetA and CetB co-operate to function as an internal membrane associated TLP. *E. coli* PAS domains interact with molecules that change in response to internal redox states, such as flavin adenine dinucleotide (FAD), to monitor cell metabolism. The authors theorise that once FAD is bound to CetB it interacts with CetA, which is present in a signalling complex with CheA and CheW, to stimulate CheA autophosphorylation and so response regulator phosphorylation (Hendrixson et al. 2001).

In *C. jejuni* a small proportion of CetA appears in soluble fractions of lysed cells, but the majority of CetA and CetB appears associated with membrane fractions. Although CetB associates with the membrane it does not have a membrane spanning region and is entirely cytoplasmic, suggesting it is a peripheral membrane protein. Interactions between CetA and CetB *in situ* have been displayed in *in vivo* cross linking experiments which identified higher molecular weight CetA associated proteins in wild type cells, which did not occur in Δ*cetB* deletion strains (Elliott & Dirita 2008).

The cell metabolism may interact with the chemotaxis signal transduction system directly viayew small molecule phosphate donors such as acetyl phosphate. These can phosphorylate response regulators independently of a histidine kinase, as has been shown for CheY (discussed previously section 1.5.2). Intra-cellular acetyl phosphate levels correlate with the nutritional status of the cell (Wolfe et al. 2003), acetyl phosphate has been shown to act as a global regulator for a number of systems *in situ*, including biofilm synthesis in *E. coli* (Wolfe et al. 2003; Klein et al. 2007). Direct phosphorylation of response regulators cannot be assumed and needs to be considered for each protein as some are tuned to prevent interaction with acetyl phosphate (Boll & Hendrixson 2011).

1.6.7. A New Che Protein for *C. jejuni*?

The chemotaxis system is well characterised in a number of bacteria but additional, as yet unidentified Che proteins may be present. The ChePep protein recently identified in *H. pylori* is an example of one.

H. pylori Δ*chePep* strains are slightly attenuated for colonisation in mice but in co-infection competition assays with wild type cells no Δ*chePep* cells were recovered. ChePep mutants are prone to frequent switching of flagella rotation, and reversals of cell direction not commonly observed for *H. pylori* (Howitt & Lee 2011). A *C. jejuni* homologue of this *chePep* has been identified, which carries only a 30% sequence identity to that of *H. pylori*, however the *H. pylori* Δ*chePep* strain was successfully complemented by introduction of *C. jejuni chePep*, with the cells returning to wild type swimming phenotype (Howitt & Lee 2011). Despite the sequence divergence between *C. jejuni* and *H. pylori* ChePep it appears its

structure is highly conserved and that the phenotypes observed for *H. pylori* Δ*chePep* strains would be reproduced if the deletion were replicated in a *C. jejuni* background.

The existence of *C. jejuni* ChePep may have implications for the *C. jejuni* Che system if it is a genuine homologue. *H. pylori* Δ*chePep* cells, tested against a pH gradient, show strong repellent taxis away from the acid source, after 10 seconds only 31% of wild type cells remained within a 60µm radius of the origin of the pH gradient, whereas 70% of Δ*chePep* cells remained within the radius. This would seem clear evidence of an involvement of ChePep in the Che transduction system, however it seems unclear whether its involvement with pH repulsion was a direct effect or perhaps due to a broader disruption of chemotaxis caused by the ChePep deletion as dramatic changes in cell morphology were observed for the Δ*chePep* mutants (Howitt & Lee 2011). It is important to note that ChePep contains a putative phosphate accepting domain but there is not as yet evidence of its phosphorylation (Howitt & Lee 2011), or its interaction with CheA.

1.6.8. The Flagellum

Most *C. jejuni* are motile when grown on Müeller-Hinton agar at 37 °C in microaerobic conditions. 90% of the *C. jejuni* population will have 1 or 2 flagella, of these 62% are amphitrichous, having a flagellum at each cell pole, 29% are monotrichous, having a single polar flagellum (Balaban & Hendrixson 2011).

The flagella of *C. jejuni* appear to be involved in more than just motility of the cell, as flagella also play a role in biofilm formation. *C. jejuni* lack pili or fimbrial systems for cell adherence, much of its adherence and invasion appears to be

flagella mediated (Gilbreath et al. 2011). Observed by scanning electron microscopy, flagella appear to layer over cells helping to form a 'net' over and between cells. Δ*flaA* and Δ*motA* strains do not form biofilms, implying that the flagellum is important to their formation, however the phenotype of the Δ*motA* strain suggests there is also a role for motility in biofilm formation as well (Moe et al. 2010). Bacterial biofilms are strongly associated with persistence in the environment (Golden & Acheson 2002).

C. jejuni flagella as well as being necessary for motility, are also used by the cell as a type III secretion system. The secretion of the Cia group of proteins is dependent upon flagella, of these CiaC is central to host cell invasion as Δ*ciaC* mutants are 50 fold less invasive in cell culture than wild type cells. The flagella secreted FlaC protein binds to epithelial cells, and Δ*flaC* mutants are highly attenuated for invasion. FspA appears to be a flagella secreted adhesin which binds to epithelial cells and can induce apoptosis (Guerry 2007).

Regulation of the number of flagella, and the process of cell division appear to be intimately linked. *C. jejuni flhG,* part of the ParA superfamily, has been implicated in regulating the numbers and positioning of flagella. In a Δ*flhG* mutant background, 40% of the cells produced more than one flagellum at a pole, whereas in wild type cells this arrangement represented only 1% of the population. These changes may have been due to downstream transcriptional regulation events resulting from the *flhG* deletion, however only the hook and rod proteins, under σ54 regulation, were found to have increased expression. Expression levels for the other flagellar protein subunits remained consistent, suggesting the observed increase in flagella number was not due to changes in

fla gene regulation (Balaban & Hendrixson 2011). A *flhG* deletion did however have profound effects upon cell division, resulting in a large population of mini-cells, of around 1.2 µm in diameter. Upon complementation the number of mini-cells fell but was replaced with elongated cells greater than 2 µm in length (Balaban & Hendrixson 2011).

Perhaps the effects observed for a *flhG* deletion could be due to wider effects on cell structure and division rather than having a direct role in the location and number of flagella. Poor complementation of the Δ*flhG* mutant could suggest that the phenotypes had been caused just by polar effects, or perhaps that the phenotypes were genuine and due to the deletion of *flhG*, but that just the complementation scheme was unsuccessful. The *flhG* gene was complemented in trans from a plasmid, and under the control of a different promoter. The level of FlhG expression may be critical *in situ*, it is unlikely the complementation method used in this study matched native expression levels. Unfortunately the method of complementation has left ambiguity over the meaning of the results.

1.7. Project Aims

The *C. jejuni* system is unique and little studied amongst the model Che transduction systems. No easy comparison to the *C. jejuni* Che signal transduction system exists, and although some evidence has been provided for a role for CheA and CheV response regulators, their mechanism and function are not yet clear in any of the model systems.

The Che system of *H. pylori* has a *cheA* response regulator, three *cheV* homologues but no observed *cheB* or *cheR* homologues, *B. subtilis* has one *cheV*

homologue, it has *cheB* and *cheR* homologues and a response regulator domain on *cheB*, whereas *E. coli* has no *cheA* response regulator or *cheV* but also possess a *cheB* with a response regulator domain. The complement of *C. jejuni* Che proteins and their domain arrangement, is not matched by any of the usual model systems, it seems the mechanism for adaption of the *C. jejuni* Che system is unique.

The interactions observed between CheA and CheY in both the B2H and Y2H assays support the hypothesis of a *C. jejuni* system working in a similar manner to that of *E. coli*, and the complementation of a *H. pylori* Δ*cheY* strain with the *C. jejuni* CheY homologue suggests the CheA-CheY backbone is conserved (Jiménez-Pearson et al. 2005; Bridle 2007; Parrish et al. 2007).The *C. jejuni* Che homologues have been identified and implicated in chemotaxis through deletion mutation studies (Bridle 2007; Kanungpean et al. 2011a; Reuter & van Vliet 2013) as have the receptors (Hartley-Tassell et al. 2010; Sandhu 2011; Hendrixson & DiRita 2004; Balaban & Hendrixson 2011), but the interactions between these constituent parts requires further investigation.

The aims of this study are to first create a range of expression clones, in which each of the *C. jejuni* Che proteins may be overexpressed and purified using a fused affinity tag. Using the purified proteins, an *in vitro* assay will be developed in which radiolabelled ATP will be used to visualise protein binding of Pi, so that the transfer of phosphate from CheA to the putative response regulators of CheV, CheA and CheY can be investigated. This assay will be used to confirm if the predicted response regulator domains are genuine and functional, and also if they are paired to the putative histidine kinase CheA. To investigate non-kinase

interactions between the Che proteins, an *in vitro* pull-down assay will be developed, which will utilise the cloned proteins fused affinity tag. These affinity tests will be used to probe for interactions between the Che proteins, which may suggest functions in the system for each of the response regulator domains, and explain how a CheB protein without a phosphorylatable domain may be regulated.

Hypothesis

I hypothesize that the *C. jejuni* chemotaxis system shares the common CheA/CheY two component backbone. CheA is a histidine kinase that will autophosphorylate in the presence of ATP. The predicted *C. jejuni* CheY, CheV and CheA RR homologues are genuine response regulators, which are phosphorylated by CheA. Phosphorylation of the response regulators affects the function of the proteins to which they are attached.

Chapter 2: General Materials and Methods

2.1. Media Used

Luria-Bertani Medium

10 g tryptone, 5 g yeast extract and 5 g NaCl (Oxoid, UK) were added to 400 mL ddH_2O and adjusted to 1 L was added to 400 ml, adjusted to pH7.2 and autoclaved for 20 minutes at 121-124 °C. The medium was cooled to 55 °C before being supplemented with the required antibiotics. Luria agar was made as described above with the addition of 6.4 g/400 ml Bioagar (Biogene, UK) prior to autoclaving. Luria medium was stored at 4 °C for a maximum of 4 weeks.

Müeller-Hinton Medium

Müeller-Hinton broth was made by addition of 8.4 g of Müeller Hinton broth powder (Oxoid, UK) to ddH_2O to final volume of 400 ml, covered and autoclaved for 20 minutes at 121-124 °C. The broth was allowed to cool to 55 °C before being supplemented with the required antibiotics. To make Müeller-Hinton agar 15.2 g of Müeller-Hinton agar powder (Oxoid, UK) was added to ddH_2O to a final volume of 400 ml. The agar was autoclaved for 20 minutes at 121-124 °C, allowed to cool to 55 °C before being supplemented with the required antibiotics and the plates poured. Müeller-Hinton medium was stored at 4 °C for a maximum of 4 weeks.

2.2. Growth and Storage of Strains

Escherichia coli

E. coli strains were grown either in Luria-Bertani broth or on Luria-Bertani agar, at 37 °C overnight (12-14 hours). *E. coli* grown in broth were agitated on a Gio Gyrotory® shaker at 200 rpm (New Brunswick Scientific, UK). Luria agar was supplemented with antibiotics, melted in a microwave then cooled to 55 °C before antibiotics were added and plates were poured. Luria media was supplemented to final concentrations of 20 µg/ml chloramphenicol (Sigma, UK) and/or 100 µg/ml ampicillin (Melford, UK) when antibiotic selection was required. For storage of *E. coli* strains, cells were cultured in 5ml of the Luria broth for 12-14 hours in conditions as outlined above. The culture was centrifuged at ^{32}20 *g* for 15 minutes to pellet the cells and the supernatant discarded. The pellet was resuspended in 1ml of 50% (v/v) Luria broth, 25% (v/v) glycerol, 25% (v/v) double distilled (ddH_2O), and then stored at -80 °C.

Campylobacter jejuni

C. jejuni strains were grown in Müeller-Hinton broth or on Müeller-Hinton agar (Oxoid, UK), supplemented with 10 µg/ml vancomycin (Melford, UK), 5 µg/ml trimethoprim (Sigma, UK) and 50 µg/ml kanamycin (Melford, UK), in a Whitely VA1000 (Don Whitley, UK) at 42 °C, in 85% nitrogen 10% carbon dioxide and 5% oxygen. Liquid cultures were grown with agitation on an Orbit™ 300 (Labnet International, USA) vortexer at 500 rpm overnight. Cultures grown on agar were incubated for 24-36 hours. For storage of *C. jejuni* strains, cells were cultured in

5ml Müeller-Hinton broth for 18 hours in conditions as outlined above. The culture was centrifuged to pellet the cells and the supernatant discarded. The pellet was resuspended in 1ml of 50% (v/v) Müeller-Hinton broth, 25% (v/v) glycerol and 25% (v/v) double distilled (ddH_2O), then stored at -80 °C.

The strains used in this study are described in Table 2.1, expression strains are referred to by the plasmid they contain, these are listed in Table 2.3.

Strain	Reference	Used for
Campylobacter jejuni NCTC 11168	National Collections of Type Cultures and Pathogenic Fungi, Colindale, London, UK	Obtaining genomic template for cloning
Escherichia coli DH5αE	(Hanahan, 1983)	Cloning processes
Escherichia coli Rosetta™	Novagen, UK	Expression from pGex 4-t-1 and pTRCHIS-B constructs

Table 2.1. Bacterial strains used within this study

2.3. DNA Manipulation

2.3.1. Chromosomal DNA Preparation

Chromosomal DNA was isolated and purified from *C. jejuni* NCTC 11168 according to a published method (Chen & Kuo 1993). *C. jejuni* was grown for 12-16 hours in 5 ml Müeller-Hinton broth supplemented with vancomycin,

trimethoprim and kanamycin. This suspension was used to inoculate Müeller-Hinton agar plates also supplemented with vancomycin, trimethoprim and kanamycin, and the plates were incubated for 24-48 hours. Using 2 ml of Müeller-Hinton broth, cells were washed from plates into 1.5 ml microcentrifuge tubes and pelleted in a Minispin (Eppendorf, UK) centrifuge at 12,000 *g* for 3 minutes. The supernatant was discarded and the pellet resuspended in 600 µl of Buffer P1, 200 µl of 5 M NaCl was added, the sample was thoroughly mixed and then centrifuged again at 12,000 *g* for 5 minutes. The supernatant was transferred to a new tube while the pellet was discarded. 600 µl of chloroform/iso-amyl-alcohol (24:1) was added to the tube, and the sample mixed by inversion, approximately 100 times. The sample was centrifuged at 12,000 *g* for 1 minute to form 3 distinct layers, the top layer was retained in a new 1.5 ml microcentrifuge tube whilst the bottom two were discarded. This process was repeated seven or eight times until the third layer, the interface between the top and bottom layers, appeared to be clean and without debris. To harvest the DNA, 1 ml of 100% ethanol was added and mixed, by inversion, with the supernatant from the previous step. The DNA became visible as a white precipitate and was pelleted by centrifugation at 12,000 *g* for 5 minutes, the supernatant was discarded and 800 µl of 70% (v/v) ethanol added. The DNA was pelleted again by centrifugation at 12,000 *g* for 2 minutes. The supernatant was again discarded and any ethanol remaining with the pellet was evaporated in a vacuum chamber. The DNA pellet was then resuspended in 100 µl of ddH_2O and stored at -20 °C.

2.3.2. DNA Restriction Enzyme Digestion

All restriction enzymes used were standard enzymes supplied by New England Biolabs (UK) and used as per manufacturer's instructions with the reagents supplied.

2.3.3. DNA Ligation

Ligation of overhanging DNA ends was carried out using a 3:1 molar ratio of insert to vector, in ddH_2O with 1xT4 ligase buffer at final concentrations of 0.5 mM ATP and 0.04 U/µl ligase (New England Biolabs, UK) the reaction was incubated at 16 °C for 12-14 hours.

2.3.4. DNA Purification

Purification of DNA from excised bands from agarose gels were performed using a ZymoClean™ Gel DNA Recovery Kit (Cambridge Bioscience, UK). Purifications from PCR reactions and enzyme digests were performed using an E.Z.N.A. ® Cycle Pure Kit (VWR, UK). Extraction of plasmid DNA from whole cells was performed using an E.Z.N.A. ® Plasmid Mini Kit 1 (VWR, UK). All kits were used with the solutions supplied and used purification steps carried out as per the manufacturer's instructions.

2.3.5. Ethanol Precipitation of DNA

To desalt ligated DNA it was ethanol precipitated. 3 M sodium acetate was added to the sample to 1/10 of the sample volume, plus 1 µl of glycogen (20 mg/ml Roche, UK) and 3x sample volumes of 100% ethanol. The sample was left

at room temperature for 1 hour then centrifuged at 12,000 *g* for 30 minutes in a Minispin centrifuge (Eppendorf, UK). Once a pellet had formed the supernatant was aspirated and discarded. 1 ml of 70% (v/v) ethanol was gently added to the sample and the sample was centrifuged again for 1 minute; this step was repeated 2-4 times to remove salts. In the final step as much ethanol as possible was aspirated without disturbance to the pellet, the sample was then left to dehydrate in a vacuum. Once fully dehydrated, the DNA was resuspended in ddH_2O.

2.3.6. Separation using Agarose Gel Electrophoresis

1-1.5% (w/v) of SeaKem® LE agarose powder was dissolved in a 1x TAE buffer, and heated in a microwave until dissolved. The agarose was cooled to 55 °C and ethidium bromide added to a final concentration of 10 ug/ml (Fisher Scientific, UK). DNA was visualised on the gel using a Syngene Gene Genius Bioimaging System (Syngene, UK) transluminator. DNA concentration was estimated, post electrophoresis, by comparison of the sample band intensity under UV light to a standard loading of HyperLadder™ 1 Kb standard (Bioline, UK).

2.3.7. Sanger Sequencing Protocol

Sequencing reactions were carried out using a Big dye v3.1 Terminator Cycle Sequencing Kit (Applied Biosystems™, UK), with ~200 ng of low complexity plasmid template using the program shown in Table 2.2.

Temp		Time
96 °C		10sec
96 °C	x29 cycles	10sec
50 °C		10sec
60 °C		4min
60 °C		5min

Table 2.2. A typical Sanger sequencing temperature cycle.

Following the sequencing reaction samples were cleaned by the addition of 2 µl of 2.2% (w/v) sodium dodecyl sulphate (SDS) and heated to 98 °C for 5 minutes, the reaction was then passed through a Performa® Spin Column (VH Bio, Gateshead, UK) to remove salts and dNTPs. Samples were submitted to the Protein Nucleic Acid Chemistry Laboratory of the University of Leicester who analysed the sequencing reaction using an ABI 377 DNA Sequencer (Applied Biosystems™, UK).

2.3.8. Preparation of Electrocompetant *E. coli*

A 5ml culture of *E. coli* DH5αE or Rosetta™ cells was grown overnight as outlined above, the following morning 1ml of this suspension was used to inoculate 100 ml of new Luria broth. The Luria broth was incubated as discussed previously, but until an OD_{600} of 0.5-0.7 was reached when measured using a Ultrospec 10 (Fischer Scientific, UK) spectrophotometer. The culture was split

between two 50 ml Falcon tubes and the cells pelleted by centrifugation at [32]20 *g* for 15 minutes at 4 °C. The supernatant was discarded and the pellets were resuspended in 50 ml of ddH_2O chilled to 4 °C. The previous step was then repeated but the cells were then resuspended in 25 ml of chilled ddH_2O. This suspension was centrifuged as previously but the pellet was then resuspended in ice cold 10% (v/v) glycerol (in ddH_2O), before centrifugation was repeated. In the final step the cell pellet was resuspended in 1 ml of 10% (v/v) glycerol and aliquoted into 50 µl volumes and stored at -80 °C, suitable for later electroporation.

2.3.9. Electroporation of Plasmid DNA into *E. coli*

DNA was electroporated into previously prepared electrocompetant *E. coli* in pre-chilled 2 mm electroporation cuvettes (Geneflow, UK) using a BioRad Gene Pulser and BioRad Pulse Controller (Biorad, UK) at 2.5 Kv, 200 Ω and 25 µF. Post electroporation 1 ml of Luria broth was added to the cells, which were then incubated with agitation for 1 hour at 37 °C. The suspension was centrifuged for 1 minute at 12,000 *g* for the cells to form a pellet, approximately 0.9 ml of the supernatant was aspirated and discarded and the cells resuspended in the remaining volume before being spread onto Luria agar plates supplemented with the appropriate antibiotics for the genotype desired. The plates were incubated overnight at 37 °C.

Table 2.3. Plasmids used in this study.

Name	Notes	Reference
pGex-4T-1	N' terminal glutathione tag vector	GE Healthcare (Chalfont St. Giles, UK)
pTrcHisB	N' terminal HIS tag vector	Invitrogen (Paisley, UK)
pPA016	Expression construct. *cheV* cloned into the pTrcHisB multiple cloning site.	This study
pPA017	Expression construct. *cheA* cloned into the pTrcHisB multiple cloning site.	This study
pPA018	Expression construct. *cheW* cloned into the pTrcHisB multiple cloning site.	This study
pPA019	Expression construct. *cheB* cloned into the pTrcHisB multiple cloning site.	This study
pPA020	Expression construct. *cheR* cloned into the pTrcHisB multiple cloning site.	This study
pPA021	Expression construct. *cheY* cloned into the pTrcHisB multiple cloning site.	This study
pPA022	Expression construct. *tlp1* cytoplasmic domain cloned into the pTrcHisB multiple cloning site.	This study
pPA024	Expression construct. $cheA^{HK}$ (ΔRR domain, ΔCheW domain) cloned into the pTrcHisB multiple cloning site,	This study
pPA025	Expression construct. $cheA^{RR}$ domain (including CheW domain) cloned into the pTrcHisB multiple cloning site.	This study
pPA029	Expression construct. c*heY* D57A cloned into the pGex-4T-1 multiple cloning site.	This study
pPA035	Expression construct. c*heV* cloned into the pGex-4T-1 multiple cloning site.	This study
pPA036	Expression construct. *cheA* cloned into the pGex-4T-1 multiple cloning site.	This study
pPA037	Expression construct. *cheY* cloned into the pGex-4T-1 multiple cloning site.	(Bridle 2007)
pPA046	Expression construct. *hk domain* (Δ*rr domain*, Δ*cheW domain*) cloned into the pGex-4T-1 multiple cloning site.	This study
pPA038	Expression construct. *cheV* E59K,L89Y cloned into the pGex-4T-1 multiple cloning site.	This study
pRS09	Expression construct. *tlp1* (*cj1506c*) cytoplasmic domain cloned into the pGex-4T-1 multiple cloning site.	(Sandhu 2011)
pRS10	Expression construct. $tlp_{2\text{-}4}$: c*j0262*, c*j1564*, c*j0144* cytoplasmic domain cytoplasmic domain cloned into the pGex-4T-1 multiple cloning site.	(Sandhu 2011)

2.3.10. Whole cell DNA Preparation for Diagnostic PCR

20 µl of ddH_2O was added to a 0.2 µl (ABgene, UK) PCR tube and a picked colony was suspended in 20 µl. This was heated to 98 °C for 10 minutes and centrifuged for 10 minutes at 12,000 *g*. 2 µl of the DNA preparation was used as a template in PCR reactions.

2.3.11. Diagnostic PCR

To confirm the presence of a cloned gene in a plasmid, diagnostic PCR reactions were carried out using Kapa Taq DNA Polymerase (New England Biolabs® Inc, UK). The reactions were carried out in the supplied buffer A at 1x, with concentrations of 1 mM dNTPs, 1 mM $MgCl_2$ in addition and 0.05 U/µl polymerase. 0.2 µM of each primer was added if using purified plasmid template or 0.4 µM for a whole cell DNA preparation, as above. For a 50 µl reaction using low complexity template approximately 5 ng DNA was added, for greater complexity DNA around 50 ng of template was added. A G-Storm GS1 (Labtech International, UK) thermocycler was used; a typical program as shown in Table 2.4.

Temperature		**Cycle step**	**Time**
94 °C		Initial denaturation	2 min
94 °C	x30 cycles	Denaturation	30sec
50-70 °C		Primer annealing	30sec
72 °C		Extension	1min/kb
72 °C		Final extension	5min

Table 2.4. A typical diagnostic PCR temperature cycle.

Typically a temperature of 55 °C was used for primer annealing, but if the PCR reaction failed to give satisfactory results a gradient PCR was carried out in an Eppendorf Vapo Protect Mastercycler Pro (Eppendorf, UK) to test the annealing temperature of the primers using a temperature range between 50 °C-70 °C. These results were used to select the annealing temperature of subsequent PCRs using these primers. All primers used are displayed in Table 2.6.

2.3.12. High Fidelity PCR

Low error rate PCR reactions were carried out using Phusion®High-Fidelity Polymerase (New England Biolabs® Inc, UK). An Eppendorf Vapo Protect Mastercycler Pro thermocycler was used; a typical program is Table 2.5.

<table>
<tr><th colspan="2">Temperature</th><th>Cycle step</th><th>Time</th></tr>
<tr><td colspan="2">98 °C</td><td>Initial denaturation</td><td>30sec</td></tr>
<tr><td>98 °C</td><td rowspan="3">X25 cycles</td><td>Denaturation</td><td>10sec</td></tr>
<tr><td>50-70 °C</td><td>Primer annealing</td><td>20sec</td></tr>
<tr><td>72 °C</td><td>Extension</td><td>30sec/kb</td></tr>
<tr><td colspan="2">72 °C</td><td>Final extension</td><td>5min</td></tr>
</table>

Table 2.5. A typical high fidelity PCR temperature cycle.

PCR reactions were carried out in the supplied buffer at 1x, with final concentrations of 200 µM dNTPs, 0.5 µM of each primer, 0.02 U/µl polymerase. For a 50 µl reaction using low complexity template approximately 5 ng DNA was added, for greater complexity DNA around 50 ng of template was used.

As Phusion® High-Fidelity Polymerase has a stabilising effect upon primer-template binding, the annealing temperatures used in earlier successful PCRs using Kapa Taq DNA Polymerase were not necessarily valid for use with Phusion® polymerase. In these cases a gradient PCR was carried out to test the annealing temperature of the primers using a temperature range between 50 °C and 70 °C. These results were used to select the annealing temperature of subsequent PCR reactions using these primers. All primers used are shown in Table 2.6.

Table 2.6. Primers used in this study (Sigma Aldritch, UK).

Primers	**5' – 3' Primer sequence** With restriction site underscored.	**Notes**
Primers for cloning into pTrcHisB		
CheA_F _BglII	GGAAGATCTATGGAAGATATGCAAGAAATAC	Primers to the 5' and 3' of *cheA* cds.
CheA_R_KpnI	CGGGGTACCTCTTATCCTAGTTTCAAATTTTTTC	
CheY_F_BglII	GGAAGATCTGTGAAATTGTTAGTTGTTGATGACAGTTCTAC	Primers to the 5' and 3' of *cheY* cds.
CheY_R_KpnI	CGGGGTACCTTACTCAGCTGCACCTTCTCC	
CheB_F_BglII	GGAAGATCTGTGAAGCTCATACTCATAGG	Primers to the 5' and 3' of *cheB* cds.
CheB_R_KpnI	CGGGGTACCATGCAATTTTCCTTTTATTAATCC	
CheR_F_BglII	GGAAGATCTATGGAAAAAAAAATAACTCCTAGCGAATTG	Primers to the 5' and 3' of *cheR* cds.
CheR_R_KpnI	CGGGGTACCTTTATACTTTTTCATAGTAAACACCTCTTG	
CheW_F_BglII	GGAAGATCTATGAGTAATGAAAAATTAGAGCAAATTTTGCAAAAAC	Primers to the 5' and 3' of *cheW* cds.
CheW_R_KpnI	CGGGGTACCTTAAAATTCGCGCTTAAGCAAAGC	
Flim_F_BglII	GGAAGATCTATGGCTGAGATACTCTCCCAAGAAG	Primers to the 5' and 3' of *fliM* cds.
Flim_R_KpnI	CGGGGTACCTCATATTTCTTCATCCTCCTCTTCA	

	GGCTCAT	
CheV_his_F_XhoI	CCGCTCGAGAATGTTTGATGAAAATATCGTGAAAAC	Primers to the 5' and 3' of *cheV* cds.
CheV_his_R_KpnI	CGGGGTACCTTACCCCTGTTCTTGAGATTGATG	
Tlp 2_F_BglII	GAAGATCTAACTATAAAACAAAAAATGTTTCCACTATAG	Primers to the 5' and 3' of the cytoplasmic domain shared by TLPs *Cj0262*, *Cj1564*, *Cj0144*, cds.
Tlp 2_R_KpnI	CGGGGTACCAGGGCTTGAATGATTAATTAAAACC	
Tlp1_F_BglIII	GGAAGATCTAATCATGAAAAAATTGAACCTAAG	Primers to the 5' and 3' of the cytoplasmic domain of *tlp1* (*Cj1506c*) cds.
Tlp1_R_KpnI	CGGGGTACCTTAAAATCTTTTTTTATTCACATCTTC	
CheA-HK (-W)_F_BglII	GAAGATCTATGGAAGATATGCAAGAAATAC	Primers to the 5' and 3' of the histidine kinase domain of *cheA* cds.
CheA-HK (-W)_R_KpnI	GGTACCCCGTTAAATTGCATAGAATTCCTCTTGAG	
CheA-RR_(incW)_F_BlgII	GGAAGATCTAGTTCATTTAAACTTAAAATTCCTCTTAC	Primers to the 5' and 3' of *cheA-RR* and *cheW* domain cds.
CheA-RR_(incW)_R_KpnI	GGTACCCCGTCATTACTCATATTCTTATCCTAGTTTC	
pTrcHisB _F	GTATCGATTAAATAAGGAGG	Primers to the 5' and 3' of the multiple cloning site, to check insert size.
pTrcHisB_R	CTACTCTCGCATGGGGAGAC	
Primers for cloning into pGex-4T-1		
CheA_F_Xma	TCCCCCCGGGTATGGAAGATATGCAAGAAATACT	Primers to the 5' and 3' of *cheA*, cds.
CheA_R_XhoI	CCGCTCGAGCGGCTAATTTTTCATTACTCATATTCTTATC	
CheV_gst_F_XmaI	TCCCCCCGGGAATGTTTGATGAAAATATCGTGAAAAC	Primers to the 5' and 3' of *cheV*, cds.
CheV_gst_R_XhoI	CCCGCTCGAGTTACCCCTGTTCTTGAGATTGATG	
HK(-W&RR)_GST_F	TCCCCCCGGGTATGGAAGATATGCAAGAAATACTTG	Primers to the 5' and 3' of histidine kinase domain of *cheA*, cds.
HK(-W&RR)_GST_R	CCGCTCGAGAATTGCATAGAATTCCTCTTGAG	
pGex 3'	CCGGGAGCTGCATGTGTCAGAGG	Primers to the 5' and 3' of the multiple cloning site cds, to check insert size.
pGex 5'	GGGCTG GCA AGC CAC GTT TGG TG	
Primers for cloning into pLeics vectors		
ChePep_F	TACTTCCAATCCATGATGAAAATTTTACTTTTAAATGAAAAC	Primers for ligationless cloning into pLeics-01 and pLeics-02

ChePep_R	TATCCACCTTTACTGTCATCAATCCTCTTTAAAACTAATG	vectors.
Primers for sequencing of inserts		
CheV seq prim_R	TAGACTTTATCGTGCCCTTGC	internal sequencing primers for the *cheV* gene.
ChePep_seq_F	CATTTCTAATGTATTTGTTTTAG	internal sequencing primers for the *chePep* gene.
ChePep_seq_R	AAAGAATTACAAGCTAATATAAG	
Primers for point mutation of Che gene		
Y-GST-D13K_F	TCCCCCCGGGTGTGAAATTGTTAGTTGTTGATAAAAGTTCTACTATGAGAAG	Primers to make a *cheY*^{D13K} mutant
Y-GST-D13K_R	CCGCTCGAGTTACTCAGCTGCACCTTCTCC	
Y '59_F_Modified	ATTCATTTCTGGCATTTTCCAATCTGTAATTAAAACTTTTACATC	Primers to make a *cheY*^{N59K} mutant
Y '59_R_Modified	AATTACAGATTGGAAAATGCCAGAAATGAATGGCTTG	
Y '89_F - Modified	TTCAGCTTTTCCACCATAAGTTGTAACCATGATGATAG	Primers to make a *cheY*^{E89Y} mutant
Y '89_R- Modified	CATCATGGTTACAACTTATGGTGGAAAAGCTGAAG	
Y-GST-D57A_F	AAAAGTTTTAATTACAGCTTGGAATATGCCAGAAATGAATG	Primers to make a *cheY*^{D57A} mutant
Y-GST-D57A_R	ATTTCTGGCATATTCCAAGCTGTAATTAAAACTTTTACATC	
CheA_57_F	GATGCAATGCTTATAGCGATCGAAATGCCAAGAATGGATGGATAC	Primers to make a *cheA*^{D57A} mutant
CheA_57_R	TTCTTGGCATTTCGATCGCTATAAGCATTGCATCAATATCATGTTC	
CheV-57_F	ATTATAGTAAGCGCGGTCGAAATGCCACAAATGGATG	Primers to make a *cheV*^{D57A} mutant
CheV-57_R	GTGGCATTTCGACCGCGCTTACTATAATTTTTAAAGTATC	

2.4. Protein Techniques

2.4.1. SDS-PAGE

For analysis of proteins samples were electrophoresed on denaturing SDS-PAGE gels (Laemmli 1970) of 10% or 14% (w/v) accrylamide using either a Mini-Protean® II (Bio-Rad, UK) or an OmniPAGE Mini gel tank (Geneflow, UK). Samples were prepared by mixing with an equal volume of 2x sample loading buffer (1 M Tris-HCL, 10% (w/v) SDS, 2% (w/v) Bromophenol blue, 10% (v/v), 0.2 M DTT) and heated to 98 °C for 10 minutes. Samples including membrane proteins, such as whole cell samples, were centrifuged at 12,000 *g* for 10 minutes before loading. 5 µl of a 10-170 kDa Page Ruler™ (Thermoscientific, UK) protein ladder was run alongside the samples for estimation of band size.

SDS-PAGE gels that required drying, for instance for radiolabel detection, were mounted upon 3 pieces of stacked Whatman 3MM paper, covered with Saran wrap (Dow, UK) and dried using a dry vacuum pump (Fisherbrand, UK) with heating for 3 hours.

2.4.2. Western Blotting

For immunoblotting of proteins, samples were first electrophoresised as above on a denaturing SDS-PAGE gel, then electroblotted onto a polyvinylidene (PVDF) membrane (Millipore, UK) using an OminiPAGE Mini (Geneflow, UK) in transfer buffer, as per the manufacturer's instructions.

The PVDF was blocked for 12-14 hours with a 5% (w/v) blocking buffer (skimmed milk powder in ddH_2O), then gently rinsed in ddH_2O. The relevant antibody, either Anti-GST-HRP (concentration not stated) (GE Healthcare, Amersham, UK) or anti-HIS-HRP at 1mg/ml (Fisher Scientific, UK), was diluted to 1:80,000 in 20 ml of 5% (w/v) blocking buffer and added to the membrane for 20 minutes. The membrane was then washed twice in 50 ml of PBS-T (1L of 1x PBS buffer plus 5 ml Tween® 20) then washed three times for 5 minutes, twice for 15 minutes and then a final three times for 5 minutes each, each wash using 20 ml of PBS-T. All above incubation and washing steps were performed with gentle agitation on a HBSHK1 Hybaid Shaker.

Horse radish peroxidase conjugated antibodies, bound to proteins on PVDF membrane, were visualised using an EZ-ECL kit for Chemiluminescence detection of HRP (Geneflow, UK). The image was captured using Fuji medical X-ray film (Fujifilm, UK), with a typical exposure time of approximately 1 minute.

2.4.2. Protein Expression

E. coli Rosetta™cells, carrying the relevant expression construct, were used to inoculate 5-10 ml of ampicillin supplemented Luria broth, and incubated at 37 °C for 12-14 hours with agitation on a Gio Gyrotory® shaker (New Brunswick Scientific, UK). That initial culture was used to inoculate fresh Luria broth, without ampicillin, at a ratio of 1:100 (v/v). This fresh culture was incubated as previously but until the suspension achieved an OD_{600} of 0.5-1 when measured using an Ultrospec 10 (GE Healthcare, UK). Protein expression was then induced by the addition of isopropyl β-D-1-thiogalactopyranoside (IPTG) to a final concentration of 1.4 mM and the culture incubated at 30 °C, with agitation at 200 rpm, in an

Innova 4000 (New Brunswick Scientific, UK) incubator for 3 hours. After 3 hours the culture was split between 50 ml falcon tubes and cells were pelleted by centrifugation at ^{32}20 *g*, 4 °C for 20 minutes in an Eppendorf 5810R centrifuge. The supernatants were discarded and the pellets retained in the 50 ml tubes at 4 °C overnight, before proceeding to the cell lysis and purification steps.

2.4.3. Cell Lysis

Each pellet was resuspended in 2 ml universal binding buffer (50 mM Tris-HCL, 0.5 M NaCl, in ddH_2O, pH7.6), these suspensions were pooled together with 1 cOmplete, Mini, EDTA-free Protease Inhibitor Cocktail Tablet (Roche, UK) per 10 ml of suspension, and 3.5 mg chicken egg white lysozyme (Sigma, UK) per ml of cell suspension. The cells were left to lyse at room temperature for 1 hour with agitation on a Hybaid Shaker HBSHK1. After cell lysis, the protein solution and the solutions used for protein purification were kept on ice to minimise protein degradation. Post lysis the protein solution was aliquoted into 15 ml tubes and sonicated using a Biorupter (Diagenode, Belgium) sonicator, set to high intensity for 7 rounds of 30 second bursts with 30 second pauses between bursts. The sonicator chamber was pre-chilled with ice for 10 minutes, and 1cm depth of ice left in the compartment before chilled water was added to the recommended depth. The cell lysates were centrifuged at ^{32}20 *g* for 20 minutes to pellet cell debris, the supernatants were pooled for later purification and the pellets kept for analysis or discarded.

2.4.4. Protein Purification

The following steps were carried out in a cold room at 4-6 °C. Affinity tagged protein purifications were carried out using either 5-7 ml of IMAC Ni Sepfast BG resin loaded into an IMAC BG-30, 30 ml gravity flow column (Geneflow, UK) for purification of polyhistidine (HIS) tagged proteins, or 3-5 ml of glutathione reduced white crystalline powder (Fisher Scientific, UK) in a IMAC BG-30, 30 ml gravity flow column. The gravity flow column was opened and the resin storage buffer drained from the column, 25 ml of ddH_2O was added to the column to wash away any remaining ethanol. Once the ddH_2O had run through the column it was followed by 25 ml of universal binding buffer which equilibriated the resin. At this point the lysate, from the cell lysis referred to above, was added to the column and allowed to flow though the resin. Once the lysate had passed through the column it was washed with 2 x 25 ml washes of universal binding buffer, which removed the majority of contaminants.

To elute the affinity tagged protein, 15 ml of the GST elution buffer (PBS supplemented with 10 mM reduced L-glutathione, pH7.6) or 15ml of the HIS elution buffer (50 mM Tris-HCL, 0.5 M NaCl, 200 mM Imidazole, in ddH_2O, pH7.6) was added to the column and the eluent containing the purified protein collected below.

For storage, the gravity columns were plugged and 30 ml of 20% (v/v) ethanol (in ddH_2O) was added, these were stored at 4°C for later re-use. Gravity columns were subsequently reused only for purification of the same protein.

2.4.5. Protein Concentration and Buffer Exchange

Buffer exchange and protein concentration were carried out using either 3 kDa, 10 kDa or 30 kDa Amicon® Ultra Centrifugal filters (Fisher Scientific, UK), in either 15 mL or 0.5 mL sizes. Purified protein samples were loaded into 15 ml concentrators and centrifuged at ^{32}20 *g* until the sample decreased in volume to approximately 250 µl, the sample would then be diluted with addition of protein storage buffer (50 mM Tris-HCL, 200 mM KCl, 10 mM $MgCl_2$, 0.1 mM EDTA, 1 mM DTT and 10% (v/v) glycerol, in ddH_2O, pH 7.6) to a final volume of around 15 ml, then centrifuged again. This step was repeated to dilute away the elution buffer used in the final step of purification, and swap buffers to the protein storage buffer. In the final step the sample was centrifuged until it reached a final volume of around 250 µl. If the desired volume could not be reached using a 15 ml Amicon® Ultra Centrifugal filter, then the sample was transferred to a 0.5 ml concentrator, of the corresponding kDa size, and centrifuged at 12,000 *g* to obtain the desired final volume. Final protein concentration was ascertained by Bradford assay (Bradford 1976) using Bradford reagent (Sigma, UK) and measured on a 6705 (Jenway, UK) multicell changer at UV/VIS at 595 nm.

2.4.6. Pull-Down Assays

Assays were carried out in 1x reaction buffer. During washing stages the MagneGST (Fisher, UK) resin would be pulled out of suspension using a magnetic rack, and the supernatant removed. 25 µl of resin was loaded into microcentrifuge tubes, and washed twice with 1 ml of reaction buffer (250 mM Tris-HCL, 375 mM KCl, 10 mM $MgCl_2$, 5 mM DTT, in ddH_2O, pH8.3). The ‘bait’

protein, 20 µl of 1% (w/v) BSA and 10 µl of a saturated acetyl phosphate solution (approximately 1.5 M) were added to the resin and incubated for 5 minutes. The resin was washed twice with 1 ml of reaction buffer. The 'prey' protein and 20 µl of 1% (w/v) BSA in reaction buffer were added to the resin, and incubated for 5 minutes, before two final 1 ml reaction buffer washes. The resin was resuspended in sample loading buffer, and the supernatant loaded onto SDS-PAGE gels for Coomassie staining.

2.5 Data Reproducibility and Analysis

All experiments were performed in duplicate or triplicate on at least 3 separate occasions, except where declared otherwise (precise replicates are shown in individual figure legends). Where needed, statistical analysis was carried out using One-way ANOVA (Analysis of Variance), two-way ANOVA with Dunnet's or Bonferroni post hoc tests using Graph Pad Prism Program. Statistical significance was indicated by a P value of less than 0·05.

2.6. Buffers and Solutions

Except where stated otherwise, buffers and solutions were pH adjusted using HCl or NaOH, and were sterilised by autoclaving, at 121-124 °C for 20 minutes, or filter sterilised using a 0.22 µM stericup (Millipore). Solutions were stored at 4 °C unless stated otherwise. All chemicals were sourced from Sigma-Aldritch (UK) except where stated otherwise.

Buffer P1

Supplied as 50 mM Tris-HCL, 10 mM EDTA, 100 ug/ml RNase A, pH8 (Qiagen, UK).

DTT

1M DTT (Melford, UK) stock dissolved in 0.01 M sodium acetate pH5.2, filter sterilised and stored at -20 °C.

GST Elution Buffer

PBS as above, supplemented with 10 mM reduced L-glutathione, filter sterilised and adjusted to pH7.6 (Fisher Scientific, UK)

HIS Elution Buffer

50 mM Tris-HCL, 0.5 M NaCl, 200 mM Imidazole, made in ddH_2O, filter sterilised and adjusted to pH7.6.

IPTG

100 mM IPTG (Melford, UK) stock dissolved in ddH_2O filter sterilised and stored at 4 °C.

Phosphate Buffered Saline Solution

Made with Phosphate buffered saline tablets (Oxoid, UK) 1 tablet/100 ml ddH_2O and adjusted to pH7.3.

Protein Storage Buffer

50 mM Tris-HCL, 200 mM KCl, 10 mM $MgCl_2$, 0.1 mM Ethylenediaminetetraacetic acid (EDTA), 1 mM Dithiothreitol (DTT) and 10% (v/v) glycerol made in ddH_2O, adjusted to pH 7.6, filter sterilised and stored at 4 °C.

Reaction Buffer 5x

250 mM Tris-HCL, 375 mM KCl, 10 mM $MgCl_2$, 5 mM DTT, made in ddH_2O, filter sterilised and adjusted to pH8.3.

Resin Storage Solution

20% (v/v) ethanol diluted with ddH_2O.

Sample Loading Buffer 2x

1 M Tris-HCL, 10% (w/v) SDS, 2% (w/v) Bromophenol blue, 10% (v/v) glycerol, made to final volume in ddH_2O. 0.2 M DTT was added before use.

SDS-PAGE Buffers

Stacking buffer: 0.5 M Tris-HCL, 0.4% (w/v) SDS, pH6.8

Resolving buffer: 1.5 M Tris-HCL, 0.4% (w/v) SDS, pH 8.8

Running buffer: 0.25 M Tris, 1.92 glycine, 1% (w/v) SDS.

Sodium Dodecyl Sulphate (SDS)

Made at 2% or 10%,(w/v) dissolved in ddH_2O and stored at room temperature.

Sodium Acetate

0.01 M sodium acetate dissolved in ddH2O and adjusted to pH5.2.

Transfer Buffer

25 mM Tris, 192 mM Glycine, 10% (v/v) methanol, 0.5% (w/v) SDS made in ddH_2O

Tris-Borate-EDTA Buffer

0.089 M Tris-HCL, 0.089 Boric acid, 0.002 EDTA, made in ddH_2O and adjusted to pH8.3.

Universal Binding Buffer

50 mM Tris-HCL, 0.5 M NaCl, in ddH_2O made in ddH_2O, adjusted to pH7.6, filter sterilised and stored at 4 °C.

Chapter 3: Cloning, Expression and Purification of *C. jejuni* Chemotaxis Proteins

3.1. Introduction

In silico analysis of the *C. jejuni NCTC11168* genome had identified the candidate *che* genes (Parkhill et al. 2000; Marchant et al. 2002), *C. jejuni* Δ*che* gene mutants had helped confirm this pool of candidates by comparing the chemotactic phenotype of Δ*che* gene mutants to that of wild type *C. jejuni* (Bridle 2007). However, there had been issues with the mutant strains as a positive selection system for the creation of gene mutants had not existed for *C. jejuni* when the Δ*che* gene mutants had been made, so downstream polar effects due to the insertion of antibiotic cassettes into the *che* genes could not be excluded. There had been issues with complementation of the Δ*che* strains as many of the strains had to be reverted using *C. jejuni* NCTC11168 chromosomal genome preparations rather than fully complemented. Bacterial two hybrid studies which had assayed the affinities between candidate *che* genes had indicated possible interactions between the proteins, but did not necessarily indicate functional relationships (Bridle 2007).

The evidence of the mutation and complementation studies, *che* gene homology combined with the B2H and Y2H studies, strongly supports the respective roles of the *che* genes though to different extents. To verify the functions and investigate the novel aspects of the system, such as CheV and the CheA RR domain,

additional characterisation is required. *In vitro* studies using purified proteins will be used to perform kinase assays, to confirm CheA as a functional histidine kinase, and to confirm the candidate response regulators as real, functioning response regulators that form interacting partners with CheA. Purified protein will also be used to assay affinities between candidate Che proteins while in phosphorylated and non-phosphorylated states.

An expression strain had been constructed for each of the chemotaxis proteins each contained an expression vector carrying one of the *C. jejuni* chemotaxis proteins fused to a HIS or GST tag by its N-terminal domain (Table 2.3). In each case the chemotaxis gene and a portion of its upstream affinity tag had been sequenced to confirm that the gene insert had a correct sequence, and that it was in frame with its affinity tag.

3.2. Cloning Procedure

To obtain purified Che proteins, *E. coli* Rosetta™ expression strains were created, each containing a vector with a *C. jejuni che* gene insert that could be induced to express from that insert, and using an in frame fusion to an affinity tag, then purified using an affinity chromatography column.

Glutathione S-transferase Fusion Plasmid pGex-4T-1

To obtain Glutathione S-transferase tagged *C. jejuni che* genes, the putative chemotaxis genes were cloned into plasmid pGex-4T-1. pGex4T-1 is an expression plasmid with a multiple cloning site downstream of a *glutathione S-transferase* (GST) gene, the multiple cloning site allows for insertion of an in

frame sequence to make an N-terminal GST fusion with the protein of your choice. The high affinity of the GST tag for its substrate, reduced glutathione, is exploited to purify the fusion protein from a cell lysate using affinity chromatography, utilising reduced glutathione as an eluant.

Expression of the GST fusion protein is from a *tac* promoter under $LacI^q$ regulation, $LacI^q$ is a repressor protein that binds to the operator region of *tac* and prevents transcription of downstream regions, in this case the GST tag and multiple cloning site ORF. Repression of transcription is released by exposure to IPTG which binds to $LacI^q$ and prevents its interaction with the operator sequence, releasing repression and allowing RNA polymerase to access the GST fusion template and cloned gene. The GST tag is a 26 kDa protein which when expressed is joined by a peptide polylinker to the cloned protein, there is a protease recognition sequence within the polylinker which allows the GST tag to be cleaved from the cloned protein by thrombin, a protease. Due to the large size of GST it had been anticipated that the GST tag may need to be cleaved from the expressed protein, but ultimately found this unnecessary. pGex-4T-1 is a high copy number plasmid, selection with chloramphenicol was required to maintain the plasmid.

As the method intended for later assaying the affinities between the Che proteins uses the affinity tag to anchor the bait protein to an affinity chromatography matrix, the proteins tested would require different tags to each other to avoid both directly binding to the matrix, for this reason CheV, CheA and CheY were cloned into both pGex-4T-1, to fuse to a GST tag and pTrcHisB to fuse to a HIS tag.

HIS Fusion Plasmid pTrcHisB

To obtain HIS tagged *C. jejuni che* genes, the *che* ORFs were cloned into plasmid pTrcHisB. pTrcHisB is an expression plasmid with a multiple cloning site downstream of a HIS tag, this multiple cloning site allows for insertion of an in frame sequence to make an N-terminal HIS tag fusion with the cloned protein. The high affinity of the HIS tag for metal cations is exploited to purify the fusion protein from a cell lysate using affinity chromatography. Expression of the HIS tagged fusion protein is from a *tac* promoter with downstream $LacI^q$ repression. pTrcHisB is a high copy number plasmid, selection with chloramphenicol was required to maintain the plasmid.

3.2.1. TLP HIS and Glutathione S-transferase Expression Clones

To obtain purified TLP proteins, attempts were made to express and purify TLP_1 and $TLP_{2\text{-}4}$ from the pRS09 and pRS10 plasmids constructed previously (Hartley-Tassell et al. 2010). pRS09 had had cloned into it, the C-terminal cytoplasmic domain of TLP1 (cj1506c), pRS10 received the C-terminal cytoplasmic domain shared by TLP_2, TLP_3 and TLP_4 (cj0144, cj1564 and cj0262). The putative N-terminal transmembrane regions of the TLPs had been excluded during cloning as there was a possibility of insertion of the TLPs into the membrane and/or aggregation during expression and purification. The interactions intended to be assayed were internal to the cell, measuring TLP affinity to CheA, CheV, CheB and CheR, for that reason the separately expressed cytoplasmic domains of TLPs were judged to be suitable to use in the affinity assays. Later HIS tagged

clones of TLP_1 and TLP_{2-4} were constructed due to issues found with purification from the GST tagged TLP constructs. The TLPs were cloned into pTrcHisB, as previously for the *che* genes, except that a greater proportion of the N-terminal domain was excluded for both TLPs to omit possible hydrophobic interactions around the predicted transmembrane regions, enough of the C-terminal domain was retained so that the predicted chemotaxis transduction domains should not be affected. TLP_1 was cloned from base pair 1118 to 2103, so to include the predicted HAMP domain between bases 1225 and 1386 and the predicted chemotaxis transduction domain between bases 1543 and 2103. TLP_{2-4} was cloned from base 1012 to 1998, so including the chemotaxis transduction domain from bases 1393 to 1998. When induced the vectors would begin transcription from the start site upstream of the HIS tag, provided by the expression plasmid and use the native stop codon supplied by the TLP C-terminal domain.

Expression Strain *Escherichia coli* Rosetta™

E. coli Rosetta™ cells were used for the expression of affinity tagged proteins from pTrcHisB and pGex-4T-1 plasmids. Rosetta™ cells carry deletions in known proteases to reduce proteolysis of the cloned protein. The expression of non-endogenous proteins in an *E. coli* background may be subject to bottlenecks in expression, due to differences in codon bias between the *E. coli* in which the protein is being expressed, and the species from which the cloned gene originates. *E. coli* is unlikely to express high levels of tRNAs for codons which are not prevalent within its own genome, Rosetta™ tackles this bottle neck using the pRARE plasmid, pRARE encodes for tRNAs which are rare within *E. coli*, this

allows greater efficiency in translation from mRNA transcripts originating from the subject of study, *C. jejuni* NCTC11168.

Primer Design

Primers for amplification of the *che* gene open reading frames (ORFs) were designed to amplify from the ORF start to stop codon and ensure that once cloned, the gene would be in frame with the affinity tag. Amplicons were directional cloned into expression vectors, primers for cloning of *che* genes into pTrcHisB used BglII sites on forward primers and a KpnI on the reverse. As the CheV gene itself contained a BglII site, an XhoI site was used instead. Primers for cloning into pGex-4T-1 plasmids used XmaI on forward primers and XhoI on the reverse. The template used was from a chromosomal genome preparation of *C. jejuni* NCTC11168.

PCR, Restriction Digestion and Ligation of Fragments

Each of the *che* genes was amplified by PCR using the appropriate primers (Table 2.6), the amplicons were each purified using an E.Z.N.A. ® Cycle Pure Kit. Typically around 500 ng of the PCR product was used in a restriction enzyme digest using the enzymes to both 5' sense and antisense ends. As controls 500 ng of pTrcHisB was added to restriction enzyme reactions individually, and in combination, and compared to undigested pTrcHisB after electrophoresis on an agarose gel to judge the effectiveness of the restriction digest (Fig.3.1) and so to estimate their effectiveness of digestion of the *che* amplicon. The efficiency of digestion of the amplicons could not be judged directly by agarose electrophoresis as the change in nucleotide length resulting from the digestion

would be too small to discern by this method. Digested *che* gene fragments and plasmids, pTrcHisB or pGex-4T-1, were purified again using an E.Z.N.A. ® Cycle Pure Kit, each *che* insert was then ligated overnight into either pTrcHisB or pGex-4T-1 as appropriate. Ethanol precipitation was used to concentrate and desalt the ligation mix, to prepare the new plasmid for electroporation into the Rosetta™ expression strain.

Transformation and Screening of Transformant Colonies

The ligated plasmid containing a *che* gene ORF was transformed into Rosetta™ by electroporation, surviving cells were inoculated onto Luria agar plates supplemented with ampicillin and chloramphenicol, and incubated at 37 °C overnight to select for transformants. To grow colonies must have received the *bla* gene which confers resistance to ampicillin and is present on either of the expression plasmids, pTrcHisB or pGex-4T-1, and the *cam* gene present on the pRARE plasmid, which confers resistance to chloramphenicol. Colonies were picked from these initial transformation plates and inoculated onto new Luria agar plates supplemented with ampicillin and chloramphenicol. Re-plating of successful transformant colonies reduced the 'free' DNA background, residual from the ligation mix used in electroporation, this background DNA may give false positive results during colony PCR. Clones containing an insert of the correct size were identified by colony PCR from crude cell lysates (Fig.3.1) using gene specific primers or primers that amplify across the multiple cloning site (Table 2.6). Clones with correct sized plasmid inserts were used to inoculate 5ml Luria broths and grown overnight at 37 °C with agitation, plasmids were purified from these suspensions using an E.Z.N.A. ® Plasmid Mini Kit 1. The plasmid inserts

were sequenced to verify that the *che* gene sequence was correct and that the affinity tag was in frame with the *che* gene, verified expression strains were stored as glycerol stocks at -80 °C for later use.

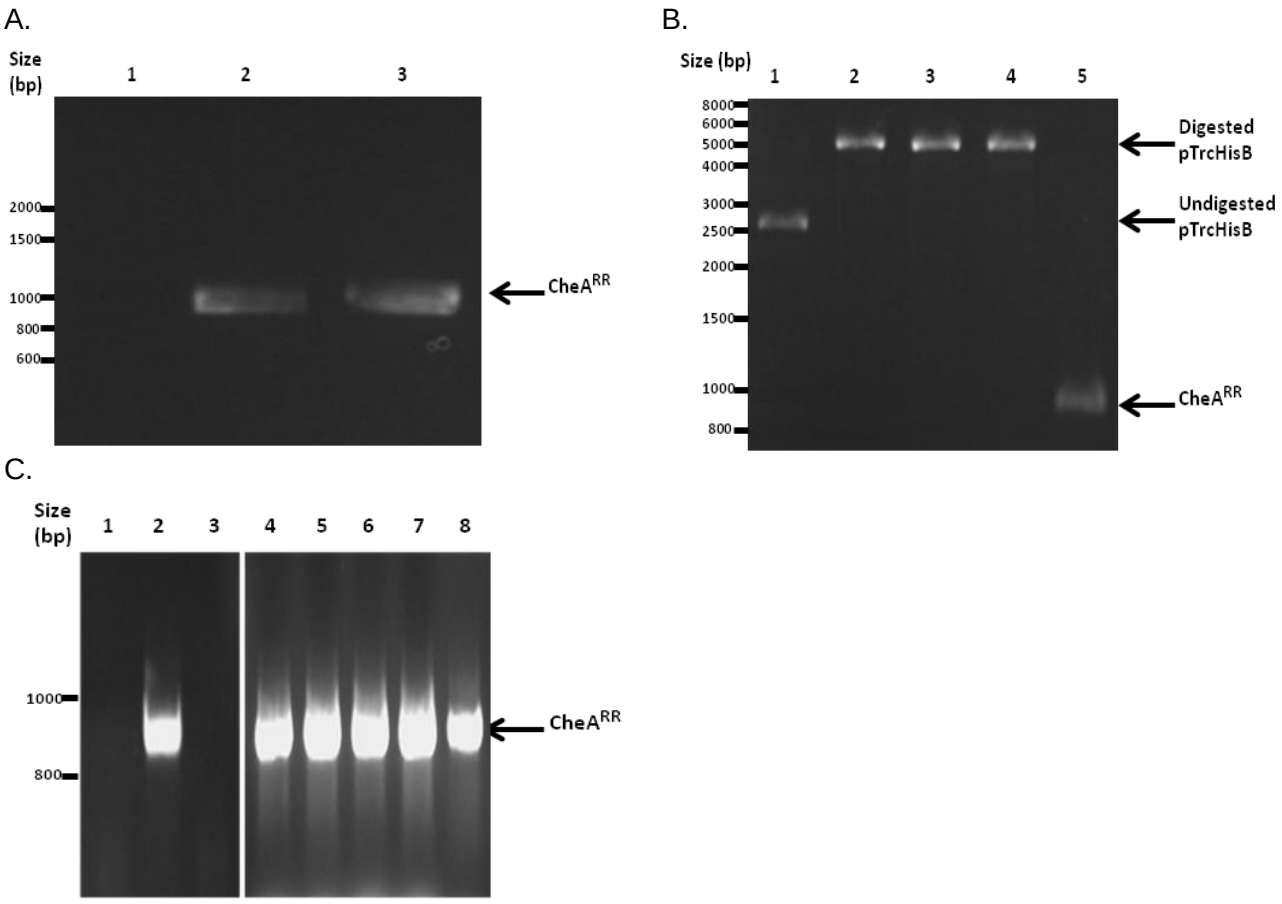

Figure 3.1. An Example of Typical Cloning Procedure. (A) shows amplified PCR products created from a *C. jejuni* NCTC11168 genome template using the CheA^{RR} gene primers (Table 2.6). Lane 1 is a negative control showing the reaction with no template added. Lanes 2 and 3 show the 913bp CheA^{RR} product produced from the NCTC11168 template. The successful CheA^{RR} PCR products were pooled, purified and concentrated. (B) shows a restriction digestion of the CheA^{RR} amplicon and the pTrcHisB plasmid using BglII and KpnI. Lane 1 contains a negative control of pTrcHisB with no restriction enzyme, a super coiled band is visible and 2 others are faintly visible, showing the undigested conformations of the plasmid. Lane 2 shows a pTrcHisB enzyme digest with BglII alone, this resulted in linear DNA which ran according to its predicted size. Lane 3 shows a pTrcHisB enzyme digest with KpnI alone, this resulted in a linear DNA which ran according to its predicted size. Lane 4 shows a restriction digest of pTrcHisB with BglII and KpnI, this resulted in linear DNA which ran according to its predicted size of 4404bps. Lane 5 shows the CheA^{RR} PCR amplicon digested by BglII and KpnI. The successfully digested pTrcHisB plasmid and CheA^{RR} PCR product were purified and concentrated. (C) displays the results of colony PCR against surviving Rosetta™ transformants. Once the cut and purified pTrcHisB and CheA^{RR} fragments had been ligated to form the expression plasmid pPA024 (Table 2.3), the plasmid was electroporated into Rosetta™ and grown on selective media. Surviving transformants were tested by colony PCR using the CheA^{RR} gene primers. Lane 1 is a negative control, with all reaction components except template DNA. Lanes 2-8 show the results of the colony PCR against colonies 1, 3, 5, 13, 15, 17, 26 respectively. Colony 3 shows a negative result, all other colonies are positive and show a product of the predicted size.

3.2.2. Expression and Purification of Che Proteins

To verify that the expression strains could produce protein from the cloned *che* gene inserts, and that the proteins produced would be fused to the N-terminal affinity tags, it was necessary to assay the induction of their expression. 5 ml of Luria broth was inoculated for each of the expression strains, each carrying a different *che* gene insert, this suspension was incubated overnight with agitation at 37 °C. The following day a 1:100 ratio of this cell suspension was used to inoculate 60 ml of fresh Luria broth, this broth was incubated as previously until it reached an OD_{600} of 0.5, at this point the Luria broth was aliquoted in 5 ml volumes into 20 ml Sterilin tubes and IPTG added to each to reach final concentrations of: 0, 0.2 mM or 0.4 mM IPTG to test Che protein expression in relation to IPTG concentration. A vector only negative control was used to demonstrate that expression must be from pGex-4T-1 or pTrcHisB.

The results of these expression tests were intended to inform the concentration of IPTG to be used in future, when expressing large batches of Che proteins. The now induced Luria broths were incubated at 30 °C for 3 hours with agitation, after 3 hours the broths were centrifuged at $^{32}20$ *g* for 20 minutes at 4 °C, the supernatant discarded, and the cell pellet resuspended in 100 µl of 2x sample loading buffer. The samples were heated to 98 °C for 10 minutes and centrifuged at 12,000 *g* for 10 minutes to create whole cell lysates for analysis. To confirm the expression of Che proteins in the expression strains, the cell lysates were loaded onto SDS-PAGE gels and electrophoresed. One of the SDS-PAGE gels was Coomassie stained to see if the expressed Che protein migrated at its

predicted molecular weight. The other SDS-PAGE gel was blotted onto a PVDF membrane, which was probed with anti-GST-HRP or anti-HIS-HRP antibodies, specific to the affinity tags. Where cloned Che proteins were not visible amongst the whole cell lysate on the Coomassie stained gel, they were visualised using the Western blotting method.

Glutathione S-transferase Tagged Che Protein Expression

Figure 3.3*A-D* shows the IPTG induction assays for the GST tagged CheA, CheY, CheV and Histidine kinase domain ($CheA^{HK}$) respectively. Each left hand gel shows the Coomassie stained SDS-PAGE gel, each SDS-PAGE gel is paired on the right with a corresponding western blot with samples arranged in the same order and probed with anti-GST-HRP.

The GST tagged CheV, CheA, CheY and $CheA^{HK}$ expression strains all expressed tagged protein, the SDS-PAGE images of Figure 3.3 display distinct bands at the approximate predicted kDa (Table 3.2) for each of the Che protein shown in Lanes 3 and 4 of Figure 3.3*A-D*. The Che band on the SDS-PAGE gels is not visible in the uninduced lanes (Lane 2 of each panel) or in the lane containing the empty Rosetta™ vector (Lane 1 of each panel), suggesting the bands in Lanes 3 and 4 are a product of the *che* gene containing pGex plasmid. When probed with anti-GST-HRP, the corresponding western blots display bands matching those of the CheV, CheA, CheY and $CheA^{HK}$ proteins on the SDS-PAGE gels. Multiple anti-GST-HRP staining bands, smaller than the predicted size of the Che proteins, appear in western blot gels A) to D). suggesting some proteolysis of the protein is taking place. Assuming these to be the desired Che

proteins, production for each appeared to peak at 0.2 mM IPTG (Lane 3), production did not increase with increased IPTG concentration.

Cloned protein	Predicted molecular weight
CheA-GST	112.12 kDa
CheY-GST	41.56 kDa
CheV-GST	62.68 kDa
$CheA^{HK}$-GST	83.86 kDa
GST	27.9 kDa

Table 3.2. Predicted molecular weight of GST tagged proteins

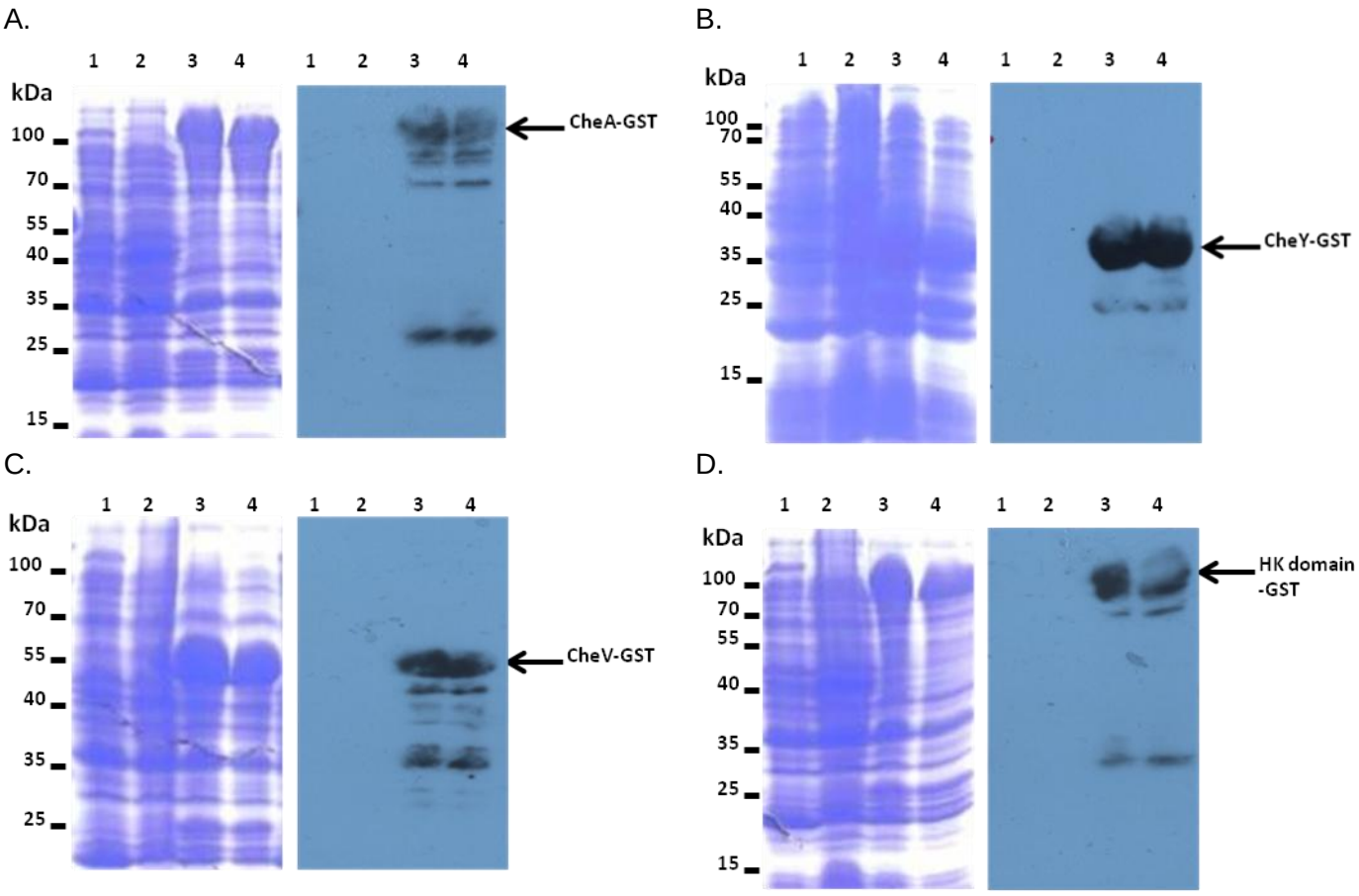

Figure 3.3. Induction assays testing optimal IPTG concentration for GST tagged Che protein expression. Expression strains were grown overnight and used to inoculate fresh Luria broth at 1:100, incubated until the suspension reached an OD600 of 0.5 then induced with different concentrations of IPTG at 30 °C. All proteins shown were GST tagged a) CheA b) CheY c) CheV d) Histidine kinase domain. Panels (A), (B), (C) and (D) show SDS-PAGE and western blots carried out using the samples from these induction tests. Each SDS-PAGE is paired with a corresponding western blot, loaded in the same order and probed with anti-GST-HRP. For each of the gels Lane 1 shows the Rosetta™ strain without an expression plasmid and induced with 1.4 mM IPTG, Lane 2 shows a Che protein expression strain with no IPTG and is therefore uninduced, Lane 3 shows a Che expression strain induced with 0.2 mM IPTG, and Lane 4 shows the same Che expression strain induced with 1.4 mM IPTG.

HIS Tagged Che Protein Expression

Induction of expression of recombinant chemotaxis proteins was initially tested at 37 °C but due to excessive proteolysis of the proteins the temperature was reduced to 30 °C. Figure 3.5*A*-*F* and Figure 3.6*A*-*E* shows IPTG induction assays for the HIS tagged CheA, CheY, CheV, Histidine kinase domain ($CheA^{HK}$), CheA response regulator ($CheA^{RR}$), CheR and CheB respectively. The left hand gel of each Figure shows the Coomassie stained SDS-PAGE gel, each SDS-PAGE gel is paired with a corresponding western blot with samples arranged in the same order and probed with anti-HIS-HRP. For each image: Lane 1 is a negative control of Rossetta™ without a pTrcHisB expression plasmid and exposed to 1.4 mM IPTG, Lane 2 is a Che protein expression strain without IPTG and therefore without induction, Lane 3 is the Che protein expression strain with 0.2 mM IPTG and Lane 4 is the Che protein expression strain with 1.4 mM IPTG.

All of the HIS tagged Che protein expression strains appeared at this point to have expressed Che protein matching their predicted molecular weight (Table 3.4). The SDS-PAGE images of Figure 3.5 and Figure 3.6 do not display a distinct band for any of the histidine tagged Che proteins, there is no distinct band visible in the induced lanes (Lanes 2-4) of the SDS-PAGE gels, at the correct kDa mass, that is not also visible in the negative control (Lane 1), however the corresponding western blots display bands at the approximate predicted kDa for each of the Che proteins (Lanes 2-4). Lane 2 of the western blots, each containing the uninduced Che expression vector, produced a band for all of the Che proteins in Figure 3.5 and Figure 3.6, this corresponded to the predicted size of each Che protein. A band of the size seen in Lanes 2-4, attributed to the Che

protein, is not seen in Lane 1 containing the empty Rosetta™ vector, suggesting the bands in Lanes 2-4 are a product of a *che* gene containing pTrcHisB plasmid. An exception to this was the western blot for CheB (Fig 3.6*C*) which, by its skewed appearance in lane 1, it appears to have suffered leakage from the adjacent lane (Lane2). Assuming these to be the desired Che proteins, production for each appeared to peak at 0.2 mM IPTG (Lane 3) with the exception of CheY which achieved greatest production at 1.4 mM IPTG (Fig 3.5*B*). For the SDS-PAGE gels shown in Figure 3.5*A,B,D* and Figure 3.6*A,B* there appears to be a decline in the total amount of protein visible correlated with increasing concentration of IPTG (Lanes 1-4). Multiple anti-HIS-HRP staining bands, smaller than the predicted size, appear in the western blot for CheV in Figure 3.6*C* Lanes 2 and 3 suggesting some proteolysis.

Cloned protein	Predicted molecular weight		Cloned protein	Predicted molecular weight
CheA	89.36 kDa		TLP1	39.85 kDa
$CheA^{HK}$	60.19 kDa		CheW	23.57 kDa
$CheA^{RR}$	36.3 kDa		FliM	44.88 kDa
CheV-His	39.83 kDa		CheB	24.25 kDa
CheY	18.4 kDa		CheR	34.71 kDa
Cj1613 (+ve control for Ig binding)	^{32}.87 kDa			

Table 3.4. Predicted molecular weight of HIS tagged proteins.

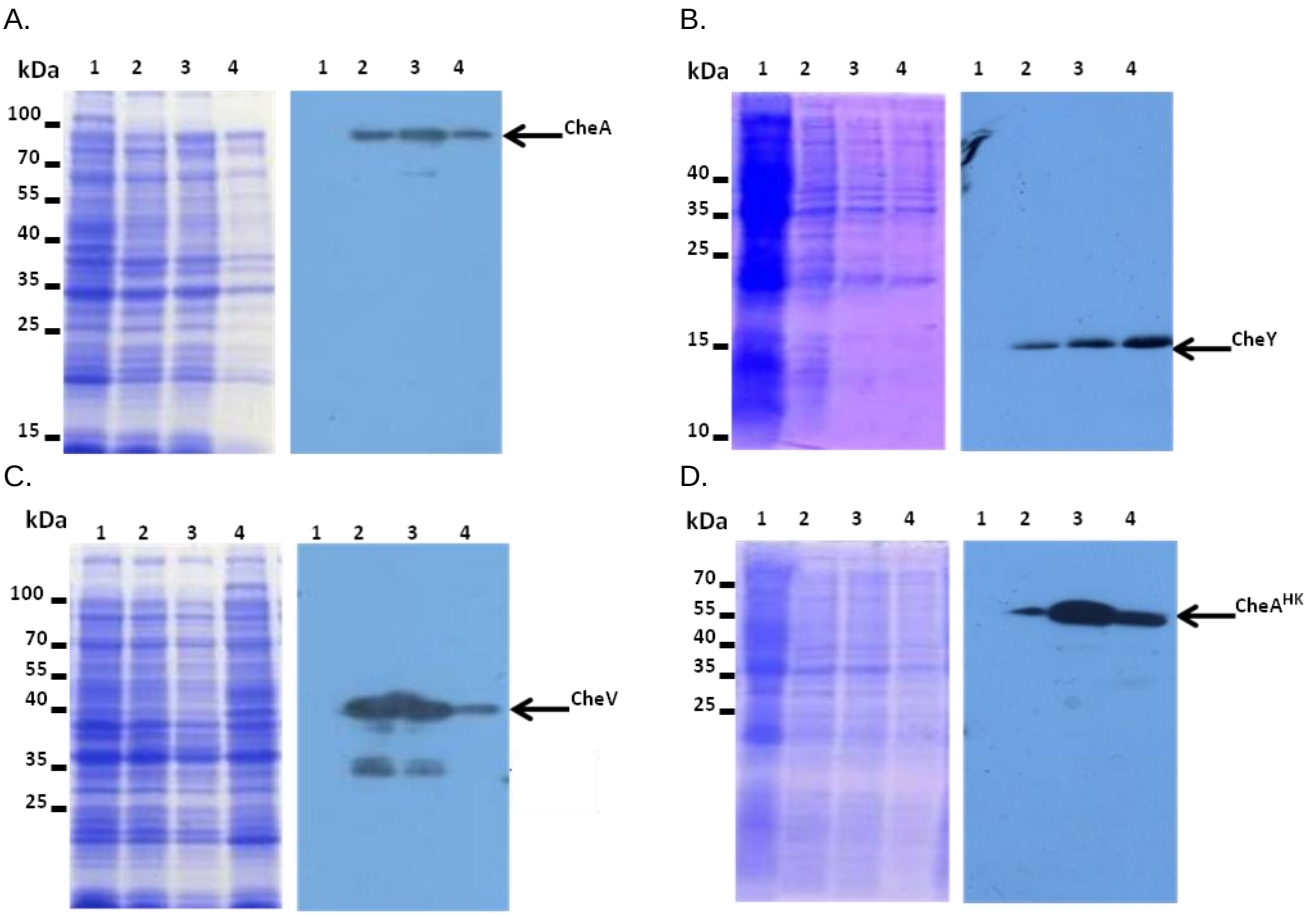

Figure 3.5. Induction assays testing optimal IPTG concentration for HIS tagged Che protein expression. Expression strains were grown overnight and used to inoculate fresh Lauria broth at 1:100, incubated until the suspension reached an OD600 of 0.5 then induced with different concentrations of IPTG at 30 °C. All proteins shown were HIS tagged a) CheA b) CheY c) CheV d) $CheA^{HK}$. Panels (A), (B), (C) and (D) show SDS-PAGE and western blots carried out using the samples from these induction tests, each SDS-PAGE is paired with a corresponding western blot, loaded in the same order and probed with anti-HIS-HRP. For each of the gels lane 1 shows the Rosetta™ strain without an expression plasmid and induced with 1.4 mM IPTG, lane 2 shows a Che protein expression strain with no IPTG which is therefore uninduced, lane 3 is the Che expression strain induced with 0.2 mM IPTG and lane 4 is the Che expression strain induced with 1.4 mM IPTG

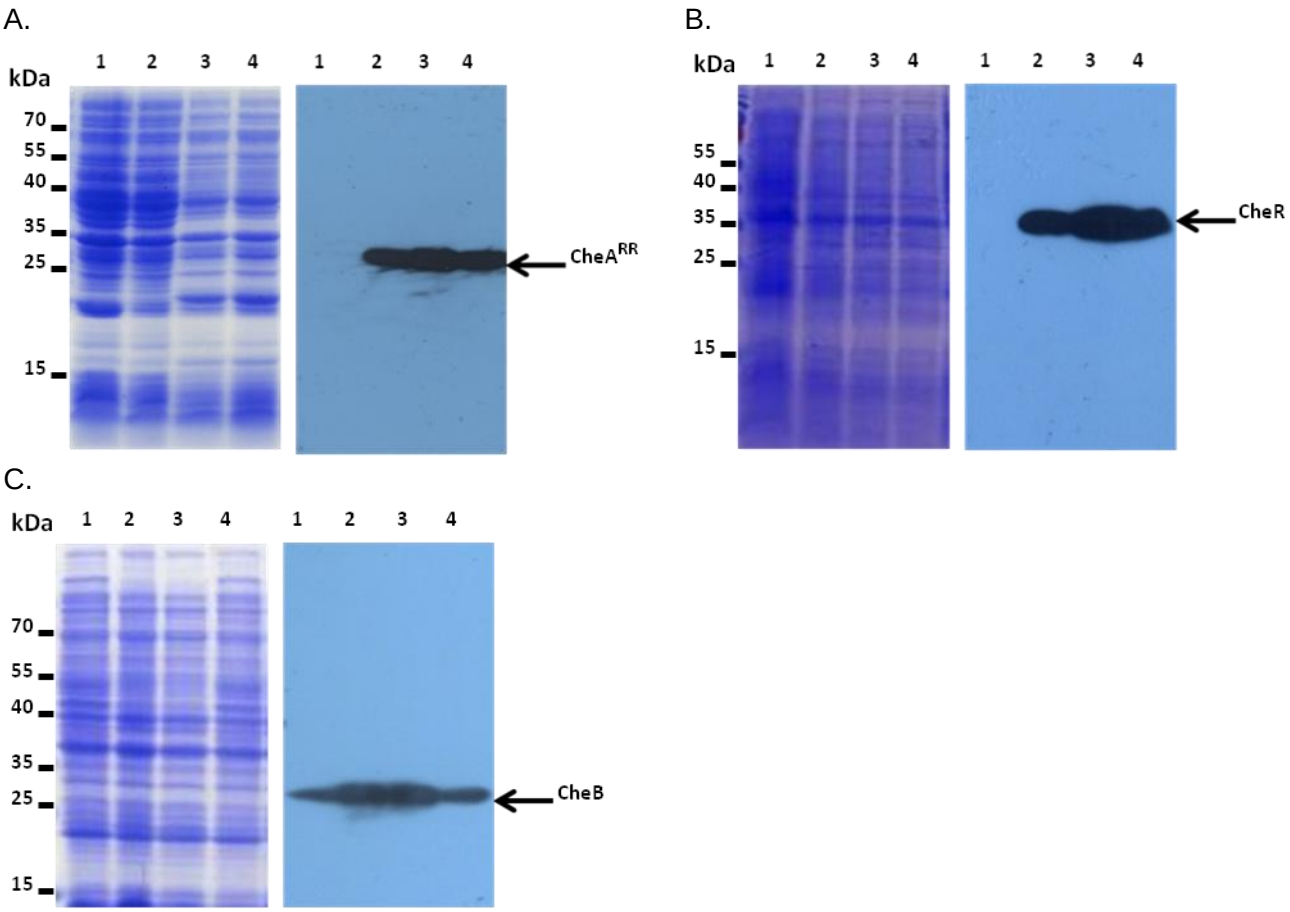

Figure 3.6. Induction assays testing optimal IPTG concentration for HIS tagged Che protein expression. Expression strains were grown overnight and used to inoculate fresh Lauria broth at 1:100, incubated until the suspension reached an OD600 of 0.5 then induced with different concentrations of IPTG at 30 °C. All proteins shown were HIS tagged a) $CheA^{RR}$ b) CheR c) CheB. Panels (A), (B) and (C) show SDS-PAGE and western blots carried out using the samples from these induction tests, each SDS-PAGE is paired with a corresponding western blot, loaded in the same order and probed with anti-HIS-HRP. For each of the gels lane 1 shows the Rosetta™ strain without an expression plasmid and induced with 1.4 mM IPTG, lane 2 shows a Che protein expression strain with no IPTG which is therefore uninduced, lane 3 is the Che expression strain induced with 0.2 mM IPTG and lane 4 is the Che expression strain induced with 1.4 mM IPTG

.

Che Protein Purification, HIS and GST tagged

The initial attempts at expression and purification of HIS tagged CheA produced a specific band at the predicted molecular weight which was also detected using anti-HIS-HRP (Fig. 3.7*A*-*D*), but these also produced multiple bands of smaller molecular weight which bound the anti-HIS-HRP, indicating that they may be proteolytic breakdown products of CheA. The temperature used during induction had initially been 37 °C, this was reduced to 30 °C and greater steps were taken to keep protein samples chilled at all times, these steps contributed to a greater purity of the CheA preparation, as judged visually by Coomassie gel separation, and reduced the apparent proteolysis of CheA to a single contaminating band (Fig 3.5). Expression and purification protocols for other expression vectors were modified to reflect this change.

Figures 3.8, 3.9 show SDS-PAGE gels of pre and post affinity chromatography processed samples for each HIS and GST tagged Che protein. Proteins are shown pre-purification, as a whole cell lysate on the left hand gel, and in the right hand gel, post-purification, buffer swapped protein in storage buffer. The protein was buffer swapped twice into protein storage buffer, achieving a 1/3600 dilution of the elution buffer and typically concentrating the protein to 4-9 µg/ul. After dilution approximately 0.05 mM of imidazole remained from the elution of the HIS tagged proteins and 0.003 mM of reduced glutathione from the elution of the GST tagged proteins. Che proteins were induced with the optimum IPTG concentration as concluded from the expression tests, 1.4 mM for CheY-HIS and 0.2 mM for all other proteins.

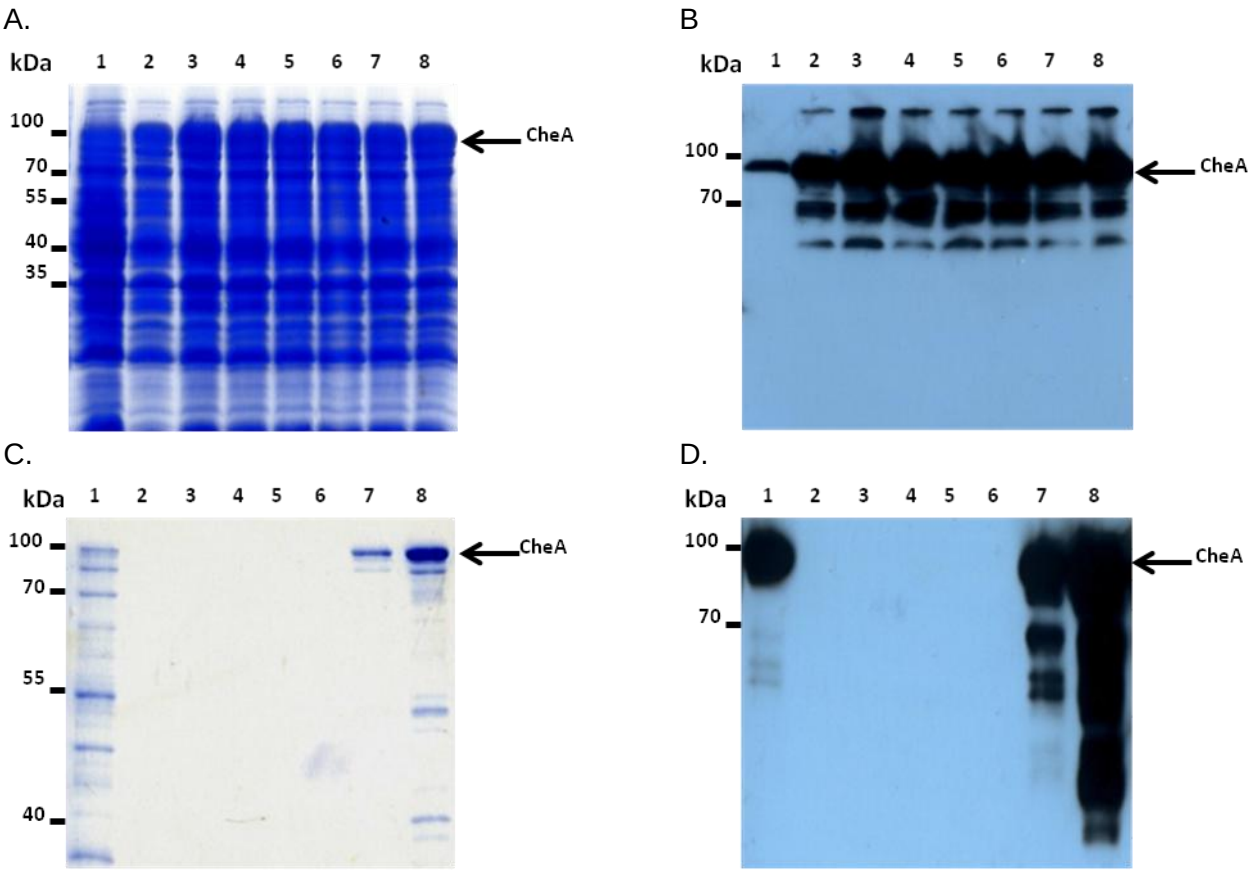

Figure 3.7 Expression and purification of His tagged CheA from suspensions induced at 37 °C. The strain was grown overnight and used to inoculate fresh Luria broth at 1:100, incubated until the suspension reached an OD600 of 0.5 then induced with different concentrations of IPTG at 37 °C. (A) shows a Coomassie stain of an SDS-PAGE gel of IPTG Induction assays against CheA. Lane1 shows the uninduced CheA vector with no IPTG, Lanes 2-8 show the vector with an increasing IPTG gradient from 0.2 mM IPTG in Lane 2, 1.4 mM in lane 8, the IPTG concentration increasing in 0.2 mM increments. (B) shows the western blot corresponding to the SDS-PAGE of (A), lanes were loaded in the same order, the membrane was blotted using anti-HIS-HRP. (C) shows a purification of HIS tagged CheA, Lane 1 shows the first flow through of the cell lysate containing CheA, Lanes 2-6 show successive washes with universal binding buffer, Lane 7 shows the elution of CheA and lane 8 the buffer exchanged and concentrated CheA. (D) shows a western blot corresponding to the SDS-PAGE of (C), lanes were loaded in the same order and the membrane was blotted using anti-HIS-HRP.

Minor contaminants do appear in the background for all of the HIS tagged proteins, however CheY, CheV, A-RR and CheR purified well enough for use in the planned assays, as they appeared on Coomassie stained SDS-PAGE gels (Fig.3.8), they have produced a clear band at the molecular weight predicted for each protein and had not required additional steps to solubilise the proteins. Proteins which had blotted with anti-HIS-HRP could be identified as breakdown products as they had retained the HIS tag of the cloned protein, whereas those which did not may still be breakdown products but as they have lost the affinity tag they cannot be identified as such, and so were labelled as contaminants. The GST tagged proteins CheY, CheV and $CheA^{HK}$ purified well enough for use in the planned assays, as they appeared on Coomassie stained SDS-PAGE gels, as they have produced a single band at the molecular weight predicted for each protein with only very low level contamination visible in the background (Fig 3.9). Despite repeated attempts to purify CheB no band was observed for CheB in any of the purifications, only minor contaminating bands appeared (Fig.3.8*G*). The proteins were excised from SDS-PAGE gels and subjected to MALDI-TOF mass spectrometry, which confirmed their identity (The Protein Nucleic Acid Chemistry Laboratory, UK) (Data not shown).

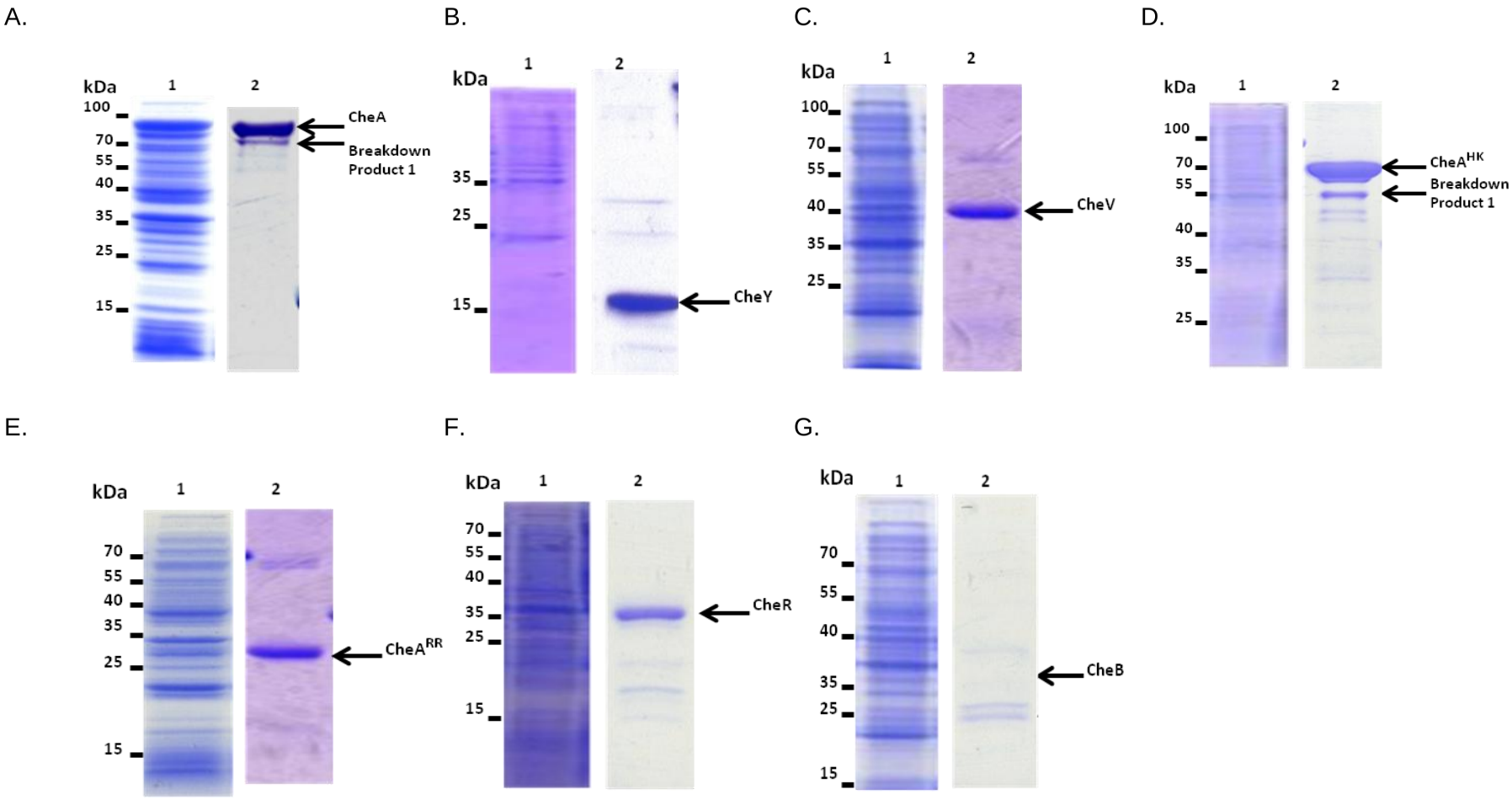

Figure 3.8. Coomassie stained SDS-PAGE gels to assess the purity of the purified HIS tagged Che proteins. Expression strains were grown overnight and used to inoculate 500 ml of Luria broth at 1:100, incubated until the suspension reached an OD600 of 0.5 then induced with IPTG at 30 °C. Che proteins were purified by affinity tag chromatography and then buffer exchanged into protein storage buffer and concentrated. The proteins displayed are HIS tagged (A) CheA (B) CheY (C) CheV (D) $CheA^{HK}$ (E) $CheA^{RR}$ (F) CheR (G) CheB. All panels show induced whole cell lysates (Lane 1) containing Che expression plasmid paired to (Lane 2) which shows the purified protein. The predicted molecular weight of the proteins shown is as follows: CheA (89.36 kDa), CheY (18.4 kDa), CheV (39.83 kDa), $CheA^{HK}$ (60.19 kDa), $CheA^{RR}$ (36.3 kDa), CheR (34.71 kDa), CheB 24.25 (kDa).

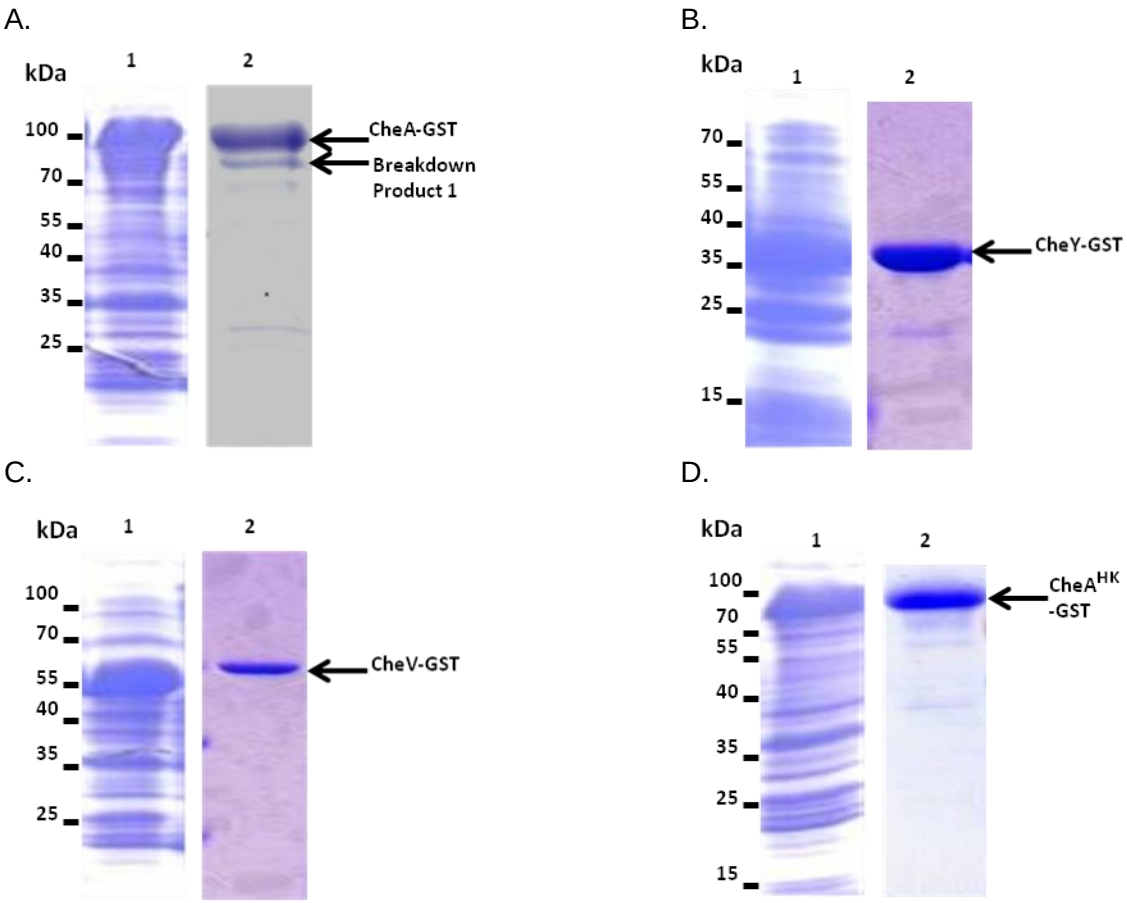

Figure 3.9. Coomassie stained SDS-PAGE gels to assess the purity of the purified GST tagged Che proteins. All proteins shown were GST tagged a) CheA-GST b) CheY-GST c) CheV-GST d) $CheA^{HK}$-GST. Expression strains were grown overnight and used to inoculate 500 ml of Luria broth at 1:100, incubated until the suspension reached an OD600 of 0.5 then induced with IPTG at 30 °C. Che proteins were purified by affinity tag chromatography and then buffer exchanged into protein storage buffer and concentrated. Lane 1 of panels (A), (B), (C) and (D) show induced whole cell lysates containing Che expression plasmid paired to Lane 2 which shows the purified protein. The predicted molecular weights of the proteins shown is as follows: CheA-GST (112.12 kDa), CheY-GST (41.56 kDa), CheV-GST (62.68 kDa) and $CheA^{HK}$ (83.86 kDa).

3.2.3. TLP Expression and Purification Results

HIS Tagged TLP Cytoplasmic Domains

GST tagged TLP_1 and TLP_{2-4} expression vectors had been constructed in a previous study (Sandhu 2011), these constructs contained only the cytoplasmic portion of the TLP proteins, which is predicted to be soluble and therefore should not cause the protein to form aggregates during over expression. Membrane association or formation of aggregates would be problematic for expression and purification of the TLP proteins. The GST tagged TLP constructs had previously been PCR verified and sequenced to confirm the insert had the correct sequence. When induced the the TLP expression clones had been found to produce amounts of each cloned protein clearly visible by Coomassie staining on SDS-PAGE gels. The SDS-PAGE gel in Figure 3.10 shows whole cell lysates of induced TLP_{2-4} (Lane1) and TLP_1 (Lane2), which both show a distinct band at the predicted molecular weight of the protein, 63 kDa for TLP_1 and 65 kDa for $TLP_{2-4.}$ The bands observed for both TLPs corresponded to those they had seen during western blot analysis using anti-GST-HRP, which strongly suggested these were the expressed GST tagged TLP cytoplasmic domains. Extensive efforts had been made during the previous study, to purify the GST tagged TLP_1 and TLP_{2-4} cytoplasmic domains (Sandhu 2011) but multiple sequential steps had been required to purify the protein and each successive step had given diminishing returns. Cleavage of the GST tag would be required before the use of TLP_1 or TLP_{2-4}, and as cleavage had not been achieved during the course of the earlier study, it was decided instead to construct HIS tagged expression vectors for both of the TLP cytoplasmic domains.

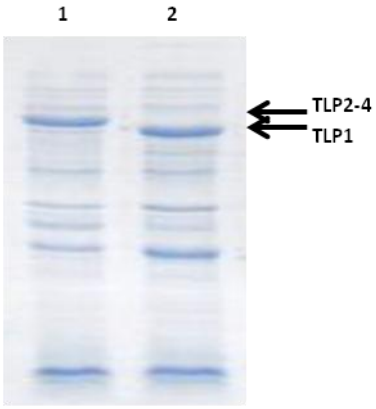

(Sandhu 2011)

Figure 3.10. Coomassie stained SDS-PAGE of induced GST tagged TLP1 and TLP2-4 expression clones. Expression strains were grown to an OD_{600} of 0.5, then induced with 1.5 mM IPTG for 3 hours at 30 °C. Lane 1 contains TLP_{2-4}-GST cell lysate, Lane 2 contains TLP_1-GST cell lysate.

The induced HIS tagged TLP_1 did not display a distinct band on an SDS-PAGE gel however the corresponding western blot using an anti-HIS-HRP antibody did show a band at 40 kDa, the predicted molecular weight of HIS tagged TLP_1 (Fig.3.11*A*). The putative TLP_1 band is not visible in Lane 1 containing Rosetta™ without the pTrcHisB vector, strongly suggesting that the band present in Lanes 2-4 is the polyhisitdine tagged TLP_1. TLP_1 was visible in lane 2 despite the lack of IPTG. Addition of IPTG increased production of the putative TLP_1 protein but the peak of production appeared at 0.2 mM rather than 1.4 mM. No proteolysis is apparent from the western blot shown in Fig. 3.11A.

Affinity chromatography of TLP_1 from cell lysate resulted in a purified polypeptide with no significant contamination visible on an SDS-PAGE gel post buffer exchange and sample concentration Fig. 3.11*B*. The purified band migrated at the predicted molecular weight of TLP_1 (Fig.3.11*B*).

Affinity chromatography of TLP_{2-4} from cell lysate produced two distinct bands under Coomassie staining (Fig.3.11*C*), the bands were of equal density and

otherwise showed no obvious background contamination (Lane 8). The upper most band ran at approximately 40 kDa, the predicted molecular weight of TLP_{2-4}, the lower band ran at approximately 30 kDa. Both bands were later analysed by mass spectrometry, the 40 kDa band was found to be the HIS TLP_{2-4}, the 30 kDa band was found to be the *E. coli* 50S ribosomal protein RL2. Repeated attempts to purify TLP_{2-4} all found it to co-purify with RL2, pre-treatment of the sample with 8 M Urea, 0.2% (v/v) Triton-X-100 or 1.5% (v/v) Triton-X-100 failed to prevent co-purification of RL2 with $TLP_{2-4,}$ the proteins maintained an equal concentration with either treament. The addition of 10 mM DTT to the TLP_{2-4}/RL2 sample before incubation at 90 °C for 30 minutes separated the proteins so that when the treated sample was again purified by affinity chromatography, a pure, soluble TLP_{2-4} sample without RL2 contamination was achieved (Fig.3.11*D*). The proteins were subsequently subjected to MALDI-TOF mass spectrometry which confirmed their identity.

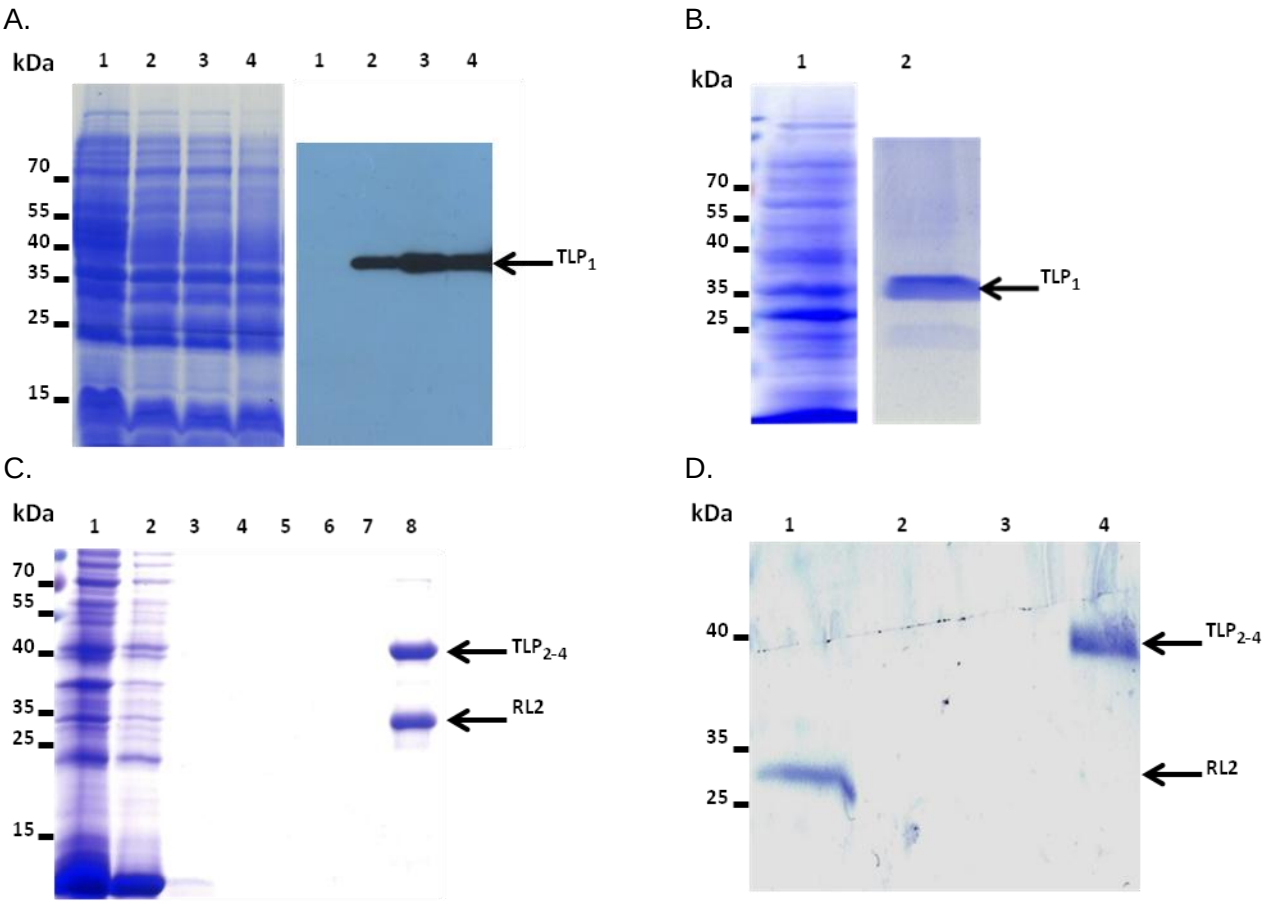

Figure 3.11 Expression and purification of HIS tagged TLP_1 and TLP_{2-4}. (A) shows an SDS-PAGE gel and its corresponding anti-HIS-HRP western blot, of an IPTG Induction assay against HIS tagged TLP1. The strain was grown overnight and used to inoculate fresh Luria broth at 1:100, incubated until the suspension reached an OD600 of 0.5 then induced with different concentrations of IPTG. Lane 1 shows a Rosetta™ strain without an expression plasmid and induced with 1.4 mM IPTG, Lane 2 shows the TLP1 vector with no IPTG, Lanes 3 and 4 shows the strain plus 0.2 mM and 1.4 mM IPTG respectively. (B) is a Coomassie stained SDS-PAGE gels of an induced whole cell TLP1 lysate paired, on the left, paired with the purified protein protein on the right. (C) shows the initial purification of TLP2-4, Lane1 is the first flow through of the cell lysate containing TLP2-4, Lanes 2-7 show successive washes with universal binding buffer, Lane 8 shows the elution of TLP2-4 with HIS elution buffer, and the co-elution of RL2. (D) is the post DTT heat treated TLP2-4 sample after being affinity purified again. Lane 1 is the flow through of the sample containing TLP2-4 and RL2, Lanes 2 and 3 are washes using universal binding buffer, Lane 4 shows the elution of pure TLP2-4. The predicted molecular weight of TLP_1 is 39.85 kDa, TLP_{2-4} is predicted to be 39.53 kDa.

.

3.3. Discussion

Purified Che and TLP proteins would be required to perform the planned *in vitro* kinase and affinity assays between the chemotaxis proteins. To acquire the purified proteins it was necessary to clone the genes into expression vectors, to test their expression under induction by IPTG and then to purify the expressed Che and TLP proteins using affinity tag chromatography.

An ORF library of sequenced expression clones had been available from Source Bioscience, but their clones contained an N-terminal GST tag and a HIS tag. The clones possessed an enterokinase cleavage site downstream of the GST tag but also a HIS tag downstream of the cleavage site, therefore any cleaved protein would have retained that HIS tag. As differential tagging would be required for the affinity assays, and which affinity tag would be used had yet to be decided, the ORF library was considered to be unsuitable.

Cloning of *che* genes

No difficulties were encountered during cloning from the *C. jejuni* NCTC11168 genome, the design of the primers gave allowance for the frequent occurrence of repeat tracts in the *C. jejuni* genome and the primers were lengthened to avoid the lower T_m found in primers designed to hybridise to regions of high A:T content.

Post electroporation into Rosetta cells, the majority of transformed cells were found to be positive for the relevant *che* gene when tested by colony PCR. The majority of the colony PCR positive *che* clones were also found to have a correct,

in frame *che* gene ORF when sequenced, the success of the cloning protocol was probably due to the exceptionally low error rate (4.4×10^{-7}) of the Phusion™ polymerase used.

Expression vectors for all of the required Che and TLP proteins were successfully produced.

Che and TLP Protein Expression

Expression vectors had previously been induced and incubated at 37 °C but due to the proteolysis initially observed during CheA expression and purification the incubation temperature was reduced to 30 °C (Fig.3.7). The reduced induction temperature improved the stability of CheA and did not severely reduce production of CheA. The induction temperature was reduced to 30 °C for all of the Che and TLP proteins.

The results at this point indicated that all of the *che* and *tlp* vectors were producing their chemotaxis proteins and that these had fused to their affinity tags. Although SDS-PAGE gels of the expression tests had only shown distinct bands for GST tagged proteins, and not for the HIS tagged proteins, the corresponding western blots using antibody specific to the affinity tags had blotted bands of the correct predicted size for all Che and TLP proteins. That these blotted bands were not visible in Lane 1 of each of the gels, where Rosetta™ without an expression vector was run, suggested that these bands were not products of the Rosetta™ cells but were the product of the *che* and *tlp* expression vectors.

Expression from the HIS vectors resulted in little obvious proteolysis, proteolysis was more of a problem for GST tagged proteins, with: CheA, CheY, CheV and

CheA^{HK} showing breakdown products (Fig.3.3). It is important to note that the affinity tag to which the HRP conjugated antibodies bind, is fused to the N-terminal of each the protein, therefore any proteins degraded from the N-terminal end may be present but would not be visible by western blotting.

For the majority of the clones the peak of Che or TLP production was at 0.2 mM IPTG, only HIS tagged CheY saw an increase in production when the IPTG concentration was increased from 0.2 mM to 1.4 mM, the reasons why this should be are unclear. The HIS tagged CheV construct displayed a decrease in CheV production, apparent from the western blot (Fig.3.5), and a decrease in total protein present, it is not possible to say whether this could have been due an actual fall in the mass of protein produced by each cell or a reduction in the number of cells possibly due to a combined toxic effect of CheV production and/or IPTG toxicity. It was notable that CheV suspensions consistently grew to lower densities than those of other expression vectors.

All of the HIS vectors 'leaked', they allowed transcription and so protein production from the affinity tag and MCS insert before the addition of IPTG, a problem not observed for any of the GST tagged proteins. That the cloned protein was produced despite the lack of induction by IPTG could have implications for storage of the HIS vectors in the Rosetta™ as this may cause selective pressure against the *che* insert and/or the affinity tag, perhaps selecting for a mutation within the promoter or tag which could permanently prevent translation and transcription from the cloned ORF or translate a truncated Che protein.

Che and TLP Protein Purification

All of the Che and TLP proteins, with the exception of the HIS tagged CheB had purified adequately enough for the use in the planned *in vitro* assays. As the cloned proteins had been found in the soluble fraction of cell lysates and had not been packaged into inclusion bodies, this gave greater confidence that the proteins were in a native conformation. Although it is easier to get a high level of purity from protein from inclusion bodies, the proteins require re-solubilisation and then refolding to get the protein into an 'active' conformation. After these processes it is impossible to be certain that the conformation of the protein is correct, if a sample of the relevant Che protein in the correct conformation was available it may be possible to compare the tryptophan resonance of a new preparation to a standard, but without that standard with which to compare, it cannot be known for certain.

The identity of all of the purified chemotaxis proteins, HIS and GST tagged, was confirmed by excision of a bands from an SDS-PAGE gels and then MALDI-TOF mass spectrometry.

The quantity of Che or TLP protein produced by HIS tagged pTrcHisB clones, was much less than that of GST vectors containing the same cloned gene. However, the total yield from HIS vectors was easily increased by increasing the total volume of Luria broth and so further optimisation was not necessary to increase the total mass of Che protein produced to a practical level for batch purification. Typically GST tagged proteins were grown in 100 ml of Luria broth, whereas the same HIS tagged protein would need to be grown in 500 ml of Luria broth.

Proteolysis was a greater issue during initial expression and purification attempts but reduction of the induction temperature from 37 °C to 30 °C and a greater stringency toward maintaining a low temperature during the purification steps, prevented much of the proteolysis of CheA and $CheA^{HK}$ seen in earlier assays (data not shown). Breakdown products which may have been degraded from the N-terminal end would not be visible on western blots, these were not a concern post purification as the loss of the N-terminal of the protein would also exclude them from purification as the affinity tag was lost. Breakdown products which did retain an affinity tag would co-purify with full length protein, however these were not a cause for concern as they would also be detected by western blotting.

The attempted purification of CheB did not produce a band at the predicted molecular weight, despite previously having been present on the western blot during the expression tests, only two contaminating bands were seen (Fig.3.8). Possibly the HIS tag had been obscured by the CheB protein and so prevented the HIS tag from binding to the Nickel resin during purification.

The CheB sample had to be denatured to be analysed by SDS-PAGE, it may be that denaturation exposed the HIS tag so that in the western blots it would be visible although during the purifications it had actually been obscured. Alternately, it may have been that CheB was in the insoluble fraction of the cell lysate so that when the cells were lysed and centrifuged before purification, CheB was discarded along with the pellet.

If CheB was present in the pellet in inclusion bodies, it could easily have been purified from these, unfortunately due to time constraints these fractions were not analysed by SDS-PAGE or western blot so the question cannot be answered.

TLP_1 and TLP_{2-4} tagged with GST were found to be unsuitable for purification, both TLPs were insoluble associating with the pellet after cell lysis (Sandhu 2011). Re-solubilisation and refolding protocols did not appear to result in a correct conformation as the GST tag, whose activity is predictable and measurable, did not retain its normally high affinity on the purification column. Fortunately the HIS tagged TLPs had been found to associate with the soluble faction after cell lysis and had been much easier to purify.

TLP_{2-4} had co-purified in equal amounts with a ribosomal protein RL2. TLP_{2-4} and RL2 were successfully separated heating to 90 °C with 10 mM DTT, however as this suggested the proteins had been covalently linked and also that the treatment required to separate the proteins was probably denaturing, it was decided not to use TLP_{2-4} in pull-down assays. Given more time it may have been possible to show a functional conformation of TLP_{2-4} by assaying its interaction with CheV. HIS TLP_1 was successfully purified, however the level of purity achieved in Figure 3.11 could not be repeated in subsequent attempts, fortunately this did not exempt its use in the planned affinity assays.

Conclusion

In summary all the pGex-4T-1 and pTrcHisB vectors produced Che and TLP proteins which could easily be purified from them, with the exception of CheB and TLP_{2-4}, the purified proteins did not contain contaminants which could predictably

cause issues when used in later assays, and also could be buffer exchanged and concentrated without excessive proteolysis. The identity of all of the cloned proteins was confirmed by mass spectrometry, details can be found in the appendix, therefore these clones and the proteins produced by this expression and purification method were suitable for the intended phosphorylation and affinity assays. As $TLP_{2\text{-}4}$ and CheB could not be purified without further efforts and their absence did not obstruct the overall aims, the decision was made to continue without them.

Chapter 4: Characterisation of CheA Kinase Activity

4.1. Introduction

To understand the signal transduction properties of the Che system in *C. jejuni*, it would be necessary to characterise phosphate transfer interactions between CheA and the predicted response regulators of CheY, CheV and CheA's own response regulator domain ($CheA^{RR}$).

The predicted Che response regulators had been successfully expressed and purified in Chapter 3. To characterise Che kinase interactions would require the development of an *in vitro* assay to detect transfer of phosphate between these purified proteins.

4.1.1. Development of the *in vitro* Phosphate Transfer Assay

My preliminary attempts to observe Che response regulator phosphorylation had used native non-denaturing PAGE gels and Acrylamide-pendant Phos-tag™, however these methods were unsuited to this application for numerous reasons, including the nature of the Che proteins.

A widely used radiolabelling method was settled upon to observe phosphate transfer from CheA to response regulators. ATP with a gamma phosphate group

radiolabelled ([γ-^{32}P] ATP), was used to locate the phosphate group after it has been removed from ATP by CheA^{HK}, and passed to a response regulator. The CheA^{HK} and a response regulator were mixed in the presence of [γ-^{32}P] ATP diluted with unlabelled ATP, in reaction buffer (50 mM Tris, 75 mM KCl, 75 mM $MgCl_2$, 1 mM DTT), samples taken at intervals and the reaction halted by adding an equal volume of sample loading buffer, and heat treating the sample at 98 °C for 20 minutes in a G-Storm GS1 thermocycler.

Sample loading buffer denatures proteins therefore preventing further phosphate transfer, including autophosphorylation of the CheA^{HK} domain, transfer of phosphate from the CheA^{HK} to a response regulator or hydrolysis of Pi from a response regulator. To give a snapshot of the location of the ^{32}P molecules at the point each sample was taken, the samples were loaded sequentially onto an SDS-PAGE gel, the proteins were separated by SDS-PAGE and the gel dried and visualised using X-ray film (Kodak, UK).

Labelled ATP, ADP and Pi were present in each sample but would run through the polyacrylamide gel and not be retained, therefore a signal was emitted only from the points on the gel to which a protein modified with ^{32}P had migrated. This method was suitable to test the autophosphorylation of the CheA histidine kinase domain and CheA dependent phosphorylation of CheY, CheV and the CheA RR domain.

All of following assays used HIS tagged Che proteins unless stated otherwise, the HIS tag was not removed from any Che proteins for any of the assays.

4.1.2. CheA v.s. CheY Individual Assays

Initial tests centred on the CheA-CheY kinase interaction as this phosphate transfer was central to the known chemotaxis systems that use a Che protein transduction system and so could be used to establish and optimise the assay.

In the first set of assays CheA and CheY were exposed to [γ-^{32}P] ATP individually and in combination, to test that CheA could autophosphorylate and to show that if CheY did become phosphorylated, that it was CheA dependant (Fig.4.1*A*). Neither CheA, CheY nor the combined proteins produced a radioactive signal without the addition of [γ-^{32}P] ATP, showing that any radioactive signal in other lanes originated from the [γ-^{32}P] ATP. In lane 3 in which CheY was exposed to [γ-^{32}P] ATP without CheA present, no radioactive signal was observed demonstrating that CheY could not accept Pi directly from ATP. Interestingly CheA and CheY in combination with [γ-^{32}P] ATP did not produce a band for either protein (Lane 5), whereas CheA alone with [γ-^{32}P] ATP demonstrated autophosphorylation of CheA (Lane 6). Therefore using CheA and CheY demonstrated that phosphorylation depended on the presence of labelled ATP and that in contrast to CheA, CheY was not able to autophosphorylate from ATP, nevertheless it was not possible to detect phosphorylation of CheY by CheA under these conditions.

4.1.3. CheA vs CheY Time Course Assay

Phosphorylation of CheA had been observed when it was exposed to labelled ATP individually but not when in combination with CheY. As the previous assays

had sampled at only one time point for each of the reactions it was possible that phosphorylation events had occurred but not been observed as the ATP substrate had been exhausted by 20 minutes. To investigate this possibility a CheA and CheY time course was attempted, the proteins were mixed together in the presence of [γ-^{32}P] ATP with multiple samples taken over a 20 minute period (Fig 4.1*B*). At no point during the assay was a labelled band observed for CheA or CheY.

4.1.4. Pre-exposure of CheA to [γ-^{32}P] ATP

Neither CheA nor CheY had been observed to be radiolabelled in the previous assay, despite CheA previously being observed labelled by ^{32}P when incubated with radiolabelled ATP alone. It was speculated that perhaps a large enough proportion of the population of CheY had not become modified by ^{32}P, at one time, to become visible, an increase in the amplitude of the radiolabelled signal was attempted by pre-exposing CheA to [γ-^{32}P] ATP for 20 minutes to allow the majority of the CheA molecules to autophosphorylate, before adding CheY to increase the amount of phospho CheA available to CheY, and so the probability of observing either protein radiolabelled (Fig 4.1*D*). CheA was observed phosphorylated, however when CheY was added no band appeared at its predicted molecular weight of 18.4 kDa, and there was not a decrease in CheA phosphorylation which would be consistent with a transfer to CheY.

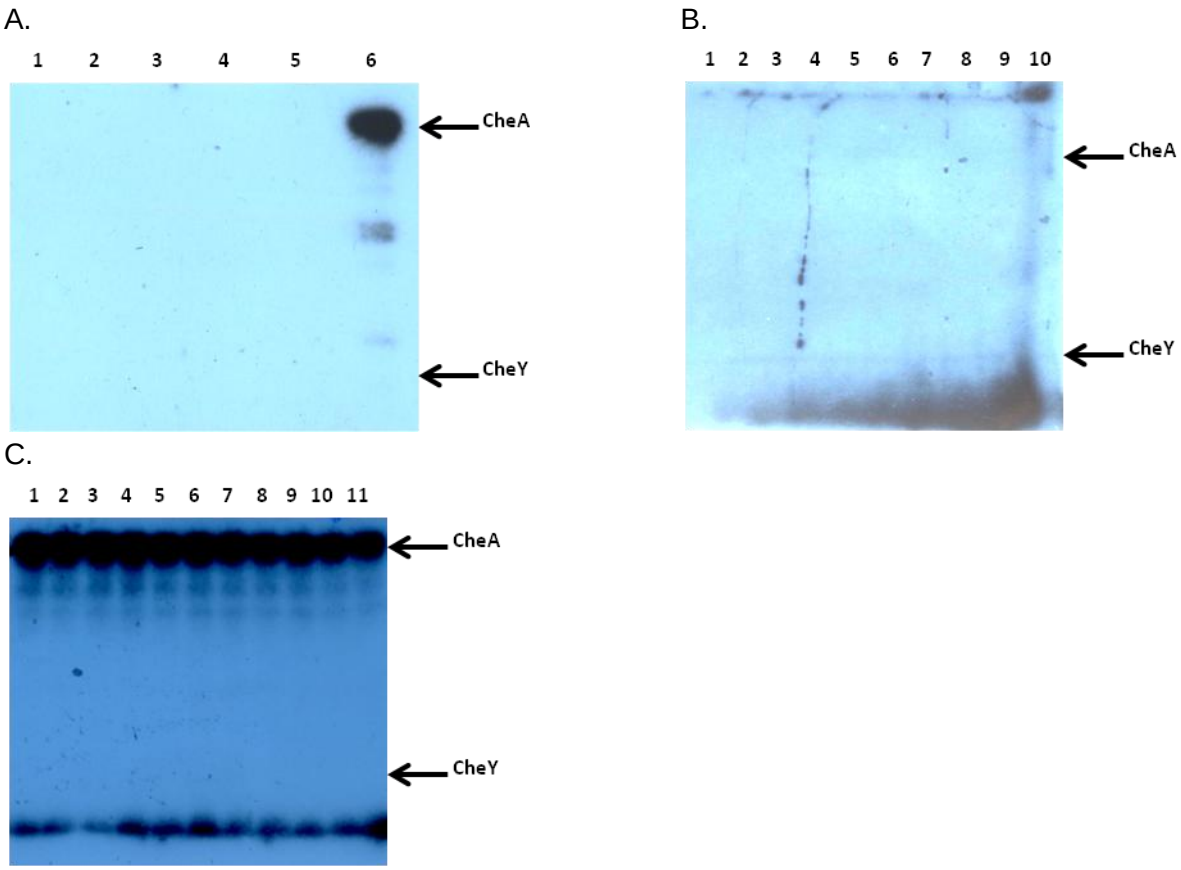

Figure 4.1. Autoradiographs of kinase assays between CheA and CheY. Reactions took place at pH7.6 at room temperature. (A) the results of individual reactions are shown, each was allowed to progress for 15min before the reaction were halted with 5x sample loading buffer with 0.2 M DTT and heat treated at 98 °C for 10 minutes. Each used 0.25 µM undiluted [γ-^{32}P] ATP, where used 10 µM CheY or 2 µM CheA was added. Lane 1 shows CheA alone with no ATP, Lane 2 is CheY alone with no ATP, Lane 3 is CheY alone plus labelled ATP, Lane 4 is CheA and CheY with no ATP, Lane 5 shows CheA and CheY with labelled ATP and Lane 6 shows CheA alone plus labelled ATP (n=3). (B) is a time course kinase assay using 2 µM CheA against 10 µM CheY, both proteins were mixed and 1.5 µM undiluted [γ-^{32}P] ATP added. Samples were taken at 0, 1, 2, 4, 6, 8, 10, 12, 15, 20 minutes, these are shown in Lanes 1-10. As samples were taken the reactions were halted using sample loading buffer and were heat treated at 98 °C for 10 minutes (n=4). (C) is a time course kinase assay using 2 µM CheA against 2 µM CheY, both proteins were mixed and 1.5 µM undiluted [γ-^{32}P] ATP added. Samples were taken at 0, 0.5, 1, 1.5, 2, 2.5, 3, 3.5, 5 and 6 minutes, these are shown in Lanes 1-11 (n=3).

4.1.5. Using the Isolated CheA^{HK} Domain of CheA in Kinase Assays

As some part of the CheA protein had become phosphorylated but was unable to transfer ^{32}P to CheY, it was decided to separate the domains of CheA by creating a clone of just the HK domain (CheA^{HK}) as described in Chapter 3.

CheA^{HK} required testing to ensure that it was functional and able to autophosphorylate. Two time course experiments were carried out in parallel, for both experiments [γ-^{32}P] ATP was added to CheA^{HK}, samples taken immediately after and then at intervals until the 20 minute point (Fig.4.2*A,B*). After 20 minutes CheY was added to one of the assays, whereas the other reaction was allowed to continue. Samples were taken from both timecourses over 2 minutes (Fig.4.2*A,B* Lanes 6-8).

The autophosphorylation of CheA^{HK} was apparent in both time courses. After the addition of CheY at 20 minutes the CheA^{HK} which was not exposed to CheY, appears to maintain a steady level of phosphorylation (Fig 4.2*A* Lanes 6-8), whereas the corresponding samples to which CheY had been added, showed complete dephosphorylation of CheA^{HK} after 30 seconds (Fig.4.2*B* Lanes 6-8). This demonstrated that the separately cloned CheA^{HK} was functional, and could autophosphorylate and interact with CheY. The level of phosphorylation on CheA^{HK} remained at the level attained after 15 minutes. Where CheY was added to a phosphorylated CheA^{HK} it was rapidly dephosphorylated, CheY however was not directly observed during this assay. This may have been due to rapid autodephosphorylation of CheY, insensitivity of the assay or perhaps a

combination of the two factors. Differences in the apparent strength of the radioactive signal between the two timecourse assays may be due to the development times used for each X-ray film rather than reflecting a real difference in the phosphorylation levels.

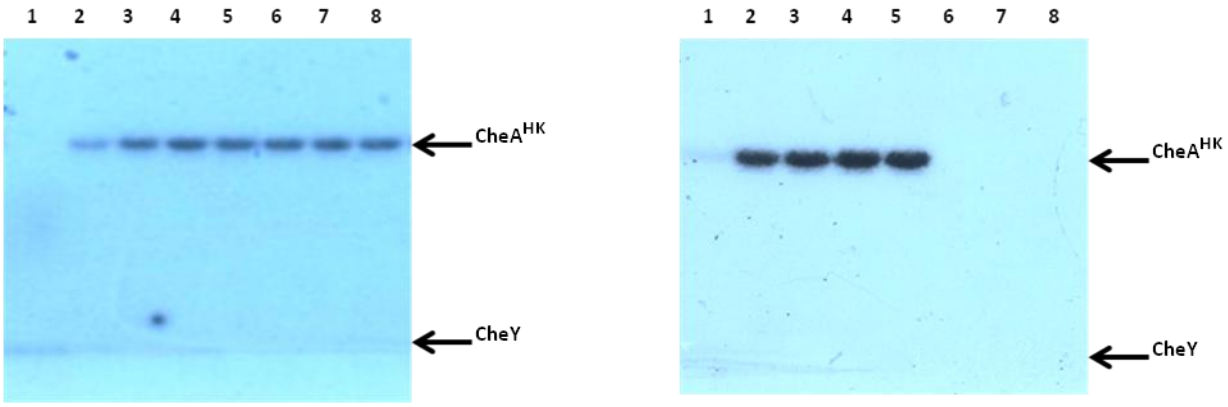

a). b).

Figure 4.2. Autoradiographs of kinase assays between CheA^{HK} and CheY. Both (A) and (B) show time course experiments carried out at pH7.6, at room temperature. Samples were halted with a 5x sample loading buffer with 0.2 M DTT and heat treated at 60 °C for 30 minutes before loading. The assays used concentrations of 20 µM CheA^{HK} and 10 µM CheY, where CheY was used. In both (A) and (B) CheA^{HK} was mixed with 0.^{32} µM [γ-^{32}P] ATP diluted with 39.66 µM unlabelled ATP, samples were taken at 0, 5, 10, 15, 20 minutes (Lanes 1-5). After 20 minutes CheY was added to the reaction in (B), in (A) an amount of reaction buffer was added to keep the reaction volumes equal between the assays. After these additions, samples were taken at 0.5, 1, 1.5 and 2 minutes (Lanes 6-8) (n=2).

4.1.6. Visualising CheY~P With Phosphor Screens

It was apparent from earlier experiments that although CheY must be interacting with $CheA^{HK}$ in a manner which affected $CheA^{HK}$ phosphorylation state, CheY had not been observed receiving Pi from CheA. Due to the apparent poor sensitivity of the autoradiographic method and the impracticalities of film exposure times measured in days/weeks it was decided to use a Typhoon 9400 (Molecular Dynamics) phosphor screen to visualise the radiolabelled proteins.

To compare the detection methods a timecourse experiment was run, intended to be visualised by both autoradiography and phosphor screen methods. As CheY had not yet been observed phosphorylated and because it had been predicted to have such a rapid rate of autodephosphorylation, the choice was made to attempt this experiment using $CheA^{RR}$. $CheA^{RR}$ was predicted to hydrolyse Pi at a much slower rate than CheY, and so would present a greater chance of observing a response regulator become phosphorylated by $CheA^{HK}$. $CheA^{HK}$ was allowed to autophosphorylate with [γ-^{32}P] ATP at room temperature for 10 minutes, the reaction was placed on a Techne Dri-Block DB-2A hotblock (Techne, UK) for 5 minutes to adjust the temperature to 30 °C, a sample was taken at this point to demonstrate $CheA^{HK}$ phosphorylation, $CheA^{RR}$ was added and samples were taken over a 30 minute period (Fig.4.3). Figure 4.3*A* shows an autoradiograph of this $CheA^{RR}$ assay, exposed for approximately 70 hours and developed for >2 minutes. A faint signal around 35 kDa, the correct molecular weight for $CheA^{RR}$, became visible and a corresponding drop in the phosphorylation of $CheA^{HK}$ was

observed, the rate of this decrease was less than that previously observed for CheY.

The phosphor screen method proved much more sensitive than autoradiography, when a phosphor screen was exposed to the same SDS-PAGE gel for approximately 16 hours, a clear band became apparent for $CheA^{RR}$ 30 seconds into the timecourse experiment (Fig 4.3*B* Lanes 3-10).

After the success of the $CheA^{RR}$ phosphorylation assay it was decided to return to CheY, to see if the technique would also be successful for this response regulator. As previously $CheA^{HK}$ autophosphorylated with labelled ATP at room temperature for 10 minutes, then was placed on ice for 5 minutes to reduce the reaction temperature, a sample was taken at this point to demonstrate $CheA^{HK}$ phosphorylation, CheY was added and samples taken at 0, 20, 40 and 60 seconds. The autoradiograph showed only a very faint smudge at the predicted molecular weight (18.4 kDa) of CheY after around 90 hours of exposure (Fig 4.03*C* Lanes 2-5), a phosphor screen exposed to the same SDS-PAGE gel for around 44 hours (Fig.4.3*D*) displayed a weak CheY band (Lanes 2-4), although not as distinctly as had been observed for $CheA^{RR}$ (Fig.4.3*A,B*). An increase in CheY phosphorylation is observed with a peak at 15 seconds, after which the signal weakened but was still visible when the final sample was taken at 46 seconds. The visible CheY band demonstrated that it was binding ^{32}P from $CheA^{HK}$, the increased sensitivity of the phosphor screen would now allow for the two component phosphorylation experiments to proceed.

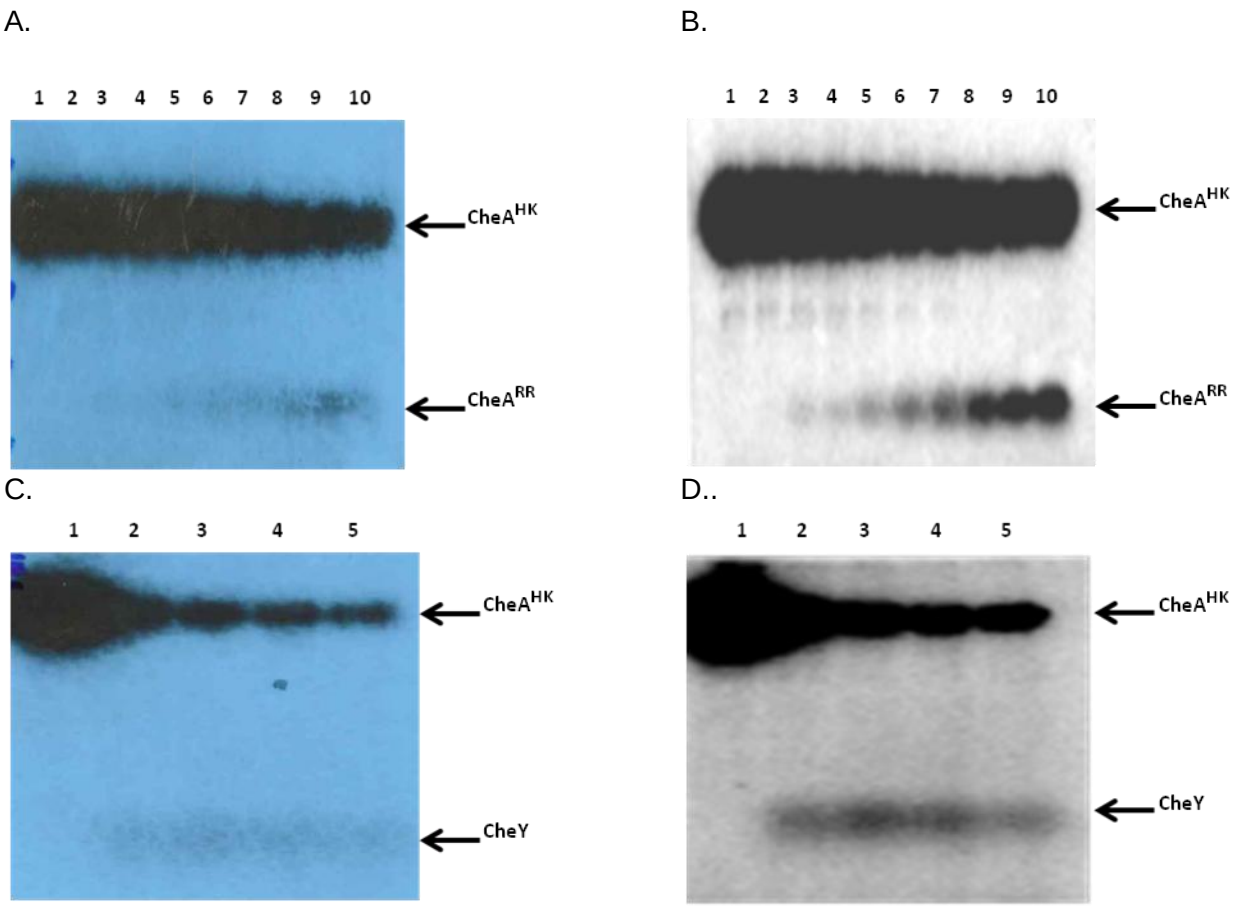

Figure 4.3 Comparison of Autoradiograph and Phosphor screen methods for visualising ^{32}P bound proteins. For the autoradiographic method x-ray film was exposed to a dried SDS-PAGE gel for approximately 70 hours then developed for >2 minutes, for the phosphor screen method, the screen was exposed to the same gel for 44 hours before being scanned. Experiments were carried out in reaction buffer at pH8.3. Samples were halted by addition of 5x sample loading buffer with 0.2 M DTT and heat treated at 60 °C for 30 minutes. (A) and (B) show autoradiograph and phosphor screen visualisations of a kinase assay of CheA^{HK} against CheA^{RR}. 20 µM CheA^{HK} was incubated with 1.3 µM [γ-^{32}P] ATP diluted with 30 µM unlabelled ATP for 10 minutes at room temperature, then for 5 minutes the temperature was adjusted to 30 °C for the assay, then a sample was taken to confirm CheA^{HK} phosphorylation (Lane 1). 20 µM CheA^{RR} was added, a sample was taken immediately after the addition of CheA^{RR} then at 0.5, 1, 2, 3, 5, 10, 20 and 30 minutes (Lanes 2-10) (n=1). (C) and (D) show autoradiograph and phosphor screen visualisations of a kinase assay of CheA^{HK} against CheY. 40 µM CheA^{HK} was incubated with 6 µM [γ-^{32}P] ATP diluted with 0.17 mM unlabelled ATP for 10 minutes at room temperature, then for 5 minutes the reaction was put on ice to reduce the temperature for the assay. A sample was taken to confirm CheA^{HK} phosphorylation (Lane1) and then 15 µM CheY was added. Samples were taken immediately after the addition of CheY, then at 15, ^{32} and 46 seconds (Lanes 2-5) (n=1).

4.1.7. Optimisation of Radiolabelled Sample Treatment

At this point in the study CheA, CheY and $CheA^{HK}$ had been successfully observed phosphorylated, but there was still a lot of variability in results which could not be explained.

Figure 4.4*A,B*, show instances where no band was apparent for CheY that had been exposed to a phosphorylated $CheA^{HK}$, despite a rapid dephosphorylation of $CheA^{HK}$ being observed. In many cases a signal had been detected in the wells or stacking portion of the SDS-PAGE gel, this could have suggested that perhaps the protein was not entering the gel, or that 'free' ^{32}P or [γ-^{32}P] ATP was in some way associating with the gel and not being removed during electrophoresis. The stacking gel/well associated errant signals were found in the lanes for time points at which greatest response regulator phosphorylation had previously been observed, the errant signals were associated with response regulator phosphorylation rather than with 'free' ^{32}P.

To investigate the origins of these errant signals and to test their association with response regulator phosphorylation, protein loading conditions were tested (Fig.4.4*C*). It was hypothesised that perhaps some aspect of the post assay sample preparation was causing these issues. $CheA^{HK}$ was allowed to autophosphorylate for 15 minutes, CheV was added, the reaction continued for 2 minutes and then stopped with sample loading buffer. A number of conditions were tested: sample loading buffer type, DTT concentration and the temperature used during the heat treatment step. Of these samples one gave a positive result

in which phosphorylated CheV was detected, the sample which was diluted with an equal volume of 5x sample loading buffer and had received no heat treatment.

Although the sample loading buffer had prevented autodephosphorylation after treatment, it appeared that the bond between the Pi group and the aspartate residue of the Che response regulators was vulnerable to increases in temperature. The protocol for sample preparation was altered accordingly, samples were diluted with equal volumes of 5x sample loading buffer and kept on ice to minimise Pi loss, until they could be loaded onto SDS-PAGE gels. SDS-PAGE gels were also run at low voltage to prevent excessive heating of the sample. In subsequent experiments little or no signal was detected in the wells or stacking gel.

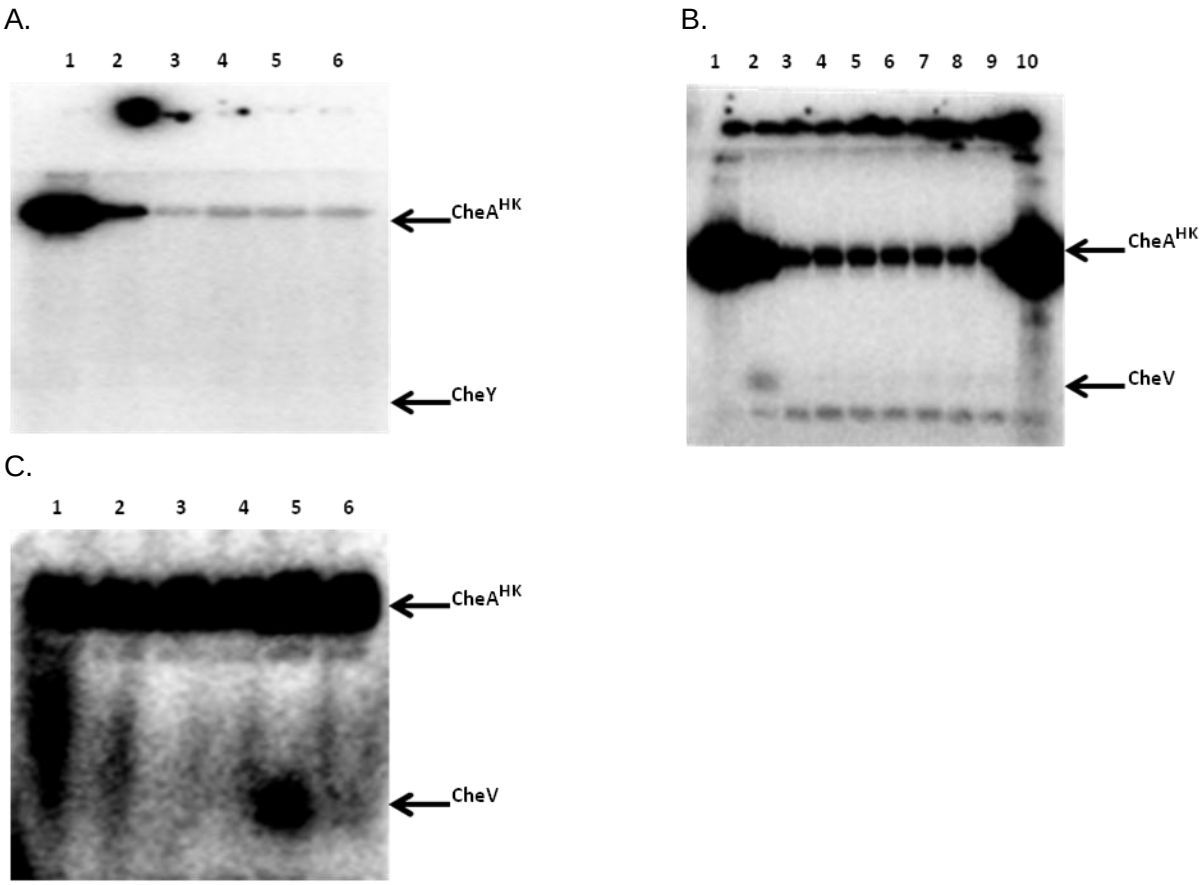

Figure 4.4. Phosphor screen visualisation of kinase experiments. The phosphor screen was exposed to the gel for 44 hours before being scanned. Experiments were carried out in reaction buffer at pH8.3, samples were treated with 5x sample loading buffer with 0.2 M DTT except where stated otherwise. (A) shows a kinase assay of $CheA^{HK}$ against CheY. 45 µM $CheA^{HK}$ was incubated with 6 µM [γ-^{32}P] ATP diluted with 0.17 mM unlabelled ATP for 10 minutes at room temperature, then for 5 minutes the reaction was put on ice to reduce the temperature for the assay. A sample was taken to confirm $CheA^{HK}$ phosphorylation (Lane1) and then 25 µM CheY was added. Samples were taken immediately after the addition of CheY, then at 20, 40, 60 seconds, and 5 minutes (Lanes 2-6) (n=2). (B) shows a kinase assay of $CheA^{HK}$ against CheV. 20 µM $CheA^{HK}$ was incubated with 1.3 µM [γ-^{32}P] ATP diluted with 30 µM unlabelled ATP for 10 minutes at room temperature, then for 5 minutes the reaction was adjusted to 42 °C before the experiment. A sample was taken to confirm $CheA^{HK}$ phosphorylation (Lane1) and then 20 µM CheY was added. Samples were taken immediately after the addition of CheV, then at 0, 2, 5, 10, 20, 30, 40, 50 minutes (Lanes 2-9) HK-15 (Lane 10) (n=2). (C) shows a comparison of sample loading conditions carried out against a $CheA^{HK}$ with CheV kinase reaction. 20 µM $CheA^{HK}$ was incubated with 1.3 µM [γ-^{32}P] ATP diluted with 30 µM unlabelled ATP for 15 minutes at room temperature. A sample was taken to confirm $CheA^{HK}$ phosphorylation (Lane1), treated with 5x sample loading buffer and heated to 60 °C for 30 minutes. The reaction was aliquoted into separate tubes to which 20 µM CheV was added, a sample loading buffer was added to each after 1 minute to halt the reaction, and then different treatment conditions were trialled before the samples were loaded on an SDS-PAGE gel. Before heat treatment a 5x sample loading buffer with 0.2 M DTT was added to each sample unless stated otherwise. In Lane 2 the sample was heated to 60 °C for 30 minutes, in Lane 3 the sample was treated with 2x sample loading buffer and heated to 60 °C for 30 minutes, in Lane 4 the sample was treated with 5x sample loading buffer with 0.4M DTT and heated to 60 C for 30 minutes, in Lane 5 the sample no heat treatment was used, in Lane 6 the sample was heated to 98 °C for 10 minutes, (n=1).

4.1.8. Verifying Kinase Activity

Additional controls were introduced to $CheA^{HK}$ to demonstrate its phosphorylation state pre and post experiment. A sample of the phosphorylated $CheA^{HK}$ was taken and mixed with sample loading buffer at the beginning of the experiment (HK-15) before a response regulator was added, to demonstrate that $CheA^{HK}$ had bound ^{32}P at the beginning of the experiment. A 10µl aliquot was also taken post HK autophosphorylation, and kept under experimental conditions until the final sample from the timecourse had been taken, after which sample loading buffer was added to stop the reaction (HK-END). The HK-END sample demonstrated the phosphorylation state of $CheA^{HK}$ in the absence of a response regulator domain, at the end of the assay.

4.1.9. [γ-^{32}P] ATP Dilution

The phosphorylation experiments had originally been intended as pulse chase assays in which CheA or $CheA^{HK}$ would be exposed to undiluted [γ-^{32}P] ATP for a period before a much larger concentration of non-radiolabelled ATP was added, to dilute the radiolabelled ATP to a point where it was effectively removed from the experiment.

The method creates a pulse of ^{32}P which accurately indicates the rate of phosphate transfer from a histidine kinase to a response regulator and the hydrolysis rates of response regulators for the Pi group. When attempting these experiments a band distinct from both $CheA^{HK}$ and CheY was consistently observed at approximately 35 kDa (Breakdown1) in all lanes (Fig. 4.5).

Breakdown1 was found to be associated with the $CheA^{HK}$ stock as it consistently appeared in HK-15 and HK-END samples as well as in the time points in between, one example is shown (Fig. 4.5). The same purified stock of $CheA^{HK}$, when used in non-pulse chase experiments using 3 µM [γ-^{32}P] ATP diluted with 30 µM of non-radiolabelled ATP, did not produce this Breakdown1 band. The band appeared to sequester all available radiolabel as where the Breakdown1 band was visible, and so phosphorylated, normally phosphorylatable response regulators did not become phosphorylated. The presence of a response regulator, such as CheY, did not reduce the signal from Breakdown1, and the band remained at a constant level of phosphorylation throughout timecourse experiments.

When purified $CheA^{HK}$ had been Coomassie stained on SDS-PAGE gels there had occasionally been a very faint band visible at the same approximate kDa as the breakdown1 band. When an older purified preparation was electrophoresed again this band appeared more pronounced suggesting it may be a breakdown product of $CheA^{HK}$. MALDI-TOF data confirmed it as a breakdown product of the $CheA^{HK}$ protein. Identified fragments mapped to the catalytic domain of $CheA^{HK}$ and confirmed the loss of the HPT domain (Fig. 4.06). If this breakdown product does represent the Breakdown1 band seen in phosphorylation experiments, the breakdown product may be able to bind ATP but then appears unable to trans-phosphorylate to a CheA HPT domain to release its ATP or transfer a Pi group to a response regulator, hence is stably phosphorylated even in the presence of response regulators.

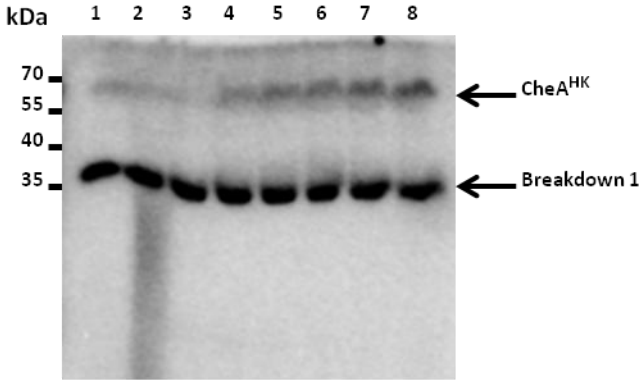

Figure 4.5 Phosphor screen visualisation of a phosphorylated CheA breakdown down product during a pulse chase assay. The phosphor screen was exposed to the gel for 44 hours before being scanned. Experiments were carried out in reaction buffer at pH8.3, samples were treated with 5x sample loading buffer with 0.2 M DTT and kept on ice before loading onto an SDS-PAGE gel. The experiment was carried out on ice at pH8.3. 40 µM $CheA^{HK}$ was incubated with 3 µM of undiluted [γ-^{32}P] ATP for 2 minutes. 1 mM of unlabelled ATP was added and the reaction mixed well, before 15 µM CheY was added. A sample was taken immediately after CheY was added (Lane 1), then at 0:20, 0:40, 1:00, 1:20, 2:00, 5:00 and 10:00 minutes (Lanes 2-8) (n=3).

Figure 4.6. Peptide fragments identified by MALDI-TOF analysis of Breakdown 1 map to CheA^{HK}. Breakdown 1 was excised from an SDS-PAGE gel and submitted for mass spectrometry to the Protein Nucleic Acid Chemistry Laboratory. This Figure shows the amino acid sequence for CheA^{HK}, underlined portions represent the peptide fragments identified by MALDI-TOF after trypsin digest of the protein. CheA^{HK} Functional domains are shown above the sequence.

4.2. Conclusion

After considerable efforts the assay had been optimised, the data shown represents the main issues encountered in establishing the assay, but it is not exhaustive. Other notable issues included: buffer composition, the temperatures of assays, the concentrations of proteins used, BSA inclusion in reactions, gel drying issues, proteolysis of CheA, sampling timing and frequency and gel shrinkage.

With the phosphorylation assay now made suitable for use, the two component interactions of CheA with CheY, CheV and $CheA^{RR}$ could be properly examined.

Kinase assays were now to be retested using the following optimised conditions $CheA^{HK}$ was allowed to autophosphorylate in the presence of 3 µM [γ-^{32}P] ATP, in the presence of 30 µM non-radiolabelled ATP, for 15 minutes in reaction buffer (50 mM Tris, 75 mM KCl, 75 mM $MgCl_2$, 1 mM DTT) and HK-15 and HK-END samples were taken. 10 µl samples were taken at intervals and aliquoted into tubes preloaded with 10 µl of chilled 5x sample loading buffer and stored on ice until loaded onto an SDS-PAGE gel. SDS-PAGE gels were dried as previously on a dry vacuum pump for 3 hours and overlayed with a phosphor screen for approximately 16 hours before the screen was scanned using the Typhoon 9400.

4.3. Optimised Kinase Assay Results

4.3.1. CheA is a Histidine Kinase Which Can Phosphorylate CheY

The following assays were used to investigate the kinase interaction between the histidine kinase domain of CheA and CheY, the $CheA^{HK}$-CheY phosphate transfer rate and autodephosphorylation of CheY.

Due to the rate at which CheY had been observed to strip phosphate from $CheA^{HK}$ and hydrolyse its Pi group, CheY assays were performed on ice to slow reactions to an observable rate. Reactions used 40 µM $CheA^{HK}$ and 15 µM HIS tagged CheY, to maximise the pool of ^{32}P available to CheY through phosphorylated $CheA^{HK}$. $CheA^{HK}$ was allowed to autophosphorylate with radiolabelled ATP at room temperature for 10 minutes, then put on ice for 5 minutes to cool the reaction, HK-15 and HK-END samples were taken, CheY was added and samples were taken at 0, 0:20, 0:40, 0:60, 1:20, 2, 5 and 10 minute time points (Fig.4.7*A*).

At the zero time point, where the sample was taken immediately after the CheY had been added to the reaction, maximum phosphorylation of CheY was observed. Most of the ^{32}P has been hydrolysed from CheY after 5 minutes but there was still weak signal present, no signal was observed after 10 minutes. A large fall in $CheA^{HK}$ phosphorylation was visible at the 0 time point (Fig.4.7*A* Lane 2), immediately after CheY had been added. After 20 seconds all of the ^{32}P appears to have been transferred from $CheA^{HK}$ to CheY (Lane 3), however

following 1 minute incubation a weak $CheA^{HK}$ band was visible and was maintained up to the 5 minute time point (Lanes 5-8), this was only observed in one experiment. The HK-15 and HK-END controls (Lanes 1 and 10) verified $CheA^{HK}$ autophosphorylation, and that loss of phosphate from $CheA^{HK}$ was due to transfer of ^{32}P to CheY and not autodephosphorylation of $CheA^{HK}$.

4.3.2. CheA Can Phosphorylate CheV

The following assays were used to investigate the kinase interactions between the histidine kinase domain of CheA and CheV, $CheA^{HK}$ -CheV phosphate transfer rate and autodephosphorylation of CheV.

CheV phosphorylation assays used a 1:1 ratio of 20 µM $CheA^{HK}$ and 20 µM HIS tagged CheV. $CheA^{HK}$ was autophosphorylated at room temperature for 10 minutes, this master mix was then either put on ice or into a hot block for 5 minutes to reach to desired temperature. HK-15 and HK-END samples were taken before CheV was added and samples were taken at intervals over 20 minutes. The assay was carried out on ice or at 42 °C. As the body temperature of the usual *C. jejuni* chicken host is 42 °C this temperature was considered to be more physiologically relevant. At 42 °C Immediate phosphorylation of CheV was observed at the 0 time point (Fig.4.7*B* Lane 2), CheV appeared to be completely dephosphorylated after 30 seconds. A marked decrease in the level of $CheA^{HK}$ phosphorylation was observed at the zero time point and almost complete dephosphorylation after 30 seconds, although this low level of phosphorylated $CheA^{HK}$ was observed for the remainder of the experiment. The HK-15 and HK-END controls (Lanes 1 and 14) verified $CheA^{HK}$ autophosphorylation, and that

loss of phosphate from $CheA^{HK}$ was due to transfer of ^{32}P to CheV and not autodephosphorylation of $CheA^{HK}$.

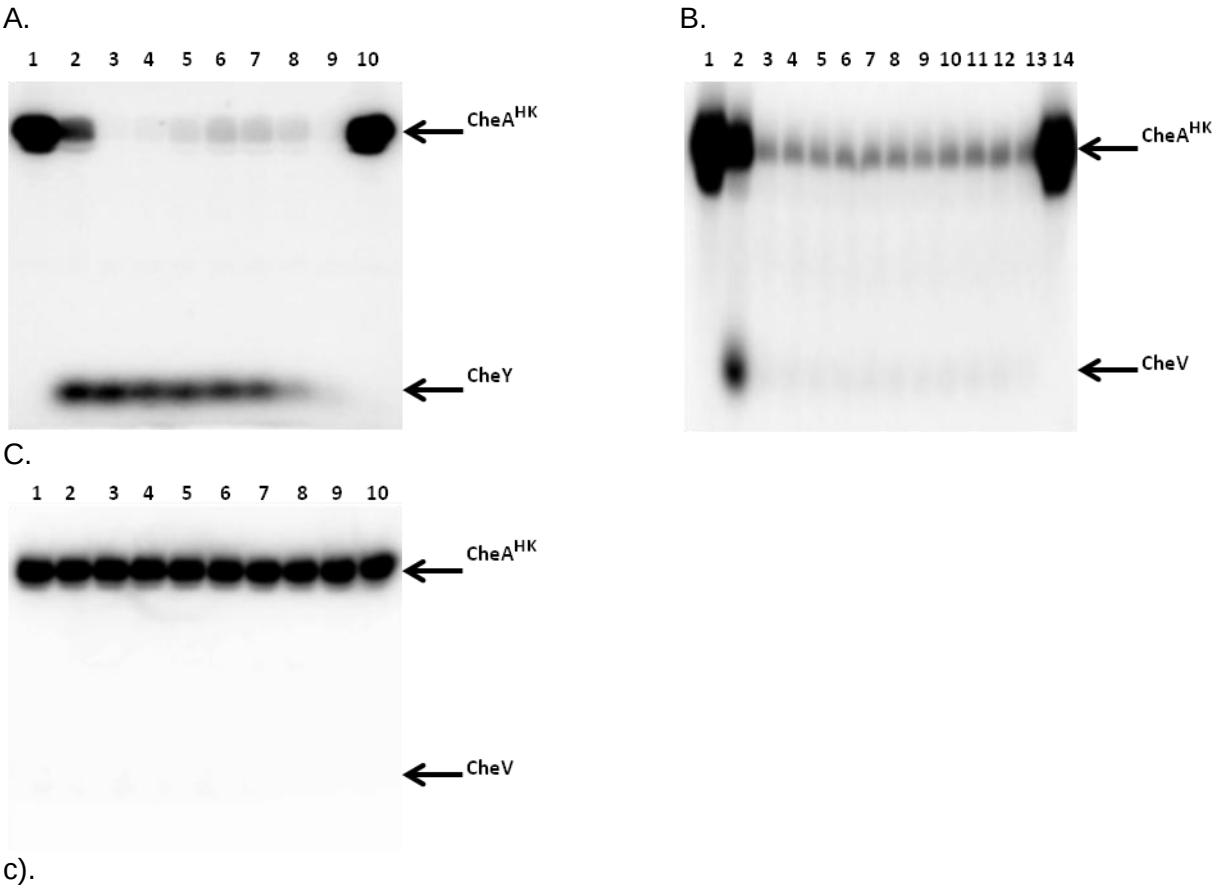

c).

Figure 4.7. Phosphor screen visualisation of $CheA^{HK}$ phosphate transfer to CheY and to CheV. Phosphor screens were exposed to gels for 44 hours before being scanned. Experiments were carried out in reaction buffer at pH8.3, samples were treated with 5x sample loading buffer with 0.2 M DTT and kept on ice before loading onto an SDS-PAGE gel. (A) shows a kinase assay between 40 µM $CheA^{HK}$ and 15 µM CheY, carried out on ice. $CheA^{HK}$ was incubated with 3 µM [γ-^{32}P] ATP diluted with 30 µM non-radiolabelled ATP, for 10 minutes. The reaction was put on ice for 5 minutes to reduce the temperature of the assay, and then a sample was taken to confirm $CheA^{HK}$ phosphorylation (Lane 1). An aliquot of the phosphorylated $CheA^{HK}$ was kept in assay conditions for the duration of the experiment, to be halted at conclusion of the assay, after the final time point was taken (Lane 10). CheY was added to the reaction master mix and a sample was taken immediately (Lane 2) then at 0:20, 0:40, 1:00, 1:20, 2:00, 3:00, 4:00, 5:00 and 10:00 minutes (Lanes 2-9) (n=4). (B) shows a kinase assay between 20 µM $CheA^{HK}$ and 20 µM CheV, carried out at at 42 °C. $CheA^{HK}$ was incubated with 1.3 µM [γ-^{32}P] ATP diluted with 30 µM non-radiolabelled ATP, for 10 minutes. The reaction was adjusted to 42 °C for 5 minutes, then a sample was taken to confirm $CheA^{HK}$ phosphorylation (Lane 1). An aliquot of the phosphorylated $CheA^{HK}$ was kept in assay conditions for the duration of the experiment, to be halted at conclusion of the assay, after the final time point was taken (Lane 14). CheV was added to the reaction master mix and a sample was taken immediately (Lane 2) then at 0:30, 1:00, 1:30, 2:00, 2:30, 3:00, 3:30, 4:00, 4:30, 5:00, and 10:00 minute (Lanes 3-13) (n=3). (C) shows a kinase assay between 20 µM $CheA^{HK}$ and 20 µM CheV, carried out at on ice. $CheA^{HK}$ was incubated with 1.3 µM [γ-^{32}P] ATP diluted with 30 µM non-radiolabelled ATP, for 10 minutes. The reaction was put on ice for 5min to reduce the temperature of the assay, and then a sample was taken to confirm $CheA^{HK}$ phosphorylation (Lane 1). An aliquot of the phosphorylated $CheA^{HK}$ was kept in assay conditions for the duration of the experiment, to be halted at conclusion of the assay, after the final time point was taken (Lane 10). CheV was added to the reaction master mix and a sample was taken immediately (Lane 2) then at 0:20, 0:40, 1:00, 1:20, 1:40, 2:00 and 5:00 minutes (Lanes 3-9) (n=3).

To reduce the reaction rate and obtain a more detailed picture of the reaction between $CheA^{HK}$~P and CheV, an identical assay was attempted on ice (Fig.4.7*C*). In repeated attempts no CheV phosphorylation or reduction in the level of phosphate on $CheA^{HK}$ was observed, however it appears that this was due to a faulty CheV preparation rather than the conditions of the assay as repetition of earlier successful assays failed using this protein stock. CheA had been shown to phosphorylate CheV but these assays had not provided data on the relative rate of phosphate transfer or CheV autodephosphorylation.

4.3.3. CheA Can Phosphorylate its Own RR domain

The following assays were used to investigate the kinase interaction between the histidine kinase and response regulator domains of CheA and autodephosphorylation from that RR domain.

Phosphorylation assays of $CheA^{RR}$ used a 1:1 ratio of 20 µM $CheA^{HK}$ and 20 µM separately expressed HIS tagged $CheA^{RR}$ domain. $CheA^{HK}$ was incubated with ATP at room temperature for 10 minutes, the temperature of the reaction was then adjusted to either 30 °C or 42 °C over 5 minutes. The HK-15 sample and HK-END aliquot were taken, $CheA^{RR}$ added to the reaction and samples taken at intervals.

At 30 °C a low level of $CheA^{RR}$ phosphorylation was visible after 30 seconds (Fig.4.8*A* Lane 3), the level of bound ^{32}P increased steadily until the 30 minute time point (Lane 10). As phosphorylation of $CheA^{RR}$ was still increasing when the 30 minute interval was taken, it was not possible to say this was the peak level of phosphorylation or if a further time point would have shown a further increase. As

$CheA^{HK}$ still displayed high levels of bound ^{32}P after 30 minutes (Lane 10) it is likely that CheA-RR phosphorylation may have increased further if unphosphorylated CheA-RR molecules were available.

Based on the results of the 30 °C assay the reaction temperature was increased to 42 °C, to try to observe full phosphorylation and autodephosphorylation of $CheA^{RR}$. At 42 ° phosphorylated $CheA^{RR}$ was observed immediately at the 0 time point (Fig.4.8*B* Lane 2), the peak level appeared to be at 2 or 5 minutes then declined steadily. Complete Pi hydrolysis was not observed after 30 minutes (Lane 9), where a low level of bound ^{32}P was still observable. The HK-15 and HK-END controls (Lanes 1 and 10) verified $CheA^{HK}$ autophosphorylation, and that loss of phosphate from $CheA^{HK}$ was due to transfer of ^{32}P to $CheA^{RR}$ and not autodephosphorylation of $CheA^{HK}$.

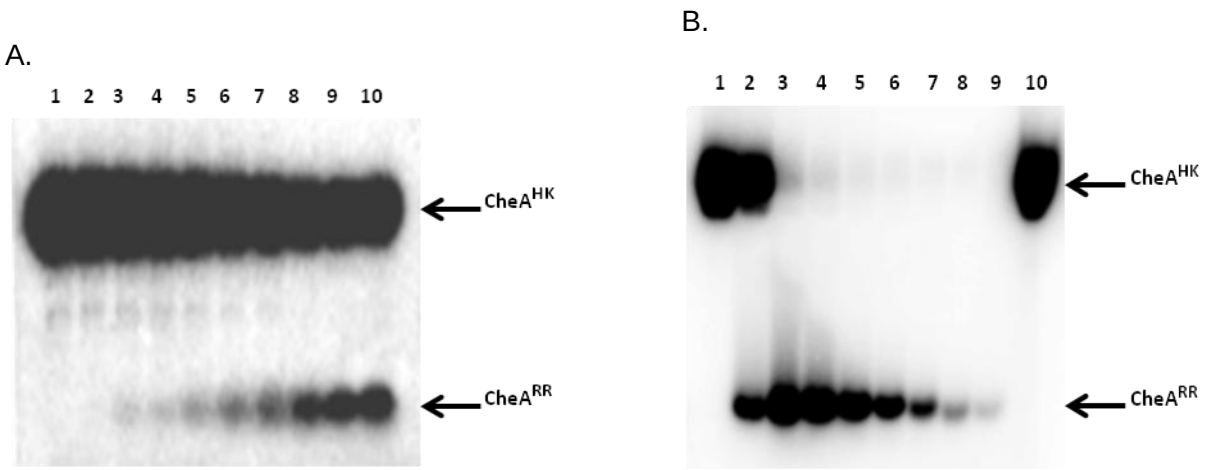

Figure 4.8. Phosphor screen visualisation of $CheA^{HK}$ phosphate transfer to $CheA^{RR}$. Experiments were carried out in reaction buffer at pH8.3. (A) shows a kinase assay (shown earlier in Fig.4.3 (B) between 20 µM $CheA^{HK}$ and 20 µM $CheA^{RR}$, carried out at 30 °C. The phosphor screen was exposed to the same gel for 44 hours before being scanned. $CheA^{HK}$ was incubated with 1.3 µM [γ-^{32}P] ATP diluted with 30 µM non-radiolabelled ATP, for 10 minutes. The reaction was adjusted to 30 °C for 5 minutes, then a sample was taken to confirm $CheA^{HK}$ phosphorylation (Lane 1). $CheA^{RR}$ was added to the reaction master mix and a sample was taken immediately (Lane 2) then at 0:30, 1:00, 2:00, 3:00, 5:00, 10:00 20:00 and 30:00 minutes (Lanes 3-10). For this assay samples were halted by addition of 5x sample loading buffer with 0.2 M DTT and heat treated at 60 °C for 30 minutes. (B) shows a kinase assay between 20 µM $CheA^{HK}$ and 20 µM $CheA^{RR}$ carried out at 42 °C. $CheA^{HK}$ was incubated with 1.3 µM [γ-^{32}P] ATP diluted with 30 µM non-radiolabelled ATP, for 10 minutes. The reaction was adjusted to 42 °C for 5 minutes, and then a sample was taken to confirm $CheA^{HK}$ phosphorylation (Lane 1). An aliquot the phosphorylated $CheA^{HK}$ was kept in assay conditions for the duration of the experiment, to be halted at conclusion of the assay, after the final time point was taken (Lane 10). $CheA^{RR}$ was added to the reaction master mix and a sample was taken immediately (Lane 2) then at 2, 5, 10, 15, 20, 25, and 30 minutes (Lanes 3-9). For this assay samples were halted by addition of 5 x sample loading buffer with 0.2 DTT and kept on ice until loaded (n=3).

4.3.4. Testing CheA Dependant Response Regulator Phosphorylation

It was necessary to demonstrate that the phosphorylation of each response regulator was dependent upon $CheA^{HK}$, and not the result of a transfer of Pi directly from [γ-^{32}P] ATP.

For each of the response regulators two reactions were setup using the reaction conditions confirmed during the individual RR assays. The first reaction included all previous elements of the successful individual RR assay, the second was a replica of the first except that it excluded $CheA^{HK}$. Results of these assays are shown in Figure 4.9. Lanes 1 and 2 show CheY in the presence and absence of $CheA^{HK}$ respectively. Where $CheA^{HK}$ was present CheY became phosphorylated, where $CheA^{HK}$ was excluded no CheY phosphorylation was observed.

Lanes 3 and 4 show $CheA^{RR}$ in the presence of $CheA^{HK}$ and without, respectively, where $CheA^{HK}$ was present $CheA^{RR}$ became phosphorylated, where $CheA^{HK}$ was excluded no $CheA^{RR}$ phosphorylation was observed. Lane 3 also shows a minor contaminant which has become weakly phosphorylated. As this band was not visible in Lanes 1, 4 or 5 it seems the contaminant may be present in the $CheA^{RR}$ stock, and possibly be a breakdown product of $CheA^{RR}$ which has retained the response regulator domain. This contaminant was not observed in any other experiments which used $CheA^{RR}$.

Lanes 5 and 6 in Figure 4.9 show CheV in the presence and absence of $CheA^{HK}$ respectively. Where $CheA^{HK}$ was present CheV became phosphorylated, where $CheA^{HK}$ was excluded no CheV phosphorylation was observed.

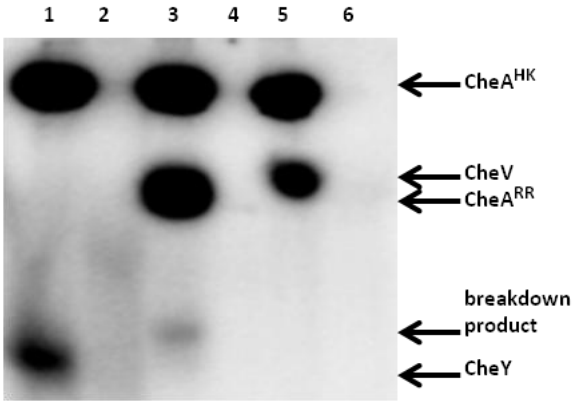

Figure 4.9. Phosphor screen visualisation of a $CheA^{HK}$ dependant RR domain phosphorylation test. Phosphor screens were exposed to gels for 44 hours before being scanned. Experiments were carried out in reaction buffer at pH8.3, samples were treated with 5x sample loading buffer with 0.2 M DTT and kept on ice before loading onto an SDS-PAGE gel. A diluted mixture of 3 µM [γ-^{32}P] ATP with 30 µM non-radiolabelled ATP was used. The experiments shown in Lanes 1 and 2 took place on ice. In Lane 1 20 µM $CheA^{HK}$ was incubated with ATP for 10 minutes, then put on ice for 5 minutes to reduce the temperature for the experiment, 15 µM CheY was added to the reaction and the reaction halted immediately. In Lane 2 ATP was added to 15 µM CheY and the reaction halted immediately. The assays in Lanes 3 and 4 were carried out at 42 °C. In Lane 3 20 µM $CheA^{HK}$ was incubated with ATP for 10 minutes, then heated to 42 °C for 5 minutes, 20 µM $CheA^{RR}$ was added to the reaction and the reaction halted immediately. In Lane 4 ATP was added to 20 µM $CheA^{RR}$ and the reaction halted after 2 minutes. The experiments shown in Lanes 5 and 6 were carried out at 42 °C. In Lane 5 20 µM $CheA^{HK}$ was incubated with ATP for 10 minutes, then heated to 42 °C for 5 minutes, 20 µM CheV was added to the reaction and the reaction halted immediately. In Lane 6 ATP was added to 20 µM CheV and the reaction halted immediately (n=3).

4.3.5. Competitive Kinase Transfer Assays

To test the relative affinity of the response regulators for $CheA^{HK}$, CheY, CheV and CheA-RR were combined in a timecourse experiment in which the response regulators would compete to receive Pi from phosphorylated $CheA^{HK}$.

The competition assay was carried out on ice and the separately expressed CheA-RR domain was used rather than the full length CheA. CheA-RR was used so that $CheA^{HK}$ could be pre-exposed to [γ-^{32}P] ATP and to avoid confusion

between phosphorylation of the HK domain or A-RR domains present on the full length CheA protein. 15 µM CheY, 15 µM CheV and 15 µM CheA-RR were prepared together as a mastermix so they could be added simultaneously. $CheA^{HK}$ was allowed to autophosphorylate at room temperature with diluted radiolabelled ATP for 10 minutes then put on ice for 5 minutes to reduce the reaction temperature. The HK-15 and HK-END samples were taken, the response regulator mix was added and then samples were taken at 0:00, 0:20, 0:40, 1:00, 1:20, 2, 5, 10 and 15 minutes.

CheY, the primary response regulator, bound much greater amounts of ^{32}P from $CheA^{HK}$ than CheV or CheA-RR (Fig.4.10*A* Lanes 2-8). As previously observed, CheY became phosphorylated and reached its peak phosphorylation at the zero time point (Lane 2). CheY phosphorylation was observed up to the 5 minute time point (Lane 8). CheV showed a similar reaction rate to that of CheY, some phosphorylation of CheV was visible at the zero time point (Lane 2) as had been found with CheY. Peak CheV phosphorylation appeared around the 40 or 60 second time point (Lane 4-5), CheV followed a similar phosphorylation pattern to that of CheY in that it was found phosphorylated at the 5 minute time point (Lane 8) but not at 10 minutes (Lane 9), autodephosphorylation of CheV appeared similarly rapid to that of CheY. Interestingly a weakly phosphorylated $CheA^{RR}$ was also observed (Lanes 2-10), this is curious due to the low temperature of the assay and considering that phosphorylation of $CheA^{RR}$ had not been observed previously in assays conducted at this temperature.

The HK-15 and HK-END controls verified HK autophosphorylation, and that loss of phosphate from $CheA^{HK}$ was due to transfer of ^{32}P to the response regulators and not autodephosphorylation of $CheA^{HK}$.

A repeat of the competition assay using full length CheA was attempted with incubation on ice. 40 µM CheA, 15 µM CheY and 15 µM CheV were combined with radiolabelled ATP. The separately expressed $CheA^{HK}$ was not included in the experiment and CheA was not pre-exposed to labelled ATP. At no point during the timecourse did any of the response regulators, or the HK domain of full length CheA, become visibly phosphorylated (Fig.4.10*B*).

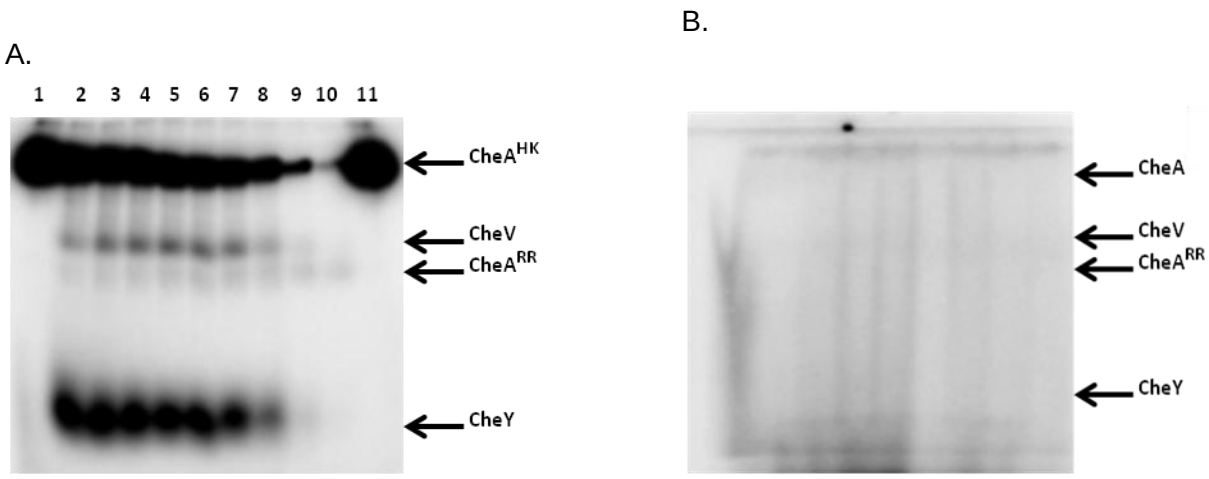

Figure 4.10. Phosphor screen visualisation of competition assays between response regulator domains. Phosphor screens were exposed to gels for 44 hours before being scanned. Experiments were carried out in reaction buffer at pH8.3, samples were treated with 5x sample loading buffer with 0.2 M DTT and kept on ice before loading onto an SDS-PAGE gel. (A) shows a phosphate transfer assay between prephosphorylated 40 µM $CheA^{HK}$ with 15 µM CheY, 15 µM CheV and 15 µM $CheA^{RR}$ and was carried out on ice. $CheA^{HK}$ was incubated with 6 µM [γ-^{32}P] ATP diluted with 0.17 mM non-radiolabelled ATP, for 10 minutes. The reaction was put on ice for 5 minutes to reduce the temperature of the assay, and then a sample was taken to confirm $CheA^{HK}$ phosphorylation (Lane 1). An aliquot of the phosphorylated $CheA^{HK}$ was kept in assay conditions for the duration of the experiment, to be halted at conclusion of the assay, after the final time point was taken (Lane 11). A master mix containing CheY, CheV and $CheA^{RR}$ was added to the reaction and a sample was taken immediately (Lane 2) then at 0:20, 0:40, 1:00, 1:20, 2:00, 5:00,10:00 and 15:00 minutes (Lanes 3-10) (n=2). (B) shows a phosphate transfer assay between 40 µ M full length CheA with 15 µM CheY, 15 µM CheV and 15 µM $CheA^{RR}$ carried out on ice and without any pre-loading of CheA with labelled ATP. CheA, CheY, CheV and $CheA^{RR}$ were put in a reaction together. 6 µM [γ-^{32}P] ATP diluted with 0.17 mM non-radiolabelled ATP was added to the reaction, a sample was taken immediately (Lane 1), then at 0:20, 0:40, 1:00, 1:20, 2:00, 5:00,10:00 and 15:00 minutes (Lanes 2-10) (n=1).

CheA Can Phosphorylate its Native, Fused RR Domain

The properties of the separately expressed CheA response regulator domain had been explored in the previous assays, however in *C. jejuni* the protein would be expressed fused to the HK domain and would demonstrate different dynamics in interactions with the HK domain than those displayed in assays that used the separately expressed domains.

A repeat was attempted of the assay attempted in Figure 4.1*B* in which whole length CheA and CheY were combined before radiolabelled ATP was added. In the original experiment neither CheA nor CheY had been visibly phosphorylated, but the autoradiography method had been used for that assay, so an attempt was made to rerun the experiment using the phosphor screen and the now optimised method. 40 µM CheA was combined with 15 µM CheY, diluted labelled ATP was added, samples were taken immediately after the addition of ATP then at 0:20, 0:40, 1:00. 1:20, 2, 5, 10, 15 and 20 minutes (Fig.4.11).

CheY was not seen to phosphorylate during the assay, however it appeared that technical problems had occurred during the gel drying stage and so this result for CheY was questionable as CheY may have been visible if the gel had been adequately dried. CheA did become visibly phosphorylated over the course of this experiment. At high exposure the first phosphorylation of CheA became visible at the zero time point, immediately after the labelled ATP had been added (Lane 1). The level of ^{32}P bound increased steadily until the end of the assay at 20 minutes.

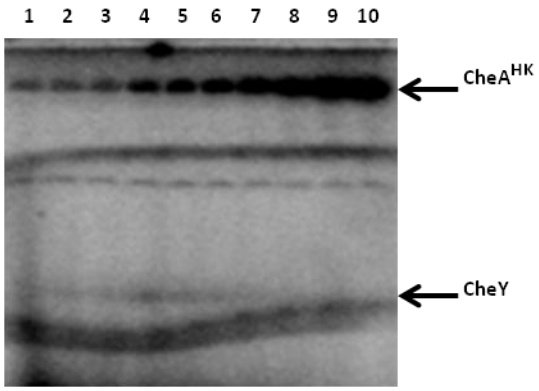

Figure 4.11 Phosphor screen visualisation of whole CheA phosphate transfer to CheY. Phosphor screens were exposed to gels for 44 hours before being scanned. Experiments were carried out in reaction buffer at pH8.3, samples were treated with 5x sample loading buffer with 0.2 M DTT and kept on ice before loading onto an SDS-PAGE gel. (A) shows a kinase assay between 40 µM CheA and 15 µM CheY, carried out on ice. CheA were put in a reaction together then 1.3µM [γ-^{32}P] ATP diluted with 30 µM non-radiolabelled ATP, a sample was taken immediately (Lane 1) then at 0:20, 0:40, 1:00, 1:20, 2:00, 5:00, 10:00, 15:00 minutes and 20:00 minutes (Lanes 2-10) (n=1).

To further investigate the dynamics of the interactions between the HK and CheA-RR domains of whole length CheA the ImageQaunt TL software provided with the Typhoon 9400, was used to quantify phosphorylation of CheA.

When a band was observed for whole length CheA the intensity of that band would represent ^{32}P bound to both the HK and RR domains. To attempt to view just the ^{32}P which HK had transferred to the CheA-RR domain, whole length CheA was allowed to autophosphorylate and transfer Pi groups to the response regulator domain before CheY was added to 'strip' ^{32}P from the HK domain. The intensity of any band observed for CheA now would represent just that phosphate left upon the CheA-RR domain, using the data from this assay it was considered possible to estimate the rate of transfer of Pi from a native fused CheA HK domain to its RR domain.

The time course assay to ‘strip’ CheAs HK domain was carried out at 30 °C, a sample was taken before diluted radiolabelled ATP was added to the reaction. Samples were taken at 0, 5, 10 and 15 minutes. After the 15 minute sample was taken, CheY was added to a final concentration of 20 µM to strip phosphate from the HK domain. The reaction continued for a further 5 minutes before being halted. The sample taken before labelled ATP was added showed that the detection of a radioactive signal from CheA was due to the addition of radiolabelled ATP (Fig.4.12*A* Lane 1). The assay displayed increasing CheA phosphorylation up to a peak at 15 minutes (Fig.4.12*A* Lane 4, Fig.4.2*B*), this increase may have continued if incubation had been continued further.

Once CheY was added a sharp decrease in CheA phosphorylation was observed, the phosphorylation dropped to 55.4% of its peak at 15 minutes (Fig.4.12*A* Lane 5, Fig.4.12*B*), a comparative fall in phosphorylation was observed in a replica experiment, with CheA phosphorylation falling to 46% of its previous peak at 15 minutes (Fig.4.12*C,D*).

The previous CheA phosphor transfer experiment (Fig. 4.12) had given only a snapshot of CheA-RR phosphorylation, observing a single timepoint at 20 minutes. It was decided to attempt to moniter phosphorylation of a native, fused CheA-RR over time. A time course assay was carried out in which CheY was added to samples for 20 seconds before each reaction was halted, to strip ^{32}P from the HK domain. The assay ran at 42 °C in order that the reaction rate for CheY should be sufficient to strip Pi from HK in 20 seconds (Fig.4.13). To moniter changes in phosphorylation levels of CheA in the presence and absence of CheY two parallel time courses were run. One in which CheA was allowed to

autophosphorylate and pass Pi between its domains unhindered, and one in which the CheY would be added before the reaction was halted.

The results of the parallel time course assays are shown in Figure 4.3 and Table 4.4 and show the difference in phosphorylation levels of CheA in the presence and absence of CheY at each time point. The phosphorylation level shown by CheA diverges for the two assays after the addition of [γ-^{32}P] ATP, with 45.12% of ^{32}P residing on the RR domain, until HK and RR phosphorylation levels begin to converge again after 4 minutes. After 7 minutes 96% of the ^{32}P bound to CheA appears to have been retained by the CheA-RR domain as there is only a small fall in signal from that sample to which CheY was added, indicating little of the ^{32}P remained on the HK domain.

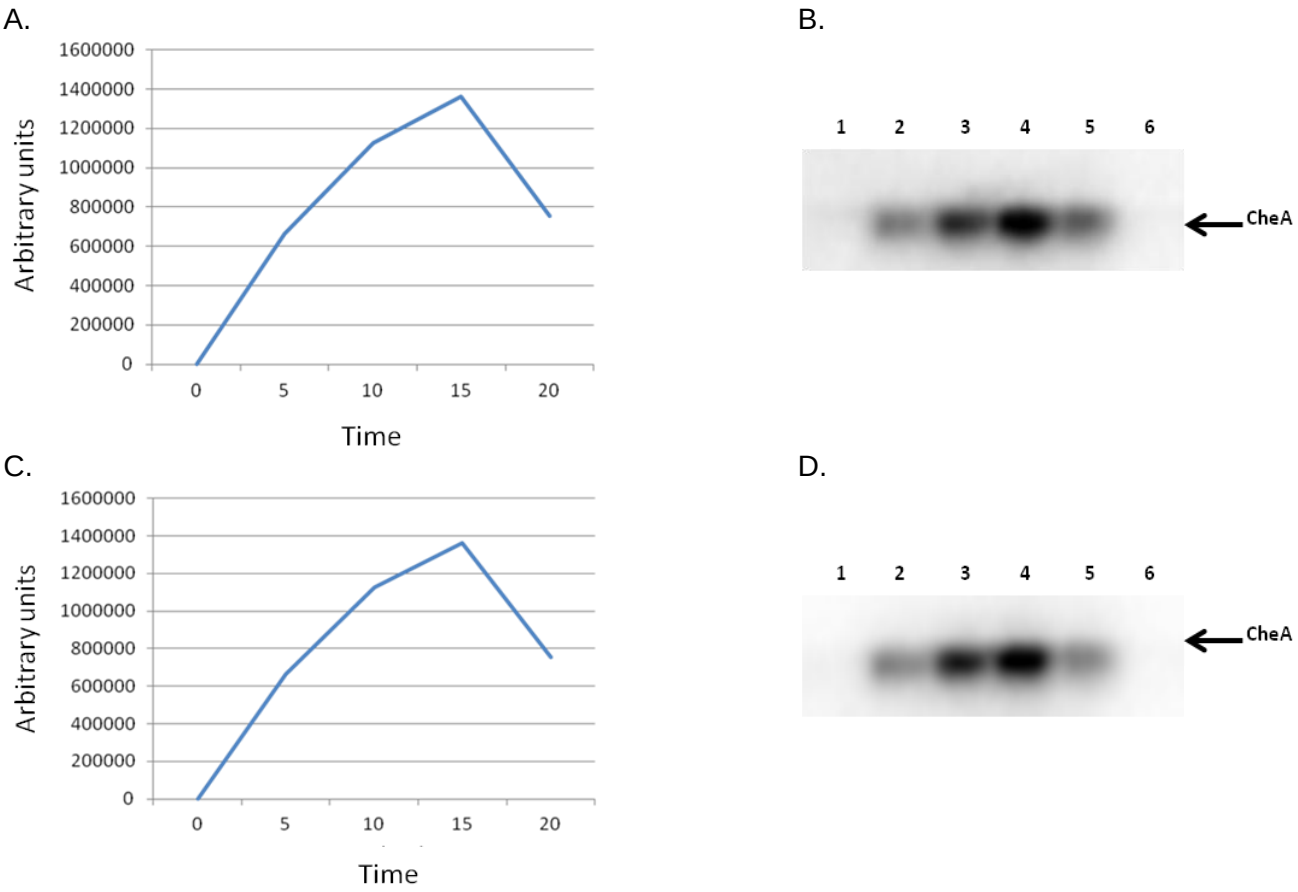

Figure 4.12. Phosphor screen assays and associated graphs to show internal phosphate transfer from HK to RR domains within CheA. Phosphor screens were exposed to gels for 44 hours before being scanned. Experiments were carried out in reaction buffer at pH8.3 at 30 °C, samples were treated with 5x sample loading buffer with 0.2 M DTT and kept on ice before loading onto an SDS-PAGE gel. Quantification of the phosphor screen signal was carried out using the ImageQaunt TL software. (A) and (B) show data from an assay in which 5 µM full length CheA was exposed to 0.25 µM [γ-^{32}P] ATP diluted with 9.4 µM non-radiolabelled ATP. Before the labelled ATP was added, an aliquot of the CheA reaction was taken to kept in assay conditions for the duration of the experiment and halted at conclusion of the assay (Lane 6). Labelled ATP was added, a sample was taken immediately (Lane 1) then at 5, 10 and 15 minutes (Lanes 2-4). After the 15 minute sample was taken CheY was added to 20 µM, the reaction continued until the final 20 minute sample was taken (Lane 5). (B) and (C) show a direct repeat of the experiments in (A) and (B) (n=3).

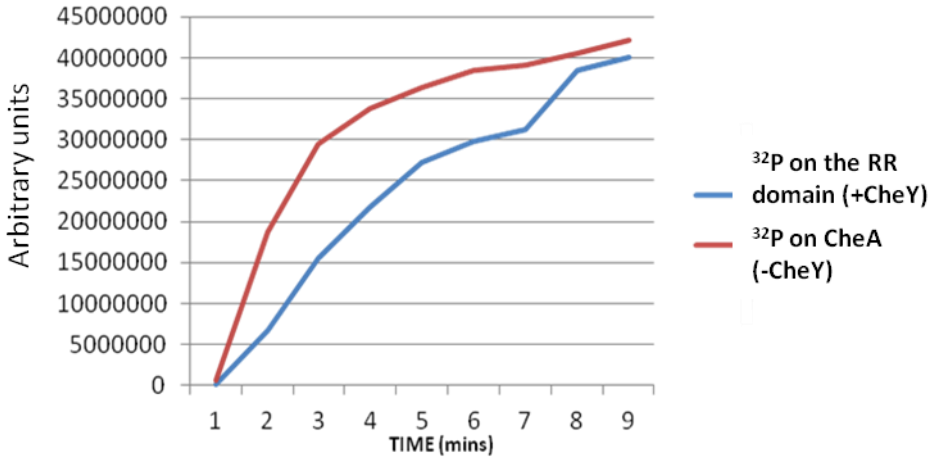

Figure 4.13. A graph of data from an assay of internal phosphate transfer from HK to RR domains within whole length CheA. The Phosphor screens from which this data was gathered, were exposed to gels for 44 hours before being scanned. Experiments were carried out in reaction buffer at pH8.3 at 42 °C, samples were treated with 5x sample loading buffer with 0.2 M DTT and kept on ice before loading onto an SDS-PAGE gel. Quantification of the phosphor screen signal was carried out using the ImageQaunt TL software. Two parallel time courses were run in which 0.25 µM [γ-^{32}P] ATP diluted with 9.4 µM non-radiolabelled ATP was added to 20 µM CheA, a sample was taken immediately, following samples were taken at 1, 2, 3, 4, 5, 6, 7, 8 and 9 minutes. For the ^{32}P upon the RR domain set, CheY was added to each sample for 20 seconds before the reaction was halted (n=2).

Table of ^{32}P retained by RR domain	
Time (min)	% ^{32}P retained by RR domain
0	0.09
1	0.36
2	0.52
3	0.64
4	0.75
5	0.77
6	0.8
7	0.95

Table.4.14 Table showing the amount of ^{32}P retained by CheA RR domain calculated from data shown in Fig.4.13.

4.4. Discussion

To understand the mechanism for transduction of chemotactic signals within *C. jejuni* investigations were needed to discern the ability of CheA to phosphorylate the putative Che response regulators *in vitro*. Experiments were carried out to test the hypothesis that CheA was a histidine kinase and that CheY, CheV and CheA-RR were real response regulators and interacting partners with CheA.

4.4.1. Assay Development

To confirm the function of the putative histidine kinase and response regulators it was necessary investigate Pi transfer using radiolabelled phosphorylation assays. As the laboratory did not have practical experience in this field and the dynamics of these particular response regulators provided challenging conditions for the assay, extensive development of the methodology was required.

The interaction of CheA with CheY was chosen as the basis on which to optimise the assay, as this reaction is central to all identified Che transduction systems. This choice was perhaps unfortunate, as the rate at which CheY accepted phosphate from CheA and the rapid rate at which it then hydrolysed its Pi group, made it difficult to visualise ^{32}P on CheY and therefore difficult to optimise conditions for the assays.

4.4.2. CheA v.s. CheY Individual Assays

For the original assay in which each protein was taken individually and in combination with and without labelled ATP (Fig.4.1*A*), these assays used a single 20 minute time point for each reaction, and so no phosphorylated band had been

observed for CheA or CheY. CheA had become fully phosphorylated and transferred all of the available ^{32}P to CheY, which had itself rapidly autodephosphorylated, so that when the sample was taken at 20 minutes, the majority of the [γ-^{32}P] ATP had already been converted into 'free' ADP and Pi and so neither protein could be seen.

Although the assay was unsuccessful in observing CheY phosphorylation, the data obtained was the first direct demonstration that *C. jejuni* CheA was a histidine kinase and could autophosphorylate using ATP as its substrate.

4.4.3. CheA v.s. CheY Time Course Assay

Rapid autodephosphorylation of CheY had prevented it being observed in the previous assay, and this finding was repeated in the time course assay (Fig.4.1*B*), in which CheA and CheY were added together before exposure to labelled ATP. Over the course of the assay no signal was observed for CheA or CheY. From this it could be hypothesised that perhaps CheY was preventing autophosphorylation of CheA from ATP, or as was later shown, that the transfer of Pi from CheA to CheY occurred at a rate greater than the rate of CheA autophosphorylation. CheY had prevented an accumulation of ^{32}P on the CheA population so that it did not become detectable by autoradiography. A later return to this assay using optimised conditions and a phosphor screen for visualisation, showed some accumulation of ^{32}P on CheA as a signal could be observed, although none was evident for CheY (Fig.4.11). It is important to note that the pattern of parallel lines across the CheA-CheY gel are consistent with gel drying problems, and so CheY may have been visible on this gel with proper

preparation. Due to the time constraints of the project this assay was not attempted again.

Pre-exposure of CheA to [γ-^{32}P] ATP

As at this point in the study phosphorylated CheY had not been observed, it was decided to pre-expose CheA to labelled ATP to maximise the amount of phosphorylated CheA available at one time and so increase the probability of observing phosphorylated CheY.

The assay resulted in a constant level of CheA phosphorylation that CheY did not affect (Fig. 4.1*C*). It was hypothesised from this result that when CheA was allowed to autophosphorylate in isolation, without a competing response regulator, the phosphate was passed from the HK domain of CheA to its own CheA-RR, and that from this domain the phosphate was unavailable to CheY, hence the stable phosphorylation of CheA and the lack of signal from CheY. This hypothesis was later shown to be the case when the separately expressed CheA^{HK} was used to successfully phosphorylate CheY.

Using the Isolated CheA^{HK} Domain

The separately expressed CheA^{HK} protein could be exposed to labelled ATP without the ^{32}P being shuttled to a CheA RR domain, so it could be observed phosphorylated and still be used as a kinase to CheY.

In the parallel time course assay CheY was shown to take phosphate from CheA^{HK} but had not itself yet been observed phosphorylated, therefore it was possible at this point that CheY was a response regulator which very rapidly

autodephosphorylated, or that CheY was acting as a phosphatase against $CheA^{HK}$.

Visualising CheY~P with Phosphor Screens

The adoption of phosphor screens for visualisation of the phosphorylated proteins allowed for much improved optimisation of the assay. Phosphorylation of CheY and $CheA^{RR}$ had been directly demonstrated and autoradiography had been shown not to be sensitive enough for adequate detection of the phosphorylated Che proteins.

Sample Treatment

The removal of the 30 minute 60 °C heat step during sample preparation had a significant effect upon the sensitivity of the assay, with greater amounts of ^{32}P found visible on response regulators with the removal of this step, and the prevention of errant signals found in the wells or stacking gel.

[γ-^{32}P] ATP Dilution

Unfortunately constant phosphorylation conditions were necessary to prevent the appearance of the Breakdown1 band that had pervaded early attempts at pulse chase experiments (Fig.4.5).

Breakdown1 had appeared in multiple samples during pulse chase experiments and had been present in HK-15 and HK-END samples. MALDI-TOF mass spectrometry had confirmed breakdown1 as mapping to the HIS-Kin domain of HK but not to the Hpt domain which receives Pi during transphosphorylation within the CheA homodimer (Stock et al. 2000). Later attempts to repeat pulse

chase experiments using the final optimised conditions, still resulted in a $CheA^{HK}$ associated Breakdown1 band.

Assay Development Conclusion

CheY had been chosen as a focus for optimisation of the test as the CheA-CheY interaction is central to known Che transduction systems, and as previously *C. jejuni cheY* had been used to complement a *H. pylori* Δ*cheY* strain (Jiménez-Pearson et al. 2005). The response regulators of CheV and CheA RR are not as common across species and it could not have been as reliably predicted that they would interact with CheA, as CheY may. The use of the CheA-CheY interaction to optimise the assay had caused additional issues as the extremely rapid autodephosphorylation of CheY in combination with the insensitive autoradiography method had prevented detection of phosphorylated CheY, in addition the response regulator domain of the histidine kinase CheA had made it unsuitable for pre-exposure to labelled ATP. For these reasons, in retrospect, it may have been advisable to develop the assay using another, slower acting two component system.

The test was optimised and reliable at this point, and had been shown to work for the histidine kinase and all three of the RR domains.

4.4.2. Optimised Phosphorylation Assay Results

CheY phosphorylation by CheA

An imbalance of 40 µM $CheA^{HK}$ to 15 µM CheY had been used to improve the probability of visualising CheY by maximising the number of $CheA^{HK}$s available to

the CheY population. Early CheY phosphorylation experiments had suggested that in the optimised conditions CheY would autodephosphorylate within a minute of accepting Pi (data not shown) however these experiments were carried out before the 60 °C sample preparation heat step had been removed. Later experiments with CheY displayed visible though weak CheY phosphorylation for upto 5 minutes (Fig.4.7), a result later matched in competition experiments (Fig.4.10).

During competition experiments CheY had displayed a similar phosphorylation profile to that seen in the previous individual response regulator phosphorylation assays, CheY was immediately phosphorylated and had retained its ^{32}P for 10 minutes, after 15 minutes a signal was no longer detectable. The band observed for CheY was much stronger than that seen for CheV or $CheA^{RR}$ showing $CheA^{HK}$ had a strong preference to transfer its Pi group to CheY, a finding which correlated with the hypothesis that CheY was the primary response regulator, and the primary method of transducing signals. The $CheA^{HK}$ dependant response regulator phosphorylation assay, shown in Figure 4.9 showed that $CheA^{HK}$ was responsible for the phosphorylation of CheY and that in the absence of $CheA^{HK}$ CheY could not obtain phosphate directly from ATP.

The hypothesis that CheY was a response regulator had been demonstrated, it had received ^{32}P from $CheA^{HK}$ and so was not acting as a phosphatase but as a response regulator paired to CheA.

CheV phosphorylation by CheA

Δ*cheV C. jejuni* strains are attenuated for chemotaxis, predicted interactions of CheV with CheA and Cj0700 suggest CheV's RR domain interacts with CheA to become phosphorylated (Bridle 2007). *B. subtilis* mutants in which only the CheW domain of CheV is expressed, show only 75% of their wild type chemotactic motility (Rosario et al. 1994). These studies strongly suggest the RR domain of CheV is real and that the function of the protein is related to chemotaxis.

Phosphorylation of CheV homologues by CheA has been confirmed in *B. subtilis* (Karatan et al. 2001), and inferred through dephosphorylation of CheA in *H. pylori* (Jiménez-Pearson et al. 2005). This section of this study confirms CheV phosphorylation by CheA in *C. jejuni*, and compares that interaction to CheA's kinase activity toward CheY and CheA response regulator.

At 42 °C the rate of Pi transfer from $CheA^{HK}$ to CheV was extremely rapid. The majority of ^{32}P had transferred from $CheA^{HK}$ to CheV by the 0 time point. This sample being taken immediately post addition of CheV to the phosphorylated $CheA^{HK}$ reaction. Complete hydrolysis of ^{32}P was observed by the 20 second time point. If it had been possible to take samples quicker, then samples at 12.5, 15 or 17.5 seconds may have allowed detection of CheV phosphorylation, however for practical and safety reasons this was not possible. 42 °C had been chosen as an elevated temperature for the assays as this is the body temperature of chickens, which are the usual *C. jejuni* host and the reservoir for human disease.

Attempts at this same phosphorylation assay with incubation on ice were repeatedly unsuccessful, with no CheV phosphorylation or dephosphorylation of $CheA^{HK}$ apparent. However, the lack of CheV activity during these assays was due to an error in the preparation of this particular batch of CheV protein rather than being an effect of temperature upon the experiment, as previously successful CheV phosphorylation assays were unsuccessful using this preparation.

The faulty CheV preparation hypothesis was confirmed by later successful CheV phosphorylation seen in the kinase competition assays, which were carried out on ice using a different CheV preparation. During these experiments CheV displayed a similar phosphorylation profile to that of CheY, the bands shown for CheV were weaker than that of CheY, showing that $CheA^{HK}$ had a preference to transfer Pi to CheY over CheV. However CheV became visibly phosphorylated immediately after the addition of the response regulator mix to the reaction and retained ^{32}P for 10 minutes, as did CheY. This was a very different picture to that displayed by the initial CheV phosphorylation experiments performed with incubation on ice.

Optimisation of the temperatures used for *C. jejuni* CheV kinase experiments may have allowed for more detailed data on Pi transfer and hydrolysis rates to be collected. In a previous study *B. subtilis* CheV kinase assays with CheA at room temperature, showed much slower autodephosphorylation rates than suggested by this study for *C. jejuni* CheV. *B. subtilis* CheV was strongly phosphorylated at 1 minute post exposure to CheA and remained phosphorylated when a final sample was taken after 4 minutes (Karatan et al. 2001), this contrasts strongly

with the *C. jejuni* results, although these were obtained following incubation at 42 °C.

The role of CheV in *C. jejuni* may be very different to that of *B. subtilis*, and so may require faster hydrolysis of Pi groups than *B. subtilis*. Studies of the *H. pylori* CheV homologues have been unable to observe phosphorylation of $CheV_{1-3}$ by CheA, possibly due to their very fast rates of autodephosphorylation (Jiménez-Pearson et al. 2005).

Interestingly during the individual response regulator assays against CheV, phosphorylation of $CheA^{HK}$ had remained at a weak but stable level after 20 seconds, and was sustained for a further 10 minutes (Fig.4.7*B*). This residual $CheA^{HK}$ phosphorylation was not observed during CheY assays, which had displayed no $CheA^{HK}$ phosphorylation after 20 seconds, or during the CheA-RR phosphorylation assays after 10 minutes (Fig.4.8*A,B*). If CheV had remained phosphorylated for a longer period then the number of CheV molecules available to strip ^{32}P from $CheA^{HK}$ would have been lower, and a greater amount of ^{32}P would have remained on $CheA^{HK}$, however the population of CheV had rapidly hydrolysed Pi after 20 seconds. If residual $CheA^{HK}$ phosphorylation had been observed during CheA-RR assays which had been carried out at 42 °C, then it may have been concluded that perhaps some part of the CheA population had undergone a conformational change, due to the higher incubation temperature. This may have prevented interaction with CheV and so a part of the $CheA^{HK}$ population would retain ^{32}P. However this does not appear to be the case as complete transfer of ^{32}P from $CheA^{HK}$ to CheA-RR had been observed at 42 °C (Fig.4.8).

A refractory period for the phosphorylation of CheV, preventing re-phosphorylation of CheV for a period after initial phosphorylation and hydrolysis of Pi, may have been plausible if the remaining $CheA^{HK}$ phosphorylation had not persisted for 10 minutes. The rapid changes needed to adapt during chemotaxis would however surely not be served by a refractory period this long, and there is no evidence for a refractory period in the literature.

The hypothesis that CheV is a response regulator that forms a two component partner with the histidine kinase CheA, was supported by these assays.

Autophosphorylation of CheA and Pi Transfer to its RR Domain

Previous studies of *C. jejuni* chemotaxis had not studied the effects of a $cheA^{\Delta RR\ Domain}$ mutation. It was unknown if the domain was involved in chemotaxis or if it was phosphorylated by CheA, however the closely related *H. pylori* becomes severely attenuated for chemotaxis if the *cheA RR* domain is deleted. Cells show the same swimming phenotype as a Δ*cheY* mutant, strongly implicating a role for CheA RR domain in *H. pylori* chemotaxis as its deletion is terminal to the chemotaxis system (Foynes et al. 2000).

The use of the separately expressed $CheA^{RR}$ in phosphorylation assays had confirmed that this domain was functional and that it was partnered to the CheA HK domain (Fig.4.8). Without a separately expressed $CheA^{RR}$ domain it would not have been possible to distinguish between phosphorylation of the HK or CheA RR domain.

At 42 °C CheA-RR had become visibly phosphorylated immediately after it was added to phosphorylated $CheA^{HK}$, a weak signal was visible after 25 minutes but

no longer after 30 minutes. At 30 °C the CheA^{RR} domain had become visibly phosphorylated after 30 seconds and was still gaining Pi groups when the final sample was taken at 30 minutes. At 42 °C or 30 °C the rate of transfer of Pi from CheA^{HK} and the rate of hydrolysis of Pi from CheA^{RR} was much slower than that observed for CheY on ice and CheV on ice, even at this greatly increased temperature.

In competition assays using CheA^{HK}, CheY, CheV and the separate CheA^{RR} assay performed on ice, only low levels of phosphorylation of CheA^{RR} was observed. In competition with CheY and CheV, the CheA^{RR} had a very low level of phosphorylation and was barely visible (Fig.4.10). However it is important to note that this phosphorylation was visible from as early as 0 or 20 seconds and continued up to the 15 minute time point supporting the earlier evidence from individual RR phosphorylation assays that CheA^{RR} autodephosphorylation rate was slower than that of CheY and CheV (Fig.4.8).

Although the separately expressed CheA^{RR} domain had allowed for observation of its phosphorylation, it was not a native protein. The RR domain would normally be expressed as part of CheA, covalently bound to the HK domain, so would have a much higher effective concentration, and so quite different kinetics to those observed in the separate CheA^{RR} assays.

To investigate native CheA RR domain kinetics competition assays using whole length CheA were carried out. However, these were unsuccessful with neither the response regulators nor the HK of CheA becoming visible (Fig.4.10). That phosphorylation of neither protein had been observed may have been due to it

not being possible to pre-expose the HK domain of CheA to labelled ATP, as the ^{32}P would have been shuttled to the CheA-RR domain before the assay had begun, or that too many response regulators had been competing for the phosphorylated HK domain of CheA for any of the proteins to become visible.

To attempt to observe native CheA-RR phosphorylation parallel timecourses were run using whole CheA, one in which CheA autophosphorylated and internally transferred Pi unhindered (Fig.4.12), and another in which CheY was added to each sample 20 seconds before the reaction was halted (Fig.4.13), to strip ^{32}P from the HK domain so that ^{32}P remaining on the RR domain could be measured. The two time courses could be compared to discern the levels of Pi bound to either HK or RR domains. Previous experiments using $CheA^{HK}$ against CheY had suggested that 40 µM HK, while on ice, was completely stripped by 15 µM CheY within 20 seconds of addition of CheY (Fig.4.7). To increase the probability of a totally dephosphorylated HK domain in this assay, incubation was performed at 42 °C and the CheA exposed to CheY for 20 seconds. The exposure time had to be minimised in order that the result for this time curve could still be comparable to that in which CheA had been allowed to phosphorylate normally. In retrospect these assays should have been run at 30 °C to match the temperature of previous experiments so that easier comparisons could be made.

The increase in temperature had a dramatic effect upon the transfer of phosphate to CheA-RR. The assays shown in Figures 4.12*A,B* had been carried out at 30 °C, here 55% and 46% respectively of the phosphate appeared to have been retained on CheA-RR domain after 15 minutes. At 42 °C, in the dual time course experiment, 96% of the phosphate appeared to be RR bound after only 7

minutes. The rates of CheA-RR phosphorylation observed were much higher when the domain was fused to its HK domain than had previously been observed using the separately expressed $CheA^{RR}$ domain. The decrease in the proportion of ^{32}P bound to the HK domain in the dual time course assay (Fig.4.13) was interesting given that as whole length CheA was used. Both domains were necessarily present in a 1:1 ratio, so although it may have been reasonable to expect that an increasing number of Pi groups would be found on the RR domain, given its relatively slow autodephosphorylation rate, it would still be reasonable to expect that if both domains were able to bind phosphate at the same time, then strong phosphorylation of the HK domain should still be seen after 7 minutes. However, this was not the case as 96% of the ^{32}P appeared to be bound to the RR domain at 7 minutes after CheY was added.

The lack of HK phosphorylation after 7 minutes could indicate a role for CheA-RR in modulating the autophosphorylatory activity of the HK domain. There is evidence of this type of regulation in *M. xanthus*, as its CheA homologue FrzE, can prevent autophosphorylation of its histidine kinase domain when its RR domain is in its non-phosphorylated, inactive state (Inclán et al. 2008).

Perhaps phosphorylated CheA-RR may reduce autophosphorylation of HK in *C. jejuni*. This would have interesting consequences for chemotaxis signal transduction if true, however this had been a preliminary assay and time had not allowed for follow up experiments. Only 52.36 µM diluted labelled ATP had been added to 20 µM of CheA, so given the low ratio of ATP to CheA molecules, the fall in ^{32}P associated with the HK domain be due to the majority of the ATP being taken by HK and passed to the RR domain within the first few minutes of the

experiment, and so fewer ATP molecules were available to the CheA HK domain in the later part of the experiment.

The individual time course assays shown in Figure 4.12, had used a similar ratio of CheA to ATP but had shown only 46% or 55% of phosphate as CheA-RR bound. Phosphate had still been available to the HK domain, perhaps due to the lower reaction temperature at the point these experiments ended, not all the RR domains were occupied and 'free' ATP was still available to HK. If time were available to repeat this experiment, CheA would be reduced to match the 5 µM used in the assays described in Figure 4.12, total concentration of ATP used increased and HIS tagged CheA used to avoid changes in protein dynamics due to the properties of the GST tag.

Despite ambiguity remaining over rates of transfer between the HK and RR domains of CheA, the HK domain has been shown to form a two component pair with the CheA-RR domain as hypothesised.

4.4.3. Conclusion

As hypothesised CheY, CheV and CheA-RR are response regulator domains that formed two component systems with CheA. CheA was shown to be a histidine kinase which autophosphorylates from ATP and passes Pi onto its partnered response regulators.

CheY is the principle response regulator and is strongly favoured by CheA for the transfer of phosphate, CheY accepts phosphate from CheA at a very rapid rate and has an autodephosphorylatory activity which, taken together, are consistent

with its predicted role of interacting with the flagella as seen in other chemotaxis signal transduction models.

Kinase assays against CheV performed on ice, with a CheV stock which had been demonstrated to be functional, may have given results that could be used to draw greater comparisons with those observed for CheY, as it appears that although CheY was the preferred interacting partner of the HK domain, CheV displayed transfer and hydrolysis rates comparable to that of CheY during the competition experiments.

The native fused CheA RR domain had a far higher affinity for Pi than had been suggested in assays using the separately expressed domain. The function of the RR domain and its native dynamics remain unknown, perhaps CheA's RR domain may modulate the autophosphorylatory activity of CheA but without further data this remains unclear.

Continuous phosphorylation of $CheA^{HK}$ using diluted [γ-^{32}P] ATP had prevented sequesteration of available radiolabel by the Breakdown 1 protein, this had previously prevented assays of $CheA^{HK}$ or response regulator phosphorylation. Continuous phosphorylation conditions however did not give as accurate data on the dynamics between the Che proteins as pulse chase experiments may have done.

It is important to note that the phosphorylation assays were carried out *in vitro* and without knowledge of the stoichiometry of the response regulators within the *C. jejuni* cell, also that the effective concentration of each of these may have been affected by interacting partners that were not included within these experiments.

Chapter 5: Affinity Tag Pull-Down Experiments

5.1. Introduction

The phosphate exchange experiments had confirmed that CheA has histidine kinase activity and that CheY, CheV and CheA-RR are response regulators, partnered to CheA. The phospho transfer assays had demonstrated the order of preference in which CheA transfers phosphate to each of the proteins and suggests CheA-RR phosphorylation may hamper autophosphorylation of the CheA HK domain. From phosphate transfer studies alone it could not be determined how the Che proteins interact to form the transduction system. Assays of affinities between the proteins could be used to suggest functional interactions between them, and allow for differences in affinity between phosphorylated and non-phosphorylated response regulators to be tested.

5.2. Previous Studies

Bridle's bacterial two hybrid study had suggested interactions which may take place between the Che proteins (Bridle 2007). CheV had been predicted to interact with CheB, suggesting that it may have a role in regulating CheB's de-methylation of TLP receptors, but CheV had also been shown to interact with CheA which might indicate a role in TLP cluster formation.

The bacterial two hybrid assays had provided insights into how the Che proteins may interact but these observations had been restricted by limits of the technique. Both false positive and negative results may occur in bacterial two hybrid assays

due to the fusion of the adenylate cyclase domains to the bait and prey Che proteins, although this had been controlled for by testing both combinations of the adenylate cyclase domains fused to bait and prey proteins, at both N-terminal and C-terminal ends (Bridle 2007). As the assays occurred *in situ* within *E. coli* it was not possible to control the phosphorylation state of the *C. jejuni* Che proteins during the assay, and also it would not be possible to alter their phosphorylation state to observe any change in affinity this may cause.

5.3. The Affinity Tag Pull-Down Assay

Pull-down assays are another method by which to probe protein-protein interactions. As these tests would be carried out i*n vitro* the phosphorylation state of response regulators would be controllable, therefore it would be possible to perform the tests with Che proteins in phosphorylated or non-phosphorylated states.

Our study used an affinity tag pull-down assay, this assay uses an affinity tag to immobilise a protein, which once immobilised can act as ‘bait’ for non- labelled ‘prey’ proteins. Non- tagged proteins are incubated with the ‘bait’ before washes to remove any proteins that have not interacted with the bait. Samples are loaded onto SDS-PAGE gels for identification of retained proteins. Retained proteins are said to have shown an affinity to the ‘bait’ which suggests the ‘bait’ and ‘prey’ proteins have a functional interaction *in situ*.

5.4. Testing Phosphorylation of the GST-Tagged Che Proteins

In the phosphate transfer assays the separately expressed $CheA^{HK}$ had been used to phosphorylate Che response regulators. The presence of $CheA^{HK}$ in a pull down assay, in addition to the bait and prey proteins, would complicate interpretation of the results. $CheA^{HK}$ may link bait and prey proteins together using the HK domain as a bridge, leading to a false positive result, or the obstruction of a bait-prey interaction site by HK may lead to false negatives.

Acetyl phosphate offers an alternative method of looking at the influence of phosphorylation on Che RR domains, as it can directly phosphorylate response regulators independently of Che^{HK} (Feng et al. 1992; McCleary & Stock 1994).

Acetyl Phosphate and Direct Phosphorylation of Response Regulators

Acetyl phosphate (Ac-P) is a small molecule phosphate donor which had been shown to phosphorylate response regulators directly, independently of histidine kinase. Ac-P had been shown to phosphorylate diverse response regulators in a number of bacteria (Wolfe et al. 2003; Klein et al. 2007; McCleary et al. 1993), including the $CheV_{1-3}$ proteins of *H. pylori* (Pittman et al. 2001), but it was necessary to demonstrate that Ac-P would be able to transfer phosphate to the Che response regulator domains of *C. jejuni*. Ideally, radiolabelled acetyl phosphate would have been used to test direct phosphorylation of the response

regulators, but it was not possible to purchase Ac-P in a labelled form, and the laboratory lacked facilities to safely manufacture radiolabelled Ac-P.

In the absence of a directly labelled Ac-P assay, it was decided to develop a blocking assay to demonstrate phosphorylation of RR domains by Ac-P. The Ac-P would be used to phosphorylate each response regulator domain before exposing it to a ^{32}P labelled CheA^{HK}. As a control a parallel test would expose the same response regulator to ^{32}P labelled CheA^{HK}, to show the level of phosphate transfer from CheA^{HK} achieved when unlabelled Ac-P was not present. Unlabelled Pi groups would bind to the response regulators to occupy the domain and block their phosphorylation by radiolabelled ^{32}P via CheA^{HK}. Less radioactive signal should therefore be observed from proteins which had successfully accepted unlabelled phosphate from Ac-P when compared to the control.

CheA^{HK} Dependant Phosphorylation of GST-Tagged Che proteins

It was necessary to demonstrate that the purified GST tagged CheY (CheY-GST), CheV-GST and CheA-RR-GST domains could be phosphorylated by ^{32}P via CheA^{HK} as the GST tagged version of these proteins had not been verified as functional, and the 26 kDa GST tag may interfere with the folding and final conformation of the proteins.

5.4.1. Results

The aim of these experiments was to show that Ac-P could directly phosphorylate *C. jejuni* Che response regulators *in vitro*, and so would be suitable to use to phosphorylate the RR domains in affinity tag pull-down assays.

Scheme for the Experiments

Each response regulator (10 µM) was exposed to 200mM Ac-P for 8 minutes at room temperature before the reaction was adjusted to the intended experimental temperature for 2 minutes. Separately 10 µM $CheA^{HK}$ was exposed to 3 µM [γ-^{32}P] ATP diluted with 30 µM unlabelled ATP for 10 minutes at room temperature then adjusted to the intended experimental temperature for 5 minutes. A sample of the response regulator/Ac-P mix was taken after the 10 minute incubation to demonstrate that this reaction was not radiolabelled (Ac-P-10). An aliquot was also taken and kept in experimental conditions, to be halted after the final sample of the time course was taken, to demonstrate that a radioactive signal would not have accumulated on the response regulator over the course of the experiment without the addition of the $CheA^{HK}$/labelled ATP mix (Ac-P-End).

The $CheA^{HK}$/labelled ATP mix was added to the RR/Ac-P mix, samples were taken at intervals, halted with 5x sample loading buffer and kept on ice. Samples were loaded sequentially onto SDS-PAGE gels which were dried and visualised using the Typhoon 9400. To minimise variance between the sample and control time course assays, the experiments were run concurrently, where sampling intervals allowed, they used the same diluted labelled ATP stock and were run on the same SDS-PAGE gel to allow for direct comparison of the results.

$CheA^{HK}$ Dependant/Independent Phosphorylation of CheY-GST

The GST tagged CheY (CheY-GST) was tested as outlined above, incubation was carried out on ice and samples were taken at 0, 2, 5, 10 and 15 minutes. Figure 5.1*A* shows an SDS-PAGE gel of the non-Ac-P exposed CheY-GST

phosphorylation assay. CheY-GST became strongly phosphorylated immediately at the 0 timepoint, the signal dropped but remained strong after 2 minutes (Lanes 2 and 3), a clear signal was not observed for CheY-GST after 5 minutes (Lanes 4-6). A similar pattern was observed for $CheA^{HK}$ dephosphorylation, $CheA^{HK}$ remains phosphorylated but with declining signal up to 5 minutes (Lanes 2-4) a proportion of $CheA^{HK}$ appears to remain phosphorylated up to the 15 minute time point but did not show a signal easily distinct from the background noise (Lane 5-6). Quantitative analysis of the SDS-PAGE gel supports these observations from Fig.5.1*C*, CheY-GST was immediately phosphorylated and then rapidly hydrolysed its phosphate group. No phosphorylated protein was present in the Ac-P-10 or Ac-P-End samples.

Figure 5.1*B* shows an SDS-PAGE gel of the Ac-P exposed CheY-GST. CheY-GST became immediately detectable at the 0 timepoint (Lane 2) but showed strongest phosphorylation at the 2 minute timepoint (Lane 3) a weak signal was visible after 5 minutes (Lane 4) but this may be a low level of residual radiation retained by the gel after electrophoresis. $CheA^{HK}$ was strongly phosphorylated at the 0 timepoint (Lane 2), a clear signal was visible up until the 5 minute time point (Lanes 2-4) and possibly up to the 15 minute sample (Lane 6) No band was present in the Ac-P-10 or Ac-P-End samples.

Comparison of the plus Ac-P (Fig.5.1*B*) and minus Ac-P timecourses (Fig.5.1*A*) shows a delayed emergence of a CheY-GST signal where Ac-P was present. Without Ac-P, CheY-GST reached its peak phosphorylation immediately after the $CheA^{HK}$/ATP mix was added (Lane 2) whereas with Ac-P the strongest signal from CheY-GST was detected at 2 minutes. In addition this signal at its peak was

34% of that of peak CheY-GST phosphorylation when Ac-P was not present (Fig.5.1*C*). These tests indicate Ac-P had blocked phosphorylation of CheY by ^{32}P from $CheA^{HK}$, showing Ac-P had directly phosphorylated CheY.

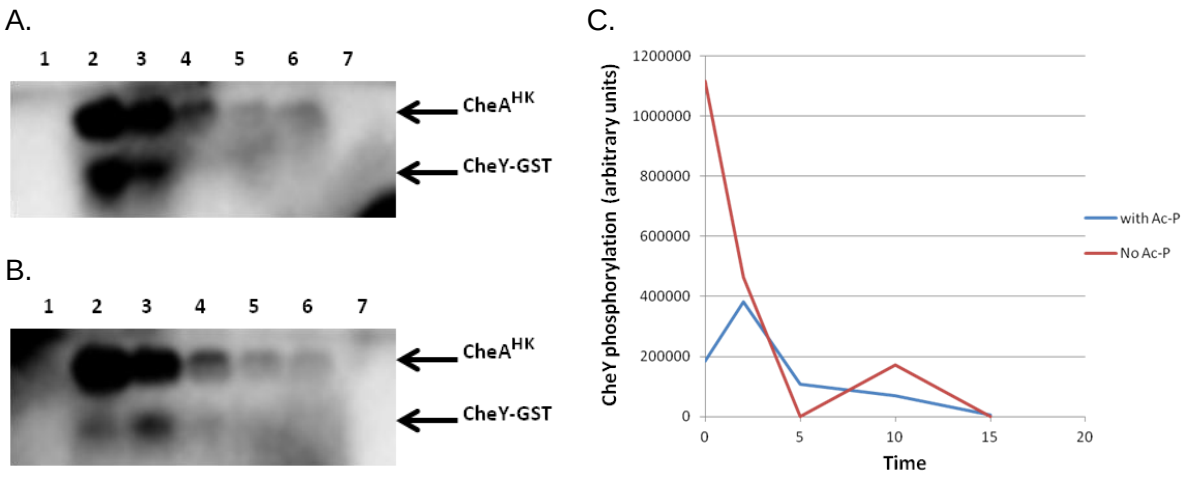

Figure 5.1 Phosphor screen visualisations and the corresponding graph, for a blocking assay of CheY-GST against ^{32}P labelled CheAHK, and unlabelled phosphate from Ac-P. Phosphor screens were exposed to gels for 44 hours before being scanned. Experiments were carried out in reaction buffer at pH8.3, samples were treated with 5x sample loading buffer with 0.2 M DTT and kept on ice before loading onto an SDS-PAGE gel. (A) 10 µM $CheA^{HK}$ was incubated with 3 µM [γ-^{32}P] ATP diluted with 30 µM non-radiolabelled ATP for 10 minutes, then put on ice for 5 minutes to reduce the temperature of the experiment. A separate reaction was prepared containing 10 µM CheY-GST and no ATP, a sample was taken from this to demonstrate that CheY-GST was not radiolabelled (Lane 1). The now phosphorylated $CheA^{HK}$ mix was added to CheY, a sample was taken immediately (Lane 2), then at 2, 5, 10 and 15 minutes (Lanes 3-6) Ac-P-END (Lane7). (B) 10 µM $CheA^{HK}$ was incubated with 3 µM [γ-^{32}P] ATP diluted with 30 µM non-radiolabelled ATP for 10 minutes, then put on ice for 5 minutes to reduce the temperature of the experiment. A separate reaction was prepared containing 10 µM CheY-GST and 200 mM Ac-P, this reaction was allowed to proceed for 10 minutes. A sample was taken from the CheY-GST/Ac-P reaction this to demonstrate that CheY-GST was not radiolabelled (Lane 1). The now phosphorylated $CheA^{HK}$ mix was added to the CheY/Ac-P mix, a sample taken immediately (Lane 2), then at 2, 5 10 and 15 minutes (Lanes 3-6) Ac-P-END (Lane7). (C) shows a plot of the data collected for (A) and (B) using the ImageQant TL software (n=2).

$CheA^{HK}$ Dependant/Independent Phosphorylation of CheV

The GST tagged CheV (CheV-GST) was tested as outlined under the scheme for experiments heading. Figure 5.2*A* shows the non-Ac-P exposed CheV-GST phosphorylation assay. Peak CheV-GST phosphorylation occurred at the 0 time point and steadily decreased until the final 2 minute point (Fig.5.2*C*) at which time a weak band was faintly observed (Lanes 2-6). $CheA^{HK}$ remained phosphorylated over the course of the experiment, its phosphorylation steadily declining over the 2 minutes of the assay. No band was present in the Ac-P-10 or Ac-P-End samples. Figure 5.2*B* shows an SDS-PAGE gel of the Ac-P exposed CheV-GST phosphorylation assay. Peak CheV-GST phosphorylation occurred at the 0 time point and steadily decreased until the final 2 minute point (Fig.5.2*C*) at which time a very weak band was observed (Lanes 2-6). $CheA^{HK}$ remained phosphorylated over the course of the experiment, its phosphorylation steadily declined over the 2 minutes of the assay. No band was present in the Ac-P-10 or Ac-P-End samples.

When compared in the plus Ac-P (Fig.5.2*B*) and minus Ac-P timecourses (Fig.5.2*A*), CheV-GST reached its peak phosphorylation at the 0 time point in both assays and remained phosphorylated for the duration of the experiment, the CheV-GST plus Ac-P assay showed a lower level of phosphorylation than that without Ac-P. However, in the presence of Ac-P CheV-GST reached 75% of the level of phosphorylation seen without Ac-P (Fig.5.2*C*). $CheA^{HK}$ remained phosphorylated for the duration of both assays. Counter intuitively a greater amount of ^{32}P was retained by $CheA^{HK}$ in the assay without Ac-P, the lower level of CheV-GST phosphorylation where Ac-P was present suggests that CheV was

accepting unlabelled Pi from Ac-P. However, the kinase assay in which Ac-P was not present showed $CheA^{HK}$ to retain a greater amount of ^{32}P. These tests indicate Ac-P had blocked phosphorylation of CheV by ^{32}P from $CheA^{HK}$, therefore Ac-P had directly phosphorylated CheV.

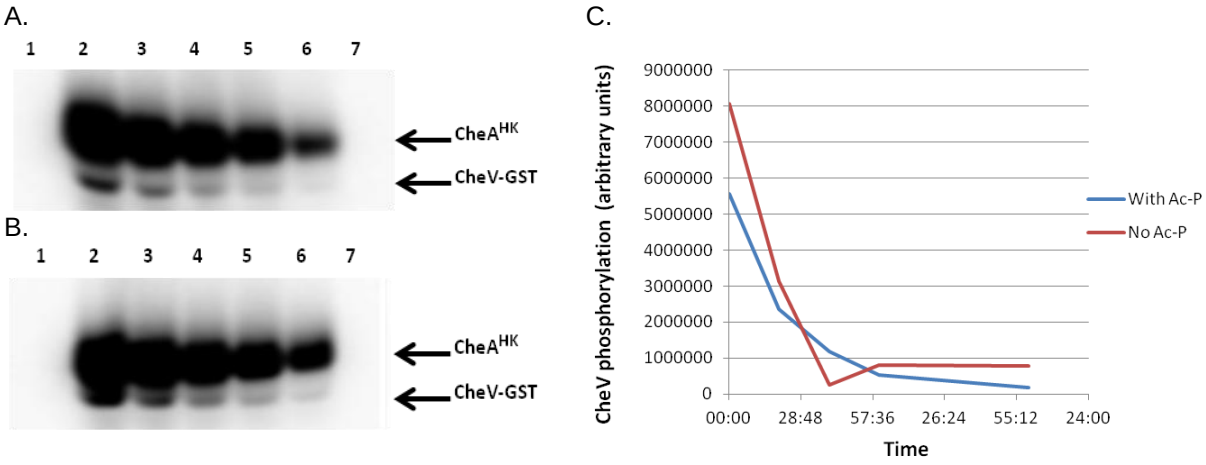

Figure 5.2. Phosphor screen visualisations and the corresponding graph, for a blocking assay of CheV-GST against ^{32}P labelled CheAHK, and unlabelled phosphate from Ac-P. Phosphor screens were exposed to gels for 44 hours before being scanned. Experiments were carried out in reaction buffer at pH8.3, samples were treated with 5x sample loading buffer with 0.2 M DTT and kept on ice before loading onto an SDS-PAGE gel. (A) 10 µM $CheA^{HK}$ was incubated with 3 µM [γ-^{32}P] ATP diluted with 30 µM non-radiolabelled ATP for 10 minutes, then put on ice for 5 minutes to reduce the temperature of the experiment. A separate reaction was prepared containing 10 µM CheV-GST and no ATP, a sample was taken from this to demonstrate that CheV-GST was not radiolabelled (Lane 1). The now phosphorylated $CheA^{HK}$ mix was added to CheV, a sample was taken immediately (Lane 2), then at 0:20, 0:40, 1 minute, and 2 minutes (Lanes 3-6) Ac-p END (Lane 7). (B) 10 µM $CheA^{HK}$ was incubated with 3 µM [γ-^{32}P] ATP diluted with 30 µM non-radiolabelled ATP for 10 minutes, then put on ice for 5 minutes to reduce the temperature of the experiment. A separate reaction was prepared containing 10 µM CheV-GST and 200 mM Ac-P, this reaction was allowed to proceed for 10 minutes. A sample was taken from the CheV-GST/Ac-P reaction to demonstrate that CheV-GST was not radiolabelled (Lane 1). The now phosphorylated $CheA^{HK}$ mix was added to the CheV/Ac-P mix, a sample taken immediately (Lane 2), then at 0:20, 0:40, 1 minute, and 2 minutes (Lanes 3-6), Ac-P END (Lane 7). (C) shows a plot of the data collected for (A) and (B) using the ImageQant TL software (n=3).

CheA-HK Dependant/Independent Phosphorylation of CheA

The whole length GST tagged CheA (CheA-GST) protein was tested rather than CheA-RR, as exclusion of a domain of CheA may have caused false positive or negative results in the later affinity tests. Testing whole length CheA-GST meant that it was not necessary to use the separately expressed $CheA^{HK}$ to phosphorylate CheA's response regulator as the native fused histidine kinase domain could be used.

As CheA incubated with ATP would pass phosphate to its RR domain, as shown in Chapter 4, quantification of CheA phosphorylation would include ^{32}P on both HK and RR domains. CheY was added to 'strip' phosphate from the HK domain so that the ^{32}P quantified subsequently would only be that which remained on the RR domain. Samples were loaded sequentially on to SDS-PAGE gels which were analysed using the Typhoon 9400.

Figure 5.3*A* and Figure 5.3*B* show the SDS-PAGE gels post Typhoon analysis and the data in Figure 5.3*C* is from quantitative analysis of the same SDS-PAGE gel carried out using the ImageQant TL software. Figure 5.3*A* shows the non-Ac-P exposed CheA-GST phosphorylation assay. CheA-GST phosphorylation first became visible in the 5 minute sample (Lane 3), peak phosphorylation occurred at the 15 minute time point (Lane 5) and may have increased further if allowed. Once CheY was added phosphorylation fell to 54% of its original total (Lane 6) (Fig.5.3*C*). No band was present in the Ac-P-10 or Ac-P-End (Blank) samples (Lanes 1 and 7). Fig 5.3*B* shows the Ac-P exposed CheA-GST phosphorylation assay, CheA-GST phosphorylation first became visible in the 5 minute sample (Lane3) peak phosphorylation occurred at the 15 minute time point (Lane 5) and

may have increased further if allowed. Once CheY was added phosphorylation, fell to 44% of its original total (Lane 6) (Fig.5.3*C*). No band was present in the Ac-P-10 or Ac-P-End samples (Lanes 1 and 7).

CheA phosphorylation for both of the assays peaked at 15 minutes, before CheY was added. After CheY was added both time course assays lost approximately half of their total ^{32}P suggesting that the strategy to 'strip' phosphate from the histidine kinase domain was successful. Notably the signal from CheA in the plus Ac-P reaction was 48% that of the CheA not exposed to Ac-P (Fig.5.3*C*). Ac-P had blocked phosphorylation of CheA's response regulator domain by ^{32}P from CheA's histidine kinase domain, it appears therefore that Ac-P had directly phosphorylated the CheA RR domain.

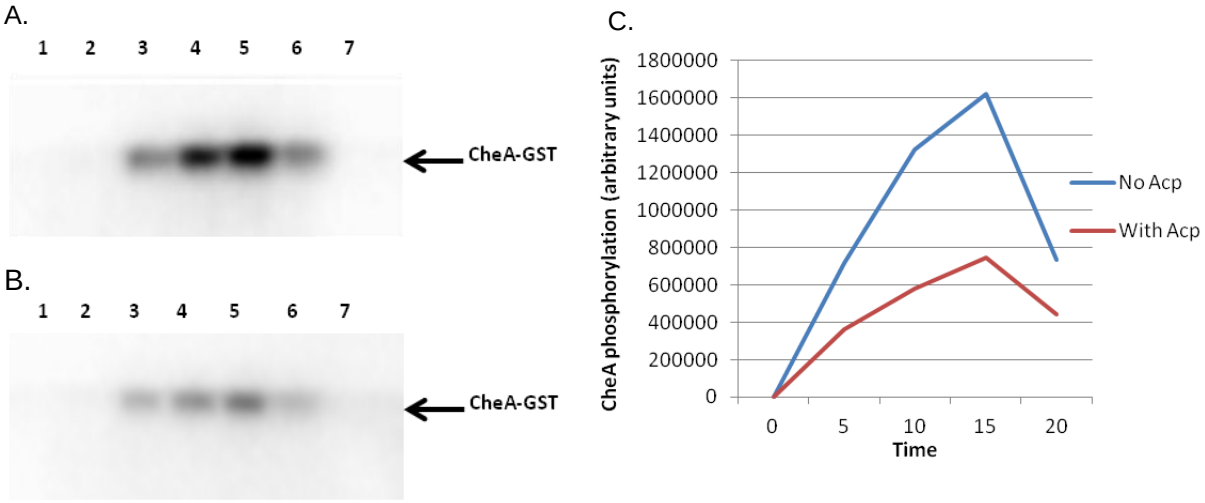

Figure 5.3. Phosphor screen visualisations and the corresponding graph, for a blocking assay of CheA-GST RR domain, against ^{32}P labelled CheAHK and unlabelled phosphate from Ac-P. Phosphor screens were exposed to gels for 44 hours before being scanned. Experiments were carried out in reaction buffer at pH8.3, samples were treated with 5x sample loading buffer with 0.2 M DTT and kept on ice before loading onto an SDS-PAGE gel. (A) a reaction containing 10 µM CheA-GST was heated to 30 °C, a sample was taken to demonstrate that CheA-GST was not radiolabelled (Lane 1). 3 µM [γ-^{32}P] ATP diluted with 30 µM non-radiolabelled ATP was added to the reaction and sample taken immediately (Lane 2) following samples were taken at 5, 10 and 15 minutes (Lanes 3 -5). After the 15 minute sample was taken CheY was added to 20 µM and the reaction allowed to proceed to the 20 minute point (Lane 6) Ac-P END (Lane7). (B) A reaction containing 10 µM CheA-GST was heated to 30 °C and exposed to 200 mM Ac-P for 10 minutes, a sample was taken to demonstrate that CheA-GST was not radiolabelled (Lane 1). 3 µM [γ-^{32}P] ATP diluted with 30 µM non-radiolabelled ATP was added to the reaction and sample taken immediately (Lane 2) following samples were taken at 5, 10 and 15 minutes (Lanes 3 -5), After the 15 minute sample was taken CheY was added to 20 µM and the reaction allowed to proceed to the 20 minute point (Lane 6) Ac-P END (Lane7). (C) shows a plot of the data collected for (A) and (B) using the ImageQant TL software (n=4).

5.4.2. Conclusion

It was necessary to confirm that the purified GST tagged response regulators CheY, CheV and CheA (RR) were functional and able to be phosphorylated via HK, as the large 26 kDa GST tag may have prevented correct folding of the response regulators or interfered with their function. Once ^{32}P phosphorylation of the RR domains by HK was confirmed, it was possible to test direct phosphorylation by acetyl phosphate.

$CheA^{HK}$ Dependant Phosphorylation of CheY-GST, CheV-GST and CheA-GST

CheY-GST, CheV-GST and CheA-GST all became phosphorylated by ^{32}P modified $CheA^{HK}$ and were able to autodephosphorylate after (Fig.5.1-5.3). The GST tag did appear to have some effect upon the rate of hydrolysis for CheV. The HIS tagged CheV protein had completely dephosphorlyated after 30 seconds (Fig.4.7), but CheV-GST under the same conditions was still clearly phosphorylated after 1 minute and a faint signal was still visible at up to 2 minutes (Fig.5.2). This may also have been true for the GST tagged CheY and CheA but the data collected using these proteins did not cover relevant timepoints or strictly comparable experiments were not carried out (Data not shown). When the HIS tagged CheY had been tested it had been clearly phosphorylated for up to 5 minutes, as was CheY-GST, but the next sample in both assays was taken after

10 minutes, at which point neither protein displayed a clear phosphorylation signal, therefore without intervening samples, no clear conclusion could be made.

For CheA there were no assays made in comparative conditions, partly due to the complication of working with the full length protein and having both HK and RR domains present, so no clear conclusion as to the relative Pi hydrolysis rate could be drawn.

Acetyl Phosphate and $CheA^{HK}$ Independent Response Regulator Phosphorylation

The acetyl phosphate phosphorylation tests demonstrated direct phosphorylation of CheY, CheV and $CheA^{RR}$. When taken in comparison to the non-Ac-P exposed assays, those response regulator domains that were pre-exposed to Ac-P showed lower levels of phosphorylation than the control assay. The unlabelled Ac-P was expected to effectively block the access of the ^{32}P, from $CheA^{HK}$, by phosphorylating the RRs with unlabelled Pi groups and making it unavailable so that where Pi from Ac-P had bound, less of the population of that RR population could become radiolabelled.

CheY-GST displayed 34% of the level of phosphorylation reached when Ac-P was not present, this was 48% for CheA-GST and 75% for CheV-GST, each paired plus and minus Ac-P assay had been carried out using the same radiolabelled ATP stock and buffers to minimise variation between the assays. It seems likely given the evidence that the Ac-P had directly phosphorylated the RR domains, however at this time it was not possible to exclude that the presence of Ac-P had in some manner interfered with the interaction of $CheA^{HK}$ and an RR

rather than itself phosphorylated the RR, though this was later demonstrated not to be the case.

The same amount of Ac-P was added to each of the three RRs but the effect upon their phosphorylation afterwards by radiolabelled $CheA^{HK}$ was variable. The Ac-P concentration used was far in excess of a value physiologically relevant to *C. jejuni*. This was chosen to overcome the inherently insensitive design of the test, but these differences may reflect an ability of the RRs to interact with Ac-P in the cell. CheY-GST appeared to have accepted the most Pi from Ac-P as it had bound only 34% of ^{32}P when compared to the control, CheV took 75% of its non-Ac-P exposed level of ^{32}P. However, the varying affinities of the Che RR domains for $CheA^{HK}$, reflected in the order of preference for $CheA^{HK}$ to phosphorylate CheY, CheV then $CheA^{RR}$ (see Chapter 4), would also have affected the rate of Pi transfer from the histidine kinase to each non-phosphorylated response regulator.

Tests to investigate the Ac-P with CheA-GST reaction were more complex as the whole length protein contained two possible phosphorylation sites, the HK and RR domains. As phosphate bound to the HK domain would act as a high background possibly obscuring comparisons of the plus and minus Ac-P assays, CheY was added before the final time point to 'strip' Pi from the HK domain. CheY had been shown to efficiently dephosphorylate $CheA^{HK}$ and the integrated CheA Histidine kinase domain (see Chapter 4). At 20 minutes, after the addition of CheY, CheA-GST plus Ac-P retained 48% of the radiolabel observed in the non-Ac-P assay, so demonstrating Ac-P had blocked phosphorylation of CheA

RR domain with ^{32}P from CheA HK domain, by itself directly phosphorylating the integrated CheA RR domain.

It was possible that Ac-P hindered HK-RR interactions rather than itself phosphorylating the RRs, it may have been possible to correct for this by carrying out the assays in a different manner. The phosphorylation experiments could have been carried out on glutathione resin with the GST tagged RR immobilised, so that after exposure to Ac-P any remaining acetate or Ac-P could be washed away, before adding the radiolabelled HK. This would have excluded the possibility of Ac-P having interfered with the interaction of HK and RR. However, due to the observed rates of hydrolysis from the Che RR domains, it seems unlikely that the necessary washing steps could be carried out before Pi hydrolysis had occured.

Another approach would have been to use radiolabelled Ac-P, this would have allowed for much lower concentrations to be used and the results would have been more physiologically relevant. However, it is not possible at present to purchase [^{32}P] Ac-P, and it was impractical to make it in the laboratory due to safety concerns and a lack of suitable facilities. It was not clear from the existing evidence that the rate of transfer from Ac-P to a fast reacting RR, such as CheY, would have allowed for enough of the RR population to become radiolabelled so as to be detectable.

The pull-down assay is a method to demonstrate an interaction between proteins, if a ‘prey’ protein is pulled down by the ‘bait’ it is suggestive of a functional interaction between the proteins *in situ*. As it would now be possible to carry out

pull-down assays using phosphorylated or non-phosphorylated protein, these assays may shed more light on the function of the Che proteins and what part their phosphorylation state may play in this role.

5.5. Pull-down Assays Between the Che Proteins

The pull-down assays here used the GST tag to immobilise the GST tagged bait response regulator onto a glutathione resin. A prey protein was added to the resin which was then washed. The GST bait protein would be retained on the resin using its GST tag, whereas the prey protein would only be retained if there is a strong enough interaction between the proteins.

HIS tagged proteins were used as prey proteins as the RR proteins had shown to be functional in the earlier phosphorylation assays, suggesting that the tag had not interfered with protein folding. The His tag was not removed before assays were carried out as it would not bind to the glutathione resin and there was little risk of it effecting protein-protein interactions during the affinity assays.

5.5.1. Results

5.5.1.1. Pull-Down Assay Optimisation

It was decided to optimise the pull-down protocol around the CheA-CheY interaction as this was the most predictable. Being the primary response regulator CheY was likely to have the highest affinity for CheA and so be the easiest to observe in the early stages of test optimisation. Also a reduction in the affinity of phosphorylated *E. coli* CheY for CheA has previously been observed (Li

et al. 1995), so the phosphorylation conditions could also be optimised with this test.

Preliminary Tests

In preliminary tests CheY-GST was used as bait and the His tagged CheA as a prey protein, no phosphorylation of CheY-GST was attempted in this experiment. 25 µl of glutathione resin was used in a microcentrofuge tube so that the resin could easily be pelleted and resuspended for washing steps. The resin was loaded into the tube and washed 5 times in reaction buffer, CheY-GST and CheA were added and incubated together with the resin for 5 minutes, before the resin was washed three times with PBS. The final wash was removed and the resin resuspended in sample loading buffer, this would dissociate the proteins from the resin. The sample supernatant was loaded onto an SDS-PAGE gel for electrophoresis, which was Coomassie stained afterwards for analysis (Fig.5.4*A*). CheA tested alone did not bind directly to the resin itself (Lane 1). CheY was shown to bind to the resin (Lane 2). When mixed together both CheY-GST and CheA were detected in samples eluted from the resin (Lane 3). A smaller polypeptide at around 34 kDa which appears to be a breakdown product of CheY-GST also bound to the GST resin,but this had not been observed in earlier tests using that purified CheY preparation. This result suggested that CheY-GST had pulled-down CheA, which implied an interaction between CheA and CheY. However, although evidence had pointed to the smaller polypeptide present in the CheY-GST preparation being a breakdown product of CheY-GST, this had not been proved. This may have been another protein that had bound to the resin pulled-down CheA, giving the impression that CheA had been retained by CheY-

GST. It was possible that CheA had interacted with the GST portion of CheY-GST and not the Che protein itself, as this had not been separately controlled for.

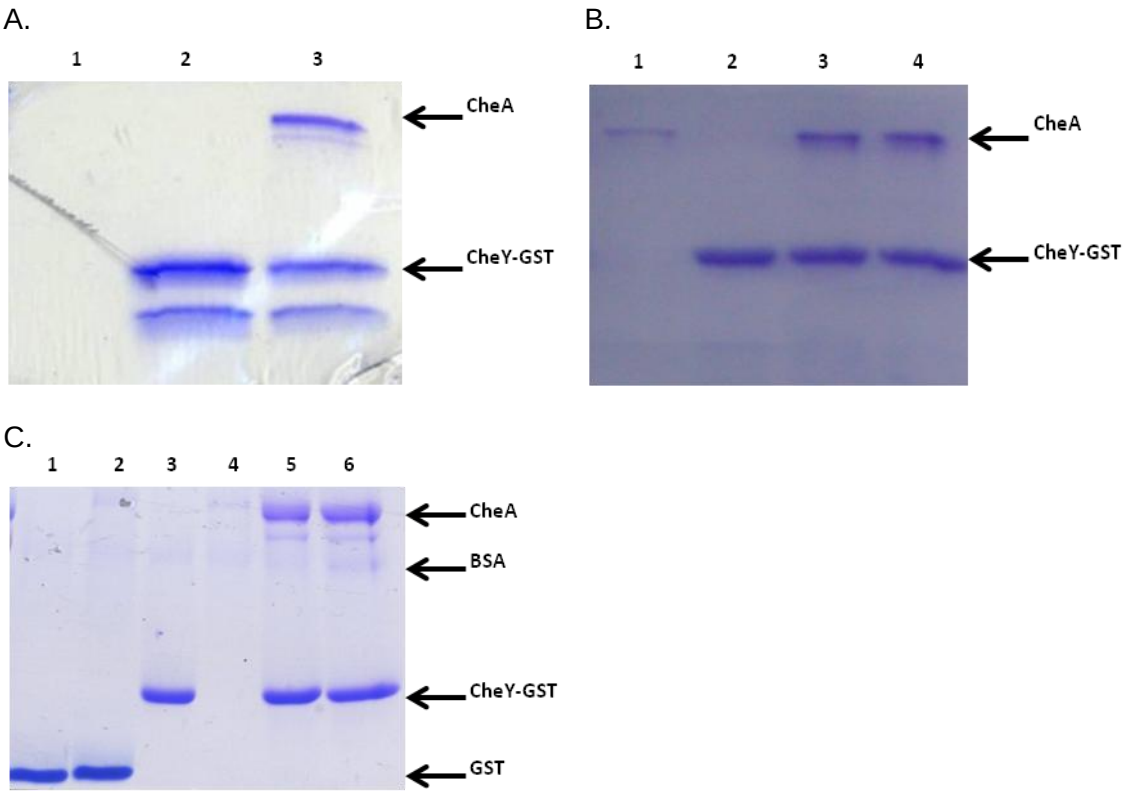

Fig 5.4 Coomassie stained SDS-PAGE gels of pull-down assay optimisation. These assays immobilise purified CheY-GST on glutathione resin, to test it's affinity to purified HIS tagged CheA. The proteins that appear do so as they have been retained by either a GST tag or their affinity to a protein that possesses a GST tag. The experiment in (A) used 25 µl of glutathione resin and PBS as a reaction/wash buffer. To wash the resin before use, the resin was pelleted by centrifugation at 12,000 *g* for 1 minute, then resuspended in fresh PBS for each wash, the resin was washed four times in total. 25 µg CheY-GST and/or 25 µg CheA were added to the relevant reactions, outlined in the scheme below. The reactions were incubated at room temperature for 5 minutes before being washed three times, with PBS as previously. Once the resin was pelleted from the final washing step, the supernatant was aspirated and discarded. The resin was resuspended in 20 µl of 5x sample loading buffer with 0.2 M DTT, the sample was re-pelleted and the supernatant for each sample was loaded sequentially onto an SDS-PAGE gel. The assays in each lane were: CheA alone on the resin (Lane 1), CheY-GST alone (Lane 2), and a test lane of CheY-GST and CheA (Lane 3) (n=1). The experiment shown in (B) was carried out as outlined for the assay in (A) except reaction buffer was used in place of PBS, 25 µl of MagneGST (Fisher, UK) magnetic beads which were pulled out of suspension using magnetic racks were used rather than the resin, and Ac-P was used in one of the tests to directly phosphorylate CheY-GST. The assays in each lane were: CheA alone on the resin (Lane 1), CheY-GST alone (Lane 2), CheY-GST with CheA (Lane 3) and phosphorylated CheY-GST with CheA (Lane 4). The conditions of the experiment in (C) were as for that in (B) except it used 20 µl of MagneGST beads, which were blocked with 20µl of 1% BSA for 5 minutes before use, then excess BSA was removed with a wash before the experiment began. The assays in each lane were: GST tag alone (Lane 1), GST tag with CheA (Lane 2), CheY-GST alone (Lane 3) CheA alone (Lane 4) CheY-GST with CheA (Lane 5) and phosphorylated CheY-GST with CheA (Lane 6) (n=2).

Updating the Pull-down Assay for Optimal Phosphorylation Conditions

In Figure 5.4*B* the protocol was kept the same but the assay was carried out in reaction buffer instead of PBS and MagneGST (Fisher, UK), a magnetic immobilised glutathione resin was used instead. The resin used together with a magnetic separation stand (Fisher, UK) allowed for faster separation of the supernatant and resin. The magnetic stand almost instantly pulled the resin out of suspension and allowed the supernatant to be removed easily so that the washes could be completed much faster than if the centrifuge steps for the normal resin had been used. As the washes could be completed quicker this increased the probability of the chosen RR retaining its phosphate for the duration of the experiment.

A new CheY-GST purified protein preparation was tested and Ac-P phosphorylated CheY-GST was trialled against CheA. The new CheY-GST preparation proved successful with only a single band at the correct molecular weight observed in all of the plus CheY-GST lanes (Lanes 2, 3 and 4). CheA was pulled-down by CheY-GST in the presence and absence of Ac-P (Lanes 3 and 4). CheA had been shown to interact with CheY-GST, no modulation of this binding affinity was observed with CheY-GST in a phosphorylated state.

A Changed Protocol and New Controls

The SDS-PAGE gel in Figure 5.4*C* shows the CheY-GST to CheA interaction with additional controls and with a phospho CheY-GST versus CheA assay. The incubation and washing protocol was updated for this assay.

No effect of phosphorylation of CheY-GST on CheA binding was apparent in this assay, lane 5 shows CheY-GST versus CheA without pre-incubation with Ac-P, this lane shows an equally strong CheA band to lane 6 in which CheY-GST had been exposed to Ac-P.

The new protocol did not negatively affect the amount of protein recovered from each pull-down. A GST versus CheA control showed only a very faint band at the size of CheA (Lane 2), similar in intensity to that seen for CheA alone on resin (Lane 4). CheA was pulled-down by phosphorylated and non-phosphorylated CheY (Lanes 5 and 6). A faint band was visible at the molecular weight of the BSA, at approximately 66.4 kDa (Lanes 1-6).

Final Optimisation

An amendment was made to the protocol shown in Figure 5.4, in which additional BSA was added at the same time as the prey protein CheA. The optimised protocol is shown in Chapter 2. This final optimisation was successful as phosphate dependent dissociation of CheA from CheY-GST was now observed (Fig.5.5)

5.5.1.2. Optimised Pull-Down Assay Results

CheY Interactions

CheY-GST Interaction With CheA

The CheY affinity to CheA was tested and the effect of CheY phosphorylation upon its affinity to CheA observed. In Figure 5.5*A* faint CheA bands are visible in CheA versus GST (Lane 3), CheA alone on resin (Lane 5) and very faintly in the phosphorylated CheY-GST versus CheA assays (Lane 7), but these bands are not as clear and dense as that shown for CheY-GST versus CheA (Lane 6). Dissociation of the phosphorylated CheY from CheA had been demonstrated (Lane 7). CheA with sample loading buffer was run alongside the final CheY-GST versus CheA assay as a size comparison (Lane 1). BSA was visible in all assays in which it was loaded (Lanes 2-7). CheA had been pulled-down by CheY-GST, but it was not pulled down when CheY-GST was in a phosphorylated state.

CheA-GST Interaction With CheY

To test the reverse of the previous CheY-GST and CheA experiment, and to test the effect of CheA-RR phosphorylation upon CheY binding, CheA-GST affinity to CheY was tested (Fig.5.5*B*). Purified CheY was loaded as a size marker in lane 7. CheY did not bind to either of the negative controls, the GST tag alone (Lane 2) or the resin alone (Lane 4), CheY is faintly visible in both of the test lanes, CheA-GST with CheY (Lane 5) and phosphorylated CheA-GST with CheY (Lane 6). BSA is visible in all assays in which it was loaded (Lanes 1-6). CheY had

been pulled down by CheA-GST, no difference was seen in the amount of CheY pulled down between phosphorylated, and non-phosphorylated CheA-GST.

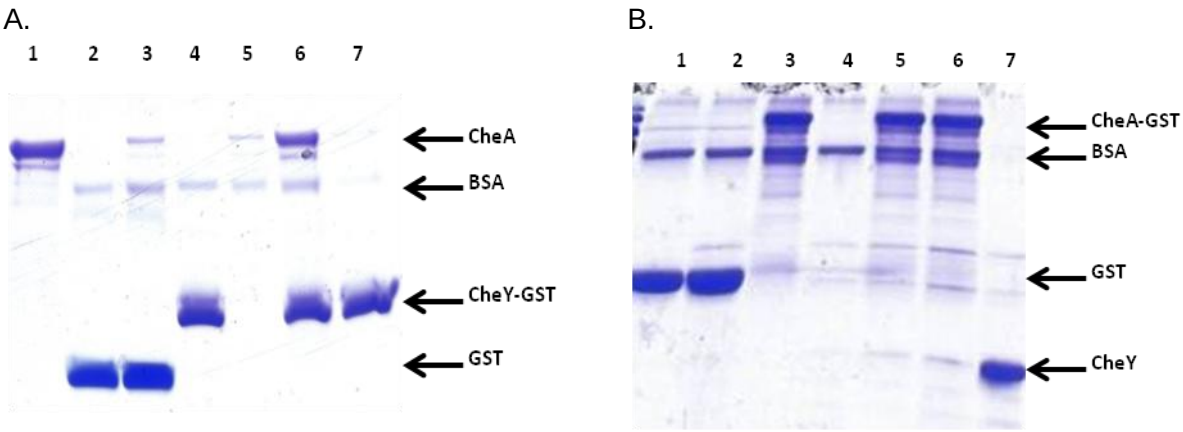

Figure 5.5. Coomassie stained SDS-PAGE gels of pull-down assays between CheY and CheA. These assays used the final updated experimental protocol, which included additional BSA to be added when the 'prey' protein was added to an assay. 30 µg of the bait protein or GST tag was used with 50 µg of the prey protein, in reaction buffer which was used as a reaction/washing buffer. The volume of MagneGST beads used was reduced to 20 µl. Acetyl phosphate was used in some assays to directly phosphorylate the GST tagged protein. For each assay 20 µl of the beads were placed into a 1.5 ml microcentrifuge tube, the resin was washed twice, 20 µl of 1% (w/v) BSA and the bait protein were added to the beads and incubated for 5 minutes, the resin was washed again twice, 20 µl of 1% (w/v) BSA and the prey protein was added to the beads, which were incubated for 5 minutes before the resin was washed again twice. The final wash was aspirated, the beads were resuspended in 20 µl of 5 x sample loading buffer with 0.2 M DTT and then captured again so the sample could be aspirated and loaded onto an SDS-PAGE gel. The proteins that appear in each gel do so as they have been retained by a either a GST tag or their affinity to a protein that possesses a GST tag (n=2). (A) CheA loaded straight onto the gel as a size standard (Lane 1), GST alone (Lane 2), GST plus CheA (Lane 3), CheY-GST alone (Lane 4), CheA alone (Lane 5) CheY with CheA (Lane 6) and phosphorylated CheY-GST with CheA (Lane 6). The experiment in (B) used CheA-GST and HIS tagged CheY. The assays in order were: GST alone (Lane 1) GST with CheY (Lane 2), CheA-GST alone (Lane 3), CheY alone (Lane 4), CheA-GST with CheY (Lane 5), phosphorylated CheA with CheY (Lane 6), CheY loaded straight onto the gel as a size standard (Lane 7) (n=3).

CheB and CheR Interactions

CheV-GST Interaction With CheR

Figure 5.6*A* shows an SDS-PAGE gel of a pull-down experiment between Che-V-GST and CheR. Purified CheR was loaded as a size control in lane 7. CheR has been retained in all of the assays in which it was loaded, in the negative controls of GST with CheR (Lane 2) and resin alone with CheR (Lane 4) and the test lanes of CheV-GST with CheR and phosphorylated CheV-GST with CheR (Lanes 5 and 6 respectively). A clear BSA band is visible in lanes 1 – 6. CheR had been pulled down in all lanes, including the negative controls.

CheA-GST Interaction With CheR

Figure 5.6*B* displays an SDS-PAGE of a pull-down experiment between Che-A-GST and CheR. Purified CheR was loaded as a size control in lane 8. CheR has been retained in all of the assays in which it was loaded, in the negative controls of GST with CheR (Lane 2) and resin alone with CheR (Lane 4) and the test lanes of CheA-GST with CheR, phosphorylated CheA-GST with CheR, and CheA-GST with CheR plus ATP (Lanes 5-7 respectively). A clear BSA band is visible in lanes 1 – 7. CheR had been pulled down in all lanes, including the negative controls.

CheV-GST Interaction With CheB

CheB was an important candidate for the affinity tests but it had not been successfully purified, many contaminants remained in the CheB stock. A strong affinity between CheV and CheB may be able to pull-down CheB from the complex mixture in a pull-down experiment, so the experiment was attempted.

Figure 5.7*A* displays the SDS-PAGE gel of the pull-down assay between CheV-GST and CheB. The CheB stock was loaded in lane 7 for comparison. A complex mixture of proteins was retained in all of the assays in which the CheB mixture was loaded, in the negative controls of GST with CheB (Lane 2), resin alone with CheB (Lane 4) and the test lanes of CheV-GST with CheB (Lane 5) and phosphorylated CheV-GST with CheB (Lane 6). A clear BSA band is visible in lanes 1 – 6. CheB was not separately pulled down from the complex mixture in any of the assays.

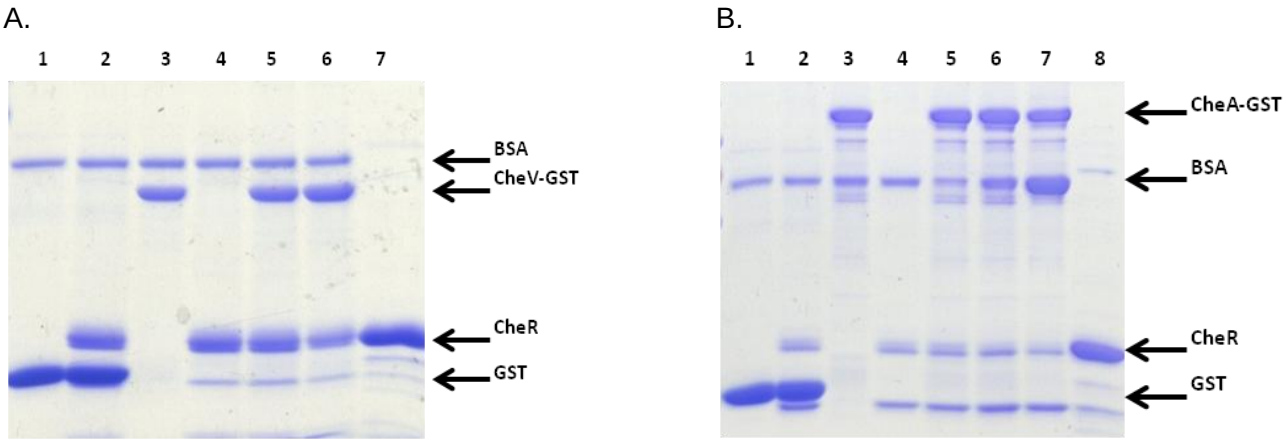

Figure 5.6. Coomassie stained SDS-PAGE gels of pull-down assays between CheV-GST and CheR, and CheA-GST with CheR. These assays used the updated experimental protocol detailed previously in Figure 5.5. 30 µg of the bait protein or GST tag was used with 50 µg of the prey protein, in reaction buffer which was used as a reaction/washing buffer. MagneGST beads were used to immobilise the GST tagged proteins. The proteins that appear in each gel do so as they have been retained by a either a GST tag or their affinity to a protein that possesses a GST tag. The experiment in (A) used immobilised CheV-GST to test it's affinity to CheR. The loading order is as follows: GST alone (Lane 1), GST and CheR (Lane 2), CheV-GST alone (Lane 3), CheR alone (Lane 4), CheV-GST and CheR (Lane 5), phosphorylated CheV-GST and CheR (Lane 6), CheR loaded directly on the gel for size comparison (Lane 7) (n=3). (B) CheA-GST was immobilised and its affinity to CheR tested. Assays in order: GST alone (Lane 1), GST with CheR (Lane 2), CheA-GST alone (Lane 3), CheR alone (Lane 4), CheA-GST with CheR (Lane 5), phosphorylated CheA-GST with CheR (Lane 6) a repeat of phosphorylated CheA-GST and CheR (Lane 7) and CheR loaded directly onto the gel as a size comparison (Lane 8) (n=2).

CheV Interactions

CheV-GST Interaction With TLP_1

At the point at which these experiments were carried out no purified TLP_1 stock was available so a partially purified complex mix was used. A high affinity between CheV-GST and TLP_1 may be able to pull-down TLP_1 from its contaminants.

In Figure 5.7*B* the negative controls showed that the TLP_1 did not interact with the GST domain of the CheV-GST protein as no band appeared (Lane 3) and that TLP_1 was not retained by the resin itself as no band appeared for that assay (Lane 5). When CheV-GST and TLP_1 were present together TLP_1 was retained by CheV-GST, where CheV-GST was unphosphorylated less TLP_1 was retained (Lane 6) than where CheV-GST was phosphorylated (Lane 7).

The same experiment with an increased amount of protein is shown in Figure 5.7*C*. The controls were run as previously except that the TLP_1 alone on the resin showed a very faint band for TLP_1 and also for one of the contaminating bands which persisted after the washing process. TLP_1 loading had been increased to make the total amount of TLP_1 available to CheV-GST larger and to account for the mass of the other proteins in this complex mixture. However, the lanes in which TLP1 and CheV-GST were present together both show much clearer distinct bands, also the pattern of increased phosphorylation of CheV-GST leading to increased retention of TLP1 was also repeated (Lanes 5 and 6)

Taken together the results of these experiments provide good evidence that CheV phosphorylation increases its affinity towards the TLP1 cytoplasmic domain.

CheV Interaction With CheA

Interactions between CheV and CheA had previously been indicated (Bridle 2007), these assays tested the affinity of CheV-GST for CheA in both phosphorylated and non-phosphorylated states.

An initial CheV-GST with CheA assay, shown in Figure 5.8*A*, had displayed an uncertain but promising sign of an interaction between the proteins. A very weak CheA band appeared to have been pulled-down by phosphorylated CheV-GST (Lane 7) when compared to the non-phosphorylated CheV-GST (Lane 6). However, where CheA was exposed alone to glutathione resin (Lane 5) this lane showed a more intense band. The CheA with GST assay showed no binding (Lane 3). Pure CheA was included as a size control in lane 1.

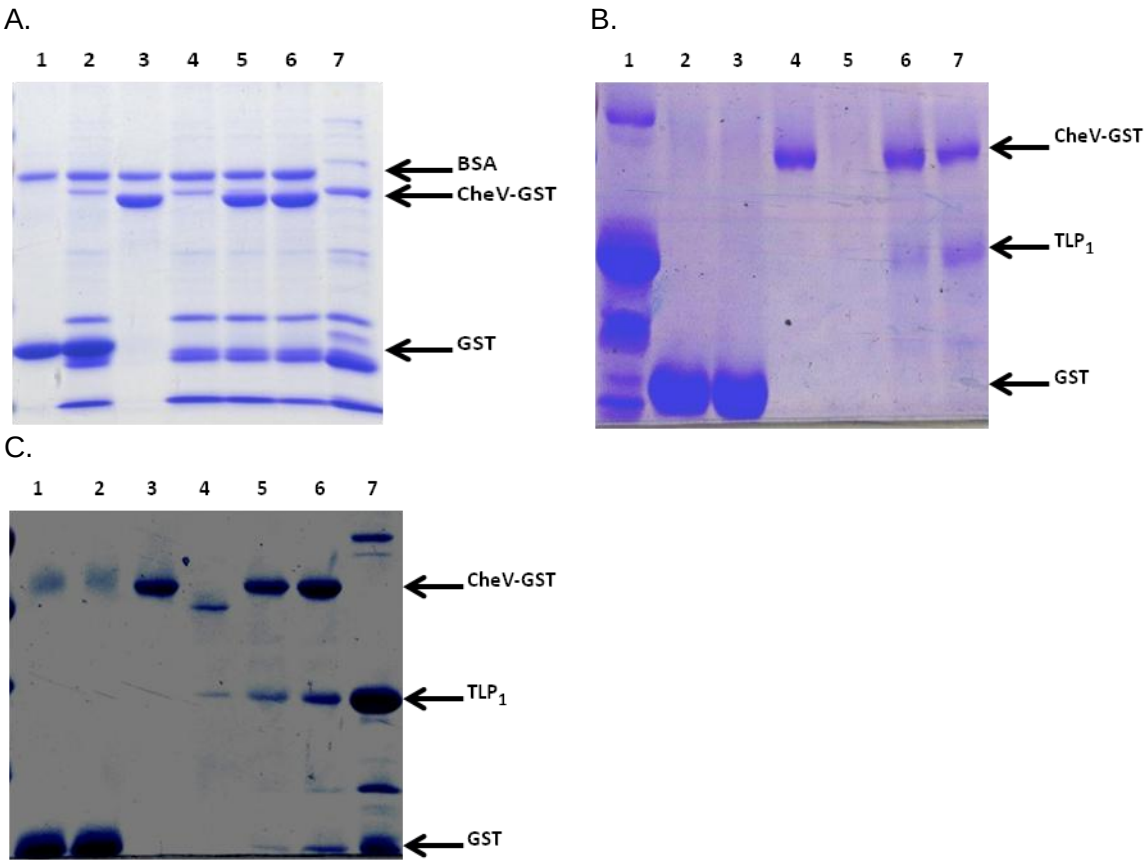

Figure 5.7. Coomassie stained SDS-PAGE gels of pull-down assays between CheV-GST and CheB, and CheV-GST with TLP_1. These assays used the updated experimental protocol detailed previously in Figure 5.5. 30 µg of the bait protein or GST tag was used with 50 µg of the prey protein, in reaction buffer which was used as a reaction/washing buffer. The proteins that appear in each gel do so as they have been retained by a either a GST tag or their affinity to a protein that possesses a GST tag. The experiment in (A) used immobilised CheV-GST to test it's affinity to CheB. The loading order is as follows: GST alone (Lane 1), GST and CheB (Lane 2), CheV-GST alone (Lane 3), CheB alone (Lane 4), CheV-GST and CheB (Lane 5), phosphorylated CheV-GST and CheB (Lane 6), CheB loaded directly on the gel for size comparison (Lane 7) (n=2). The assay shown in (B) tests CheV-GST affinity to TLP_1. Lanes are as follows: TLP_1 loaded directly as a size standard (Lane 1), GST alone (Lane 2), GST with TLP_1 (Lane 3), CheV-GST alone (Lane 4), TLP_1 alone (Lane 5) CheV-GST with TLP_1 (Lane 6), phosphorylated CheV-GST with TLP_1 (Lane 7). (C) shows a repeat of the experiment of (B) but the loading order is different. GST alone (Lane 1), GST with TLP_1 (Lane 2), CheV-GST alone (Lane 3), TLP_1 alone (Lane 4), CheV-GST with TLP_1 (Lane 5), phosphorylated CheV-GST with TLP_1 (Lane 7) (n=3).

Numerous attempts to repeat the results of this assay resulted in no interaction being detected between the CheV-GST bait and CheA prey protein, many conditions were tried including using a greater mass of protein but no interaction was detected between the proteins using this method. The opposite assay using CheA-GST against CheV was attempted multiple times but no interaction between the proteins was observed (Fig.5.8*B*).

The time taken between phosphorylation of the proteins and completion of the final washing steps was reduced to maximise phosphorylated protein during the assay. CheV-GST and CheA were combined together with Ac-P for varying amounts of time before the washing steps commenced (Fig.5.8*C*). In this assay polypeptide migrations at the molecular weight of CheA were detected in the plus Ac-P for 1 and 2 minute assays (Lanes 2 and 3) and not for any of the assays including the negative, no Ac-P assay (Lane 1).

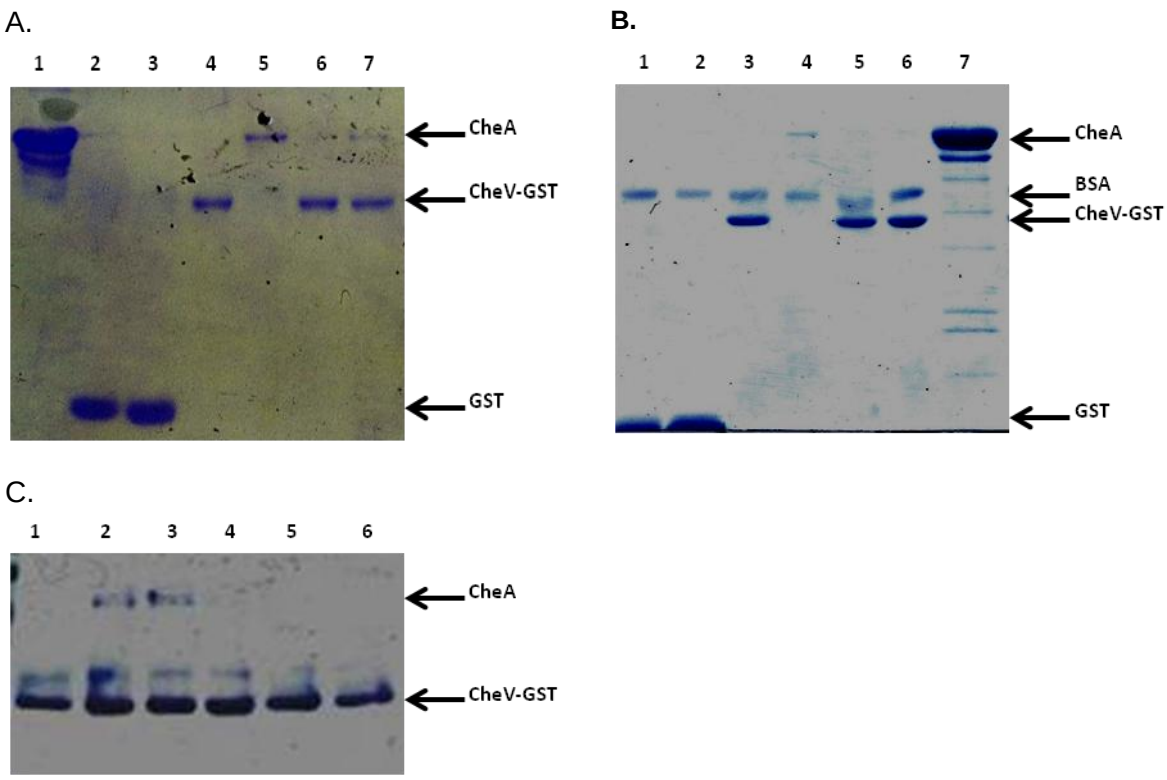

Figure 5.8. Coomassie stained SDS-PAGE gels of pull-down assays between CheV-GST with CheA, and CheA-GST with CheV. These assays used the updated experimental protocol detailed previously in Figure 5.5. 30 µg of the bait protein or GST tag was used with 50 µg of the prey protein, in reaction buffer which was used as a reaction/washing buffer. MagneGST beads were used to immobilise the GST tagged proteins. The proteins that appear in each gel do so as they have been retained by a either a GST tag or their affinity to a protein that possesses a GST tag. The experiment in (A) used immobilised CheV-GST to test its affinity to CheA. The loading order is as follows: CheA loaded directly on to the gel for size comparison (Lane 1), GST alone (Lane 2), GST with CheA (Lane 3), CheV-GST alone (Lane 4), CheA alone (Lane 5), CheV-GST with CheA (Lane 6), phosphorylated CheV-GST with CheA (Lane 7) (n=1). (B) displays a repeat of the experiment in (A) but with a different sample loading order. GST alone (Lane 1), GST with CheA (Lane 2), CheV-GST alone (Lane 3), CheA alone (Lane 4), CheV-GST with CheA (Lane 5), phosphorylated CheV-GST with CheA (Lane 6), CheA loaded directly onto the gel as a size comparison (Lane 7) (n=6). (C) The experimental protocol was changed for this assay. In all lanes CheV-GST and CheA were combined in the presence of Ac-P for varying amounts of time before washing commenced. no Ac-P control (Lane 1), 1 minute incubation (Lane 2), 2 minute incubation (Lane 3) 4 minute incubation (Lane 4), 10 minute incubation (Lane 5), 20 minute incubation (Lane 6) (n=1).

5.6. Discussion

The aim of the affinity tag pull-down assays had been to verify interactions previously observed in the bacterial and yeast two hybrid studies (Bridle 2007; Parrish et al. 2007), and to identify previously unobserved functional relationships between chemotaxis proteins. With these assays I hoped to also expand upon that data, by examining the effect of phosphorylation upon chemotaxis protein interactions.

5.6.1. Pull-Down Assay Optimisation

It was decided to base optimisation of the pull-down assay upon the interaction of CheY with CheA, as the kinase assays had shown CheY to be the primary response regulator so increasing the likelihood of an interaction being observed (Chapter 4). As I also wished to optimise the phosphorylation aspect of the pull-down assay, the CheY-CheA interaction was ideal as large changes in the affinity for CheA of phosphorylated and non-phosphorylated CheY had been previously observed (Lee et al. 2001).

The washing protocol was modified to prevent exposure of the prey response regulator to Ac-P, so that if the interaction of two response regulators were being tested Ac-P could be removed from the assay before the prey protein was added to the reaction. The additional BSA added with the prey protein acted as a blocking agent and allowed for dissociation of the phosphorylated CheY-GST from CheA, when the non-phosphorylated CheY-GST did not (Fig.5.5). If CheY-GST and CheA were the only proteins present even a large drop in the affinity of

CheY-GST for CheA may still result in CheA being pulled-down, as no competing proteins present would be present in the cell. BSA also plays a role in supporting native tertiary conformation of proteins when used *in vitro*, the conditions of these assays may have caused non-native conformations in CheA/CheY that prevented dissociations that would have occurred *in situ*. The introduction of negative controls against direct binding of prey proteins to the glutathione resin and the GST tag ensured that the interactions observed were between the bait and prey proteins, and not due to interactions with the resin or affinity tag.

It may be argued that Ac-P had interfered with protein-protein interactions directly rather than by phosphorylating the RR domains. However, the majority of Ac-P had been removed by washing before the prey protein was added. If it were the case that any remaining Ac-P may generally interfere with protein-protein interactions, that hypothesis would be inconsistent with the increases in CheV-GST to TLP_1 affinity that had been observed when CheV-GST had been pre-exposed to Ac-P (Fig.5.7).

5.6.2. CheY Interactions

CheY-GST Interaction with CheA

CheY was observed to have a strong interaction with CheA (Fig.5.5), this was consistent with the competitive phosphorylation assays which had suggested CheY was the primary response regulator, and was consistent with results of the bacterial and yeast two hybrid assays which had shown strong interactions between CheY and CheA (Bridle 2007; Parrish et al. 2007).

An advantage of *in vitro* pull-down assays over *in vivo* affinity methods was shown by the displayed decrease in the affinity of phosphorylated CheY-GST to CheA. This was consistent with the predicted role of primary response regulator, which once phosphorylated, would dissociate from CheA in order to interact with the flagella, switch as previously observed for *E. coli* CheY (Lee et al. 2001).

CheA-GST with CheY

Our assay was intended to confirm the result of the previous CheY-GST to CheA affinity assay by reproducing it with immobilised CheA-GST with CheY as the prey protein. This test allowed the CheA-RR domain to be phosphorylated so that its effect upon CheY binding could be investigated. Binding of CheY to the GST tagged CheA was observed, however the CheY bands for both phosphorylated and non-phosphorylated CheAs were quite faint, and no obvious difference in the level of CheY binding was seen between them (Fig.5.5). For these reasons it was not possible to say that the phosphorylation of CheA-RR domain affected binding of CheY to the CheA protein.

There had not been sufficient time to repeat this assay, the low molecular weight of CheY made it more difficult to visualise as the mass of CheY would be much lower than that of CheA when both were present in equimolar amounts, and so CheY would be less visible after Coomassie staining. With further optimisation, such as: an increase in the mass of both proteins used, visualisation by silver staining or the use of western blots, an affect of CheA-RR phosphorylation may have been observed.

5.6.3. CheB and CheR Interactions

CheR with CheV-GST and CheA-GST

A good level of purification had been reached with CheR and although some level of contamination had persisted, it only became pronounced when high concentrations of the stock were present in a reaction. No interaction can be said to have been observed for CheR in assays with either CheV-GST or CheA-GST as in either case CheR bound to both of the negative controls (Fig.5.6). The CheR protein had been purified relatively easily and had been found in the soluble fraction of the supernatant during purification once the Rosetta expression cells had been lysed, suggesting that the protein had been soluble, consequently it is difficult to explain how it may have bound so strongly to the beads in the negative control (Chapter 3).

CheB with CheV-GST

An interaction between CheV and CheB had been predicted in the bacterial two hybrid assays, however it had not been possible to pull down CheB from its contaminants using CheV-GST (Fig.5.7). It may be that with another Che protein as bait, this would have been possible but the predictions of the B2H system suggested CheV would be the prime candidate to do this.

5.6.4. CheV Interactions

CheV-GST Interaction with TLP_1

In repeat experiments CheV-GST was shown to interact with the cytoplasmic domain of TLP_1, and phosphorylated CheV-GST had bound more TLP_1 molecules than non-phosphorylated CheV-GST (Fig.5.7).

The nature of the interaction between CheV and $TLP_{1,}$ and its regulation by phosphate, may be shared by other *C. jejuni* TLPs however this had not been investigated. It had been intended to repeat these assays for the cytoplasmic domain shared by TLP_{2-4} however during purification the domain had co-purified with the ribosomal protein RL2, with which it had strongly bound. Eventually the proteins had been separated by heating in the presence of DTT but for this reason it was not possible to be certain of a functional conformation of the protein. Given more time a CheV-GST with TLP_{2-4} assay would have been attempted to investigate whether this interaction was common to other TLPs.

CheV-GST Interaction with CheA

Despite early promise and numerous attempts to repeat or optimise the experiment I did not see a reproducible interaction between CheV and CheA, whether that assay was based on immobilised CheV-GST with CheA or CheA-GST with CheV (Fig.5.8).

Perhaps the lack of a detected interaction between CheA and CheV was in some way due to the affinity tags which were fused to the purified proteins. The bacterial two hybrid assays (Bridle 2007) had displayed a CheV-CheA interaction

but the results had not been entirely consistent. The assays had used the two adenylate cyclase domains fused to CheA and CheV in both combinations, that is to say each combination of adenylate cyclase domains was tried on CheA and CheV at N-terminal and then C-terminal ends, in case of an inhibitory effect of the adenylate cyclase upon normal function the bait or prey protein.

Bridle's study (2007) had found that a CheA interaction with CheV was only detected when C-terminal rather than N-terminal fusions of adenylate cyclase to CheA had been used. CheA may be sensitive to fusion of large domains at the N-terminal end. However, the affinity tagged clones produced and used in this current study had been fused at the N-terminal end of CheA and had been shown to be functional, indeed phosphorylation of CheV-GST by HIS tagged $CheA^{HK}$ has been shown (Chapter 4).

Perhaps a CheV-CheA interaction is dependent upon a phosphorylated CheA-RR domain and that had not been detected by the assay, because in all of the pull-down assays in which a phosphorylated CheA-RR was used, the GST tagged version of CheA had been used. It may be that the GST tag interferes with the CheV-CheA interaction so that in the one experiment (Chapter 5) in which it may have been possible to see this interaction it had been inhibited by the nature of the CheA-GST used.

The final experiment in which CheV-GST had been placed with the HIS tagged CheA and phosphorylated together, I did see some increased binding of CheV-GST to CheA (Fig.5.8). As the proteins were phosphorylated together it is impossible to say whether the interaction was due to the phosphorylation of either

or both proteins. However for the reasons stated in the paragraph above, it may be feasible that what I had observed was a CheA-RR dependant increase in affinity that had in previous assays been hindered by a GST tag upon CheA. However, this assay had been intended to shorten the time taken for the experiment to minimise autodephosphorylation of CheV to increase the opportunity of a phosphate dependant interaction being observed. Given CheA-RR's slow Pi hydrolysis rate and that the CheV-CheA interaction was only observed at 1 and 2 minutes and not after 5 minutes, it seems unlikely that the effect observed was due solely to CheA-RR phosphorylation. The interaction could be said to be dependent on CheV or on combined CheV and CheA phosphorylation. Phosphorylation may play some role in increasing the affinity between these proteins, but clear supporting evidence is unavailable so far.

5.7. Conclusion

In this section I pool the findings of this study with the previous findings in *C. jejuni* and related model systems, which will inform later discussion of model systems to follow in Chapter 6.

CheY Participation in the *C. jejuni* Chemotaxis System

The hypothesis of a *C. jejuni* Che transduction system with a two component CheA/CheY backbone is strongly supported by our study. CheA had been shown to be a histidine kinase which autophosphorylated using ATP as a Pi donor, and that this phosphate could be transferred to either of the three predicted response regulators, CheY, CheV or $CheA^{RR}$ (Chapter 4).

There is good evidence to support the hypothesis of CheY being the primary response regulator of the *C. jejuni* Che transduction system. CheA had been shown to phosphorylate CheY in kinase assays, and that it was the preferred RR domain to receive phosphate (Chapter 4). The high affinity of CheA for CheY, observed here in Chapter 5, probably plays a role in this preference toward CheY phosphorylation as the strength of this interaction is not matched by CheV, as is apparent in the pull-down experiments (Chapter 5).

The large decrease in affinity observed in pull-down experiments of CheA with phosphorylated CheY, is consistent with the model of an activated CheY dissociating from CheA, so to diffuse and interact with the flagella motor switch (Lee et al. 2001). Unfortunately time did not allow for proper investigation of the interaction of a CheA-GST with a phosphorylated RR domain against CheY, as the CheA RR domain may play a role in the regulation of CheY binding.

CheV Participation in the *C. jejuni* Chemotaxis System

CheV phosphorylation by CheA has been shown in this study (Chapter 4) as it had been for the *B. subtilis* (Karatan et al. 2001) and *H. pylori* (Jiménez-Pearson et al. 2005) homologues previously. In the kinase competition experiments CheV had shown Pi transfer and hydrolysis rates similar to that of CheY, although CheA had shown a much stronger preference toward CheY phosphorylation (Chapter 4).

CheV had displayed an affinity for TLP_1 in the pull-down assays, as had been demonstrated previously between in *C. jejuni* (Hartley-Tassell et al. 2010), however the extension of this study into the phosphorylation state of CheV, found

an increase of the affinity between the two proteins upon CheV phosphorylation (Chapter 5). The modulation of CheV affinity for TLP_1 may be shared with other TLPs but the time in which to test this was not available, it is interesting to note that through a Y2H approach CheV has also been shown to interact with TLP_4 (Parrish et al. 2007). Given that TLP_4 shares a cytoplasmic domain with TLP_2 and TLP_3, it is likely that CheV interacts with TLP_2 and TLP_3 also.

There was a hint of a possible interaction between a phosphorylated CheA (Pi on the RR domain) and a phosphorylated CheV in pull down assays (Fig.5.8*C*). Interaction between the CheV and CheA had been previously observed in B2H (Bridle 2007), although not in the global *C. jejuni* Y2H (Parrish et al. 2007). The Y2H assay predicted 100% probability of a CheW/CheA interaction but had detected no interaction between CheV and CheA. Perhaps in *C. jejuni* this interaction does occur but is dependent upon phosphorylation of both the RR domains (Parrish et al. 2007).

Given the nature of the interactions observed between CheW, CheA and TLPs in *E. coli* receptor clusters (Bhatnagar et al. 2010; Maddock & Shapiro 1993), phosphorylation controlled modulation of affinities between CheV, which has a CheW-like domain, with TLP, and between CheV with CheA, may indicate an interesting role for CheV in TLP raft formation.

$CheA^{RR}$ Participation in the *C. jejuni* Chemotaxis System

Phosphorylation of the CheA RR domain by CheA had been successfully shown using the separately expressed $CheA^{HK}$ and $CheA^{RR}$ proteins. When these results were compared to assays using the native full length CheA, the dynamics

of phosphate transfer from fused HK to RR domains was much faster than had been indicated previously, as would be expected for covalently linked domains.

In the absence of competing response regulators, phosphate was rapidly transferred internally from the CheA HK domain to the CheA RR domain. However, how accurately this may reflect what would occur *in situ* is in doubt as CheY and CheV would also be present and competing for phosphate from CheA (Chapter 4).

In competition assays using all three response regulators $CheA^{HK}$ had shown least preference for Pi transfer to $CheA^{RR}$, however these tests had used the separately expressed domains. Attempts to use full length CheA in competition assays had been unsuccessful with none of the proteins being observed phosphorylated, presumably because the histidine kinase domain could not be pre-incubated with labelled ATP as it had been in previous kinase experiments.

It would have been interesting to test the CheA autophosphorylation rate while the CheA RR domain was phosphorylated, as CheA RR may regulate activity of the HK domain as the RR domain of the CheA homologue FrzE does (Inclán et al. 2008). This role has also been suggested for the *H. pylori* CheA homologue but is not yet supported by experimental data (Jiménez-Pearson et al. 2005).

CheB and CheR and Their Participation in the *C. jejuni* Chemotaxis System

Unfortunately *in vitro* experiments with *C. jejuni* CheB and CheR had proven unsuccessful. CheB had proven too difficult to purify in the time given, and the HIS tagged CheR had bound to GST and resin negative controls in the pull-down

assays. Therefore, this study could not contribute further to the evidence of existing studies in *C. jejuni*, that is: Δ*cheB* and Δ*cheR* strains have attenuated chemotaxis on motility plates (Bridle 2007; Kanungpean et al. 2011b), that there is evidence of modulation of TLP methylation *in vivo* (Kanungpean et al. 2011b) and that B2H had shown interactions between CheB and CheV (Bridle 2007).

The relevance of these findings to alternate *C. jejuni* signal transduction models is discussed in Chapter 6.

Chapter 6: Concluding Discussion

6.1. A *C. jejuni* Model of Chemotaxis Signal Transduction

Based on information from the literature and the present study, the following can be proposed: CheA is held together in a signalling complex with CheW/CheV and the cytoplasmic domain of a TLP receptor. The rate of CheA autophosphorylation is modulated by signals from the TLPs. Once phosphorylated, CheA primarily phosphorylates CheY, in its now activated state CheY dissociates from CheA and interacts with the flagella motor switch, alternating flagella rotation. Phospho CheA transfers Pi to CheV, in second preference to CheY. CheV is strongly associated with CheB, so that when phosphorylation of CheV causes it to associate with TLP, that also increases the effective concentration of CheB in relation to TLPs and so modulates it's methylesterase activity. CheA RR domain is third in preference of phosphorylation by the CheA histidine kinase but insufficient evidence exists with which to assign it a role. All three activated response regulators are dephosphorylated by autodephosphorylation and/or the phosphatase Cj0700, and so the system resets (Fig.6).

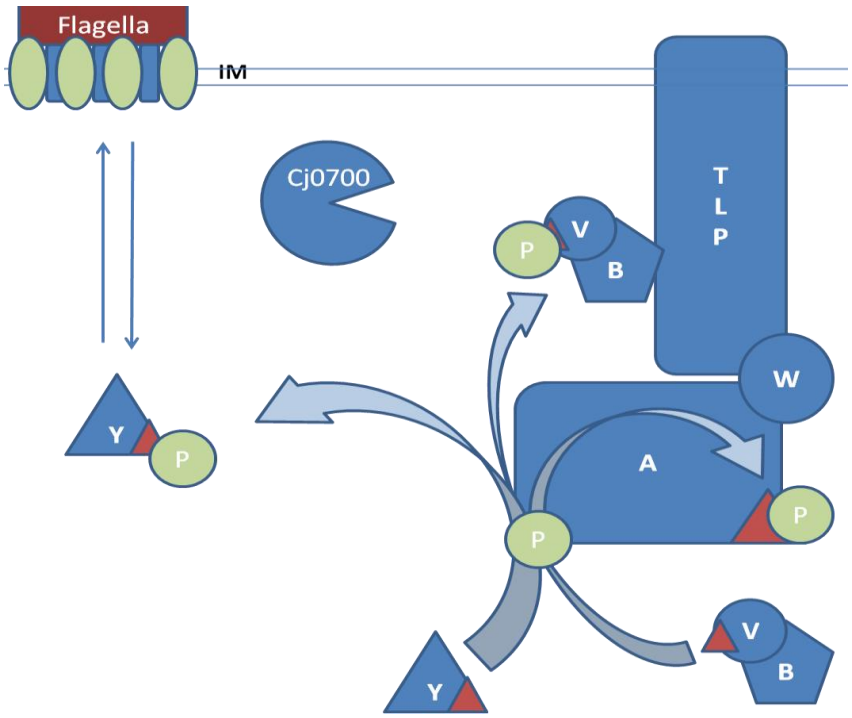

Figure 6. Routes for phosphate transfer in the model *C. jejuni* chemotaxis system. The periplasmic sensing domain of the TLP receptor regulates CheA autophosphorylation. When CheA autophosphorylates it transfers Pi to CheY, CheY then dissociates from CheA to interact with the flagella motor switch and modulate flagellum rotation. If CheY is not associated with CheA when it autophosphorylates again, it may phosphorylate CheV, which then associates with TLP so increasing the effective concentration of CheB in relation to TLP. Increasing methylesterase activity of CheB, reducing methylation levels on TLPs. CheA RR domain can also be phosphorylated by CheA but its function is unknown. Cj0700 is a phosphatase which deactivates CheY, CheV and CheA RR domain by removal of the phosphate groups.

Evidence For and Against the Current Model

Receptors and Signalling complexes

The hexagonal trimer of receptor dimer arrangements seen in *E. coli* are conserved in *C. jejuni* (Briegel et al. 2009) as in the *B. subtilis* and *H. pylori* systems to which I make reference.

Data from previous studies supports the presence of the CheA/CheW/TLP cytosolic signalling complexes shown in the proposed *C. jejuni* model, and previously observed in *E. coli* (Bhatnagar et al. 2010; Maddock & Shapiro 1993), Y2H assays show that CheA interacts with CheW, and CheW associates with TLP_4 (Rajagopala et al. 2007), which shares a common cytoplasmic domain with TLPs 2 and 3.

The CheA and CheY backbone

The preference of CheA to phosphorylate CheY, shown in the kinase competition experiments of this study (Chapter 4), and the fall in affinity between CheA/CheY when CheY became phosphorylated (Chapter 5), is consistent with the proposed model. CheY appears to be the primary response regulator of the Che system which upon becoming phosphorylated dissociates from CheA, to interact with the flagella motor switch, as in the *E. coli* model (Lee et al. 2001), although a CheY-FliM interaction has not been investigated here.

CheV

CheV phosphorylation by CheA was predicted by the B2H and Y2H assays (Bridle 2007; Rajagopala et al. 2007) and was directly observed in this study (Chapter 4). CheV was second in preference of phosphorylation by CheA but showed similar kinase and hydrolysis rates to CheY (Chapter 4), suggesting that its function required rapid activation and deactivation. These rates may suggest a role in adaptation, perhaps through CheB as suggested in the model proposed here.

Increased TLP methylation had been indicated in *C. jejuni* Δ*cheB* strains (Kanungpean et al. 2011b) and cells had attenuated chemotactic phenotypes (Bridle 2007; Kanungpean et al. 2011b), as would be predicted if the role of CheB was conserved, however the *C. jejuni* CheB lacks an RR domain. Bridle's *C. jejuni* model suggested that CheV modulates CheB's methylesterase activity but does not suggest how this may occur (Fig.6.1). Bridle's Model 6.1 shows CheB associated with TLPs, and CheV free in the cytoplasm that associates with CheB once it becomes phosphorylated and so activates CheB, but there is no evidence for a CheB association with TLPs in *C. jejuni*. A CheB/TLP interaction was not tested in the B2H assays and CheB was not included in the Y2H results, nor has its location in the cell been determined.

This study's pull-down experiments observed binding between CheV and TLP_1 that increased upon CheV phosphorylation. If as suggested by the B2H study, CheB is associated with CheV and CheV modulates its association with TLPs via its phosphorylation state, then perhaps a 'free' CheV is permanently associated

with CheB and its integration into clusters, upon phosphorylation, increases the effective concentration of CheB in relation to TLPs so increasing methylesterase activity, resulting in a decrease in the number of methyl groups upon TLPs. This could be a method by which the activity of a CheB without its own RR domain may be regulated if it were constitutively active.

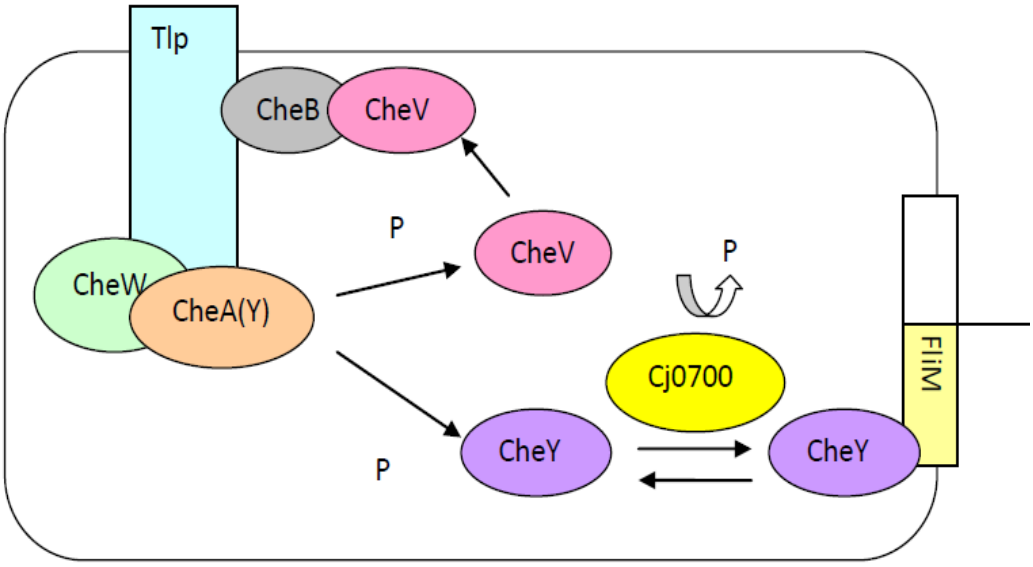

Bridle (2009)

Figure 6.1. Bridle's *C. jejuni* chemotaxis model. The periplasmic sensing domain of the transmembrane TLP regulate CheA autophosphorylation. CheA autophosphorylates and transfer Pi to CheY, CheY then dissociates from CheA to interact with the flagella motor switch. Cj0700 is a phosphatase which deactivates CheY by removal of the phosphate group. CheV is also phosphorylated by CheA, activation of CheV by phosphorylation regulates the methylesterase activity of CheB (Bridle 2009).

Control of TLP methylation state may be due to presentation of methylation sites to CheB and CheR caused by conformational changes resulting from ligand binding, rather than by activation of CheB or CheR; this appears to be the case in *B. subtilis* (Glekas et al. 2011; Kirby et al. 1999). It is important to note that the *B. subtilis* CheB does possess an RR domain so it appears its CheB is activated as well.

The *B. subtilis* chemotaxis transduction model is a useful comparison for study of adaptation in the *C. jejuni* system, as *B. subtilis* also possesses CheV, CheB and CheR proteins. In *B. subtilis* the receptors are dynamic. At rest, without the addition of an attractant MCPs are found located at the poles, when an attractant is added to cells an increased proportion of the MCPs are observed laterally associated, whereas the opposite is true of CheV which becomes predominantly polar when the cell is in the presence of an attractant (Wu et al. 2011). This would seem to contradict the proposed *C. jejuni* model of CheV being used to associate CheB with receptors, however the *B. subtilis* MCP and CheV localisations represent the location of the majority of each protein and not the entire population, and so both statements may be correct.

Cj0700

The Cj0700 phosphatase activity toward Che response regulators has been demonstrated since Bridle's model was proposed. Phosphate sink theories had suggested the additional RR domains of the *C. jejuni* system were part of a phosphate sink system, to sequester Pi from CheA and so limit the availability of

phospho CheA to CheY. B2H assays had predicted CheA to interact with CheY and CheV but these response regulators had also shown interactions with Cj0700. The CheZ orthologue Cj0700 has now been shown to have phosphatase activity against CheY and the CheA RR domain, and is suspected to hydrolyse phosphate groups from CheV although this has not yet been demonstrated (Jama 2013). Cj0700 need not necessarily be a phosphatase to CheV as CheV's rapid hydrolysis rate may in itself be sufficient to fulfil its role, but the B2H interactions observed between Cj0700 and CheV would suggest that it is a phosphatase with activity toward CheV as well.

The phosphorylation dependent changes in affinity between Che proteins seen in the pull-down assays would suggest the 'additional' RR domains had specific functions, and so an indiscriminate use of these domains as phosphate sinks would seem to conflict with the performance of their specific functions.

Bridle's model does not assign a role to CheA RR domain, possible functions will be explored in the following section.

6.1.1. Alternate Roles for CheV and CheA RR Domain

Although the evidence of this study and reviews of the literature would suggest there is a body of data supporting the *C. jejuni* model proposed here, there is insufficient evidence to conclusively assign functions to either CheV or the CheA RR domain.

Possible Alternative Roles for CheV

CheV and Receptor Raft Morphology

CheV may play a role in receptor raft morphology. It has been suggested that CheW and CheA may help the formation of larger hexagon rafts, the increase in affinity of CheV for TLP_1 (Chapter 5) may represent a method by which CheV phosphorylation could modulate the size or density of these rafts. Receptor rafts have been observed in *C. jejuni* (Briegel et al. 2009) but it is unknown if they are dynamic in response to ligands as the rafts of *B. subtilis* and *E. coli* are (Wu et al. 2011).

B. subtilis MCP and CheV localisation studies found CheV to become predominantly polar when the proportion of polar MCPs dropped. This result would suggest a disruptive role for CheV in receptor raft morphology, rather than the constructive role suggested by the CheV-TLP interaction observed by this study. However, the movement of rafts within *C. jejuni* has not been studied and may not be consistent with this finding from *B. subtilis*.

Disruption of CheA/TLP communication

In *E. coli* CheW and CheA compete for binding space on TLPs and overexpression of CheW can lead to CheA being dislodged from the signalling complex (Levit et al. 2002; Francis et al. 2002). Perhaps the increase in affinity of CheV for TLP upon phosphorylation may help it to temporarily outcompete CheA for an active site on TLP and so cause reduced communication between CheA and TLPs, and so a temporary reduced sensitivity of the system to the ligand.

Proposed roles for CheA RR domain

Regulation of CheA Autophosphorylation

The CheA RR domain may function as another regulator of histidine kinase autophosphorylation rate. FrzE the CheA homologue of *M. xanthus*, has an RR domain which can completely block FrzE HK domain autophosphorylation (Inclán et al. 2008). This regulatory role of a CheA RR domain over the HK domain has been suggested for the *H. pylori* homologue as well but this has not yet been demonstrated (Jiménez-Pearson et al. 2005).

As the kinase experiments of this study looked at populations of proteins it is impossible from this data to assess what effect CheA RR domain phosphorylation had upon HK autophosphorylation. A model in which the HK domain could not autophosphorylate or had reduced autophosphorylation if the RR domain had Pi bound, may cause signalling from the CheA to be temporarily disrupted if a persistent signal were detected. This disruption may act as a refractory period for a persistently activated CheA, for as long as it took the RR domain to dephosphorylate.

If CheA is receiving a signal to autophosphorylate, it seems likely it would transfer phosphate to CheY first, as it is likely to have a CheY bound as pull down assays observed high affinity between CheA and the unphosphorylated CheY (Chapter 5) and CheA HK domain preferentially phosphorylates CheY over other response regulators (Chapter 4). However, if CheA HK domain became phosphorylated again before a CheY molecule bound again then perhaps this Pi would be passed

to the CheA RR domain which would then modulate the efficiency of CheA transphosphorylation, or of CheA/TLP communication for a period until the RR domain lost its phosphate.

CheV Recruitment by CheA RR Domain

As I was unable to use full length CheA in competition experiments, it may be that CheA RR domain is actually second in the hierarchy of phosphorylation by HK. The CheA RR domain appears to have low affinity for phospho CheA, inferred by its low Pi transfer rate, but if the domains were covalently linked as in the native protein the RR domain may not require a high affinity to HK in order to interact with it.

The apparent interaction of phosphorylated CheA RR domain with phosphorylated CheV, though not well supported in this study, if true could act to increase the amount of ‘free’ phospho CheV associated with signalling clusters. This associated but ‘free’ phosphorylated CheV could act as a pool of CheV with which to replace CheVs, which interacting with TLP had dephosphorylated in the course of the interaction.

If the observed CheV/CheA interaction had been between a non-phosphorylated CheV and phosphorylated CheA RR domain, it could represent a method to recruit CheVs to the area around signalling complexes and increase the effective concentration of CheV to the HK domain of CheA, increasing its probability of phosphorylation. So in that model, if a persistent signal for CheA HK to phosphorylate were present, then CheY would take Pi first, then as the signal continues CheA RR domain accepts Pi which would lead it to recruit CheV, which

then could become phosphorylated and interact with the signalling complexes. The evidence around this proposed interaction is weak and may not have been included in the study if it were not for evidence from the B2H assay which showed interactions between CheA RR domain and CheV but not between CheV/HK domain (Bridle 2007).

A Role for the *C. jejuni* ChePep homologue

The ChePep protein has not been discussed at length in this study as its discovery is a recent development in the field, and due to a lack of time efforts to purify the protein during this study had to be abandoned.

The existing work was carried out in *H. pylori* which may call into question its relevance, however their Δ*chePep* mutants recovered their chemotactic phenotypes when complemented with *C. jejuni chePep* (Howitt & Lee 2011). The deletion of a component of the transduction system which is terminal to the *H. pylori* system, results in straight swimming, as that is its default if the chemotaxis system is removed, however the Δ*chePep* mutants have hyper switching phenotypes. With only one publication so far on this newly identified Che protein, there is insufficient evidence with which to form a view of its interaction with any of the existing models.

It is important to note that no kinase assays were attempted using any of the other histidine kinases or response regulators identified in *C. jejuni*, although they are not suspected of interacting with the now confirmed *C. jejuni* Che proteins, the possibility of other interacting partners donating or receiving phosphate from this system cannot be excluded.

6.2. Future Work

Investigating *C. jejuni* Motility

As even the swimming mode of *C. jejuni* is not confirmed it would be wise to begin with tethered cell assays, using antibody raised against FlaA. These assays could be used to investigate if *C. jejuni* uses a swim/tumble, swim/pause or swim/pause/reverse mode. However, these experiments would need to be combined with fluorescent microscopy tracking of *C. jejuni* swarming, as a swim/pause/reverse mode would have the same observable phenotype in tethered cell assays, as a swim/pause/tumble motility mode.

Once developed, tethered cell and fluorescent microscopy methods could be used to test the responses of wild type cells to identified attractants and repellents, and test again the swimming bias of Δ*che* mutant strains. With a more accurate picture of wild type swimming phenotypes the effect of *che* gene deletions upon the signal transduction system would be easier to discern.

Concerns exist over possible polar effects in the existing Δ*che* strains, to address these concerns, the recently developed rpsl* positive selection system could be used to produce mutant strains. Insertion or deletion of single bases within targeted open reading frames, could delete genes by creating frame shifts that would have minimal impact on downstream genes (Reyrat et al. 1998).

Improved Techniques for Measuring Protein-Protein Interaction

Pull-down assays are insensitive to weak or transient interactions and may have failed to detect interactions that occur *in situ*. The Surface Plasmon Resonance (SPR) technique would have been a far more sensitive method with which to assay affinities between the proteins. Over the time frame required for SPR to be carried out, any RR domain being investigated would autodephosphorylate, so the effect of Pi upon Che protein interactions could not be investigated using natural phosphate activation of response regulators. Beryllium fluoride is now commonly used to artificially put response regulators into a stable 'active' conformation and has been successful previously for CheY (Lee et al. 2001).

CheV Interactions

Using stable, artificial activation of response regulators and SPR in combination, the change in affinity between CheV and TLP_1 could be quantified and compared to that of CheA/TLP_1 to see if 'activated' CheV could displace CheA from signalling clusters. The interaction of CheV and CheA with either or both of their RR domains 'activated' could be tested to discern if this was a real interaction that had been observed previously.

CheA RR Domain Interactions

To investigate if the CheA RR domain is modulating the autophosphorylation of CheA, future studies could use beryllium fluoride to permanently activate CheA's

RR domain (Lee et al. 2001; Scharf 2010), and compare its autophosphorylation rate to that of a CheA with a RR domain rendered non-phosphorylatable by site directed mutagenesis. Neither CheA would be able to phosphorylate its own response regulator domain, but the beryllium fluoride treated CheA RR domain would be fixed in an active state, while the mutated CheA RR domain would be permanently inactivated. These kinases could then be incubated with labelled ATP, and their autophosphorylation rates compared.

Studies using SPR and beryllium fluoride could be used to investigate the effect of CheA RR domain phosphorylation on CheY binding, comparing non-activated CheA RR to activated. Obstruction of the CheA/CheY interaction site could be a simple method by which to adapt sensitivity of the system.

Alternately *in vitro* signalling complexes consisting of the purified constituent Che proteins, as previously carried out for *E. coli,* could have their CheY Pi transfer rates compared to complexes using CheV instead of a CheW, or using a permanently activated CheV. These tests could be used to assess the role of CheV and activated CheV in modulating CheA/TLP interactions.

ChePep

There is too little evidence available with which to assign a role to ChePep, therefore collection of more basic data is required first. Although the evidence from *H. pylori* is compelling, a *C. jejuni* Δ*chePep* mutant would need to be constructed to confirm the swimming and swarming phenotypes in *C. jejuni*. The ChePep protein would need to be purified and used in kinase assays, to test if its putative RR domain will accept Pi from CheA. Antibodies could be raised against

a purified ChePep protein and used to locate the protein *in situ*, and assess if its position was dynamic or fixed in response to MCP ligand binding, and if it co-locates with TLPs.

If *C. jejuni* ChePep was shown by swarming assays to be a genuine chemotaxis transduction protein, a strain with a non-phosphorylatable RR domain could be subjected to the repeats of the MCP ligand binding tests, to see if the RR domain was necessary to its location or its dynamic movement. B2H studies focusing on ChePep could be used to investigate possible interactions with the known Che proteins and to look for new candidate Che proteins. Although, as ChePep does not appear in the global Y2H assays, possibly due to cell toxicity, this approach may have limited opportunity for success.

Implications of the Study

Establishment of the kinase assays had proven problematic and required much greater time and effort than originally expected, nevertheless phosphorylation of the predicted CheV, CheA and CheY response regulators by CheA was confirmed. The pull down assays had shown modulation of the affinities between the Che proteins resulting from phosphorylation of response regulator domains and implicated an important role for CheV response regulator domain in TLP adaption. This study has contributed to the body of knowledge on *C. jejuni* chemotaxis, which is an important determinant in human and chicken *C. jejuni* colonisation. A greater knowledge of this transduction system may provide possible targets for disruption of colonisation, and so reduce the risk of human infection.

6.3. Acknowledgements

I would like to thank my supervisor Professor Julian Ketley for his help with the project, the members of my thesis committee, Chris and Mike. I wish to thank Richard and Sue for all their help and advice, and Claire for the great patience shown in my initial training.

I would like to thank my family, friends and all my colleagues in lab 121 for their great support through challenging times, and the Genetics department for the funding of the project.

7.0. Appendix

P00071 **Mass:** 112391 **Score:** 311 **Expect:** 4.3e-028 **Queries matched:** 27

CheA-GST tagged sequence provided by P AINSWORTH 19/09/2012 - this is not a real UniProt entry - added to database by SYA

Observed	Mr(expt)	Mr(calc)	ppm	Peptide
732.4230	731.4157	731.3926	31.6	K.VTNVSGR.G
745.4470	744.4397	744.4130	35.9	K.NLITER.E
770.4770	769.4697	769.4922	-29.25	K.NVLRLR.D
816.5250	815.5177	815.4865	38.3	K.TLLNSIR.D
905.4480	904.4407	904.4039	40.7	R.DEGDKWR.N
907.5350	906.5277	906.5076	22.2	K.VFNKFPR.V
1032.6260	1031.6187	1031.5797	37.8	K.LTQSMAIIR.Y
1038.4930	1037.4857	1037.4998	-13.54	K.MDRTLMQK.A + Oxidation (M)
1083.6830	1082.6757	1082.6448	28.6	R.NLPLIAVTSR.T
1138.5360	1137.5287	1137.5090	17.3	K.YEEHLYER.D
1182.7000	1181.6927	1181.6768	13.5	K.RIEAIPQIDK.Y
1199.7300	1198.7227	1198.7034	16.2	R.LRDEVLSLVR.L
1204.6660	1203.6587	1203.7016	-35.58	M.SPILGYWKIK.G
1225.6150	1224.6077	1224.5809	21.9	R.MDGYTLAGEIR.K
1457.6370	1456.6297	1456.6001	20.3	R.NSCDHGVEDPATR.A
1516.8210	1515.8137	1515.7966	11.3	R.AEISMLEGAVLDIR.Y
1644.7620	1643.7547	1643.7315	14.2	K.IYDDVEERYEGEK.F
1715.9120	1714.9047	1714.8811	13.8	K.ITPDIMDVVLESIDR.M
1739.8960	1738.8887	1738.8746	8.13	K.SIVEEIGDPIMHMIR.N
1748.8860	1747.8787	1747.8523	15.1	K.KVPASGSNASSMDQTIR.V
1873.9030	1872.8957	1872.8854	5.53	K.AYNEGNHIVVEITDDGK.G
1907.9820	1906.9747	1906.9571	9.25	K.SMGDYLQNIQGIAGATIR.G
1941.9140	1940.9067	1940.8972	4.92	K.SGEHDIDAMLIDIEMPR.M
1961.8970	1960.8897	1960.8619	14.2	R.DNGNDTAIGMDIEPICAR.L
2326.1500	2325.1427	2325.1331	4.14	K.YIAWPLQGWQATFGGGDHPPK.S
2773.3820	2772.3747	2772.3680	2.42	R.GVEVGMTEYITKPYSPEYLENVVR.K
2926.3820	2925.3747	2925.3727	0.70	K.QEIATPEPEVDVNQLSDSEVEAEIER.L

Figure A1. Results of mass spectrometry against suspected CheA-GST

P00072 **Mass:** 60270 **Score:** 197 **Expect:** 1.1e-016 **Queries matched:** 16

HK domain (-W -RR) HIS tagged sequence provided by P AINSWORTH 19/09/2012 - this is not a real UniProt entry - added to database by SYA

Observed	Mr(expt)	Mr(calc)	ppm	Peptide
732.4200	731.4127	731.3926	27.5	K.VTNVSGR.G
745.4390	744.4317	744.4130	25.2	K.NLITER.E
816.5090	815.5017	815.4865	18.7	K.TLLNSIR.D
907.5440	906.5367	906.5076	32.2	K.VFNKFPR.V
1038.4990	1037.4917	1037.4665	24.3	K.IYDDVEER.Y
1414.7670	1413.7597	1413.7140	32.3	K.GSSSFLNFDVLTK.L
1457.6470	1456.6397	1456.6001	27.2	R.NSCDHGVEDPATR.A
1540.6870	1539.6797	1539.6325	30.7	R.DLYDDDDKDPSSR.S
1644.7940	1643.7867	1643.7315	33.6	K.IYDDVEERYEGEK.F
1715.9280	1714.9207	1714.8811	23.1	K.ITPDIMDVVLESIDR.M
1739.9340	1738.9267	1738.8746	30.0	K.SIVEEIGDPIMHMIR.N
1748.9030	1747.8957	1747.8523	24.9	K.KVPASGSNASSMDQTIR.V
1873.9450	1872.9377	1872.8854	28.0	K.AYNEGNHIVVEITDDGK.G
1961.9190	1960.9117	1960.8619	25.4	R.DNGNDTAIGMDIEPICAR.L
2335.0510	2334.0437	2333.9814	26.7	M.GGSHHHHHHGMASMTGGQQMGR.D
2926.4620	2925.4547	2925.3727	28.0	K.QEIATPEPEVDVNQLSDSEVEAEIER.L

Figure A2. Results of mass spectrometry against suspected CheA^{HK}

P00073 **Mass:** 36324 **Score:** 133 **Expect:** 2.7e-010 **Queries matched:** 10

ARR domain (+W) HIS tagged sequence provided by P AINSWORTH 19/09/2012 - this is not a real UniProt entry - added to database by SYA

Observed	Mr(expt)	Mr(calc)	ppm	Peptide
1083.6420	1082.6347	1082.6448	-9.28	R.NLPLIAVTSR.T
1199.6960	1198.6887	1198.7034	-12.20	R.LRDEVLSLVR.L
1225.5740	1224.5667	1224.5809	-11.54	R.MDGYTLAGEIR.K
1362.6990	1361.6917	1361.7078	-11.84	R.VPIDDIYTIEGK.N
1540.6090	1539.6017	1539.6325	-19.99	R.DLYDDDDKDPSSR.S
1907.9310	1906.9237	1906.9571	-17.49	K.SMGDYLQNIQGIAGATIR.G
1941.8670	1940.8597	1940.8972	-19.29	K.SGEHDIDAMLIDIEMPR.M
1957.8650	1956.8577	1956.8921	-17.56	K.SGEHDIDAMLIDIEMPR.M + Oxidation (M)
2334.9440	2333.9367	2333.9814	-19.15	M.GGSHHHHHHGMASMTGGQQMGR.D
2773.3110	2772.3037	2772.3680	-23.19	R.GVEVGMTEYITKPYSPEYLENVVR.K

Figure A3. Results of mass spectrometry against suspected CheA^{RR}

P00074 **Mass:** 62866 **Score:** 251 **Expect:** 4.3e-022 **Queries matched:** 18

CheV-GST tagged sequence provided by P AINSWORTH 19/09/2012 - this is not a real UniProt entry - added to database by SYA

Observed	Mr(expt)	Mr(calc)	ppm	Peptide
770.4220	769.4147	769.4446	-38.88	K.GLVQPTR.L
905.3890	904.3817	904.4039	-24.50	R.DEGDKWR.N
1032.5690	1031.5617	1031.5797	-17.45	K.LTQSMAIIR.Y
1094.5380	1093.5307	1093.5630	-29.53	-.MSPILGYWK.I
1138.4900	1137.4827	1137.5090	-23.14	K.YEEHLYER.D
1182.6700	1181.6627	1181.6768	-11.90	K.RIEAIPQIDK.Y
1327.6570	1326.6497	1326.6820	-24.30	K.VYEGIYGVNVSK.V
1397.6080	1396.6007	1396.6293	-20.44	K.TGSNEMELVDFR.I
1402.6310	1401.6237	1401.6565	-23.36	K.FNASDFFNEIAK.V
1516.7690	1515.7617	1515.7966	-23.04	R.AEISMLEGAVLDIR.Y
1611.7760	1610.7687	1610.7974	-17.81	K.FTGTALILDDSMTAR.K
1655.7230	1654.7157	1654.7517	-21.75	K.EMMQQMGFQVVEAK.D
1666.7530	1665.7457	1665.7709	-15.09	R.GSPEFPGMFDENIVK.T
1801.8220	1800.8147	1800.8716	-31.60	K.TGSNEMELVDFRIFK.Q + Oxidation (M)
1846.8840	1845.8767	1845.9117	-18.95	K.WMQITEPESTMLKPR.V
1862.8860	1861.8787	1861.9066	-14.98	K.WMQITEPESTMLKPR.V + Oxidation (M)
1951.9550	1950.9477	1950.9786	-15.81	K.LEELSQIYGESLNDTLK.I
2162.9910	2161.9837	2162.0289	-20.89	K.IIVSDVEMPQMDGFHFAAR.I

Figure A4. Results of mass spectrometry against suspected CheV-GST

P00076 **Mass:** 18451 **Score:** 59 **Expect:** 0.0071 **Queries matched:** 4

CheY-HIS tagged sequence provided by P AINSWORTH 19/09/2012 - this is not a real UniProt entry - added to database by SYA

Observed	Mr(expt)	Mr(calc)	ppm	Peptide
1540.5710	1539.5637	1539.6325	-44.67	R.DLYDDDDKDPSSR.S
1811.8160	1810.8087	1810.8845	-41.84	K.KYEDMPIIMVTTEGGK.A
1887.9800	1886.9727	1887.0618	-47.21	K.AGVNNYIVKPFTPQVLK.E
2334.8790	2333.8717	2333.9814	-47.00	M.GGSHHHHHHGMASMTGGQQMGR.D

Figure A5. Results of mass spectrometry against suspected CheY

1. P00077 **Mass:** 41757 **Score:** 246 **Expect:** 1.3e-021 **Queries matched:** 19

CheY-GST tagged sequence provided by P AINSWORTH 19/09/2012 - this is not a real UniProt entry - added to database by SYA

Observed	Mr(expt)	Mr(calc)	ppm	Peptide
770.4290	769.4217	769.4446	-29.78	K.GLVQPTR.L
905.3840	904.3767	904.4039	-30.03	R.DEGDKWR.N
1013.4410	1012.4337	1012.4583	-24.23	K.HNMLGGCPK.E
1032.5670	1031.5597	1031.5797	-19.39	K.LTQSMAIIR.Y
1048.5520	1047.5447	1047.5746	-28.56	K.LTQSMAIIR.Y + Oxidation (M)
1094.5450	1093.5377	1093.5630	-23.13	-.MSPILGYWK.I
1138.4920	1137.4847	1137.5090	-21.38	K.YEEHLYER.D
1149.6200	1148.6127	1148.6328	-17.52	R.LLLEYLEEK.Y
1182.6510	1181.6437	1181.6768	-27.98	K.RIEAIPQIDK.Y
1235.6070	1234.5997	1234.6227	-18.64	K.LLVVDDSSTMR.R
1248.6250	1247.6177	1247.6398	-17.66	R.GSPEFKDEIVK.L
1516.7840	1515.7767	1515.7966	-13.14	R.AEISMLEGAVLDIR.Y
1683.7370	1682.7297	1682.7895	-35.54	K.YEDMPIIMVTTEGGK.A
1811.8740	1810.8667	1810.8845	-9.81	K.KYEDMPIIMVTTEGGK.A
1888.0520	1887.0447	1887.0618	-9.06	K.AGVNNYIVKPFTPQVLK.E
2102.0460	2101.0387	2101.0588	-9.54	K.VLITDWNMPEMNGLELVK.K
2269.0980	2268.0907	2268.1313	-17.90	R.LLLEYLEEKYEEHLYER.D
2326.1090	2325.1017	2325.1331	-13.50	K.YIAWPLQGWQATFGGGDHPPK.S
2347.1340	2346.1267	2346.1492	-9.57	R.LGHDDVLEAEHGVEAWDLLTK.N

Figure A6. Results of mass spectrometry against suspected CheY-GST

P00078 **Mass:** 41713 **Score:** 254 **Expect:** 2.1e-022 **Queries matched:** 18

CheY delta 56 GST tagged sequence provided by P AINSWORTH 19/09/2012 - this is not a real UniProt entry - added to database by SYA

Observed	Mr(expt)	Mr(calc)	ppm	Peptide
770.4160	769.4087	769.4446	-46.68	K.GLVQPTR.L
905.3750	904.3677	904.4039	-39.98	R.DEGDKWR.N
963.4950	962.4877	962.5225	-36.17	M.SPILGYWK.I
1032.5510	1031.5437	1031.5797	-34.90	K.LTQSMAIIR.Y
1094.5220	1093.5147	1093.5630	-44.16	-.MSPILGYWK.I
1138.4730	1137.4657	1137.5090	-38.09	K.YEEHLYER.D
1149.6020	1148.5947	1148.6328	-33.19	R.LLLEYLEEK.Y
1182.6370	1181.6297	1181.6768	-39.83	K.RIEAIPQIDK.Y
1235.5880	1234.5807	1234.5587	17.9	K.MFEDRLCHK.T
1516.7550	1515.7477	1515.7966	-32.27	R.AEISMLEGAVLDIR.Y
1801.8800	1800.8727	1800.9403	-37.54	K.ERAEISMLEGAVLDIR.Y
1811.8140	1810.8067	1810.8845	-42.94	K.KYEDMPIIMVTTEGGK.A
1887.9990	1886.9917	1887.0618	-37.14	K.AGVNNYIVKPFTPQVLK.E
2057.9970	2056.9897	2057.0689	-38.50	K.VLITAWNMPEMNGLELVK.K
2269.0460	2268.0387	2268.1313	-40.83	R.LLLEYLEEKYEEHLYER.D
2326.0610	2325.0537	2325.1331	-34.14	K.YIAWPLQGWQATFGGGDHPPK.S
2347.0680	2346.0607	2346.1492	-37.70	R.LGHDDVLEAEHGVEAWDLLTK.N
2357.1090	2356.1017	2356.1991	-41.32	K.KFELGLEFPNLPYYIDGDVK.L

Figure A7. Results of mass spectrometry against suspected CheY$^{\Delta 56}$

P00072 **Mass:** 60270 **Score:** 179 **Expect:** 6.8e-015 **Queries matched:** 13

HK domain (-W -RR) HIS tagged sequence provided by P AINSWORTH 19/09/2012 - this is not a real UniProt entry - added to database by SYA

Observed	Mr(expt)	Mr(calc)	ppm	Peptide
745.4090	744.4017	744.4130	-15.12	K.NLITER.E
907.5040	906.4967	906.5076	-11.96	K.VFNKFPR.V
1038.4580	1037.4507	1037.4665	-15.24	K.IYDDVEER.Y
1457.5890	1456.5817	1456.6001	-12.62	R.NSCDHGVEDPATR.A
1540.6230	1539.6157	1539.6325	-10.90	R.DLYDDDDKDPSSR.S
1644.7110	1643.7037	1643.7315	-16.87	K.IYDDVEERYEGEK.F
1739.8560	1738.8487	1738.8746	-14.87	K.SIVEEIGDPIMHMIR.N
1748.8220	1747.8147	1747.8523	-21.49	K.KVPASGSNASSMDQTIR.V
1821.0110	1820.0037	1820.0342	-16.74	K.RLDHLMNLIGELVLGK.N
1873.8510	1872.8437	1872.8854	-22.23	K.AYNEGNHIVVEITDDGK.G
1961.8410	1960.8337	1960.8619	-14.35	R.DNGNDTAIGMDIEPICAR.L
2616.2430	2615.2357	2615.2941	-22.33	R.EADQMTDKEAFALIFKPGFSTAAK.V
2926.2760	2925.2687	2925.3727	-35.54	K.QEIATPEPEVDVNQLSDSEVEAEIER.L

Figure A8. Results of mass spectrometry against Breakdown 1.

PA03 Campylobacter **Mass:** 39509 **Score:** 215 **Expect:** 1.7e-018 **Queries matched:** 15

MebesTLP2 - Sequence provided by P Ainsworth 24/01/2011 - this is not a real UniProt entry - added to database by SI

Observed	Mr(expt)	Mr(calc)	ppm	Peptide
828.3890	827.3817	827.4065	-29.94	K.IFEEYK.S
927.5430	926.5357	926.5549	-20.70	K.LLDVLQAR.V
954.5420	953.5347	953.5545	-20.79	R.NPQLIELK.N
1062.5380	1061.5307	1061.5506	-18.69	R.GFAVVADEVR.K
1101.5490	1100.5417	1100.5462	-4.06	R.GLEQDNQAVK.E
1190.6400	1189.6327	1189.6455	-10.76	R.GFAVVADEVRK.L
1257.6400	1256.6327	1256.6473	-11.59	K.RGLEQDNQAVK.E
1349.6750	1348.6677	1348.6722	-3.30	K.TSDVITQSEEIK.N
1540.6380	1539.6307	1539.6325	-1.16	R.DLYDDDDKDPSSR.S
1745.8930	1744.8857	1744.8956	-5.63	K.ESVQTVSVVEGGNLTAR.I
2178.0730	2177.0657	2177.0600	2.63	K.SNDEFGQISNAINENILATK.R
2261.1360	2260.1287	2260.1183	4.62	K.EQTAGITQINDSVAQIDQTTK.D
2334.9880	2333.9807	2333.9814	-0.30	M.GGSHHHHHHGMASMTGGQQMGR.D
2350.9900	2349.9827	2349.9763	2.72	M.GGSHHHHHHGMASMTGGQQMGR.D + Oxidation (M)
2402.2850	2401.2777	2401.2336	18.4	R.NKLENASGSVELTTNALGDEIVK.M

Figure A9. Results of mass spectrometry against TLP_2.

RL2_ECO24 **Mass:** 29956 **Score:** 148 **Expect:** 8.3e-010 **Queries matched:** 12

50S ribosomal protein L2 OS=Escherichia coli O139:H28 (strain E24377A / ETEC) GN=rplB PE=3 SV=1

Observed	Mr(expt)	Mr(calc)	ppm	Peptide
705.3680	704.3607	704.3565	5.94	K.NSKSGGR.N
784.4670	783.4597	783.4715	-15.07	R.GVRPTVR.G
894.4620	893.4547	893.4607	-6.66	R.DGAYVTLR.L
906.4220	905.4147	905.4243	-10.54	R.LEYDPNR.S
955.5220	954.5147	954.5134	1.34	K.DGIPAVVER.L
1099.6340	1098.6267	1098.6437	-15.46	K.GKPFAPLLEK.N
1164.6400	1163.6327	1163.6299	2.45	R.SAGTYVQIVAR.D
1197.6700	1196.6627	1196.6513	9.53	R.NKDGIPAVVER.L
1249.6660	1248.6587	1248.6615	-2.25	K.HPVTPWGVQTK.G
1497.7660	1496.7587	1496.7405	12.1	R.ATLGEVGNAEHMLR.V
1688.7660	1687.7587	1687.7485	6.05	R.GTAMNPVDHPHGGGEGR.N
2239.1370	2238.1297	2238.1427	-5.78	K.AGDQIQSGVDAAIKPGNTLPMR.N

Figure A10. Results of mass spectrometry against RL2.

PA02_Campylobacter **Mass:** 39804 **Score:** 295 **Expect:** 1.7e-026 **Queries matched:** 26

MebesCheV - Sequence provided by P Ainsworth 18/01/2011 - this is not a real UniProt entry - added to database by SI

Observed	Mr(expt)	Mr(calc)	ppm	Peptide
716.3910	715.3837	715.4129	-40.81	R.RINWK.D
757.3950	756.3877	756.4130	-33.39	R.IKEDPR.F
795.3640	794.3567	794.3810	-30.61	K.TDIDFGK.I
995.4770	994.4697	994.4794	-9.68	R.MFDENIVK.T
1108.7100	1107.7027	1107.7016	1.03	R.GVVIPVVNLAK.W
1306.6740	1305.6667	1305.6565	7.85	K.GVQEAGGEGYLVK.F
1327.6980	1326.6907	1326.6820	6.61	K.VYEGIYGVNVSK.V
1397.6440	1396.6367	1396.6293	5.34	K.TGSNEMELVDFR.I
1402.6780	1401.6707	1401.6565	10.2	K.FNASDFFNEIAK.V
1413.6450	1412.6377	1412.6242	9.58	K.TGSNEMELVDFR.I + Oxidation (M)
1540.6570	1539.6497	1539.6325	11.2	R.DLYDDDDKDPSSR.M
1611.8240	1610.8167	1610.7974	12.0	K.FTGTALILDDSMTAR.K
1627.8280	1626.8207	1626.7923	17.5	K.FTGTALILDDSMTAR.K + Oxidation (M)

1655.7860	1654.7787	1654.7517	16.3	K.EMMQQMGFQVVEAK.D
1801.8190	1800.8117	1800.8716	-33.26	K.TGSNEMELVDFRIFK.Q + Oxidation (M)
1846.9340	1845.9267	1845.9117	8.14	K.WMQITEPESTMLKPR.V
1862.9440	1861.9367	1861.9066	16.2	K.WMQITEPESTMLKPR.V + Oxidation (M)
1952.0190	1951.0117	1950.9786	17.0	K.LEELSQIYGESLNDTLK.I
2084.0330	2083.0257	2082.9932	15.6	K.DIPIVFNSSLSNEFMNEK.G
2163.0630	2162.0557	2162.0289	12.4	K.IIVSDVEMPQMDGFHFAAR.I
2179.0800	2178.0727	2178.0238	22.5	K.IIVSDVEMPQMDGFHFAAR.I + Oxidation (M)
2335.0220	2334.0147	2333.9814	14.3	M.GGSHHHHHHGMASMTGGQQMGR.D
2344.2720	2343.2647	2343.2362	12.2	K.IPSLTELPGVPDYIEGIFDLR.G
2351.0510	2350.0437	2349.9763	28.7	M.GGSHHHHHHGMASMTGGQQMGR.D + Oxidation (M)
2359.1880	2358.1807	2358.1566	10.2	R.FKDIPIVFNSSLSNEFMNEK.G
2764.4230	2763.4157	2763.3814	12.4	K.DGVEGINKLEELSQIYGESLNDTLK.I

Figure A11. Results of mass spectrometry against CheV.

P00072 **Mass:** 60270 **Score:** 240 **Expect:** 5.4e-021 **Queries matched:** 23

HK domain (-W -RR) GST tagged sequence provided by P AINSWORTH 19/09/2012 - this is not a real UniProt entry - added to database by SYA

Observed	Mr(expt)	Mr(calc)	ppm	Peptide
732.4020	731.3947	731.3926	2.89	K.VTNVSGR.G
745.4200	744.4127	744.4130	-0.34	K.NLITER.E
816.4900	815.4827	815.4865	-4.61	K.TLLNSIR.D
817.4130	816.4057	816.4090	-3.95	R.KAEDQAR.R
907.5300	906.5227	906.5076	16.7	K.VFNKFPR.V
1038.4960	1037.4887	1037.4665	21.4	K.IYDDVEER.Y
1336.6950	1335.6877	1335.6605	20.4	K.LTHHMEDVLNK.A
1386.7880	1385.7807	1385.7402	29.3	K.LNGVIEIDSELGK.G
1414.7560	1413.7487	1413.7140	24.6	K.GSSSFLNFDVLTK.L
1620.8180	1619.8107	1619.7573	33.0	K.VPASGSNASSMDQTIR.V
1644.7750	1643.7677	1643.7315	22.1	K.IYDDVEERYEGEK.F
1697.9580	1696.9507	1696.9188	18.8	K.EAFALIFKPGFSTAAK.V

1715.9340	1714.9267	1714.8811	26.6	K.ITPDIMDVVLESIDR.M
1731.9080	1730.9007	1730.8761	14.3	K.ITPDIMDVVLESIDR.M + Oxidation (M)
1739.9290	1738.9217	1738.8746	27.1	K.SIVEEIGDPIMHMIR.N
1748.8930	1747.8857	1747.8523	19.1	K.KVPASGSNASSMDQTIR.V
1755.9170	1754.9097	1754.8695	22.9	K.SIVEEIGDPIMHMIR.N + Oxidation (M)
1873.9290	1872.9217	1872.8854	19.4	K.AYNEGNHIVVEITDDGK.G
1946.9770	1945.9697	1945.9480	11.2	R.LTAISEGESPVVATDSNEK.S
1961.9040	1960.8967	1960.8619	17.8	R.DNGNDTAIGMDIEPICAR.L
2399.2040	2398.1967	2398.1724	10.1	K.QTTNAAPKPTNNTANKPTESGEK.K
2527.2910	2526.2837	2526.2674	6.48	K.QTTNAAPKPTNNTANKPTESGEKK.V
2926.3860	2925.3787	2925.3727	2.07	K.QEIATPEPEVDVNQLSDSEVEAEIER.L

Figure A12. Results of mass spectrometry against CheA^{HK}-GST.

8.0. References

Ames, S.K., Frankema, N. & Kenney, L.J., 1999. C-terminal DNA binding stimulates N-terminal phosphorylation of the outer membrane protein regulator OmpR from *Escherichia coli*. *Proceedings of the National Academy of Sciences of the United States of America*, 96(21), pp.11792–7.

Baker, M.D., Wolanin, P.M. & Stock, J.B., 2006. Signal transduction in bacterial chemotaxis. *BioEssays: news and reviews in molecular, cellular and developmental biology*, 28(1).

Balaban, M. & Hendrixson, D.R., 2011. Polar flagellar biosynthesis and a regulator of flagellar number influence spatial parameters of cell division in *Campylobacter jejuni*. *PLoS Pathogens*, 7(12).

Bhatnagar, J. et al., 2010. Structure of the ternary complex formed by a chemotaxis receptor signaling domain, the CheA histidine kinase, and the coupling protein CheW as determined by pulsed dipolar ESR spectroscopy. *Biochemistry*, 49(18), pp.3824–41.

Boll, J.M. & Hendrixson, D.R., 2011. A specificity determinant for phosphorylation in a response regulator prevents in vivo cross-talk and modification by acetyl phosphate. *Proceedings of the National Academy of Sciences,* 108(50), pp.20160-5

Borrok, Kolonko, K.., 2008. Chemical probes of bacterial signal transduction reveal that repellents stabilizeand attractants destabilize the chemoreceptor array. *ACS: Chemical Biology*, 3(2), pp.101–109.

Bradford, M.M., 1976. A rapid and sensitive method for the quantitation of microgram quantities of protein utilizing the principle of protein-dye binding. *Analytical Biochemistry*, 72, pp.248–54.

Bren, a & Eisenbach, M., 2001. Changing the direction of flagellar rotation in bacteria by modulating the ratio between the rotational states of the switch protein FliM. *Journal of Molecular Biology*, 312(4), pp.699–709.

Bridle, O., 2007. An investigation into chemotaxis in *Campylobacter jejuni*. PhD, University of Leicester.

Briegel, A. et al., 2009. Universal architecture of bacterial chemoreceptor arrays. *Proceedings of the National Academy of Sciences of the United States of America*, 106(40), pp.17181–6.

Cai, S.J. & Inouye, M., 2002. EnvZ-OmpR interaction and osmoregulation in *Escherichia coli*. *The Journal of Biological Chemistry*, 277(27), pp.24155–61.

Cantwell, B.J. et al., 2003. CheZ Phosphatase localizes to chemoreceptor patches. *Journal of Bacteriology*, 185(7), pp.2354–2361.

Chen, W.P. & Kuo, T.T., 1993. A simple and rapid method for the preparation of gram-negative bacterial genomic DNA. *Nucleic Acids Research*, 21(9), p.2260.

Corry, J.E. & Atabay, H.I., 2001. Poultry as a source of *Campylobacter* and related organisms. *Symposium series (Society for Applied Microbiology)*, (30), p.96S–114S.

DEFRA, 2013. *Zoonoses Report 2012*.

Elliott, K.T. & Dirita, V.J., 2008. Characterization of CetA and CetB, a bipartite energy taxis system in *Campylobacter jejuni*. *Molecular Microbiology*, 69(5), pp.1091–103.

Everest, P.H. et al., 1992. Differentiated Caco-2 cells as a model for enteric invasion by *Campylobacter jejuni* and *C. coli*. *Journal of Medical Microbiology*, 37(5), pp.319–25.

Falke, J.J. et al., 1997. The two-component signaling pathway of bacterial chemotaxis: a molecular view of signal transduction by receptors, kinases, and adaptation enzymes. *Annual Review of Cell and Developmental Biology*, 13, pp.457–512.

Feng, J. et al., 1992. Role of phosphorylated metabolic intermediates in the regulation of glutamine synthetase synthesis in *Escherichia coli*. *Journal of Bacteriology*, 174(19), pp.6061–70.

Ferré, A., Mora, J. De & Ballado, T., 2004. Biochemical study of multiple CheY response regulators of the chemotactic pathway of *Rhodobacter sphaeroides Journal of Bacteriology*.186(15) pp.5172-7.

Ferrero, R.L. & Lee, a, 1988. Motility of *Campylobacter jejuni* in a viscous environment: comparison with conventional rod-shaped bacteria. *Journal of General Microbiology*, 134(1), pp.53–9.

Foussard, M. et al., 2001. The molecular puzzle of two-component signaling cascades. *Microbes and Infection*, 3(5), pp.417–24.

Fouts, D.E. et al., 2005. Major structural differences and novel potential virulence mechanisms from the genomes of multiple campylobacter species. *PLoS Biology*, 3(1).

Foynes, S. et al., 2000. Helicobacter pylori possesses two CheY response regulators and a histidine kinase sensor , CheA , which are essential for chemotaxis and colonization of the gastric mucosa *Helicobacter pylori*. *Infection and Immununity*. 68(4) pp.2016-23

Francis, N.R. et al., 2002. Subunit organization in a soluble complex of tar, CheW, and CheA by electron microscopy. *The Journal of Biological Chemistry*, 277(39), pp.36755–9.

FSA, 2009. FSA report for the UK survey of *Campylobacter* and *Salmonella* contamination of fresh chicken at retail sale.

Gao, R. & Stock, A.M., 2009. Biological insights from structures of two-component proteins. *Annual Review of Microbiology*, 63, pp.133–54.

Garrity, L.F. & Ordal, G.W., 1997. Activation of the CheA kinase by asparagine in Bacillus subtilis chemotaxis. *Microbiology*, 143(9), pp.2945–51.

Gilbreath, J.J. et al., 2011. Change is good: variations in common biological mechanisms in the epsilonproteobacterial genera *Campylobacter* and *Helicobacter*. *Microbiology and Molecular Biology Reviews,* 75(1), pp.84–132.

Glekas, G.D. et al., 2011. Site-specific methylation in *Bacillus subtilis* chemotaxis: effect of covalent modifications to the chemotaxis receptor McpB. *Microbiology*, 157(1), pp.56–65.

Golden, N.J. & Acheson, D.W.K., 2002. Identification of motility and autoagglutination *Campylobacter jejuni* mutants by random transposon mutagenesis identification of motility and autoagglutination *Campylobacter jejuni* mutants by random transposon mutagenesis. *Infection and Immunity*. 70(4):1761-71.

Guerry, P., 2007. *Campylobacter* flagella: not just for motility. *Trends in Microbiology*, 15(10), pp.456–61.

Hamer, R. et al., 2010. Deciphering chemotaxis pathways using cross species comparisons. *BMC systems biology*, 4(3).

Hartley-Tassell, L.E. et al., 2010. Identification and characterization of the aspartate chemosensory receptor of *Campylobacter jejuni*. *Molecular Microbiology*, 75(3), pp.710–30.

Hegde, M. et al., 2011. Chemotaxis to the quorum-sensing signal AI-2 requires the Tsr chemoreceptor and the periplasmic LsrB AI-2-binding protein. *Journal of Bacteriology*, 193(3), pp.768–73.

Hendrixson, D.R., Akerley, B.J. & DiRita, V.J., 2001. Transposon mutagenesis of *Campylobacter jejuni* identifies a bipartite energy taxis system required for motility. *Molecular Microbiology*, 40(1), pp.214–24.

Hendrixson, D.R. & DiRita, V.J., 2004. Identification of *Campylobacter jejuni* genes involved in commensal colonization of the chick gastrointestinal tract. *Molecular Microbiology*, 52(2), pp.471–84.

Higgins, D. & Dworkin, J., 2012. Recent progress in *Bacillus subtilis* sporulation. *FEMS Microbiology Reviews*, 36(1), pp.131–48.

Hofreuter, D. et al., 2006. Unique features of a highly pathogenic *Campylobacter jejuni* strain. *Infection and Immunity*, 74(8), pp.4694–707.

Hood, a M., Pearson, a D. & Shahamat, M., 1988. The extent of surface contamination of retailed chickens with *Campylobacter jejuni* serogroups. *Epidemiology and Infection*, 100(1), pp.17–25.

Howitt, M.R. & Lee, J.Y., 2011. ChePep Controls *Helicobacter pylori* Infection of the Gastric Glands and Chemotaxis in the Epsilonproteobacteria. *Molecular Biology*. 2011 Jul 26;2(4).

Hugdahl, M.B., Beery, J.T. & Doyle, M.P., 1988. Chemotactic behavior of *Campylobacter jejuni*. *Infection and Immunity*, 56(6), pp.1560–6.

Inclán, Y.F., Laurent, S. & Zusman, D.R., 2008. The receiver domain of FrzE, a CheA-CheY fusion protein, regulates the CheA histidine kinase activity and downstream signalling to the A- and S-motility systems of *Myxococcus xanthus*. *Molecular Microbiology*, 68(5), pp.1328–39.

Jama, A., 2013. Personal comunication. *Unpublished data*.

Jenal, U. & Galperin, M.Y., 2009. Single domain response regulators: molecular switches with emerging roles in cell organization and dynamics. *Current Opinion in Microbiology*, 12(2), pp.152–60.

Jiménez-Pearson, M.-A. et al., 2005. Phosphate flow in the chemotactic response system of *Helicobacter pylori*. *Microbiology,* 151(Pt 10), pp.3299–311.

Kanungpean, D., Kakuda, T. & Takai, S., 2011a. False positive responses of *Campylobacter jejuni* when using the chemical-in-plug chemotaxis assay. *The Journal of Veterinary Medical Science*, 73(3), pp.389–91.

Kanungpean, D., Kakuda, T. & Takai, S., 2011b. Participation of CheR and CheB in the chemosensory response of *Campylobacter jejuni*. *Microbiology*, 157(5), pp.1279–89.

Karatan, E. et al., 2001. Phosphorylation of the response regulator CheV is required for adaptation to attractants during *Bacillus subtilis* chemotaxis. *The Journal of Biological Chemistry*, 276(47), pp.43618–26.

Ketley, J. & Korolik, V., 2008. *Campylobacter*, Edition 3. *American Society for Microbiology Press*, Washington, DC, USA.

Kirby, J.R. et al., 1999. CheY-dependent methylation of the asparagine receptor, McpB, during chemotaxis in *Bacillus subtilis*. *The Journal of Biological Chemistry*, 274(16), pp.11092–100.

Kirby, J.R. et al., 1997. Methanol production during chemotaxis to amino acids in *Bacillus subtilis*. *Molecular Microbiology*, 24(4), pp.869–78.

Klein, A.H. et al., 2007. The intracellular concentration of acetyl phosphate in *Escherichia coli* is sufficient for direct phosphorylation of two-component response regulators. *Journal of Bacteriology*, 189(15), pp.5574–81.

Krell, T. et al., 2011. Diversity at its best: bacterial taxis. *Environmental Microbiology*, 13(5), pp.1115–24.

Lamarche, M.G. et al., 2008. The phosphate regulon and bacterial virulence: a regulatory network connecting phosphate homeostasis and pathogenesis. *FEMS Microbiology Reviews*, 32(3), pp.461–73.

Lee, S.Y. et al., 2001. Crystal structure of activated CheY. Comparison with other activated receiver domains. *The Journal of Biological Chemistry*, 276(19), pp.16425–31.

Lertsethtakarn, P. & Ottemann, K.M., 2010. A remote CheZ orthologue retains phosphatase function. *Molecular Microbiology*, 77(1), pp.225–35.

Levit, M.N., Grebe, T.W. & Stock, J.B., 2002. Organization of the receptor-kinase signaling array that regulates *Escherichia coli* chemotaxis. *The Journal of Biological Chemistry*, 277(39), pp.36748–54.

Li, J. et al., 1995. The response regulators CheB and CheY exhibit competitive binding to the kinase CheA. *Biochemistry*, 34(45), pp.14626–36.

Li, M. et al., 2011. Chemotaxis kinase CheA is activated by three neighbouring chemoreceptor dimers as effectively as by receptor clusters. *Molecular Microbiology*, 79(3), pp.677–85.

Liarzi, O. et al., 2010. Acetylation represses the binding of CheY to its target proteins. *Molecular Microbiology*, 76(4), pp.932–43.

Lowenthal, A.C. et al., 2009. A fixed-time diffusion analysis method determines that the three cheV genes of *Helicobacter pylori* differentially affect motility. *Microbiology*, pp.1181–1191.

Maddock, J.R. & Shapiro, L., 1993. Polar location of the chemoreceptor complex in *Escherichia coli*. *Science*, 259(5102).

Manson, M.D., 1992. Bacterial motility and chemotaxis. *Advances in Microbial Physiology*. *Elsevier.*

Marchant, J., Wren, B. & Ketley, J., 2002. Exploiting genome sequence: predictions for mechanisms of *Campylobacter* chemotaxis. *Trends in Microbiology*, 10(4), pp.155–9.

McCleary, W.R. & Stock, J.B., 1994. Acetyl phosphate and the activation of two-component response regulators. *The Journal of Biological Chemistry*, 269(50), pp.31567–72.

McCleary, W.R., Stock, J.B. & Ninfa, A.J., 1993. Is acetyl phosphate a global signal in *Escherichia coli*? *Microbiology*, 175(10), pp.2793–2798.

Varughese, KL. 2002. Molecular recognition of bacterial phosphorelay proteins. *Current Opinion in Microbiology*, pp.142–148.

Moe, K.K. et al., 2010. The mode of biofilm formation on smooth surfaces by *Campylobacter jejuni*. *The Journal of Veterinary Medical Science*, 72(4), pp.411–6.

Mortensen, N.P. et al., 2011. The role of *Campylobacter jejuni* cytolethal distending toxin in gastroenteritis: toxin detection, antibody production, and clinical outcome. *Acta Pathologica, Microbiologica, et Immunologica Scandinavica*, 119(9), pp.626–34.

Ninfa, E.G. et al., 1991. Reconstitution of the bacterial chemotaxis signal transduction system from purified components. *The Journal of Biological Chemistry*, 266(15), pp.9764–70.

Noriega, C.E. et al., 2008. Autophosphorylation and dephosphorylation by soluble forms of the nitrate-responsive sensors NarX and NarQ from *Escherichia coli* K-12. *Journal of Bacteriology*, 190(11), pp.3869–76.

Parkhill, J. et al., 2000. The genome sequence of the food-borne pathogen *Campylobacter jejuni* reveals hypervariable sequences. *Nature*, 403(6770), pp.665–8.

Parrish, J.R. et al., 2007. A proteome-wide protein interaction map for *Campylobacter jejuni*. *Genome Biology*, 8(7).

Pearson, B.M. et al., 2007. The complete genome sequence of *Campylobacter jejuni* strain 81116 (NCTC11828). *Journal of bacteriology*, 189(22), pp.8402–3.

Pittman, M.S., Goodwin, M. & Kelly, D.J., 2001. Chemotaxis in the human gastric pathogen *Helicobacter pylori*: different roles for CheW and the three CheV paralogues, and evidence for CheV2 phosphorylation. *Microbiology*, 147(9), pp.2493–504.

Poly, F. & Guerry, P., 2008. Pathogenesis of *Campylobacter*. *Current Opinion in Gastroenterology*, 24(1), pp.27–31.

Pope, J.. et al., 2010. *Campylobacter* Reactive Arthritis: A Systematic Review. *Seminars in Arthritis and Rheumatism,* 37(1), pp.48–55.

Porter, S.L., Wadhams, G.H. & Armitage, J.P., 2011. Signal processing in complex chemotaxis pathways. *Nature Reviews: Microbiology*, 9(3), pp.153–65.

Rajagopala, S. V et al., 2007. The protein network of bacterial motility. *Molecular Systems Biology*, 3(128), p.128.

Rao, C. V, Glekas, G.D. & Ordal, G.W., 2008. The three adaptation systems of *Bacillus subtilis* chemotaxis. *Trends in Microbiology*, 16(10), pp.480–7.

Reuter, M. & van Vliet, A.H.M., 2013. Signal balancing by the CetABC and CetZ chemoreceptors controls energy taxis in *Campylobacter jejuni*. *PloS One*, 8(1), p.e54390.

Reyrat, J. et al., 1998. Counterselectable Markers: Untapped Tools for Bacterial Genetics and Pathogenesis. *Infection and Immunity*, 66(9).

Rosario, M.M. et al., 1994. Chemotaxis in *Bacillus subtilis* requires either of two functionally redundant CheW homologs . Chemotaxis in Bacillus subtilis Requires Either of Two Functionally Redundant CheW Homologs. *Journal of Bacteriology*, 176(9).

Sandhu, R., 2011. The transducer-like proteins of *Campylobacter jejuni*. PhD, University of Leicester.

Scharf, B.E., 2010. Summary of useful methods for two-component system research. *Current Opinion in Microbiology*, 13(2), pp.246–52.

Sheppard, S.K. et al., 2013. Genome-wide association study identifies vitamin B 5 biosynthesis as a host specificity factor in *Campylobacter*. *Proceedings of the National Academy of Sciences,* 110(29), pp.11923–11927.

Shigematsu, M. et al., 1998. *Spirochaete*-like swimming mode of *Campylobacter jejuni* in a viscous environment. *Journal of Medical Microbiology*, 47(6), pp.521–6.

Shreeve, J.E. et al., 2013. Sequential spread of *Campylobacter* infection in a multipen broiler house. *Avian Diseases*, 44(4), pp.983–8.

Smith, C.K. et al., 2005. *Campylobacter jejuni* induced cytokine responses in avian cells. *Infection and Immunity*, 73(4).

Stock, a M., Robinson, V.L. & Goudreau, P.N., 2000. Two-component signal transduction. *Annual Review of Biochemistry*, 69, pp.183–215.

Stock, J. & Levit, M., 2000. Signal transduction: Hair brains in bacterial chemotaxis. *Current Biology*, pp.11–14.

Szurmant, H. & Hoch, J. a, 2010. Interaction fidelity in two-component signaling. *Current Opinion in Microbiology*, 13(2), pp.190–7.

Szymanski, C.M. et al., 1995. *Campylobacter jejuni* motility and invasion of Caco-2 cells. *Infection and immunity*, 63(11).

Szymanski, C.M. & Gaynor, E.C., 2012. How a sugary bug gets through the day Recent developments in understanding fundamental processes impacting *Campylobacter jejuni* pathogenesis. *Gut Microbes*, 3(2) pp.135–144.

Tareen, a M. et al., 2010. *Campylobacter jejuni* proteins Cj0952c and Cj0951c affect chemotactic behaviour towards formic acid and are important for invasion of host cells. *Microbiology*, 156(10), pp.3123–35.

Terasawa, S. et al., 2011. Coordinated reversal of flagellar motors on a single *Escherichia coli* cell. *Biophysical Journal*, 100(9), pp.2193–200.

Terry, K., Go, A.C. & Ottemann, K.M., 2006. Proteomic mapping of a suppressor of non-chemotactic cheW mutants reveals that *Helicobacter pylori* contains a new chemotaxis protein. *Molecular Microbiology*, 62(4), pp.1215–1215.

Thomas, S. a, Brewster, J. a & Bourret, R.B., 2008. Two variable active site residues modulate response regulator phosphoryl group stability. *Molecular Microbiology*, 69(2), pp.453–65.

Toljander, J. et al., 2012. Public health burden due to infections by verocytotoxin-producing *Escherichia coli* (VTEC) and *Campylobacter* spp. as estimated by cost of illness and different approaches to model disability-adjusted life years. *Scandinavian Journal of Public Health*, 40(3), pp.294–302.

Vegge, C.S. et al., 2009. Energy taxis drives *Campylobacter jejuni* toward the most favorable conditions for growth. *Applied and Environmental Microbiology*, 75(16), pp.5308–14.

Wolfe, A.J. et al., 2003. Evidence that acetyl phosphate functions as a global signal during biofilm development. *Molecular Microbiology*, 48(4), pp.977–88.

Wu, K. et al., 2011. Attractant binding induces distinct structural changes to the polar and lateral signaling clusters in *Bacillus subtilis* chemotaxis. *The Journal of Biological Chemistry*, 286(4), pp.2587–95.

Yan, J. et al., 2008. In vivo acetylation of CheY, a response regulator in chemotaxis of *Escherichia coli*. *Journal of Molecular Biology*, 376(5), pp.1260–71.

Yao, R., Burr, D.H. & Guerry, P., 1997. CheY-mediated modulation of *Campylobacter jejuni* virulence. *Molecular Microbiology*, 23(5), pp.1021–31.

Zapf, J. et al., 1998. A source of response regulator autophosphatase activity: the critical role of a residue adjacent to the Spo0F autophosphorylation active site. *Biochemistry*, 37(21), pp.7725–32.